Development of methods for measuring and characterising the surface topography of additively manufactured parts

Lewis Newton

Supervisor: Prof. Richard Leach

Prof. Nicola Senin

Dr. Simon Lawes

Faculty of Engineering

University of Nottingham

This dissertation is submitted for the degree of

Doctor of Philosophy

January 2020

I would like to dedicate this thesis to all those that have supported me along the way. Mum and Dad, Celise and Ian, you have helped me get so far in life; Gran and Grandad, you've always been proud of me; Ellie and Molly, you're always there to cheer me on; Curtis, Matthew and Joe, we've had some great times together; Lars, you will always be my desk-mate; Luke and Paddy, the office was great, but China was better; Adam, your advice and debate was always appreciated and well-recieved; Nicola, thank you for your scientific rigour and excellent commentary; Richard, you gave me the greatest opportunity, have been an outstanding supervisor and have built an amazing team. I would like to thank the University of Nottingham, the University of Huddersfield and all my former schools and teachers for providing me with the education and skills to produce such a document.

Lastly, to Beer, you've really got me through!

Cheers!

Declaration

I hereby declare that except where specific reference is made to the work of others, the contents of this dissertation are original and have not been submitted in whole or in part for consideration for any other degree or qualification in this, or any other university. This dissertation is my own work and contains nothing which is the outcome of work done in collaboration with others, except as specified in the text and Acknowledgements. This dissertation contains fewer than 65,000 words including appendices, bibliography, footnotes, tables and equations and has fewer than 150 figures.

Lewis Newton

January 2020

Acknowledgements

I would like to acknowledge the Engineering and Physical Sciences Research Council, the Centre for Additive Manufacturing, the Manufacturing Metrology Team and the Manufacturing Technology Centre for their support during my Thesis. I would like to give thanks to Richard Leach, Nicola Senin, Bethan Smith and Evangelos Chatzivagiannis for their supervision and contribution. I would also like to thank Franz Helmli, Reinhard Danzl, Liam Blunt, Carlos Gomez and Wahyudin Syam for their support with the optimisation of the focus variation instrument. I would like to thank Charlie McGuiness for the help in fabricating samples and Dejan Basu, David Gilbert, Annie Kerwin and Ben McGrory for their support with the finishing of the additive manufactured samples.

Abstract

Surface texture metrology, concerned with small-scale features present at a surface, is a fundamental tool for the improvement of manufacturing processes. Each manufacturing process produces a surface texture with measurement performed to understand the process and assess functionality and engineering tolerance. Metal powder bed fusion (PBF), a branch of additive manufacturing (AM), uses an energy source to selectively sinter or melt powder in bed layer-by-layer; resulting in a complex surface that presents new challenges for conventional measurement. The PBF surface also creates challenges for finishing operations, which remain essential to produce surfaces that meet functional and tolerancing requirements. The thesis aims to optimise the focus variation microscope (FV), validate feature-based segmentation approaches, apply feature-based characterisation approaches to PBF surfaces and to monitor the evolution of surface topography during the application of finishing operations. Whilst optical measurement techniques are being used to measure AM surfaces, good practice is not clearly defined. Using statistical regression modelling, measurement settings of FV were modelled against metrics of measurement quality: non-measured points, repeatability error and surface texture. The results show significant general trends across all surface types that can be used to inform good practice. Increasing resolution led to reductions in repeatability error, but increased instances of non-measured points. Measurement quality was also improved by using higher intensity illumination types. Feature-based characterisation allows for the segmentation and characterisation individual features, such as particles/spatter, but still requires validation of the accuracy and validity of feature identification. Using

binary classification testing between a manual reference and three algorithmic segmentation approaches (morphological segmentation on edges, contour stability analysis and active contours), metrics for accuracy were used to compare and validate segmentation methods for different PBF test cases. No segmentation approach was best overall, with results highly dependant on the test case and a general trade-off between identifying features and the ability to accurately define feature boundaries. Feature-based characterisation is applied to PBF surfaces, offering an enhanced assessment of the dimensional properties of surface features; only currently applied to top surfaces. Active contours segmentation of the particle/spatter features was applied to surfaces with varying build orientation angle. As the build orientation angle increases, towards facing into the powder bed, there is an increasing proportion of features. The underlying surface, deprived of features, shows a reduction in parameter values when compared to the original surface - a result of removing top heights of the surface. The effect and requirements of finishing operations applied to PBF surfaces needs further understanding and assessment. Using fidicual marksers and alignment and registration in six degrees of freedom, the evolution of surface topography can be monitored after finishing is applied. Linishing, laser polishing and shot peening were shown to all have a different effect on the initial topography in terms of material removal or surface reformation. By comparing surface texture parameters and feature properties of aligned topographies between finishing condition, the changes in heights on the surface in absolute terms and within the same coordinate system is shown. Overall, the work within this thesis contributes to the development of good practice in the measurement and characterisation of additive manufactured surfaces, whilst applying novel characterisation approaches to as-built and finished AM surfaces. For future work, the determination of measurement uncertainty for the measurement and characterisation of additive manufactured surfaces is fundamental.

Table of contents

List of figures **xvii**

List of tables **xxi**

1 Introduction **1**

1.1 Motivation 1

1.2 Aims and objectives 2

1.3 Structure of the thesis 4

2 State of the art **7**

2.1 Overview of additive manufacturing 7

2.1.1 Metal additive manufacturing 9

2.1.2 Powder bed fusion - process and considerations 11

2.2 Overview of metrology 19

2.2.1 Dimensional metrology 21

2.2.2 Surface measurement technologies 22

2.2.3 Surface topography characterisation 29

2.3 Overview of finishing operations applied to AM surfaces 38

2.3.1 Methods for the finishing of AM surfaces 39

2.4 Surface topography measurement for AM 44

2.4.1 General considerations for AM 45

2.4.2 Measurement techniques applied to AM 48
2.5 Surface texture characterisation for AM 50
2.5.1 Parameter-based characterisation 50
2.5.2 Feature-based characterisation 53
2.6 Discussion 55
2.7 Summary 58

3 Focus variation measurement of metal additive surfaces 61
3.1 Introduction 61
3.2 Methodology 63
3.2.1 Samples 63
3.2.2 Measurement process parameters 66
3.2.3 Experimental plan 66
3.2.4 Performance indicators 68
3.2.5 Data analysis 69
3.3 Results 71
3.3.1 Visual inspection of topography data 71
3.3.2 General full factorial design of experiments 76
3.3.3 Summary of the results 88
3.4 Discussion 89
3.4.1 General assumptions from the results 89
3.4.2 The meaning of measurement quality 90
3.4.3 General advice on FV configuration for measurement 91
3.5 Conclusions 93

4 Comparison and validation of surface topography segmentation methods 97
4.1 Introduction 97

4.2 Methodology 98
4.2.1 Sample surfaces 98
4.2.2 Segmentation using contour stability analysis 100
4.2.3 Morphological segmentation on edges 101
4.2.4 Segmentation using active contours 102
4.2.5 Comparison of segmentation methods 103
4.3 Results 108
4.3.1 LPBF top surface 109
4.3.2 EBPBF angled surface 112
4.3.3 EBPBF side surface 115
4.3.4 Summary of the comparison results 118
4.4 Discussion 119
4.4.1 Limits of the segmentation validation method 119
4.4.2 Additional computational costs of segmentation 120
4.4.3 Measurement uncertainty for feature-based characterisation 121
4.5 Conclusions 121

5 Characterisation of surface topography for EBPBF surfaces produced at different build orientations 125

5.1 Introduction 125
5.2 Methodology 128
5.2.1 Measurement test part 128
5.2.2 Measurement strategy 128
5.2.3 Feature-based segmentation 129
5.2.4 Feature-based characterisation of surface texture 131
5.2.5 Parameter-based characterisation of surface texture 131
5.3 Results 132

5.3.1 Visualisation of the surface 132
5.3.2 Feature-based characterisation 133
5.4 Discussion 144
5.5 Conclusion 147

6 Monitoring the evolution of surface topography 149
6.1 Introduction 149
6.2 Methodology 151
6.2.1 Samples 151
6.2.2 Relocation landmarks 151
6.2.3 Measurement strategy 151
6.2.4 Finishing operations 152
6.2.5 Re-measurement and registration of topographies 152
6.2.6 Surface texture characterisation 153
6.2.7 Feature-based evaluation of surface topography 154
6.3 Results 155
6.3.1 Surface texture characterisation 155
6.3.2 Feature-based characterisation of side surfaces 164
6.4 Discussion 171
6.5 Conclusion 174

7 Conclusions 177
7.1 Thesis summary 177
7.2 Contributions to the field 180
7.3 Areas for future work 184

References 187

Appendix A Design of experiment results for optimisation of focus variation 197

A.1 Coefficient of determination (R^2) results for each ANOVA model 197

A.2 Main effects plots for each ANOVA model 199

List of figures

2.1 Process flow diagram of additive manufacturing 9
2.2 Principle of directed energy deposition 10
2.3 Principle of sheet lamination 11
2.4 Principle of powder bed fusion 11
2.5 Laser powder bed fusion process 12
2.6 Electron-beam powder bed fusion process 13
2.7 Melting and scanning principles of LPBF 16
2.8 Examples of various supports for PBF processes 18
2.9 List of finishing techniques that have been applied to AM surfaces 20
2.10 Calibration hierarchy or traceability pyramid 22
2.11 Diagram of contact stylus measurement system 24
2.12 Effect of lay on profile measurement 25
2.13 Diagram for the numerical aperture of a microscope objective lens 26
2.14 Operation principle of focus variation 28
2.15 Separation of waviness from roughness with filters 30
2.16 Definition of a surface profile 31
2.17 Graphical representation of calculation of *Ra*. 33
2.18 Graphical representation of calculation of *Rsk*. 34
2.19 Prodecure to extract surface texture components 36

2.20 EBPBF surface topography segmented using morphological segmentation . 38
2.21 Material removal mechanisms for abrasion 39
2.22 Graphical representation of the staircase effect 46
2.23 Example features of PBF surface 47
2.24 Commonly investigated truncheon test part. 52

3.1 Schematic diagram of the focus variation technology 64
3.2 Samples of various PBF test parts 65
3.3 Procedure for calculating Q3 from measurment data 70
3.4 Top views of topography models with RGB colour map 72
3.5 Height map visualisations with changing magnification 74
3.6 Height map visualisations with changing vertical resolution 75
3.7 Height map visualisations with changing lateral resolution 77
3.8 Height map visualisations with changing illumination 78
3.9 Main effect plots for Q3 at 10× magnification. 79
3.10 Main effect plots for Q3 at 20× magnification. 80
3.11 Main effect plots for Q3 at 50× magnification. 81
3.12 Main effect plots for NMP at 10× magnification. 83
3.13 Main effect plots for NMP at 20× magnification. 84
3.14 Main effect plots for NMP at 50× magnification. 84
3.15 Main effect plots for surface parameter, *Sa*, at 10× magnification. 85
3.16 Main effect plots for surface parameter, *Sa*, at 20× magnification. 86
3.17 Main effect plots for surface parameter, *Sa*, at 50× magnification. 87

4.1 Example surface topography height maps 99
4.2 Pre-processing for performance indicators for individual feature assessment 105
4.3 Binary classification test results for the LPBF top surface 110
4.4 Precision, recall and specificity for the LPBF top surface 111

4.5 Performance indicators for the whole LPBF top surface 112
4.6 Binary classification test results for the EBPBF angled surface 113
4.7 Precision, recall and specificity for the EBPBF angled surface 114
4.8 Performance indicators for the whole EBPBF angled surface 115
4.9 Binary classification test results for the EBPBF side surface 116
4.10 Precision, recall and specificity for the EBPBF side surface 117
4.11 Performance indicators for the whole EBPBF side surface 118

5.1 'Bracelet' test part 128
5.2 Topographic height maps built at varying orientation 133
5.3 Active contour approach applied to angled surface 134
5.4 Object maps from the active contour process 135
5.5 Boxplots of feature count with respect to surface orientation 136
5.6 Boxplots of feature height with respect to surface orientation 137
5.7 Boxplots of feature area with respect to surface orientation 138
5.8 Characterisation applied to surface with particles removed 139
5.9 Boxplots of percentage particle coverage with respect to surface orientation 140
5.10 Boxplots of surface parameter, *Sa*, with respect to build orientation 141
5.11 Boxplots of surface parameter, *Sq*, with respect to build orientation 142
5.12 Boxplots of surface parameter, *Sz*, with respect to build orientation 143
5.13 Boxplots of surface parameter, *Ssk* with respect to build orientation 145
5.14 Boxplots of surface parameter, *Sku* with respect to build orientation 146

6.1 Layout of relocation landmarks 152
6.2 Alignment principle 153
6.3 Surface characterisation of the pre- and post- linished 0° surface 156
6.4 Surface characterisation of the pre- and post- laser polished 0° surface . . . 158
6.5 Surface characterisation of the pre- and post- shot-peened 0° surface 160

6.6 Surface characterisation of the pre- and post- linished 90° surface 161
6.7 Surface characterisation of the pre- and post- laser polished 90° surface . . 163
6.8 Surface characterisation of the pre- and post- shot-peened 90° surface . . . 165
6.9 Segmentation mask applied pre- and post-linished side surface 167
6.10 Feature attributes for pre- and post-linished side surface 168
6.11 Segmentation mask applied pre- and post-laser polished side surface 169
6.12 Feature attributes for pre- and post-laser polished side surface 170
6.13 Segmentation mask applied pre- and post-shot peened side surface 172
6.14 Feature attributes for pre- and post-shot peened side surface 173

A.1 Main effects plots for Q3 for the 10× magnification 200
A.2 Main effects plots for NMP for the 10× magnification 201
A.3 Main effects plots for *Sa* for the 10× magnification 202
A.4 Main effects plots for Q3 for the 20× magnification 203
A.5 Main effects plots for NMP for the 20× magnification 204
A.6 Main effects plots for *Sa* for the 20× magnification 205
A.7 Main effects plots for Q3 for the 50× magnification 206
A.8 Main effects plots for NMP for the 50× magnification 207
A.9 Main effects plots for *Sa* for the 50× magnification 208

List of tables

3.1 Sample block material, commercial machine, and sample part size 63

3.2 Selected FV measurement process parameters and their values 67

4.1 Classification of pixels in the segmentation map 106

5.1 Optimised threshold values for height thresholding 130

6.1 Finishing operations and key parameter values 152

A.1 Coefficient of determination (R^2) results for the 10× objective ANOVA models 198

A.2 Coefficient of determination (R^2) results for the 20× objective ANOVA models 198

A.3 Coefficient of determination (R^2) results for the 50× objective ANOVA models 198

Chapter 1

Introduction

1.1 Motivation

With newer manufacturing technologies, such as additive manufacturing (AM), there is always a need to quantity and qualify the ability to produce components. The applicatio of metrology, the science of measurement, is concerned with the suitability of measurement instruments and their calibration as well as the quality control of the manufacturing process being measured. In order to support the adoption of AM technologies, good practice by following standards and correctly using measurement instruments can allow for meaningful measurements to qualify the process.

Surface texture refers to the small-scale features present at a surface, but not those that contribute to the form, or overall shape of the part. Surface texture metrology is a fundamental tool for the improvement of manufacturing processes. Each manufacturing process produces a surface texture, and measurement is performed to ensure suitability of a surface with respect to its application. If required, surface finishing operations can be applied to modify the initial surface until a desired texture is achieved.

Powder bed fusion (PBF) is a branch of AM that uses an energy source (commonly a laser) to selectively sinter to powder within a bed to produces parts layer-by-layer. As a

result, within PBF there is a complex physical interaction between the build process and the material feedstock that can produce complex topographies that are highly dependent on the geometry of the part being built. It is these complex surfaces that present new challenges for conventional surface texture measurement instruments - with high slopes, varying reflectivity and large height ranges. This as-built topography also results in challenges for finishing operations, which act to alter or remove features on the surface and are often necessary to produce surfaces that suitable for a desired function.

Using surface texture metrology, AM surfaces can be measured, visualised and characterised to assess quality, functionality and finishing requirements as well as offer a method to relate the parameters of the build process (or any subsequent post-process) to features and heights on the surface.

1.2 Aims and objectives

The aim of the thesis is to develop methods or methodology for the measurement and characterisation of surface texture of as-built and post-processed AM parts. The use of focus variation (FV) microscopy was investigated as a surface texture measurement instrument, due to its prevalence in industry, its inherent ability to capture high slope angles on surfaces and its known suitability in measuring rough surfaces and excessive height ranges - all common challenges for metal PBF surfaces. Metal PBF is investigated in this thesis as one of the most common methods of producing AM parts, with focus on the electron beam powder bed fusion process. The finishing operations investigated in this thesis range from conventional grinding to more non-conventional approaches: shot peening and laser polishing.

Firstly, the FV method contains a variety of measurement settings that can be adjusted to ensure a high quality of measurement (i.e. full coverage, lower repeatability errors); this needs to be suitably tailored to the various surfaces throughout the research. A suitable

evaluation of optimised settings for the measurement of complex additive surfaces, both as-built and finished, is required to determine what can constitute good practice for this particular measurement technique.

Secondly, the additive surface contains a variety of features as a result of the layer-by-layer process. To better understand the additive process, newer descriptive measures could offer better suitability to research and industry alongside the current parameters used in the evaluation of surface texture.

This requires the use of algorithmic feature-based assessment of surface topographies that act to 'break-down' the surface into deterministic sets of topographic formations from which dimensional properties can be assessed. For example, surfaces produced using powder-based methods may contain varying levels of particles depending on the orientation of the build. By characterising the proportion of features on the surface and parameters of the underlying surface, requirements for any subsequent finishing operations can be estimated and better adapted to each surface.

Thirdly, post processing is an essential part of the AM supply chain. Whilst there is increasing development of processes to reduce the requirement of post-processing, it is still required for many applications to meet desired functionality and tolerancing. Depending on the process applied, features present on the surface can influence the finishing process and even contribute to the creation of newer features. Each process leaves a 'fingerprint' on the surface and in order to assess the suitability of surface texturing methods for AM, then greater understanding into the evolution of the surface topography through the post-process is required.

In summary, the objectives are:

1. Determine the optimum instrument settings and good practice for the measurement of surface topography of additive surfaces using focus variation

2. Develop methodologies to identify and describe/ define features on the PBF surface, such as investigating variation of features with respect to build orientation

3. Develop methodologies that can quantitatively monitor the evolution of surface topography before and after post processing

1.3 Structure of the thesis

In Chapter 1, the motivation of the thesis is presented alongside a breakdown of the aims and objectives.

In Chapter 2, a review of relevant literature is presented to analyse the state of the art within the field to inform the research conducted throughout the thesis. The themes throughout this thesis are measurement technologies, characterisation approaches and finishing operations for metal PBF.

In Chapter 3, a study on the influence of changing measurements settings of the focus variation microscope on the measurement results for metal PBF surfaces is presented. The purpose of this chapter is to facilitate the development of good practice guidelines for the measurement of metal additive manufactured surfaces using the focus variation microscope.

In Chapter 4, a methodology to allow for the comparison and validation of feature-based segmentation approached is presented. The purpose of this chapter is to provide quantitative and qualitative metrics regarding the quality and efficacy of various segmentation approaches when applied to different metal powder bed fusion surface test cases in order to allow for meaningful comparison.

In Chapter 5, an investigation into how the surface topography of AM parts is affected by build orientation is presented. The purpose of this chapter is to study how surface texture parameters and segmented topographical formations, such as particles/spatter features and their properties, differ with respect to build orientation.

In Chapter 6, a methodology to allow for the comparison of surfaces topographies that are altered by a finishing operation using alignment and registration is presented. The purpose of this chapter is to makes use of fidicual markers and areal topography data to align and register topographies in six degrees of freedom; this can further allow for assessments of the evolution of surface topographies and identified features as a result of finishing in terms of absolute changes of heights on the surface.

In Chapter 7, the conclusions and future work of the thesis are presented in terms of how the contributions of the work address the aims and objectives of the thesis.

Chapter 2

State of the art

In this chapter, a review of the state of the art for the surface texture metrology for additive manufacturing is presented. More specifically, this chapter covers the basics of metal additive manufacturing, metrology and the common surface finishing approaches applied to metal additive surfaces before investigating in more detail the measurement technologies being used for measurement and the characterisation approaches - including feature-based characterisation - applied to metal powder bed fusion surfaces as well as those subsequently finished.

2.1 Overview of additive manufacturing

Additive manufacturing (AM) is the general term for a series of technologies that, using geometric representation of a designed part, creates physical objects by successively adding material [1, 2]. With three-dimensional (3D) model data, material can be joined layer upon layer to create parts and contrasts subtractive (shape acquired through selective removal of material) and formative (shape acquired through application of pressure to a body of raw material) manufacturing approaches. A layer refers to material laid out or spread to create a surface on which the joining process is applied to create an approximate ‘slice’ of the 3D

model data that represents the final part [1].

Within AM there are seven process categories as defined in the ISO 17296-2 [2]:

- Binder jetting
- Directed energy deposition
- Material extrusion
- Material jetting
- Powder bed fusion
- Sheet lamination
- Vat photo-polymerization

Increasingly more materials are being made available for the technologies within AM. However, some technologies, such as vat photo-polymerization which requires a UV curable photo-polymer, are limited in the material they can use due to the nature of the process.

With AM there is more flexibility for the design of parts, because the part is built up in layers, complex forms can be approximated into layers (theorised as slices) which when sub-sequentially built up produce the desired part [1]. As a result, assemblies can be consolidated into a reduced number of parts and complex bio-mimetic structures can be realised. Another capability of AM is that internal structures can be built without access and foams and lattices can be produced building up the geometry in layers. AM generally requires little part-specific tooling for and between the production of the part, making the approach competitive for the production of low volume parts and a suitable tool for prototyping [1]. Increasingly, AM is moving into the production of direct, final parts. This low volume, batch manufacturing

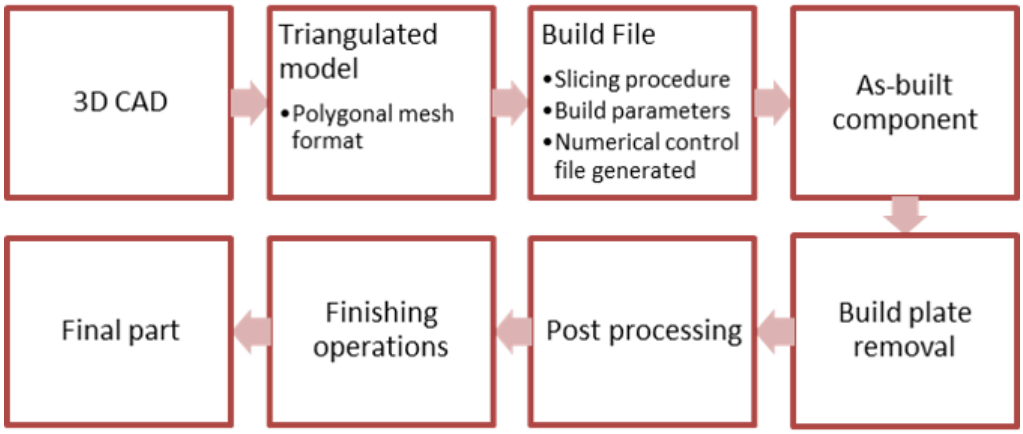

Fig. 2.1 Process flow diagram of additive manufacturing, from 3D computer-aided design data to final part

allows for the mass customisation of parts created a greater volume of bespoke products. The process from design to manufacture for an AM part can be visualised in Figure 2.1.

2.1.1 Metal additive manufacturing

The creation of direct full metal parts, where the final part is wholly metal as-built without the need for infiltration, is currently commercially limited to only a few process categories. Specifically, these are directed energy deposition, sheet lamination, and powder bed fusion [2, 3].

Directed energy deposition

Directed energy deposition (DED) is a process in which focused thermal energy (laser, electron beam, plasma arc, etc.) is used to fuse materials by melting as they are being deposited [2] (Figure 2.2). Like traditional welding but acting in three dimensions, the metals used here are either wire- or powder-based and include aluminium alloys and steels using metal inert gas (MIG), as well as titanium alloys using Tungsten inert gas (TIG) and plasma arc welding [4]. The surfaces produced are characterised by large weld tracks. DED is

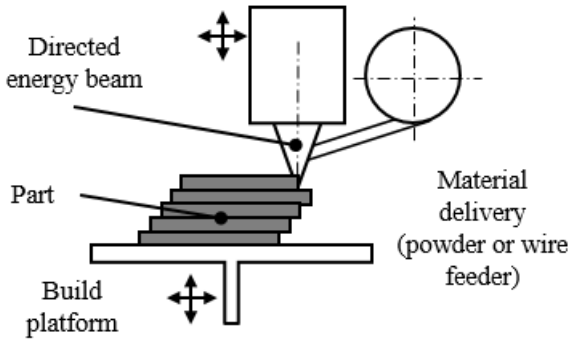

Fig. 2.2 Principle of directed energy deposition

scalable to produce larger metal AM parts and can be integrated with 5-axis control. With 5-axis control, DED is able to deposit layers in many directions offering more degrees of freedom in which to build, however, the weld size is relatively large as is the the minimum feature resolution.

Sheet lamination

Sheet lamination is a process in which sheets of material are bonded to form a part [2](Figure 2.3). For metals, this is typically performed via application of ultrasound (ultrasonic consolidation). For ultrasonic metal additive manufacturing (UAM), ultrasonic welding can be used to integrate layers of material (including different materials) provided they can be rolled as layers [5]. The geometry of each layer can be cut or machined before and/or after adhesion. UAM parts possess machined surfaces on the sides, and surface structure on the upper surfaces possess topographical formations resulting from a process of rolling compression.

Powder bed fusion

Powder bed fusion (PBF) is a process in which thermal energy is used to selectively fuse regions of a powder bed, the build area in which powder material (referred to as feedstock) is

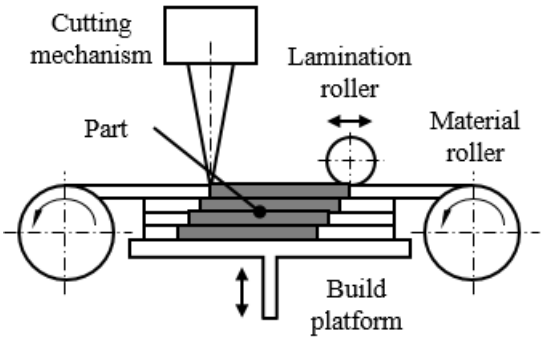

Fig. 2.3 Principle of sheet lamination

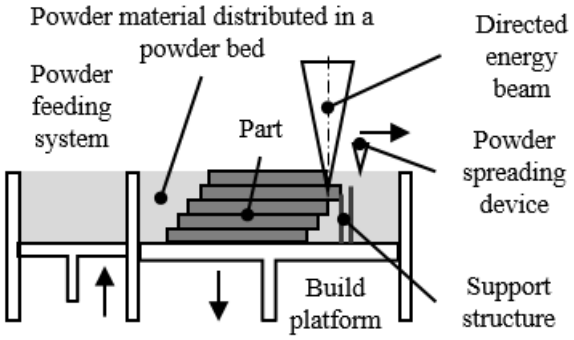

Fig. 2.4 Principle of powder bed fusion

deposited [2] (Figure 2.4). PBF is one of the most commonly used AM process for metal fabrication, with its surfaces presenting unique metrological challenges [6, 7].

2.1.2 Powder bed fusion - process and considerations

While the principles discussed in Section 2.1.1 cover all of the technologies of metal AM, the work of this Thesis focused more specifically on those produced using powder bed fusion (PBF), with this process being divided into two sub-technologies determined by their mechanism in which energy is applied to the powder bed: laser-based and electron beam-based.

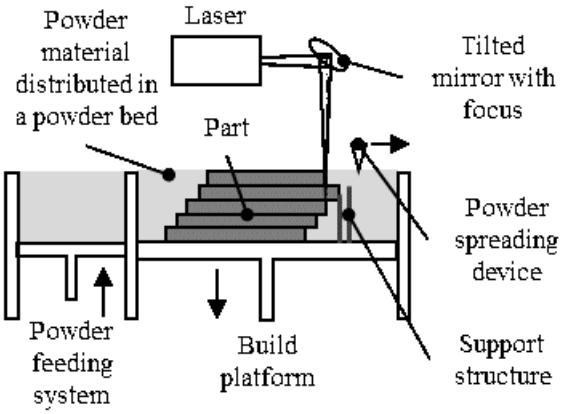

Fig. 2.5 Laser powder bed fusion process

Laser based processes

The process of the laser powder bed fusion (LPBF), shown in Figure 2.5, is typically as follows [1, 3, 8]:

- An appropriate atmosphere is generated, typically inert gas atmosphere.
- The build chamber is heated to reduce thermal gradients and cooling effects during processing.
- A layer of powder is deposited over the build platform from the powder feeding system, which is spread to achieve a defined layer thickness.
- The laser scans over regions of the powder bed layer, melting the powder where it passes. These melted regions then solidify and form a single layer, which adheres to the layer (or build platform) below.
- The build platform is then lowered by a step defined by the layer thickness.
- Another layer is deposited, spread and fused, repeating until fabrication is complete.

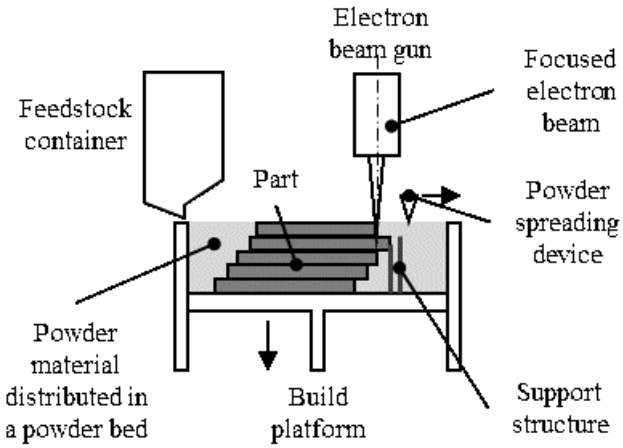

Fig. 2.6 Electron-beam powder bed fusion process

Electron beam based processes

The process of electron beam powder bed fusion (EBPBF) is like that of LPBF, but with some differences [9], as shown in Figure 2.6 and below:

- A vacuum environment is generated in the build chamber.
- The build chamber is heated to reduce thermal gradient.
- A layer of powder is deposited and spread from the powder feed system.
- An electron beam gun scans a larger region of the chamber, approximating the layer and a region around it. This is a pre-heating step and acts to semi-sinter the powder into a ‘cake’.
- After this, the electron beam scans at a lower speed to melt the powder particles, to form the solid layer which adheres to the layer (or build platform) below.
- The build platform is then lowered by a step defined by the layer thickness.

Powder considerations

PBF powder can be fabricated from a variety of methods, commonly gas atomisation [1], producing a normal distribution of sizes between some limits specific to the type of system being used [10]. Powder particle sizes range from approximately 15 µm to 50 µm for laser-based systems and 45 µm to 100 µm for electron beam systems [11]. The specific range is dependent on the material and can be further refined depending on the build process. The particle size range used influences packing density (which is linked to part porosity), as well as the required layer thickness and the size of spatter and adhered particles that are found on as-built part final surfaces [1, 12].

Material considerations

Materials available for both metal PBF processes include titanium alloys (such as Ti6Al4V), steels (such as stainless-steel alloy 316L) and nickel super alloys (such as Inconel 625 and Inconel 718). LPBF is also able to print materials such as copper, gold and aluminum alloys (mostly AlSi10Mg) [1]. The chosen material will influence the optical properties of the final surface (such as reflectance), which will affect the interaction between the surface and the measurement instrument [13].

Process considerations

There are a variety of process settings that affect the powder bed fusion process [1]. When considering the parameters that influence the input energy that causes the powder bed to melt, the energy density equation can be used to explain the relationship between power of the energy beam, P, scanning velocity, v, diameter or spot size of the energy beam, D, hatch distance (width between weld tracks), h, and layer thickness, t. This equation provides a volumetric expression of energy, E, expressed in J/mm^3 [1, 14].

$$E = P/(v\,D\,H\,t). \tag{2.1}$$

This equation is often used experimentally to help determine the settings used for the process. Depending on the parameter, a value too low or too high can often lead to either: insufficient energy density - characterised by incomplete melting, low density parts, pores, and reduced adhesion of particles on side surfaces; or excessive energy density - which can lead to increased potential for spatter (particles that eject from the bed which then fall back on the bed, and often onto the surface) as well as which can contribute to porosity, build failure and excessive surface roughness [14–16]. Diagrams showing the melting process of LPBF and the aspects of contouring (outer shape) and hatching (in-fill) that make up the scan strategy for the continuous scan of a single layer can be seen in Figure 2.7.

Build plate and support removal

In order to remove the part from the build plate, the powder surrounding the part needs to be removed. For LPBF, it is often a simple case of raising the build plate within the chamber and brushing away the loose powder, which can then be sieved, filtered and recycled in a later build [1]. However, for EBPBF there is a sintered cake that surrounds the part. To remove the cake, loose powder is often grit blasted on the build which breaks up the weaker 'cake' [9]. The loose powder from the build and the broken-up cake can then be re-processed and recycled.

Supports are used in metal PBF to control thermal effects and assist with the fabrication of overhanging build geometry, with some examples seen in Figure 2.8. Some of the more common methods or removal are by manual mechanical means, band-sawing, and the use of wire electro-discharge machining (EDM) [1, 17, 18].

Manual mechanical removal is a human operation often results in tool marks and scratches being accidentally applied to the surface [1], and the surfaces in general are dominated by

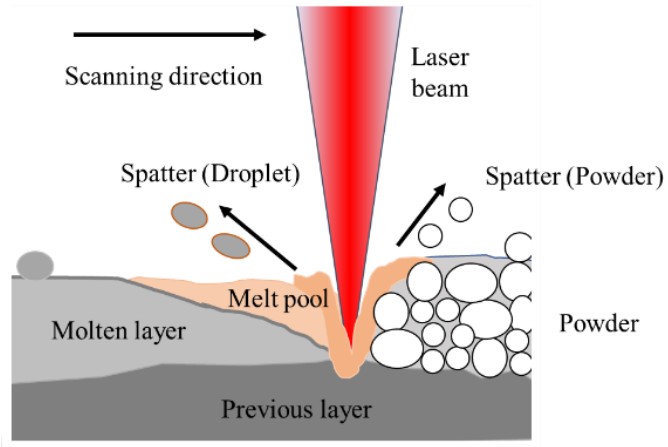

(a) Diagram of melt phenomena for LPBF

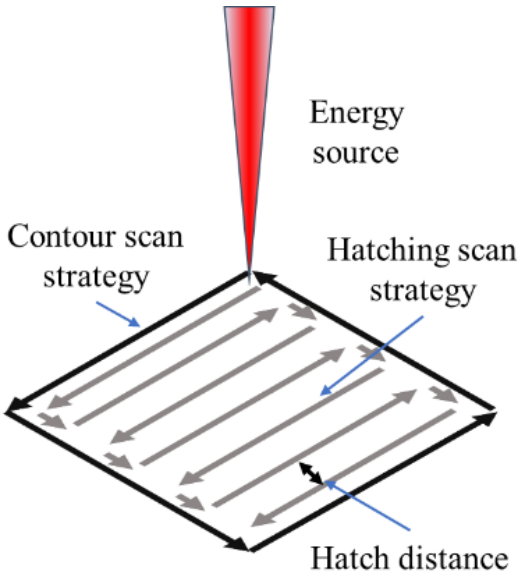

(b) Diagram of scanning principle for AM

Fig. 2.7 Melting and scanning principles in the production of a layer for laser powder bed fusion

a large remainder of stumps that made up the original support strategy. These stumps are often very large features compared to the layer thickness and particle sizes of the respective processes and can also be large in height.

Wire EDM uses spark erosion from a charged wire that acts as a cutting tool to remove supports from the part. The resultant surface features a relatively smooth surface related to the shape of the wire, but can contain small pits due to the nature of spark erosion randomly affecting the surface and micro-crystalline features due to impurities which are not eroded by the process [18].

For the removal of loose powder on AM parts and the sintered 'cake' more specifically EBPBF process, ultrasonic cleaning is the use of a bath of solvent that can be excited via ultrasound [19]. The operating principle can be compared to ultrasonic cavitation abrasion, where the ultrasound causes cavitation bubbles to collapse close to the surface in order to dislodge partially melted powders or to propel abrasive particles to abrade the surface [20]. Together, the mechanisms of ultrasonic cleaning work to remove material and alter the surface; leaving craters through cavitation and flattened regions and scratches from propelled particles. It is often used to prepare samples prior to further post processing, measurement or application.

Post processing

Post processing refers to the process steps taken after a build in order to achieve desired properties in the final product. Post processing commonly includes the application of heat treatments [21, 22], such as hot isostatic pressing (HIP)[17], and surface texture modification operations (often referred to as surface finishing), which in this Thesis are considered separately. Heat treatments are used to control and improve part micro-structure and mechanical properties and can act to reduce the sizes of internal porosity [1, 21, 22]. These steps are often used before any subsequent finishing operations are applied.

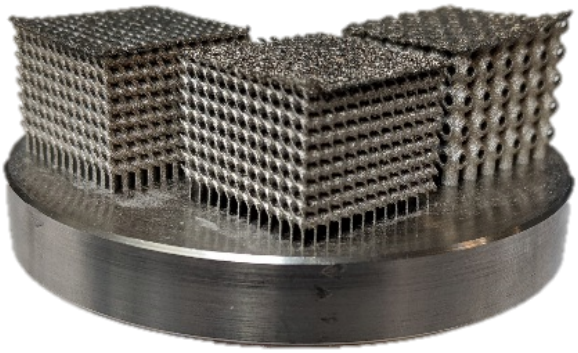

(a) LPBF lattice parts attached to the build plate using supports

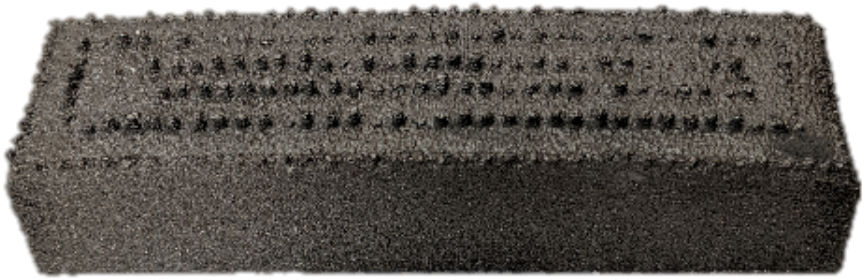

(b) EBPBF bottom surface after support removal

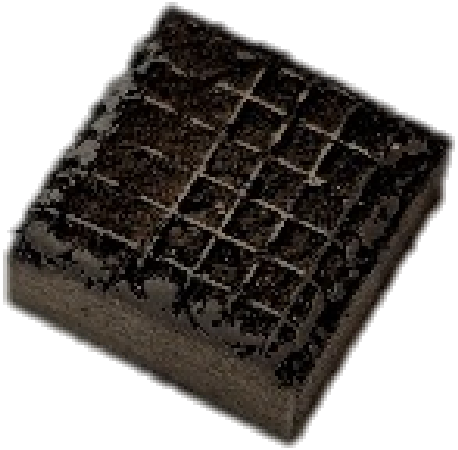

(c) LPBF bottom surface after support removal

Fig. 2.8 Examples of various supports for PBF processes

Surface finishing for additive manufacturing

Surface finishing is used to refer to specific steps taken to improve surface texture, using finishing operations such as mass finishing and conventional machining. In such operations, surfaces interact with the finishing mechanism in order to produce parts of a desired surface quality. Each finishing technique has its own process inputs and limitations and results in its own characteristic process mark or 'signature' on the surface [23, 24] . Finishing operations act in several ways: removing asperities (high points, such as particles) from the bulk surface, re-forming the surface, or even filling in the deeper recesses by adding material to alter the surface. Finishing operations can be manual or automatic and are either applied to multiple parts in batches or individually applied to each part.

By possessing information about the finishing processes and their parameters, scales of interest and the scale of interaction can be better determined for the measurement process. A non-exhaustive list of finishing techniques that have been applied to AM surfaces can be seen in Figure 2.9:

2.2 Overview of metrology

According to the international vocabulary of metrology (VIM)[36], metrology refers to the science of measurement and its application, including all theoretical and practical aspects of measurement, measurement uncertainty and its field of application.

Measurement is the process of obtaining quantity values that can be attributed to a quantity, referred to as a measurand, with an associated measurement uncertainty. Measurement uncertainty is defined as the parameter that characterises the dispersion of the quantity values of the measurand.

There are many components of uncertainty, such as components from systematic effects, which can be either corrected for (as with instruments that are measuring assigned values of

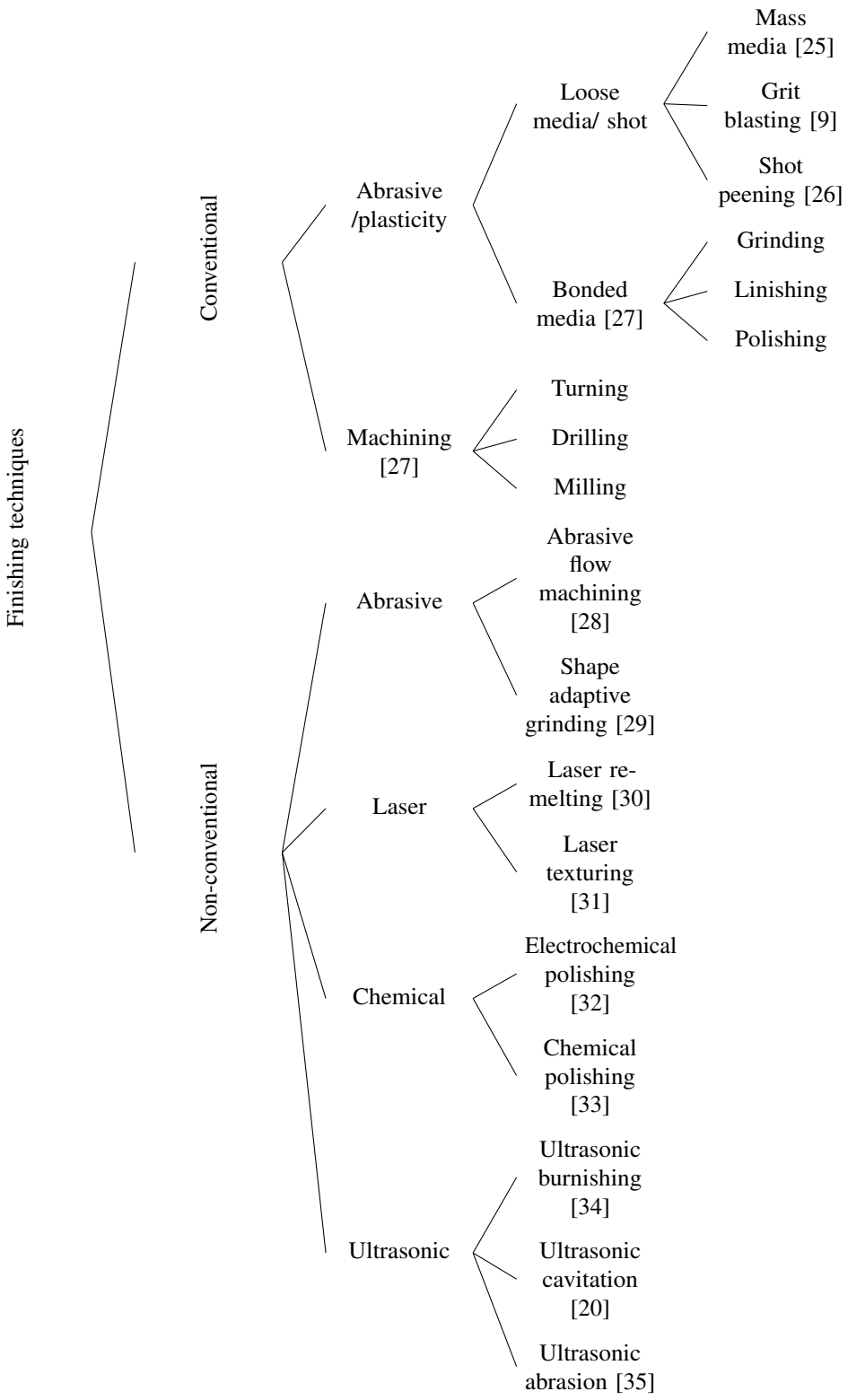

Fig. 2.9 List of finishing techniques that have been applied to AM surfaces

measurement standards) or incorporated (as for definitional uncertainty - that is, the component of uncertainty in the definition of a measurand) [37]. Measurement uncertainty can be evaluated as either Type A or Type B. Type A evaluation is the evaluation of a component of measurement uncertainty using the statistical analysis of a series of measurands obtained under defined measurement conditions and are often characterised as standard deviations. The types of defined measurement conditions vary, but for a repeatability condition of measurement, measurements are taken with the same measurement procedure, operators, measurement system, operating conditions and location with replicate measurements taken over a short period of time [37]. Type B evaluation is the evaluation of a component of measurement uncertainty by any other means than a Type A evaluation. This evaluation is generally based on information and may come in the form of a published quantity value of a certified reference material, obtained from a calibration certificate or obtained from limited deduced through personal experience [37].

Traceability is paramount in metrology and is a property of a measurement result in which it can be related to a reference through an unbroken chain of calibrations (comparison of measurement, each contributing to measurement uncertainty) [36–38]. Traceability requires an established calibration hierarchy (traceability pyramid) which relates the work-piece being measured to the international standard, which, in the case of dimension, is the metre (See Figure 2.10). In general, the uncertainty of each calibration increases as you move down the traceability chain towards the work-piece [37].

2.2.1 Dimensional metrology

Dimensional metrology covers several smaller fields of measurement, such as measurement of length, displacement, form and surface texture [39]. Dimensional measurements are routinely made in order to compare dimensional measurands to specification. These specifications

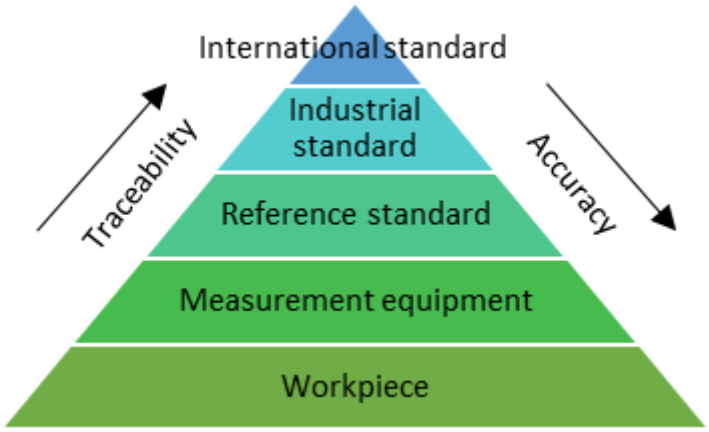

Fig. 2.10 Calibration hierarchy or traceability pyramid

indicate a dimension that is to be measured and a tolerance on that dimension, which determines whether a specific part fails or passes during an inspection process.

Form and surface texture metrology

Form can be understood as an assessment of deviations of surfaces or paths from fundamental definitions of geometrical primitives [39]. Simply put, form metrology deals with the overall shape of a part. Form measurement includes, for example, the measurement of straightness, roundness and cylindricity (deviation from lines, circles and cylinders); and flatness and parallelism (deviation from planes and the relation of geometries from one another).

Surface texture metrology (also referred to as surface metrology) deals with local deviations of a surface from a defined form (typically a perfectly flat plane) [40]. Simply put, it deals with geometrical irregularities present at a surface, but not those that contribute to the form or shape of the surface. It is this branch of metrology that is considered by the research within this Thesis.

2.2.2 Surface measurement technologies

There are seven technologies capable of measuring surfaces that are currently covered within the ISO 25178-60X series.

Of these, only the following are commonly applied in the measurement of AM surfaces [6, 7, 41]. These technologies are:

- Contact stylus [42]
- Coherence scanning interferometry [43]
- Focus variation microscopy [44]
- Confocal microscopy [45]

In addition to these approaches, X-ray computed tomography and other conventional form measurement technologies have increasingly been used to measure parts to extract surface information [46, 47]. In general, form measurement systems capture data either as point clouds in an (x, y, z) format or as 3D triangulated meshes. These 3D datasets can be rasterised in order to convert to the current standard of (x, y) datasets, as in [46, 48], whilst other research is investigating how to use 3D datasets for conventional assessments [49, 50].

The primary instruments used within this Thesis, and discussed in some detail, were the contact stylus - a profile measuring contact instrument - and the focus variation microscope - a non-contact optical areal measurement instrument.

Contact stylus

The contact stylus instrument is one of the oldest and most common technologies used within surface metrology [13, 51], including its use in AM [6]. These instruments employ mechanical contact between a probe and the surface being measured. whilst traversing the surface along a profile, transducers convert the vertical movement of the stylus into an electrical signal that can be encoded by a computer into measurement data. As the motion of a stylus can more easily be modelled, the contact stylus have found themselves to be one of the few measurement technologies that can be used in a traceable way [13, 51]. The measurement principle can be seen in Figure 2.11.

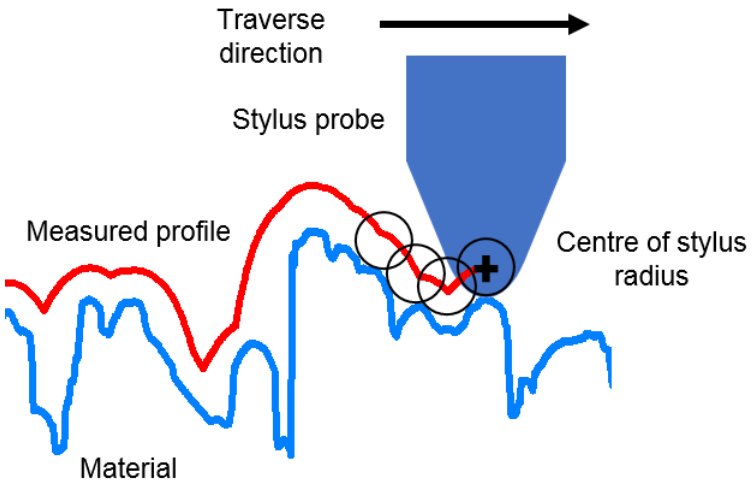

Fig. 2.11 Diagram of contact stylus measurement system. The stylus moves a spherical probe, which can be modelled as a ball, over the surface.

Contact systems traverse the surface with a spherical diamond tip probe, commercially made with radii ranging from 2 µm to 10 µm, dragging along the surface at a constant speed, recording at regular sampling intervals [51–53]. This traversing can be easily modelled as a ball rolling along the surface [51]. Due to the stylus size and geometry some aspects of the surface, such as smaller valleys and pits, may not be penetrated which will give a distorted of filtered measure of the surface texture. The lateral resolution, or the shortest wavelength where a stylus can reach the bottom of the surface is given by $\lambda = 2\pi\sqrt{ar}$ (where λ is the smallest wavelength, a is the amplitude of the surface and r is the tip radius)[51]. Because the stylus is always moving downwards from above, it can never detect any re-entrant features (features that lie underneath other parts of surface) on the surface. The effect of force can influence the measurement process and results. Too low a force can run the chances of 'stylus flight' where there is risk of no contact with the surface as it scans after peaks, meaning speed needs to be reduced to compensate [54]. Too high a measurement force causes excessive scratch damage to the surface being measured. Other measurement process considerations are stylus wear, that is, damage to the stylus tip and its effect on the measurement with a

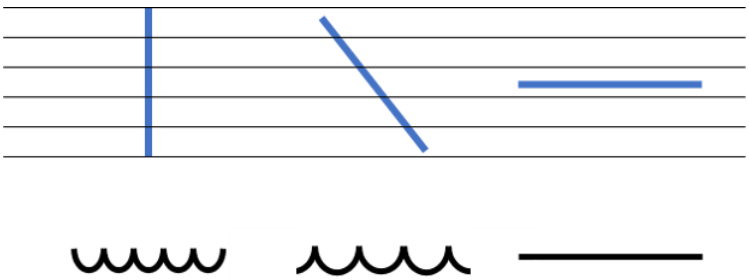

Fig. 2.12 Effect of lay on profile measurement

damaged tip no longer possessing its specified tip radius making it more difficult to accurately model as well as creating erroneous results. Areal scanning time is a limitation for most of the profile scanning technologies, including contact stylus. Whilst profile measurement can result in high resolution measurement with small sample spacing, rasterised scanning of a large area with an equivalent profile spacing to this sampling results in a large amount of points being collected and many profile measurements being taken [51]. This large amount of profiles being measured can lead to long measurement times. In order to capture the most representative profile of the surface, it is good practice to ensure that the surface profile is perpendicular to the lay of the surface [53], where the lay is the dominant direction of surface pattern (Figure 2.12).

While offering the opportunity for traceable measurement, when compared to non-contact optical measurement systems, contact stylus are slow and limited to acquiring profile data - it is possible to raster scan adjacent profiles, but this only increases the time taken to measure a surface [13, 51].

Optical measurement systems

Optical systems are non-contact in nature and whilst removing the risk of damage to the sample due to the mechanical interaction of the stylus, it makes the modelling of the electro-magnetic interaction more difficult and therefore leads to difficulties with traceability and

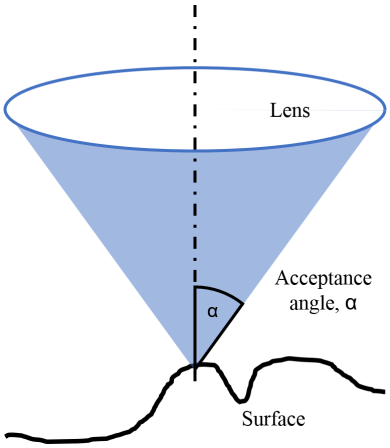

Fig. 2.13 Diagram for the numerical aperture of a microscope objective lens

comparison with contact methods [51]. Optical methods are potentially much faster than stylus instruments especially for areal scanning and capturing 3D datasets.

The magnifications of optical instruments used to measure surface topography vary from 2.5× to 150× depending on the application and type of surface being measured. Within each objective, there will be a differing value of numerical aperture (NA) which will determine the largest slope angle on the surface that can be measured and affects the optical resolution. The NA of a given objective is given by:

$$NA = n \sin \alpha \tag{2.2}$$

where n is the refractive index of the surrounding medium (for air the value is one), and α is the acceptance angle. This equation is valid for both the case of specular and non-specular reflection and is represented in Figure 2.13.

Relating to the numerical aperture of the optic, the optical resolution is the ability of the optical system to resolve two points sources and is the minimum distance between two lateral features on a surface that can be distinguished. There are many criterion that can be used to quantity this value (e.g. Sparrow, Abbe, Rayleigh) and care should be taken to ensure which method is being considered [40]. The equation for resolution is:

$$r = k\lambda / NA \tag{2.3}$$

where k is a constant depending on the method being used and λ is the wavelength of light used to make the measurement [13]. The different criteria determine the value of k and these differ based on how 'resolvable' is defined. Most commonly used in the case of incoherent light are the Rayleigh and Sparrow limits ($k = 0.61$ and $k = 0.47$ respectively) [40].

In practice, the meaningful lateral resolution is determined either by the optical resolution or the pixel spacing on the detector with respect to the optic being used (pixel sampling). Typically, a higher magnification optic will possess a larger NA, therefore having a higher optical resolution. When the pixel sampling resolution is higher than the optical resolution, the optical resolution limits the level of detail in the image and determines the (meaningful) lateral resolution. For a lower magnification lens, the inverse is the case: with the decreased pixel sampling resolution typically being much closer to the lens' decreased optical resolution. This under-sampling makes the pixel spacing resolution a more meaningful definition of resolution.

Focus variation microscopy

Focus variation (FV) microscopy makes use of an optic with a limited depth of field and vertical scanning in order to capture topographical information of the surface [13, 44]. With an optic with a limited depth of field, only small regions that are in focus are sharply imaged. For a full depth of field measurement, the optic captures images through vertical scanning from which algorithms convert this into 3D information by computing the local contrast information in a local neighbourhood region for each vertical scan position. The operational principle is explained in more detail in Section 3.1.

As a result of the measurement principles of FV, this technology is particularly useful for the measurement of rough surfaces and surfaces with high slope angles as the system can

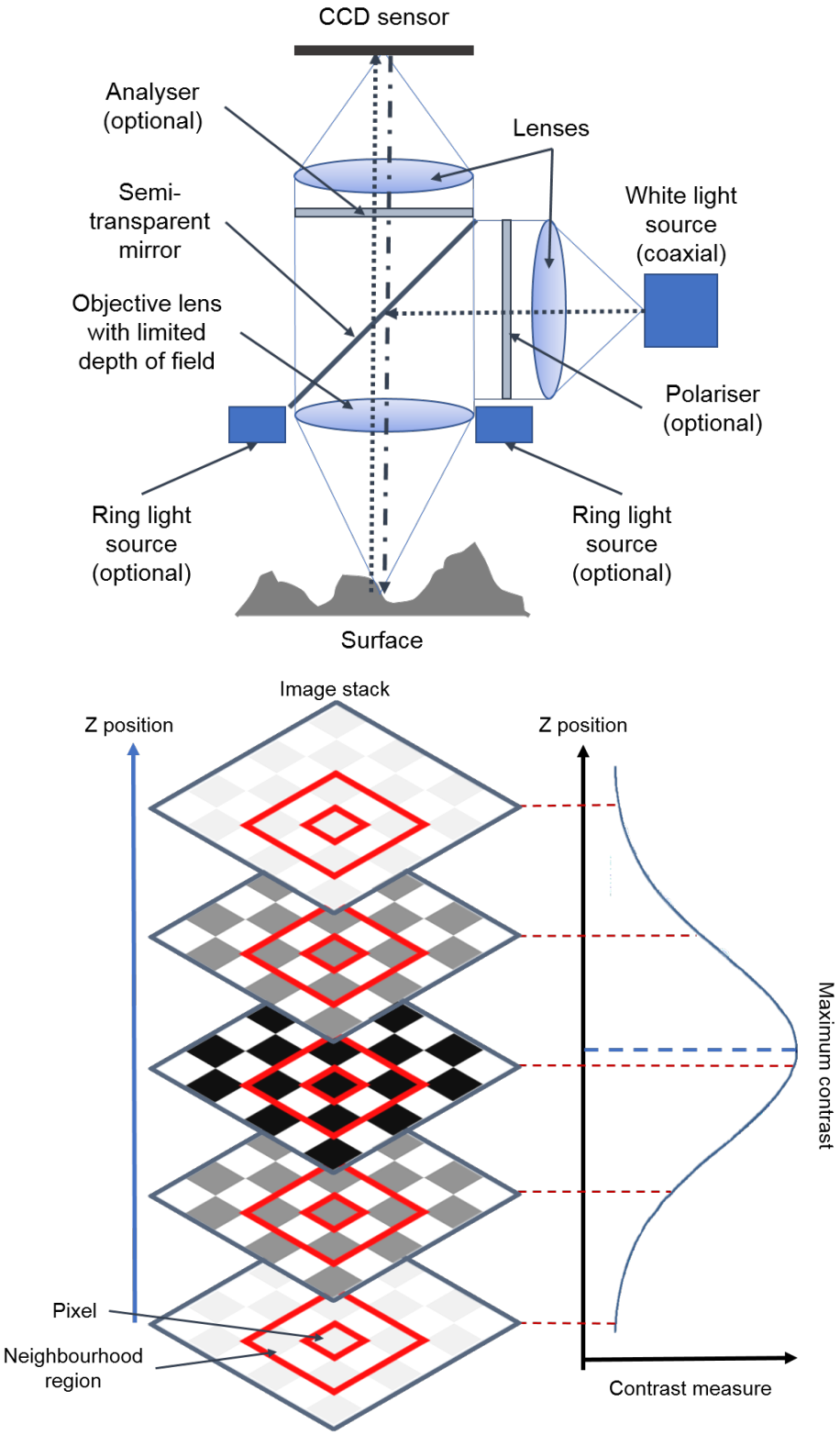

Fig. 2.14 Operation principle of focus variation

make use of both specular and diffuse reflections by adjusting light settings to overcome the limitations of the NA for the objective [55]. Ultimately, the contrast in the image is the most important aspect for measuring the surface, with the light and contrast settings available to maximise this contrast. FV systems also produce full focus colour information allowing for additional characterisation options and process understanding that may not be apparent on only height information. A main limitation of this approach is the requirement of contrast within the image, either height or colour, making the system incapable of measuring optically smooth or transparent surfaces. Whilst surfaces possessing at least a nano-scale roughness, *Ra* of 15 nm (using λc at a value of 2 μm) can be measured [56], transparent and translucent surfaces require surface replications to be made using surface transfers to measure their topography (the surface will be inverted as a result).

2.2.3 Surface topography characterisation

Surface topography refers to the overall surface structure of a part, surface form refers to the underlying shape of that part and surface texture as features that remain after the form has been removed [40, 52, 57]. After the highest spatial frequency components have been removed, the surface texture is defined. The surface texture can be either be separated out further into the components of waviness and roughness or assessed as a primary profile or surface [52]. Waviness refers to the lower spatial frequency components of the surface texture, and roughness to the higher spatial frequency components. These terms are standardised terminology within profile surface texture[52]. For areal surface texture, there is a different naming convention where the surfaces are defined by the filters applied and how they limit the scale on the surface [57]. The equivalent to the roughness profile is the S-L scale-limited surface, whilst the primary and waviness profiles are referred to as S-F surfaces (as a result it is important to correctly define filter values).

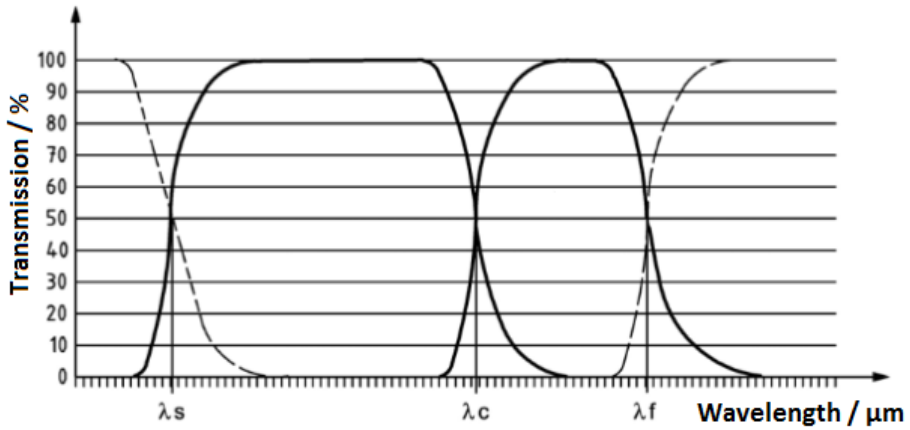

Fig. 2.15 Separation of waviness from roughness with filters. Source: ISO 4287 [52].

To extract surface texture components on which to calculate surface texture parameters, firstly the form is removed. Form removal is commonly performed by planar subtraction, polynomial fitting or filtration (known as known as the λf filter for profiles, or F-operator for surfaces) [40, 57]. Secondly, a low-pass filter (known as the λs filter for profiles or S-filter for surfaces) is applied to the surface to remove the highest spatial frequency components and finally, in order to separate out the remaining surface texture into waviness (low spatial frequency) and roughness (high spatial frequency), another filter is applied (known as the λc filter for profiles or L-filter for surfaces). Most filters are Gaussian convolution filters using 50% cut-offs, meaning that 50% of the spatial frequencies are attenuated at the value of that filter. The transmission of wavelengths over the surface and the influence of applied filters are shown in Figure 2.15.

Profile surface texture characterisation

When characterizing profiles, the following procedures are to be followed, as covered in ISO 4288 [53]. A surface profile can be defined as the profile that results from the intersection of a surface by a specified plane, that is, the plane in which the measurement is taken. Profile

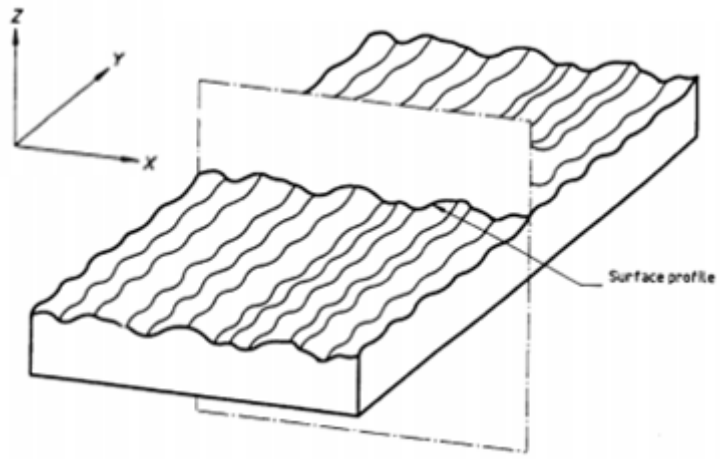

Fig. 2.16 Definition of a surface profile. Source: ISO 4287 [52]

measurements are taken along the lay of the surface, that is, the direction perpendicular to manufacturing process tool mark, see Figure 2.16.

The sampling length of the profile is generally determined by and equal to the wavelength of the filter used to separate out the roughness and waviness components. The evaluation length is the complete length of the profile to be characterised and is taken as five times the sampling length. Within ISO 4288 there are recommended default values for sampling length (and therefore filter wavelength) that relate to estimated parameter values of the surface being measured. Generally, the smoother the surface (lower the value of estimated parameter), the smaller the roughness sampling length recommended and therefore the smaller the evaluation length recommended. A surface is characterised by taking many profile measurements (sometimes up to 10) over the same surface and averaging the parameter results.

For stylus measurements, a total traverse length of seven sampling lengths is usually taken to allow for run up and slow-down of the physical stylus. Profile measurement results in a two-dimensional (2D) representation of the surface, with the height data, being a function of the one dimension of the profile, represented by $z(x)$. Terminology for profile measurement is found in ISO 4287 [52] whilst the rules and procedures are covered in ISO 4288 [53].

For the characterisation of surface texture, the most common parameter is the *Ra* parameter, which is the arithmetic mean deviation of the assessed profile, and this is used to characterise a wide range of engineering surfaces [6, 51, 52]. However, there are many more amplitude, spacing, hybrid and curve-based parameters that can characterise an assessed profile. Parameters are used in order to relate statistical properties of the heights to better understand the interactions of the surface and the functionality [40, 51].

Profile parameters

It is worth noting that the following parameters, prefixed by an $R-$, refer to those characterised only on the roughness surface. Equivalent parameters, prefixed with $P-$ and $W-$, refer to those computed on the primary (texture component - unfiltered by the λc) and waviness profiles respectively [52]. $R-$parameters are calculated for each sampling length and averaged to calculate a parameter for the evaluated profile. Common amplitude parameters used for the assessment of surface texture are explained below [52, 58].

Ra, the arithmetic mean height of the assessed profile, which is the mean of the absolute ordinate (height) values, $z(x)$, over the length, l (Figure 2.17) [52]. It is the most commonly used parameter to characterise a surface, it is expressed as:

$$Ra = \frac{1}{l}\int_0^l |z(x)|\,dx. \tag{2.4}$$

Rq, the root mean square height of the assessed profile [52]. This parameter is closely related to the arithmetic mean and is used in a similar way. It is expressed as:

$$Rq = \sqrt{\frac{1}{1}\int_0^1 |\mathrm{z}^2(\mathrm{x})|\,\mathrm{dx}}. \tag{2.5}$$

Rsk, skewness of the assessed profile. This parameter is the quotient of the mean cube value of ordinate (height) values, $z(x)$, and the cube of *Rq* within a sampling length, lr [52].

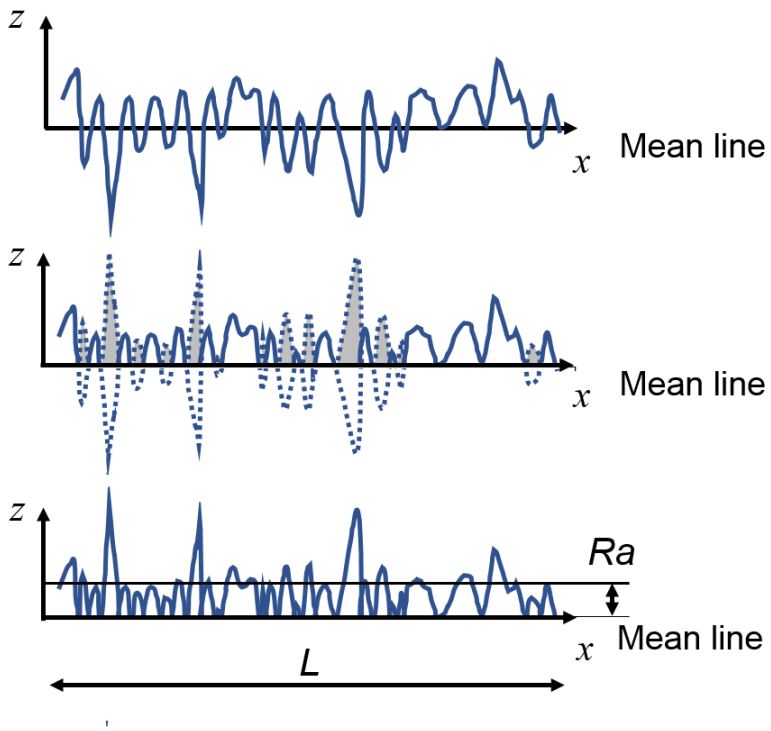

Fig. 2.17 Graphical representation of calculation of *Ra*.

This parameter can be used to describe the distribution of heights about the mean plane and is negative when the bulk of the surface is above the mean plane and positive when the bulk is below the mean plane (Figure 2.18). The equation for *Rsk* is:

$$Rsk = \frac{1}{Rq^3}\left[\frac{1}{lr}\int_0^{lr} z^3(x)\,dx\right] \tag{2.6}$$

Rku, kurtosis of the assessed profile. This parameter is the quotient of the mean quartic value of the ordinate (height) values, $z(x)$, and the fourth value of *Rq* within a sampling length, *lr* [52]. This parameter measures the sharpness or 'spikiness' of the surface distribution, and is expressed as:

$$Rku = \frac{1}{Rq^4}\left[\frac{1}{lr}\int_0^{lr} z^4(x)\,dx\right] \tag{2.7}$$

Rz, the maximum height of the profile, which is the sum of the largest profile peak height and the lowest profile valley depth within a sampling length [52]. The *Rz* is considered an

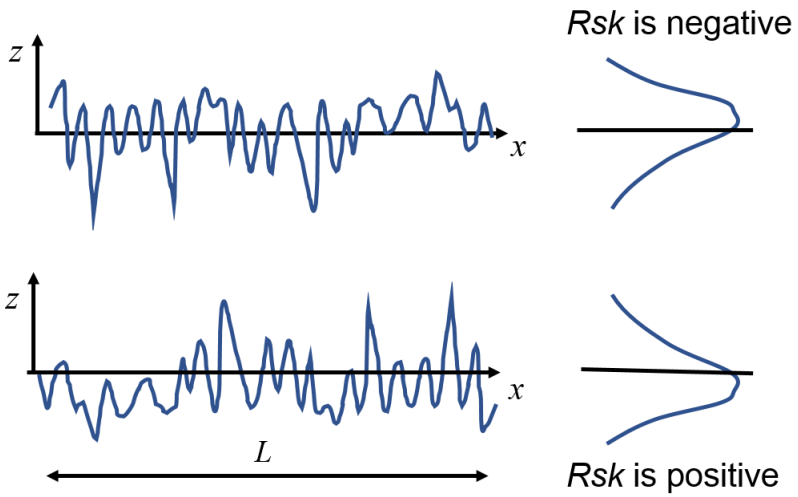

Fig. 2.18 Graphical representation of calculation of *Rsk*.

'extreme' parameter as it can be easily influenced by outliers in the data but is widely used in industry as a measure of roughness.

There are many other parameters that can be calculated on a profile, grouped within in ISO 4287 [52], including:

- Spacing parameters - These parameters are calculated on profile elements (a grouped peak and a valley region defined at the mean line of a sampling length) and characterise the dimensional aspects of these elements (i.e. width) or number.
- Hybrid parameters - Hybrid parameters are determined from both amplitude and spacing information. For example, the $R\Delta q$, is the root mean square slope of the assessed profile and is a measurement of the angular slope of the profile.
- Curves and related parameters - A material ratio curve is plotted form the heights of the profile over the evaluation length (similar to a cumulative probability density curve, where 0% is air and 100% is the bulk material). On this curve, height values on the surface can correspond to a level of material ratio and from which peak, core and valley regions can be determined and characterised.

Areal surface texture characterisation

There are known limitations of profile characterization as fundamentally a profile contains less information and is limited to a single plane of measurement (presented as a 2D representation of height along a measurement axis), making it highly dependent on surface lay [40]. It is also possible that a discrete pit on the profile is part of a larger valley in the areal surface map. As a result of its and because of these limitations, areal characterization (i.e. representing the areal nature of the measurement) is being increasingly used over profile-based characterization [59]. Areal surface measurement results in a 3D representation of the surface with the height data, being a function on the two dimensions of the plane, so that heights, $z(x,y)$ [57]. The sampling area refers to the xy plane in which a measurement is performed, typically this is size of the field of view of an optical measurement system but can also be made of stitched measurement areas or even a rasterised array of parallel profiles. The components of the surface are not defined explicitly as waviness and roughness but are defined by the filtering methods applied to them. The process flow for extracting components of the surface topography can be seen in Figure 2.19.

Areal surface texture parameters

Areal parameters are like profile parameters, but act in both dimensions of the plane. Also, instead of relating to the surface component (such as $R-$ parameters being calculated on the roughness surface), all areal surface texture parameters are referred to as either $S-$ parameters (calculated on height on the specific scale limited surface), or $V-$ parameters (volume-based parameters on the specific scale limited surface)[40, 57].The areal equivalent parameter of Ra is Sa, the arithmetic mean height of the scale limited surface, which is expressed as:

$$Sa = \frac{1}{A} \iint_A |z(x,y)| \, dx \, dy \tag{2.8}$$

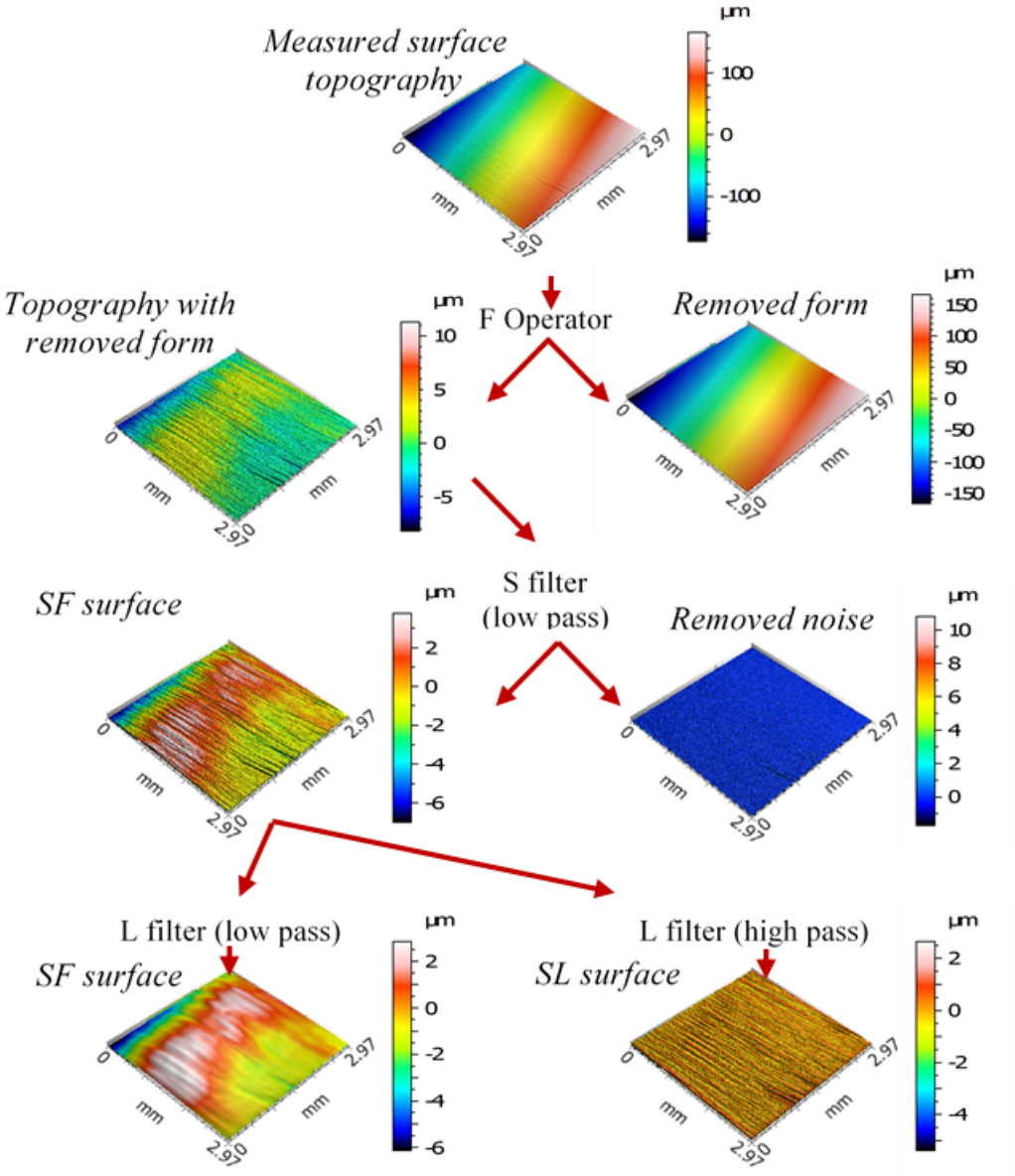

Fig. 2.19 Procedural flow from measured surface topography to scale-limited surface components

where the parameter is the arithmetical mean of the absolute of the ordinate values within a definition area, A, and $z(x,y)$ is the height of the assessed area at any position, x,y. This similarity is replicated for most of the areal parameters described in ISO 25178-2 that match the profile parameters found in ISO 4287. The parameters *Sa*, *Sq*, *Ssk*, *Sku* and *Sz* are, for example, used equivalently to their profile counterparts. The difference between profile and areal characterisation is that a single areal parameter doesn't require averaging over five regions at the size of a sampling length for each profile being evaluated. Instead, areal parameters are generally calculated over a measurement region with a length and width of five times the filter wavelength, which can be then be averaged with for repeat measurements of other parts of the surface to evaluate that surface.

Areal data allows for a whole host of other parameters that can also be calculated for specific applications [40, 57], including:

- Spatial parameters
- Functional parameters of the material ratio curve
- Functional parameters of the volumetric areal material probability curve
- Fractal dimensions and parameters

Areal feature characterisation

Areal surface data can also be characterised by the features present upon it. Within ISO 25178-2 [57], there is a standardised process for the characterization of specified features on a scale-limited surface using morphological segmentation into hills or dales (derived from the work of Maxwell) [60]. Morphological segmentation often over-segments the surface and smaller segments are pruned out to leave a suitable segmentation of the surface features [57, 60]. Pruning refers to the methods that have been defined to simplify the partitioning by aggregating individually less relevant (i.e. smaller) hills or dales to larger ones, the most

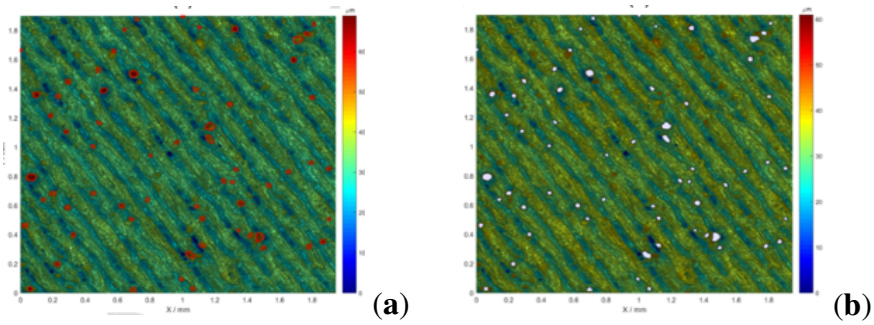

(**a**) (**b**)

Fig. 2.20 Example of EBPBF surface topography segmented using morphological segmentation on edges with features (a) highlighted in red in and (b) removed. Source: Lou et. al. [63]

common approached being Wolf and area pruning [57, 60, 61]. As a result, the topography of a surface can be decomposed into various peaks, pits, hills, dales and/or course lines and ridge lines. These topographic formations may relate to features on the surface (e.g. pores, scratches, particles, discontinuities and other singularities) and can be assessed individually characterisation of their geometric properties (area, width, height, depth, etc.) [62].

There are other methods to segment a surface topography that have since been developed, a review of the various methods of segmentation and their application is covered in Section 2.5.2. An example of a EBPBF surface that has been segmented using morphological segmentation on edges can be seen in Figure 2.20.

2.3 Overview of finishing operations applied to AM surfaces

Surface finishing is separate from any support removal or part preparation, and deals with the post-processing applied to improve or modify the AM surface to change surface texture, and to improve functionality. In this section, finishing operations applied to metal AM surfaces and their influence on functionality from the literature are assessed.

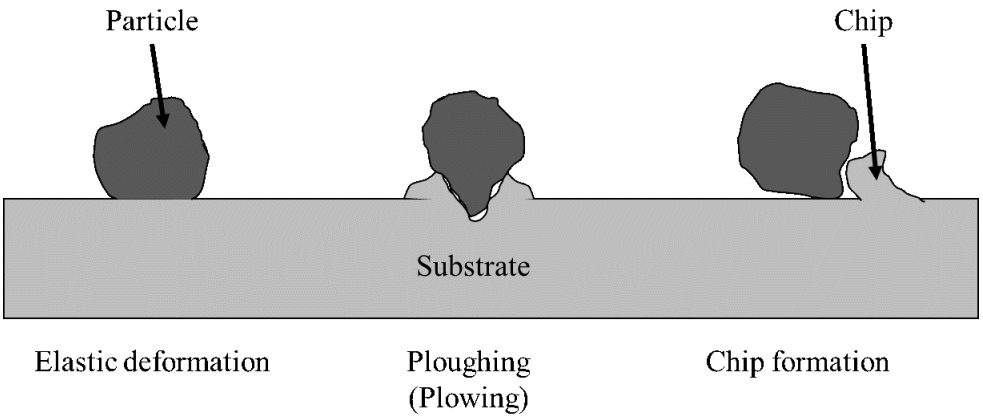

Fig. 2.21 Material removal mechanisms for abrasion

2.3.1 Methods for the finishing of AM surfaces

Conventional - Abrasive techniques

Abrasion is a mechanism of finishing that works in one of three ways, shown in Figure 2.21: elastic deformation, ploughing and chip formation [64]. These three interactions occur continuously and simultaneously to remove material. When applying these techniques, considerations are made with regards to the size, shape, and material of the abrasive particles in these processes [64]. Abrasive particles can either be loose (as grains of grit), or bonded (into a tool) which can be used to classify abrasive techniques.

Loose media includes two of the more commonly applied finishing approaches for AM parts: mass-media finishing [25] and grit blasting [9]. Mass media finishing refers to a group of processes that suspend parts within a large volume of finishing media which are agitated to abrade the surfaces. These approaches are suitable for AM parts as they can often cope with some of the more complex free-form geometries. Often applied in various stages, the resultant surface can be finished to possess a mirror finish. There is a limitation to abrasive processes known as the 'roughness limitation' in which the surface may change (due to material removal) but the roughness parameter reaches an equilibrium value [64]. Typically, the features are scratches in all directions and features of the original surface that

are smaller than what can be affected by the media. Common resultant features of a grit blasting operation can vary; rougher surfaces are often made smooth, and smooth surfaces are often made rougher. The size of features on a abraded surface is mostly likely due the size of the grit as it interacts with the surface, with a grit blasted surface possessing randomly located bumps and pits [65]. This would be the most common process applied to EBPBF parts as loose powder from the chamber is typically blasted to remove surrounding sintered cake [9].

Bonded media refers to the tools commonly found in grinding, linishing and polishing, where the media that perform the abrasive action is suspended in a matrix material to form the tool, such as one found on a grinding wheel [66]. The resultant features of these processes are directional scratches on the surface, which relate to the movement of the tool over the part as well as increased reflectivity. As the process moves into polishing by using increasingly smaller abrasives, the features are typically removed to present a defect-free surface as far as reasonably possible. Buffing is a similar process applied to achieve a mirror finish. A case study of polishing a stainless steel LPBF surface is given in [27].

Conventional - Machining techniques

Machining refers to the set of processes covering conventional turning, milling and drilling. For AM, machining can be found applied within the additive process (in-situ layer milling of edges [67]) or most typically utilised after [27, 68–71]. A lot of consideration is needed with regards to designing a part that can be both printed and subsequently machined (access to surfaces in design, limitations of tool movement). Machining is applied to achieve the required dimensional accuracy (e.g. specified form of part, correct hole size, etc.) and leaves a deterministic set of features: tool scratches and cuts on the surface. These tool markings are a result of the process variables such as tool shape, cutting angle, size, rotational speed, movement speed, etc [23].

Various publications combining traditional turning and machining of metal AM surface currently exist. An investigation of feasibility into dry and cryogenic surface of EBPBF parts is found in [68], the surface integrity is assessed for directed metal deposition parts that have been machined via milling is found in [69], the effect of machining parameters is studied to compare wrought titanium and LPBF titanium alloys in [70], a case study into using milling to improve stainless steel LPBF surface is found in [27], and an EBPBF titanium alloy was milled to determine the metallic crystal micro-structure of the sub-surface and determine wear characteristics in [71].

Non-conventional - Abrasive techniques

Abrasive flow machining (AFM) uses a slurry of abrasive, with a thick consistency, which is forced through channels to remove material. This process is useful for finishing AM freeform internal parts as the fluid acts to fill the volume of the shape of the workpiece [72]. Features of AFM are similar to that of other abraded surfaces but directed along the path of fluid flow and will depend on the properties of the abrasive used. A case study of use on an LPBF part can be found in [28].

Shape adaptive grinding (SAG) is an advanced grinding technique with a specialised tool that allows for freeform machining of hard materials, which make it suited for AM. Rigid pellets are held on an elastic tool, which follow the freeform shape of the part whilst the pellets act as smaller grinding tools to abrade the surface [29]. Features of an SAG processed surface will be very similar to those of conventional ground surfaces. A case study of use of SAG on EBPBF and LPBF titanium parts can be found in [73].

Non-conventional - Shot peening

Using plasticity rather than abrasion, shot peening uses projected shot (metal spheres) that impact the surface, each shot acting as a miniature ball peen hammer [26]. This acts to

harden the surface on impact by inducing a compressive stress on the surface presenting a variety of benefits: crack resistance, work hardening, corrosion resistance, etc [26]. The resultant surface is one dominated by plastic deformations, which appear on the surface as craters, there is an increased reflectivity and the excessive heights are flattened down. A case study of shot peening on the surfaces of LPBF samples can be found in [26]. Shot peening has been used in order to enhance fatigue properties of AM surfaces [65] as well as alter microstructure and residual stresses [26, 74].

Non-conventional - Laser-based techniques

Laser re-melting is the application of a laser in an inert environment which acts to re-melt the surface layer of a part, it can be applied in process (using the laser within the AM system) or out of process. The features found on a laser re-melted surface are newer weld tracks and ripples, and the melting of particles on the surface, however larger scale waviness on the surface is relatively unchanged [75, 76]. Due to a re-melt, there are thermal cracks that can be seen as well as an increased shininess and reflectivity with potential for iridescence. Case studies using ex-situ laser re-melting to polish the surfaces of LPBF surfaces can be found in [30, 77, 78], while a case study using in-situ laser re-melting can be found in [79].

Rather than melting the surface, laser texturing uses the laser to ablate parts of the surface to create patterns to improve characteristics associated with tribology (wear, lubrication holding, bio-integration, etc.) [75, 31]. Patterns, shapes and channels are all features that can be etched on the surface in computer designed arrays which raise challenges for conventional parameter based surface texture metrology when dealing with these large arrays of microscale structures. Laser texturing techniques may not alter the texture of the surface, but often affects the appearance by changing the reflective properties of the surface.

Non-conventional - Chemical techniques

With electro-polishing, the part is submerged in an electrolyte acting as an anode, which are subjected to an electrical current. The surface metal is dissolved with the raised heights, burrs and corners affected more so due to increased current density. The features of this process are incredibly smooth surfaces but one that which may keep waviness components of the surface. A LPBF titanium alloy surface was finished using electro polishing as part of a study of different post process techniques in [32].

Methods that simply require the submersion of the AM part in chemicals, referred simply as chemical polishing, ensures a generally even finish, with removal of the surface through dissolution controlled by the chemical mixture being used, time and temperature. Features which possess a larger surface area will be affected more by the process, with these techniques leaving a surface similar to other chemical processes such as electro polishing. Chemical etching of a metal LPBF surface was used as part of a wider study of post process techniques in [32] and on an LPBF lattice structure in [33].

Non-conventional - Ultrasonic techniques

Burnishing is the use of a rounded tool that acts to compress the surface as opposed to cutting that occurs with a traditional lathe or mill. Ultrasonic burnishing utilises ultrasonic vibrations to the burnishing tool to repeatedly impact the surface in order to improve the surface finish. This will leave rounded grooves on the surface in the way that traditional milling or turning would operate but without the features of cutting on the surface. A case study of ultrasonic burnishing on a cobalt chrome LPBF surface can be found in [34].

Cavitation abrasive finishing is the use of cavitation bubbles that collapse close to the surface in order to dislodge partially melted powders or to propel abrasive particles which can then abrade the surface. Together, these mechanisms work to remove material and alter

the surface leaving craters, flattened regions and scratches. Cavitation abrasive finishing was used on Inconel 625 LPBF sample in [20].

Ultrasonic abrasion finsishing uses an ultrasonic tool to excite a slurry of abrasive fluid, the vibrations cause the particles of the slurry to abrade the surface, it is considered more advanced as it produces less heat in the part compared to conventional grinding and the tool can be made to the shape of the surface. The features found on this surface will be similar to those found on conventionally abraded surfaces. A review of ultrasonic abrasion finishing is found in reference [35] as part of a wider review of post processing techniques used for AM .

2.4 Surface topography measurement for AM

Previously, Townsend et al. published a review paper in 2016 which reported on the literature for surface texture metrology for AM [6]. A significant amount of literature was investigated within this review, with PBF being the process under investigation in the majority of literature. Other conclusions of the review were that the general purpose of the research into the surface topography for AM parts was to build up an understanding of the manufacturing process. Other work reported investigated the relationship of surface texture of AM parts and a desired functionality. At the time of this review, test parts (artifacts) which are purpose-built samples as opposed to real, industrial parts were the most common form of part being measured, with very few case studies of parts considered. For measurement instruments used for AM, contact stylus approaches were the most common, although it is noted within the review about the loss of information from profile measurement techniques relative to areal measurement techniques.

Following on from this work, the review within these chapters deals mainly with the final inspection of parts, not in-situ or in-process monitoring. Generally, the literature covered concerns measurements performed in conventional metrology laboratory environments after the part has been removed from the respective process.

2.4.1 General considerations for AM

With new approaches to manufacturing come new challenges for measurement. The layer-based approach to manufacture allows for the fabrication of complex geometries, some of which can cause issues for conventional surface texture metrology [1, 7]. Some of these issues are general to all of AM, while others are specific to metal PBF. With the development of lattice structures and other complex internal geometries, the ability for surface texture measurement and therefore final part validation is limited, either by the line of sight access requirements of optical systems, or the contact access requirements of contact measurement systems [47]. These limitations mean that the adoption of AM in wider and more advanced applications is slowed, because of the inability to verify the conditions of such difficult-to-access surfaces. Generally, as a result of these limitations, recent research has involved the extraction of surface texture information using non-destructive volumetric measurement systems (most commonly X-ray computed tomography) and the assessment of surface quality through in-process measurement [46, 47]

Another general consideration for the surface metrology of AM is the presence of the staircase effect, which is represented by visibly offset layers of a fixed height that approximate the 3D model data [1]. Because of this effect, visuallised in Figure 2.24, local surface angle and layer thickness are often dominant influencing factors on the surface topography of side surfaces [80].

Surface texture metrology for powder bed fusion

As expressed earlier in Section 2.1.2, there are various process conditions specific to the PBF process, most notably the interaction between the energy source and the powder feedstock [12, 81]. A list of some of the more common challenges presented by PBF surfaces, visualised in Figure 2.23, are:

- large measurement ranges

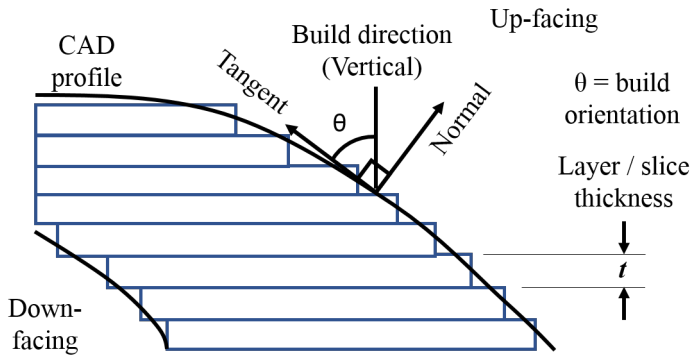

Fig. 2.22 Graphical representation of the staircase effect

- sphere-like protrusions
- surface pores (also sub-surface)
- changing reflectivity
- large scale of interest
- re-entrant features

Powder that adheres to the side surfaces and spatter particles that land on the upper facing surfaces both contribute to creating large protrusions on the surface [6, 82]. This height range is further increased by the presence of any surface pores or valley regions present [12, 83, 84]. Together, these features create issues for some measurement techniques that are limited by their vertical scanning ranges and by using a larger measurement range often means that vertical surface topography repeatability errors are often much higher than those for comparable smoother, flatter samples [85].

Optical properties, such as reflectance, vary across the materials used in PBF, as well as across single PBF surfaces. Such variations can cause issues for optical measurement techniques [13, 48]. Because of the presence of pores and deep valleys, there is often a need to use high intensity light settings in order to capture light reflected from within these regions (to obtain surface data). Simultaneously, metal PBF surfaces possess very smooth

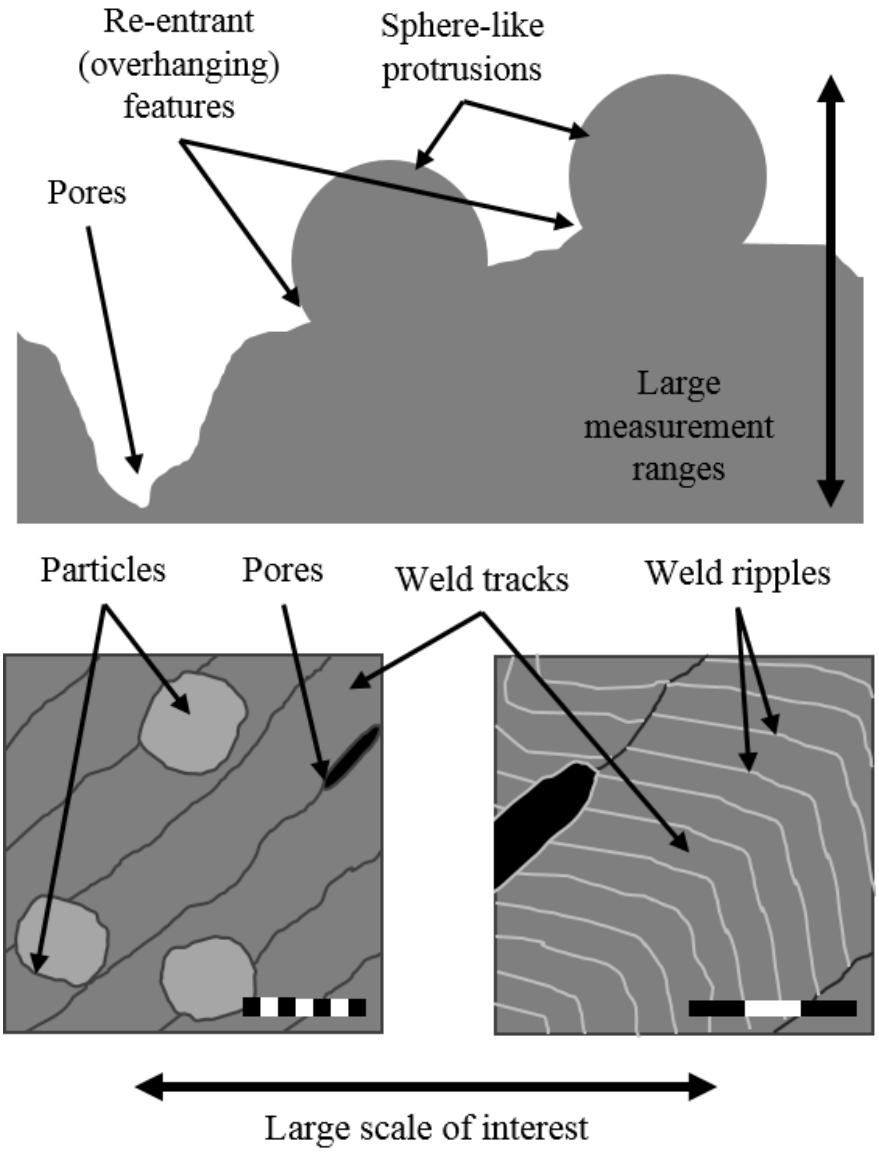

Fig. 2.23 Example features and challenges of PBF surfaces

regions that result from the melting and solidification process, which have a high reflectance and can easily produce over-saturated images in the optical instrument with high intensity illumination. Together, these factors make the determination of suitable optical measurement settings difficult [48, 86].

The surfaces typically manufactured by metal PBF are very rough, which can be seen through visual inspection and through measurement [6, 7]. Metal PBF surfaces generally possess a wide range of spatial wavelengths. These surfaces often contain large scale components hundreds of micrometres in size, such as the weld tracks or layers, in addition to spatter, un-melted powder other exogenous particles that appear as features tens of micrometres in size, and there are even higher spatial frequency components (such as weld ripples a few micrometres in size) that can be captured on the surface [48, 84].

2.4.2 Measurement techniques applied to AM

As briefly covered within Section 2.2.2, areal measurements has been increasingly used to measure surface topography - most often using optical systems. Whilst profile measurements have been critical in the assessment of conventionally machined surfaces, for AM surfaces, extracted profiles are limited in their ability to represent the surface. The dominant limitation of only being able to capture a single line along the lay proves difficult for the complex surfaces produced within PBF - dominated by weld tracks, pores and spatter or layers and sintered powders [48, 83]. Instead, both contact and optical systems have been used to capture and assess these topographies using areal measurement - with form measurement systems also being developed to capture surface topography for AM [46, 47, 87, 88].

For the measurement of PBF surfaces using conventional surface texture measurement instruments, the contact stylus has been used in [80, 89] and was noted as the most commonly used technique within the review by Townsend et al. [6]. Optical measurement instruments have increasingly been used for PBF with the application of confocal microscopy in [90]

to capture areal topography, and coherence scanning interferometry used in [82, 86, 91]. More specifically for FV, previous work has indicated this technology as providing a good compromise between quality of measurement results, versatility, ease of operation and measurement times [6, 56, 44]. These characteristics have resulted in FV being utilised in the measurement of metal additive surfaces [6, 89, 92–97]

Thompson et al. has investigated, a comparison of various measurement technologies on a metal LPBF top surface in [41, 48]. Within this work, the focus variation, coherence scanning interferometry, confocal microscopy and X-ray computed tomography were used to measure and compare the same surface - performed through registration. A form of bandwidth matching [98] was applied within this work, where bandwidths of measurement results are matched using filtering in order to offer a meaningful comparison. In summary, this work highlights the influence of various surface features on the measurement as well as, more importantly, the influence each measurement technology has on the ability to capture the same surface.

Gomez et al. investigated how the measurement configurations of the CSI influenced the measurement of various metal PBF surfaces in [86]; this work goes some way to offer a methodology in which to optimise the optical measurement systems for AM surfaces as well as to understand the interaction between the instrument and the surface. In general, further research is needed to identify optimal set-up configurations for the other measurement technologies, and the actual influence of the available measurement process parameters on the final measurement results.

2.5 Surface texture characterisation for AM

2.5.1 Parameter-based characterisation

From the review by Townsend [6] and a review of parameters used by industry by Todhunter et al. [99], it was noted that the ISO 4287 [52] profile parameters were the most commonly used, with *Ra*, the arithmetic mean height, as the most common. When areal was used, ISO 25178-2 [57] parameter *Sa*, the areal equivalent to *Ra*, was the most commonly cited parameter for assessment. Whilst the authors noted that improved understanding of the AM process can be gained by using areal datasets to visualise aspects of the AM surfaces, there was very little research on the use of feature-based parameters applied to the characterisation of AM. Across all measurements in the review, many publications did not quote experimental conditions and analytical procedures for the measurement and characterisation of surface texture. In general, the papers reviewed did not publish their measurement settings, levelling procedures, levelling operations, or filtering operations used to calculate parameters - all required to result in reproducible work.

Surface texture characterisation with relation to the AM process

Most surface texture characterisation is done to assess the influence of common PBF process parameters, highlighted in Section 2.1.2, to surface quality. Top surfaces are the most commonly investigated when changing scanning parameter settings as they directly relate to the weld tracks present on the surface. Commonly, full factorial ANOVA (analysis of variance) design of experiment analyses (sometimes reduced using the Taguchi method) are used to investigate process settings of scanning speed, laser power and hatching distance against the surface texture parameters in order to determine significant parameter choices with an aim of reducing surface texture values. The surface texture parameter, *Ra*, was investigated with respect to process settings using ANOVA for upward facing surfaces in

[16] and [100] with similar statistical assessments by use of ANOVA design of experiments used for across different materials [101], or different surface parameters [102]. Another variable that can influence surface texture is the orientation of the surface being built with respect to the build direction, and in the case of PBF, the powder bed. As a result, there have been various work on understanding the surface as a function on tilt within AM. Surface topography as a function of tilt for metal AM is mostly investigated in powder bed fusion processes, with the majority looking at LPBF [80, 82, 89, 90, 103–105] and fewer covering EBPBF [89, 91, 104]. The most common purpose of assessment of surface tilt is to build simulation models that can be used to predict final roughness parameter values using only the process parameters and the geometry from the CAD file as in [80, 103, 106–109].

Specifically concerning metal AM, artifacts are the most commonly used part to investigate surface topography change with relation to tilt. A truncheon is used in [80, 103], with upward surfaces (up-skin) being measured from 0° to 90° (in 3° increments). Blocks and coupons (simple shapes with flat surfaces individually built at angles) are also used with up-skin angles of 0° to 90° in 15° increments in [110], 0° to 90° in 30° increments in [89] and at 0°, 55° and 90° to the build direction in [91]. Downwards facing surfaces of blocks (down-skin) at 60° and 90° are found in [89], with the down-skin being the main surface investigated at 30° to 75° in 15° increments in [82]. Other artifacts include a dome with flat surfaces 0° to 90° in 30° increments in [90] and thin struts built at 0° and 45° degrees [104]. The only real part, a Pelton wheel bucket, is used as a case study to verify model prediction in [80].

The parameters that are most commonly investigated are the ISO 4287 [52] profile parameters with the most common being *Ra* [82, 90, 103, 104], typically measured perpendicularly to the layer texture direction. Other profile parameters investigated include *Rc*, *Rpc* and *RSm* [82], and *Wsa* [90]. For areal parameters (ISO 25178-2 [57]) the most common parameters investigated with relation to tilt are *Sa* and *Sq* [89, 91]. *Sdq* and *Sdr* are used in [90].

Fig. 2.24 Truncheon test part. Source: Strano et. al. [103].

Application of finishing operations for metal PBF

Metal PBF is still a relatively new technology, with an indeterminable amount of combinations of parameter combinations within the machine and material properties throughout the component that it is not easy to say a manufacturing process is entire repeatable between builds, or even between parts within the same build. These challenges presented by as-built surfaces mean that AM components will often require some finishing in order to produce a part ready to function in the required environment.

Surface texture parameters are the most common method of quantitatively comparing topographies from before and after finishing to assess surface quality.

Surface texture parameter *Ra* [52], is the most common parameter used for the evaluation of shot peening [16, 111], laser polishing [30, 79, 112], and grinding [73, 113].The areal parameter *Sa* [57], is used for the evaluation of shot peening [26] and laser polishing [77, 114].

The limitations for surface texture parameters are that they only provide a statistical assessment of the surface and often only result in a single value to represent the surface. As areal data can be visualised in 3D, there is the ability to offer qualitative assessment of surface texture. Whilst most literature regarding finished surfaces offer some qualitative assessment of the effect of a finishing operation on the surface (e.g. scanning electron microscopy images of surfaces), quantitative assessments of surface features (such as those found in [84]) are not often used.

2.5.2 Feature-based characterisation

Feature-based characterisation requires topography segmentation, i.e. partitioning of the surface into regions. Segmentation may be performed in multiple ways by means of a wide range of algorithms, but ultimately, it should lead to a partitioning that delimits the features being targeted, separating them from their surroundings. Most of the accuracy of feature-based characterisation is tied to accuracy of the segmentation step [115]. However, for complex topographies, the identification of an optimal segmentation approach is usually far from trivial. A challenge which is typically encountered is that specialised user input is often required to determine what defines the feature of interest and, in turn, what criteria should be used to identify the exact transition boundaries between a feature and its surroundings. Even when the definition of the targeted feature is sufficiently clear, the lack of a reference result of what should constitute an optimal partitioning outcome, makes it challenging to assess whether a segmentation method/algorithm performed well.

MacAuley et al. reviewed various segmentation approaches in [116]. This review covers the operational principle of a variety of segmentation approaches applied to a variety of surfaces, although none of them were AM. The work covers the following segmentation approaches: thresholding, morphological segmentation, active contours and template matching. The review also discusses the use of geometric attributes of individual segmented features and their utility in comparison to conventional areal parameter characterisation of the whole surface.

Currently, there are only a limited number of approaches being used to segment the topography of AM surfaces: thresholding [117], morphological segmentation on edges [63], and contour stability analysis [84].

Thresholding refers to the application of a binary threshold to isolate features on the surface by moving a plane to a point on the surface corresponding to a height on the surface [116], often provided by assessing a relevant value on the material ratio curve (*Spk* is used in

[117]). Thresholding requires the removal of waviness and other components on the surface that may be erroneously included as features above or below the threshold.

Morphological segmentation is included within ISO 25178-2 [57] and consists of partitioning the topography into Maxwellian hills or dales [60]. This approach over-segments the topography and requires either pruning (such as Wolf pruning [57]) or thresholding [63]. Watershed segmentation can also be applied to segment topographic edges by applying a morphological segmentation on dales on a artificial topography of absolute values of local gradient, as in [118], referred to as morphological segmentation on edges.

Contour stability, found in [84], is an edge detection method that slices planes through the topography in order produce a series of cross-sectional contours of the topography. By tracking how the contour shape and size changes, minimal changes can be defined as stable (with a threshold) and defined a contours for segmenting features of the surface. This approach privileges sharp transitions so is best applied to segment features that possess steep walls on the topography.

Although not currently applied to AM surfaces, the review by MacAuley et al. [116] identified active contours as an approach to segmentation. Active contours is a segmentation approach that requires an initial 'guess' as an input in order to iteratively refine the edges of a contour to the topography [119–121], this approach is discussed in more detail in Section 4.2.4.

Application for AM

The appeal of feature-based approaches is that they provide the opportunity to decompose a surface into its relevant constituent topographic formations (features), and thus describe the surface itself in terms of the geometric attributes of such features [84]. As opposed to texture field parameters, feature-based characterisation may provide indication as to why one

surface may be "rougher" than another, i.e. what topographic formations (features) may be contributing the most in determining the overall surface texture.

For surfaces produced using metal PBF, a typical matter of interest involves the identification and characterisation of spatter formations and un-melted particles present on the as-built topography (that is, before any finishing process). Spatter formations result from molten particles ejected during surface processing and deposited on the surface in the form of solidified aggregates [12]. Similar particle clusters (though not technically spatter), may be created by excess input energy from the melt pool, that can also act to sinter loose powder adjacent to the build geometry in LPBF [8] and for the electron beam PBF (EBPBF) process deliberately sintering a larger 'cake' region around the build geometry of the layer prior to melting the layer [9]. Forming a clear picture of location, distribution, size, shape and other geometric properties of spatter, particles and particle clusters accumulated over an as-built PBF surface, for example as a function of surface orientation during the build process, helps to achieve an enhanced understanding of the manufacturing process, and helps when assessing the surface finishing challenges [63, 84, 117, 122].

2.6 Discussion

From the literature it appears that PBF is the most common approach to produce metal parts with AM, with LPBF the most commonly used. As a result, there is definitely a research need to also consider EBPBF and to apply similar studies to this process with respect to understanding the relationship between build parameters and the surface texture. The challenges associated with this are that it is difficult to find direct correlation of build parameters with surface texture parameters, whereas feature-based characterisation may be able to offer an insight into properties of topographic structures both qualitatively and quantitatively and perhaps more significantly related to build parameters.

The physical processes of PBF are understood albeit not perfectly, however, there are an increasing number of physical models being developed in terms of the mechanisms that produce a layer, the interactions between the powder bed and the energy source and the features that are found present on final surfaces. Ultimately, the challenges lie in the suitability of surface texture characterisation approaches in relating parameters or features to these build mechanisms.

The surface condition is generally not suitable for final part application and there is often some form of post-processing in the form of finishing - however a growing research question is whether non-functional surfaces still require uniform finishing. As for the finishing operations applied to metal PBF parts, there is a wide range from batch finishing parts on all surfaces to automated approaches that can be applied adaptively to achieve surface requirements.

PBF surfaces present new challenges to the measurement of surface texture as the varying features on the surface interact with the measurement principles in a variety of ways. For example, PBF surfaces possess large measurement ranges, sphere-like protrusions, surface pores, changing reflectivity, re-entrant features and a large scale of interest; all creating unique measurement challenges for each measurement technology. These challenges only further highlight the need for good practice, which is being addressed already in some of the literature by determining optimum settings and studying the response of AM surface to measurement techniques. However, it is important that the measurement process is defined in relation to the scale of interest of relevant features on the surface which in turn relate to the AM build mechanisms and/or finishing operations that influence the surface topography.

FV appears to be suited to overcome the challenges present on the PBF surface, this technology requires investigation into optimum measurement settings specific to instrument in order to contribute to a guideline for good practice. In general, for the measurement of AM, good practice is required for all measurement technologies when being used for

the measurement of AM surfaces. Deeper understanding is required as to what features influence measurements results and their extent; with an aim to contribute to the assessment of measurement uncertainty.

For the characterisation of AM surface, parameters are the most commonly used method to assess surface texture. Profile roughness parameters are the most commonly used, with a lower adoption of areal texture parameters and limited case studies for feature-based characterisation. Due to the areal nature of the AM surface, and the presence of various features at differing scales these latter approaches require further investigation and study. Characterisation is performed

In general, for parameter-based characterisation there is still need to determine suitable values for filters to characterise PBF surfaces, due to the various sizes of features found on the surface. There is also a lack of good practice in reporting procedures for parameter-based characterisation, representing a lack of reproducibility of the literature.

Parameter-based characterisation is most commonly employed in relating the build parameters of the AM process to a resultant surface texture, with the aim to use statistical design of experiments (such as ANOVA) to build experimental models. The relationship of geometry of AM parts to the surface are also assessed experimentally with many studies investigating the relationship between build orientation and the associated surface texture. A key research question would be whether feature-based characterisation could also be used to relate dimensional properties of features to the AM process or even to application performance.

As finishing is required for most PBF surfaces produced, the surface texture is often measured before and after a process to determine the effectiveness of a particular finishing application in reducing surface roughness or achieving desired functionality or tolerance. To assess AM surface before or after finishing profile parameters are common with some examples of areal surface texture characterisation, however these are rarely measured in

matching locations and only assess a more general change in surface texture parameter between surface condition.

Feature-based characterisation can be used to offer an enhanced understanding of the manufacturing process of AM, in terms of the features present in the topography but accurate definition of these features and accurate determination of segment boundaries is essential. The research challenges of feature-based characterisation are that it remains a human-driven operation requiring specialised user input and while there are a variety of methods for segmentation, there are currently no methods to meaningfully compare the effectiveness of these approaches. A further challenge is the definition of what features are important for AM surfaces and their application, as a result, feature-based characterisation requires co-design with process specialists on a case-by-case basis in order to tailor characterisation pipelines to accurately isolate features of interest - a general definition of features for AM would support these methods.

AM is a suitable application for feature-based characterisation, as their surfaces typically consist of a wide range of features from weld ripples to particles/spatter to weld tracks. Spatter on the top surfaces of PBF parts are the most commonly investigated case study for segmentation and characterisation, however, it is the proportion of features on a surface that is typically characterised and not the dimensional components of individual features. There is a research need to investigate features over varying AM surface cases, including surfaces produced with different build parameters, surfaces built at differing orientations and perhaps for surfaces before and after a finishing operation is applied.

2.7 Summary

Through the review of the state of the art, the following key findings in relation to the aims and objectives of the Thesis can be found:

- PBF is commonly used to produce metal AM parts, producing unique measurement challenges to surface texture measurement instruments - EBPBF requires further study.
- Surfaces produced by PBF are rough and contain a large range of components over a large scale of spatial wavelengths - from small ripples to particles/spatter to weld tracks.
- FV appears as a suitable measurement technique to overcome many of the measurement challenges presented by PBF, but requires optimisation of its measurement parameters.
- Parameters are mostly used to characterise the surface, which is most often to relate to either the build process parameters or to assess effectiveness of finishing operations.
- Feature-based characterisation can offer an alternative to parameters, by characterising dimensional properties of defined and segmented surface features. But there are no methods for comparison or validation of these approaches.
- Feature-based characterisation and various segmentation approaches are already being applied to PBF surfaces to isolate particles on the surface, however, active contours segmentation is not currently used for AM test cases.
- Finishing operations are required for most PBF surfaces produced, which are assessed using parameter-based characterisation typically measured before or after over representative regions of the surface - it is uncommon for feature-based characterisation to be applied.

Chapter 3

Focus variation measurement of metal additive surfaces

The work in this chapter has been published in the journal Additive Manufacturing [123].

3.1 Introduction

As identified in Chapter 2, there is an increasing need for good practice when using measurement instruments for the measurement and subsequent characterisation of additive manufactured surfaces. FV is a relatively popular method to measure the surface topography of AM parts due to its ability to capture high slope angles while being reasonably robust to varying optical properties (e.g. reflectivity) [44, 124].

FV utilises an optic with a limited depth of field and vertical scanning in order to capture topographical information of the surface. With an optic with a limited depth of field, only small regions that are in focus are sharply imaged. For a full depth of field measurement, the optic captures images through vertical scanning from which algorithms convert this into 3D information by computing the local contrast information in a local neighbourhood region for each vertical scan position [56, 44]. The operational principle can be seen in

Figure 3.1. In recent work, a 3D linear theory for FV is discussed, which investigates the various illumination settings available to the instrument (coaxial, ring light or polarised coaxial illumination) and their effects on measurement results [55]. Other work investigates illumination in FV while at the same time varying the tilt of the surface being measured and the lateral resolution of the measurement [125]. FV has been previously used to measure titanium alloy samples made using LPBF and EBPBF [89]; however, the settings of the instrument are mentioned but not systematically investigated. FV measurement has been investigated in comparison to other measurement technologies; in [48], where the same LPBF top surface is measured with FV, confocal chromatic microscopy, coherence scanning interferometry (CSI) and X-ray computed tomography, and the results are compared. Further investigation of how individual metal AM topographic features appear as measured via different technologies can be found elsewhere [83]. Investigative work into the effect of the instrument settings on the measurement of AM surfaces has been carried out for other optical surface measurement technologies, such as CSI [86].

Within the FV system, there are a variety of settings that can be adjusted to capture surface topography. They are the magnification, illumination type, lateral resolution setting and vertical resolution setting. Magnification has an influence on the objective used and, therefore, the field of view, the NA, and optical lateral resolution. In addition, FV optics have a limited depth of focus with differing objectives also possessing changing depths of focus. For the objectives available to this instrument, higher magnification optics possess a higher optical resolution and a higher numerical aperture (NA) but a smaller field of view and depth of focus; this is inverse for lower magnifications. The illumination types available are: coaxial (light travelling along the same optical path as the detector), polarised (coaxial light with a polarizing filter to reduce saturation effects due to strong specular reflection) and ring light (ring-shaped light emitter to increase the input aperture of illumination and thus the amount of light captured at the detector even in the presence of high local slopes). Vertical

Table 3.1 Sample block material, commercial machine, and sample part size

Material	Commercial system	Build properties
Al-Si-10Mg aluminium alloy	Renishaw AM250	(20 × 20 × 20) mm cube
Inconel 718 nickel super-alloy	Renishaw AM250	(50 × 20 × 15) mm block
Ti-6Al-4V titanium alloy	Renishaw AM250	(20 × 20 × 20) mm cube
Ti-6Al-4V titanium alloy	Arcam 2XX	(70 × 20 × 15) mm block

resolution setting is a term used by the FV instrument to specify distances between images in the focal image stack, because the vertical scanning is a continuous motion, this relates to the sampling rate of images captured in the focal stack. Lateral resolution setting is a term used by the FV instrument to control the size of the region within which the contrast for each point is determined within each image of the stack.

Contributing a further understanding of FV measurement of metal additive surfaces, to identify guidelines for the optimal operation of FV instruments, this chapter explores the sensitivity of FV measurement to selected, controllable measurement process parameters. The experimentation and results illustrated in the following were obtained on a variety of materials and metal AM processes. Measurements were performed using an Alicona InfiniteFocus (IF) G5 instrument, but the findings should be broadly applicable to any conventional FV instrument [44].

3.2 Methodology

3.2.1 Samples

In this chapter, four samples produced by LPBF and EBPBF were measured (Table 3.1 and Figure 3.2). The blocks were built so that the top surface would be orthogonal to the build direction (referred to as 0° build orientation).

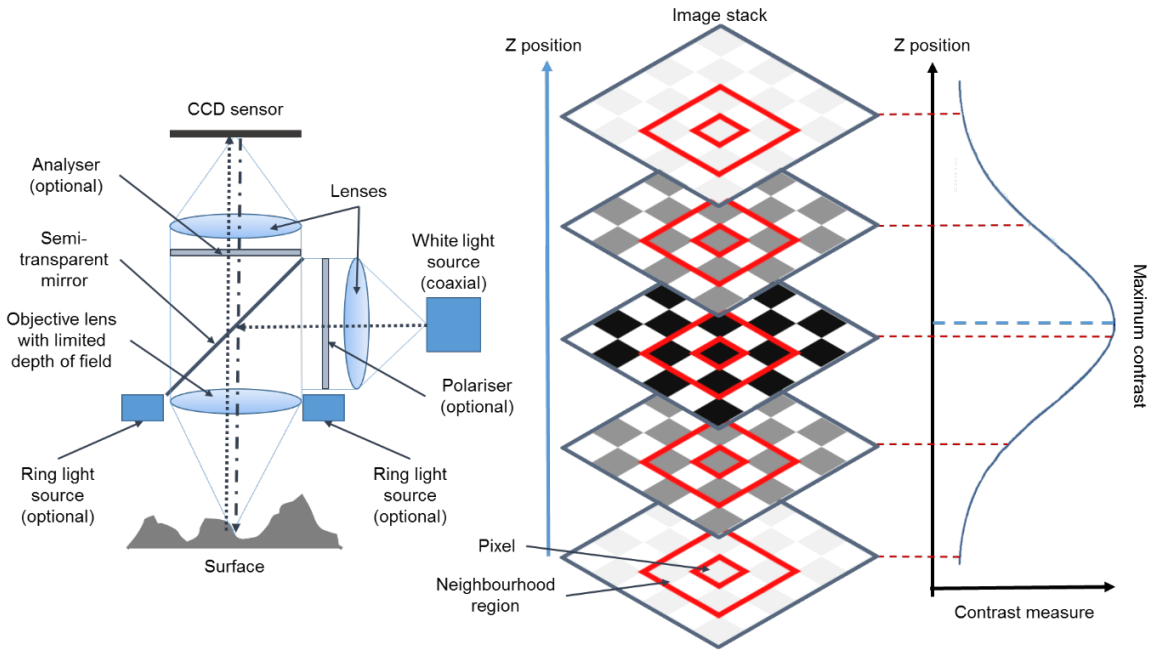

Fig. 3.1 Schematic diagram of the focus variation technology; a) elements of the optics system; b) images captured during vertical scanning, arranged as a stack. The small red square represents an example pixel where contrast is computed; the large red square represents the window of neighbouring pixels used to compute contrast c) the contrast curve associated to the example pixel, obtained by interpolation between contrast values from the image stack. The maximum of the curve (height measurement result) may not correspond to any reference height of the images in the stack.

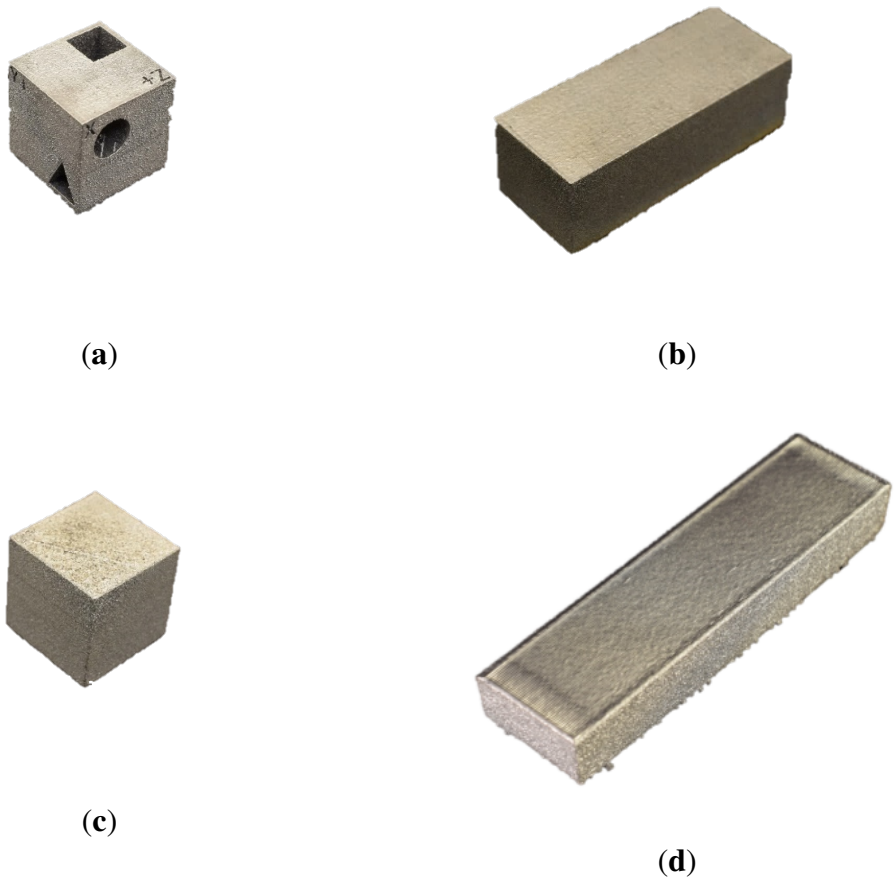

(**a**) (**b**)

(**c**) (**d**)

Fig. 3.2 Samples: (a) Al-Si-10Mg LPBF cube, (b) Inconel 718 LPBF block, (c) Ti-6Al-4V LPBF cube, and (d) Ti-6Al-4V EBPBF block.

3.2.2 Measurement process parameters

The samples were measured using an Alicona Infinite Focus G5, simply referred to as "FV instrument" henceforth. The following measurement process instrument parameters, as explained in Section 3.1, were considered:

- magnification
- illumination type
- lateral resolution
- vertical resolution

The magnifications considered were 10×, 20× and 50×, obtained by switching objective lenses (information in Table 3.2). The illumination types were: coaxial (light travelling along the same optical path as the FV probe), polarised (coaxial with a polariser [44] to reduce saturation effects due to strong specular reflection [56]) and ring light (ring-shaped light emitter to increase the input aperture of illumination and thus the amount of light captured at the detector even in the presence of high local slopes [55]). The choice of magnification directly affects the lateral and vertical resolutions that could be tested within each measurement set-up. Vertical resolution is a term used by the FV instrument to specify distances between images in the focal image stack, because the vertical scanning is a continuous motion, this relates to the sampling rate of images capture in the focal stack. Lateral resolution is a term used by the FV instrument to control the size of the region within which the contrast for each point is determined within each image of the stack.

3.2.3 Experimental plan

An experimental plan was designed to assess the influence of the selected measurement process parameters (magnification, illumination type, lateral resolution and vertical resolu-

Table 3.2 Selected FV measurement process parameters and their values. FoV is field of view and NA is numerical aperture

Magnification	10× NA 0.3 FoV (1.62×1.62) mm	20× NA 0.4 FoV (0.81×0.81) mm	50× NA 0.6 FoV (0.32×0.32) mm
Illumination type	Coaxial Polarised coaxial Ring light	Coaxial Polarised coaxial Ring light	Coaxial Polarised coaxial Ring light
Lateral resolution / µm	2, 4	1,2,3	1, 2
Vertical resolution / nm	100, 300, 900	50, 200, 500	20, 50, 200

tion) on the FV measurement results, with respect to application to metallic, AM surfaces. In Table 3.2, the measurement control parameters and their values are shown. Lateral and vertical resolution values were chosen considering the ranges automatically suggested by the instrument software once the proper magnification had been selected. More specifically, for lateral resolution, the default suggested value was taken as the largest value, and one or two (depending on magnification) smaller values (higher resolutions) were chosen, remaining within the range of acceptable values as suggested by the instrument software. For vertical resolution, the default suggestion by the instrument software was taken as the central value, together with one lower and one higher value, also within the range of acceptable values suggested by the instrument software.

From each one of the four samples described in Table 3.1 and shown in Figure 3.2, both the top surface and one of the side surfaces were selected for measurement (one region per surface), leading to a total of eight regions being measured for each instrument set-up. For each region, three measurements were performed in sequence, in repeatability conditions (i.e. same set-up and position of the probe over the region), leading to a total of twenty-four measurements per set-up. A total of sixty-three set-ups were investigated, considering the combinations of measurement control parameters illustrated in Table 3.2, leading to a grand total of 1512 measured datasets.

3.2.4 Performance indicators

Each measurement by the FV instrument produced a height map (structured grid of height values, i.e. the topography dataset), an RGB colour map (2D image of colour as given by the optical probe, mapped to the same co-ordinates as the height map, and obtained in focus-stacking mode) and a quality map (structured grid reporting an estimate of the local repeatability error associated to each height point, as computed by the FV instrument itself). The following information was extracted/computed from the datasets as quality indicators.

a) 3D topography models reconstructed from the height maps and RGB colour maps.

The height maps were converted into triangle meshes and artificially coloured based on local height information. Additional models were created using the RGB colour map as texture overlays on top of the triangle meshes. Both types of models were 3D rendered for interactive visual inspection, to acquire an initial assessment of the quality of the datasets.

b) NMP - percentage of non-measured points.

Within each height map, points for which the instrument does not acquire sufficient information were flagged by the instrument itself as non-measured. The second quality indicator, the percentage of non-measured points, was obtained as the ratio of non-measured points (as indicated by the instrument) over the total number of points of a topography dataset (in percentage).

c) Q3 - Upper quartile of the distribution of the repeatability errors associated to each measured point.

The quality map produced by the FV instrument was used to build a probability distribution of local repeatability error in height determination. The upper quartile value (Q3) of such a distribution was used as an indicator of overall quality. Q3 represents the reference value for repeatability error below which 75% of the measured points are located (Figure 3.3), so smaller Q3 values indicate better instrument performance (lower repeatability error).

d) *Sa* – arithmetical mean height of the scale-limited surface.

The ISO 25178-2 areal field texture parameter *Sa*, the arithmetical mean height of the scale-limited surface [59, 44], essentially a measure of local roughness, was considered. To compute the parameter, each dataset was processed with a form-removal operator (ISO 25178-2 F-operator) consisting of subtraction of the least-squares mean plane. No further filtering was performed (i.e. no separation of texture components at different spatial wavelengths), while this approach is not compliant with ISO 25178, it gives insight into the influence of measurement process parameters on the measured topography. Topography data processing and texture parameter computations were carried on by using MountainsMap by Digital Surf [126].

3.2.5 Data analysis

For each magnification and for each one of the eight surface regions (Table 3.1, Figure 3.2), three independent, general full factorial designs of experiments (DOEs) were generated for Q3, NMP and *Sa* respectively, to determine the sensitivity of the quality indicators to the factors: illumination type, vertical resolution and lateral resolution (levels previously illustrated in Table 3.2). In total, 24 general linear models were created.

From each full factorial DOE, regression models were fitted, and results were investigated by looking at the main effects plots and the statistical significance through ANOVA.

For every regression model, the coefficient of determination (R^2) statistics (i.e. the proportion of the variance in the dependent variable that is predictable from the independent variables) was inspected to assess the goodness of fit of the regression line between the predicted values as determined by the general linear model and the observed responses. Theoretically, if the model could explain 100% of the variance, the predicted values would always equal the observed values and all data points would fall on the fitted regression line. The model itself is 'quadratic' and considers an intercept, main effects, interactions and quadratic terms of factors so that the shape of the model can possess a curve to fit the adjusted

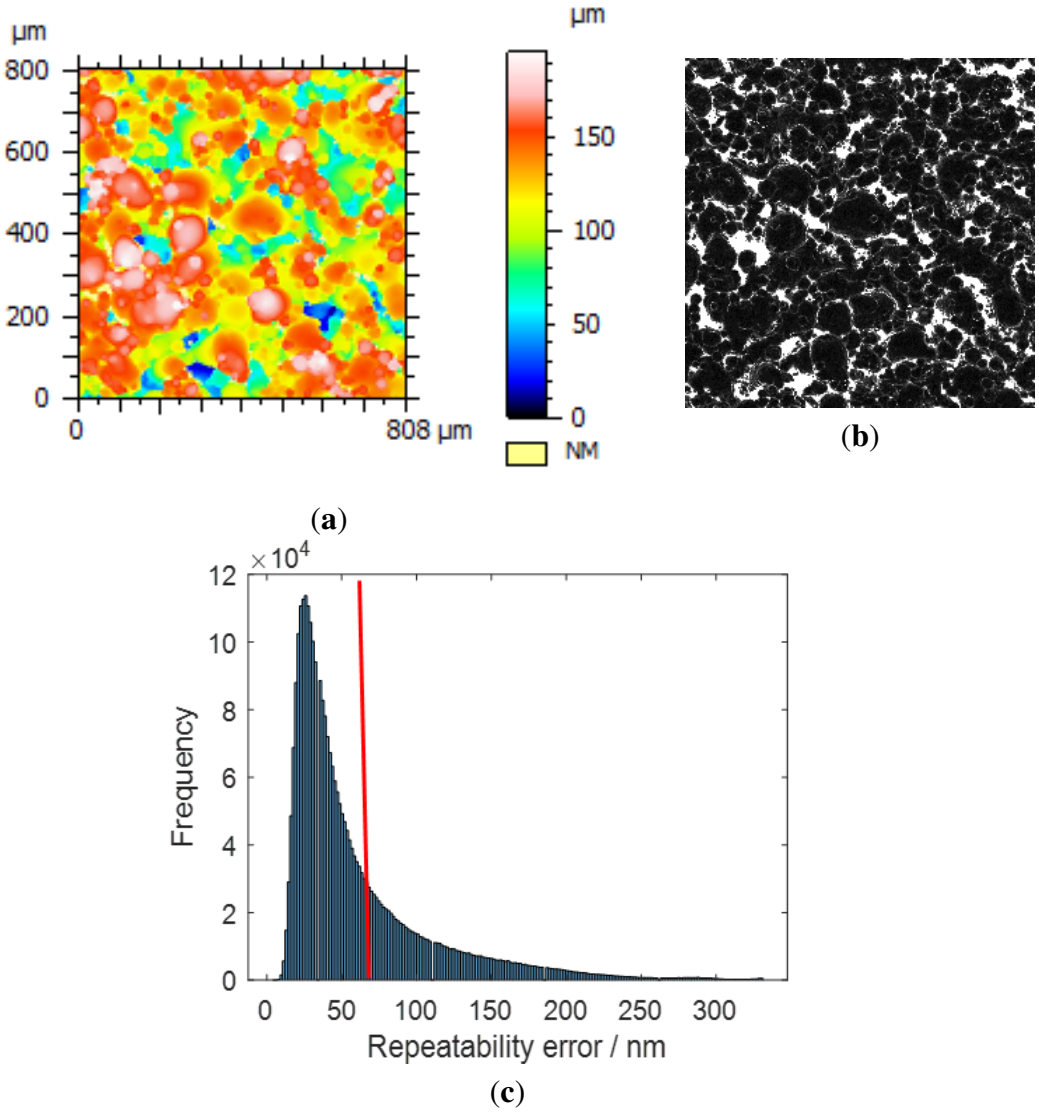

Fig. 3.3 Procedure for calculating Q3 from measurment data: (a) Example computation of Q3, the upper quartile of the repeatability error (SLM Inconel 718 side surface measured using 20× objective, coaxial light, vertical resolution at 200 nm and lateral resolution at 2 µm); a) height map; b) quality map; c) probability distribution of the local repeatability error with the position of the upper quartile indicated by the red line.

data of the model to the responses. For the analysis, only the main effects of a factor and their were significance through ANOVA were considered.

For every independent variable (factor), the p-value was reported to indicate significance of that variable in affecting the result ($p < 0.05$ indicating that changes in the factor value do indeed trigger changes in the response variable) alongside the main effects plots (which indicate changes in level means as a result of the factor). The complete results can be found in Appendix A

3.3 Results

3.3.1 Visual inspection of topography data

Top views for a selection of the specimens viewed by means of the RGB colour map overlays are shown in Figure 3.4. These maps indicate some of the measurement challenges encountered when applying the FV technology to AM surfaces featuring dark, poorly contrasted recesses and specular over-saturated plateaus. As height detection in FV is based on contrast, such surfaces offer a number of challenges. The surfaces also appear very different depending on process (LPBF or EBPBF) and whether they are top or side surfaces. The side surfaces in particular present a much larger number of attached particles, which are typically very smooth and specular. Many features also possess high aspect ratios, or high local slopes, presenting an extra challenge to measurement. The evident diversity between surface types should be noted, with topographies varying significantly depending on process, material and build orientation. This last point is a further obstacle towards the identification of a single measurement set-up which may work optimally for all surfaces.

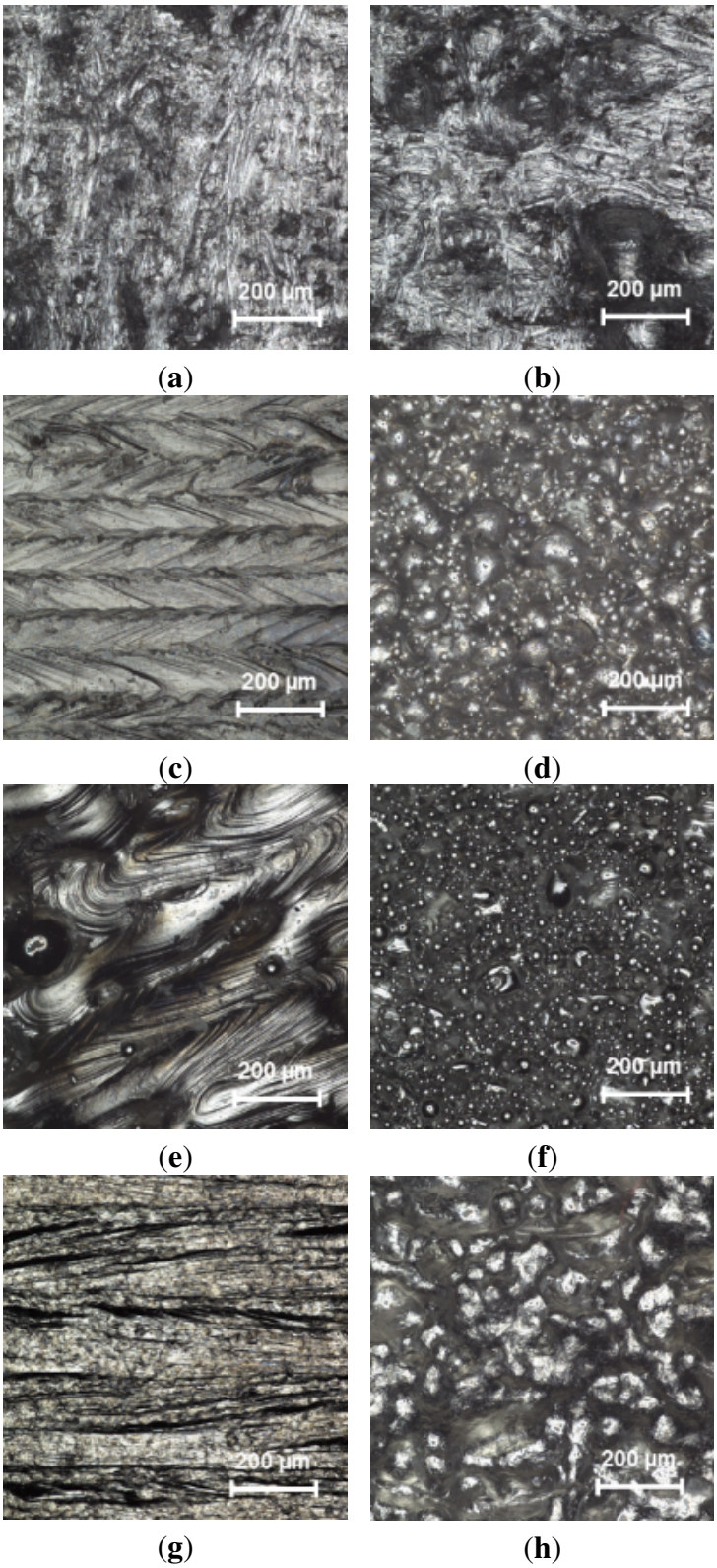

Fig. 3.4 Top views of topography models with RGB colour map overlays measured using 20× magnification, coaxial light, vertical resolution at 200 nm and lateral resolution at 2 µm; top surface (a) and side surface (b) for LPBF aluminium; top surface (c) and side surface (d) for LPBF nickel super-alloy; top surface (e) and side surface (f) for LPBF titanium alloy; top surface (g) and side surface (h) for EBPBF titanium alloy.

Effect of changing magnification

Topography models obtained using height-based colouring are shown in Figure 3.5, for an EBPBF titanium top surface as an example. The use of different objectives leads to different surface features being captured depending on observational scale. The choice of magnification is clearly dependent on investigation goals. As can be seen in the height maps in Figure 3.5, lower magnification objectives allow the capture of patterns formed by multiple weld tracks generated by the additive process (further details elsewhere [83]), as well as underlying larger-scale waviness components. At higher magnification objectives, smaller scale features, such as weld ripples, become more visible, despite there being limits to the best possible lateral resolution (smallest resolution value) due to both the optical resolution limit (related to the NA values reported in Table 3.2), and to the algorithms used by FV to resolve local height information by contrast detection [56].

Effect of changing vertical resolution

Height maps of the same surface obtained at different vertical resolution settings are shown in Figure 3.6. Changes in vertical resolution have a significant effect on measurement time (higher resolution results in slower measurement). In terms of the effects of vertical resolution on height computation, according to the principle of operation of FV, higher resolutions (smaller resolution values) lead to the generation of a higher number of images in the vertical stack produced by vertical scanning. This should lead to a higher probability of detecting a point of maximum contrast in one of the stacked images. On the contrary, lower vertical resolutions produce fewer images in the stack, leading to a higher reliance on interpolation by the maximum contrast identification algorithm. In terms of visual inspection, as shown in Figure 3.6, changes of vertical resolution do not seem to produce appreciable topographic differences.

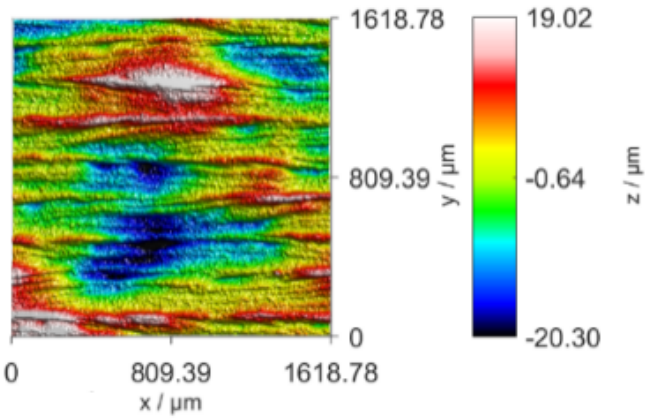

(**a**)

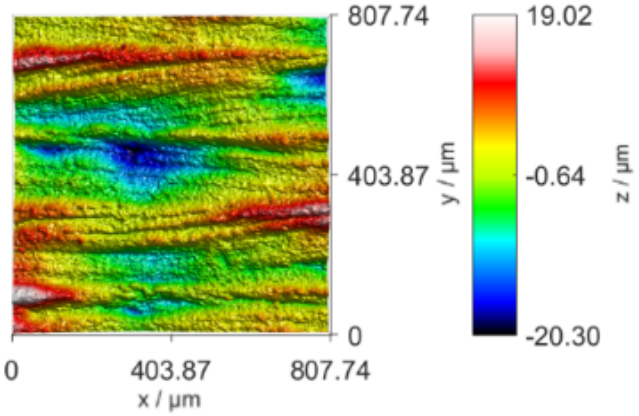

(**b**)

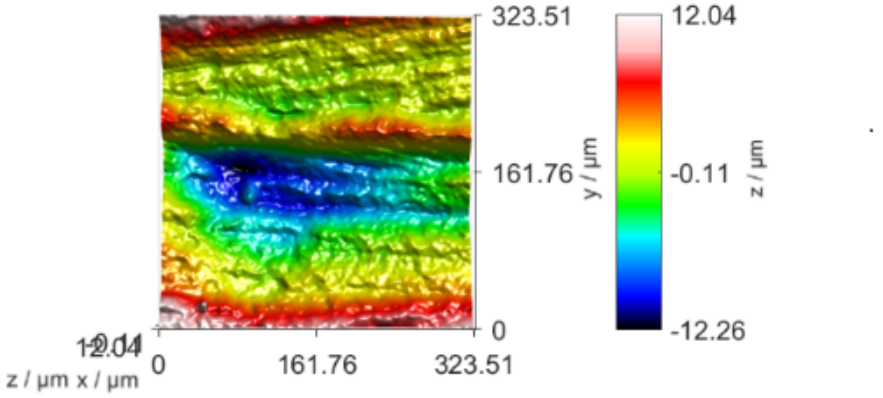

(**c**)

Fig. 3.5 Height map visualisation of an EBPBF titanium alloy top surface measured using coaxial light at (a) 10× magnification, (b) 20× magnification, and (c) 50× magnification.

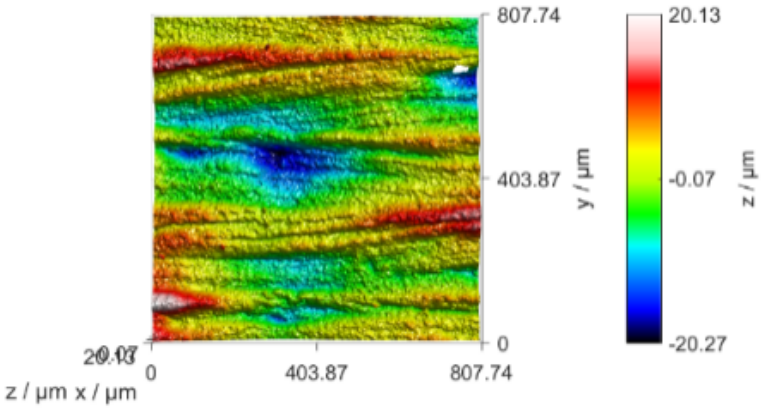

(**a**)

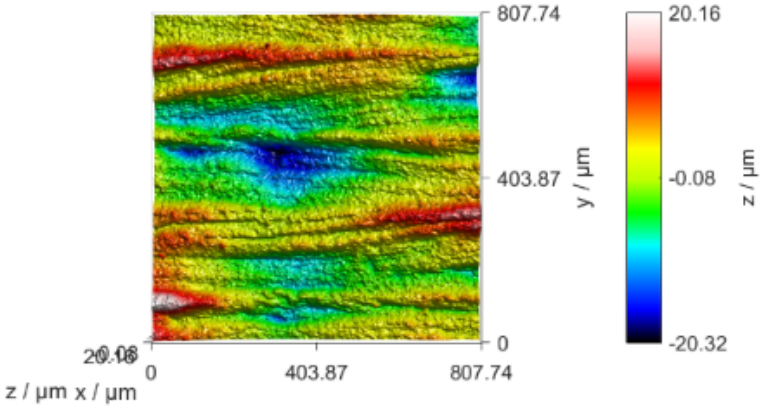

(**b**)

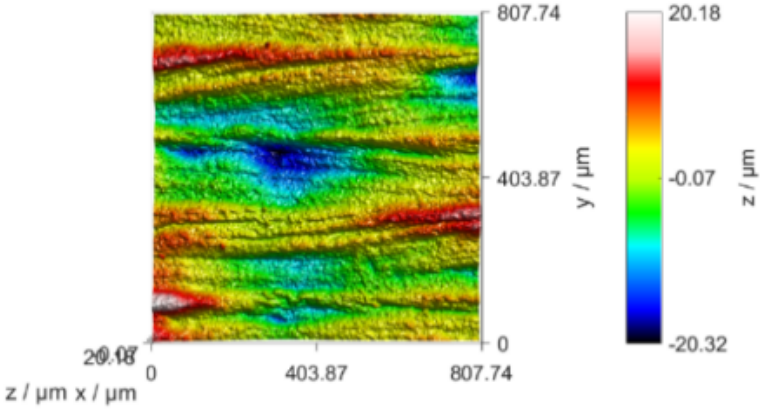

(**c**)

Fig. 3.6 Height map visualisations of an EBPBF titanium alloy top surface measured using 20× magnification, coaxial light, lateral resolution at 2 µm, and vertical resolution at (a) 50 nm, (b) 200 nm and (c) 500 nm.

Effect of changing lateral resolution

The lateral resolution setting is related to how many adjacent pixels are used to compute contrast and thus resolve local height. Changing lateral resolution (lateral scales measurable) produces a visible effect in the reconstructed height maps (see Figure 3.7), despite the size of the covered area remaining the same when magnification is not changed. Higher lateral resolution leads to an increased level of lateral detail visible in the height map which can be used to reconstruct smaller features, such as the weld ripples and adhered particles. On the contrary, lower resolutions appear to introduce a smoothing effect on topography, due to larger overlapping windows used to determine local contrast.

Effect of changing illumination type

As visible in the RGB images of the surface shown in Figure 3.8 (a-c), each illumination type results in a different appearance of the same surface. Since such appearances are what is ultimately used by the FV technology to resolve height information through contrast detection, it is useful to see how different RGB appearances correlate with differences in the respective height maps. As shown in Figure 3.8 (d-f), the height maps contain similar detail between the coaxial, polarised and ring light illuminations. However, the higher spatial frequency topography components appear more pronounced under coaxial and ring light illuminations (Figures 3.8 d & e) than with the polariser (Figure 3.8e). In Figure 3.8-c the ring light illumination setting also appears to contain extreme peaks in the measurement, which are likely due to the capture of a highly reflective features, influencing the overall range of the detected height values.

3.3.2 General full factorial design of experiments

The complete results for the general full factorial design of experiments can be found in Appendix A.

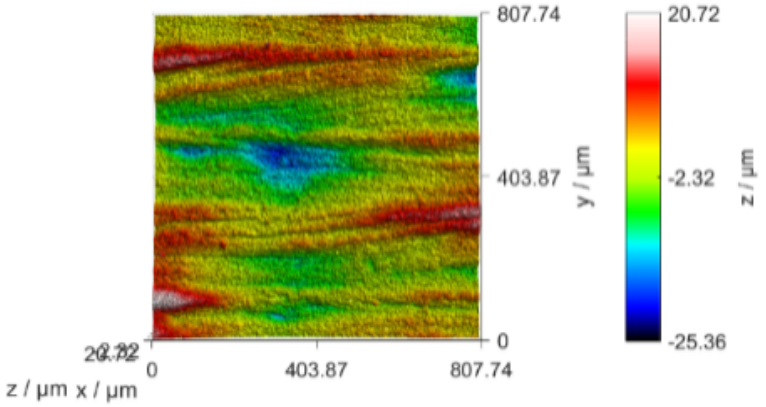

(**a**)

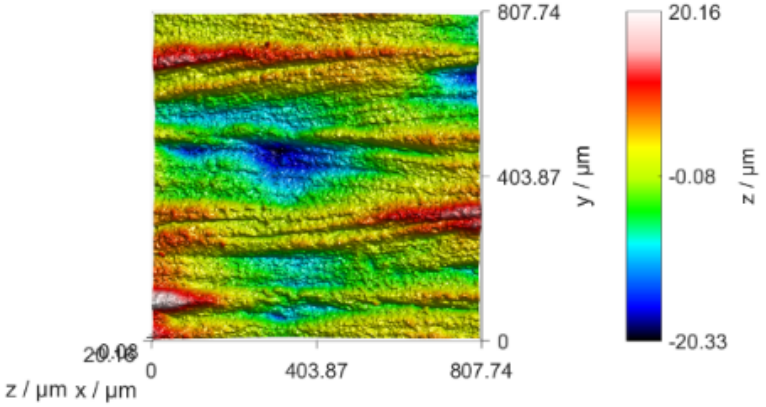

(**b**)

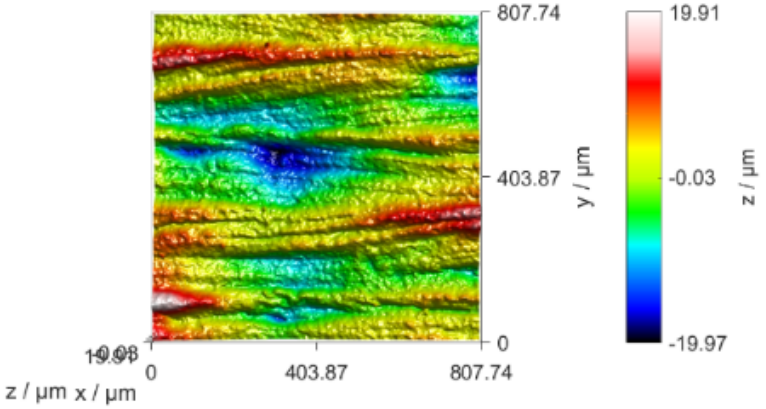

(**c**)

Fig. 3.7 Height map visualisation of EBPBF titanium alloy top surface measured using 20× magnification, coaxial light, vertical resolution at 200 nm, and lateral resolution at (a) 1 µm, (b) 2 µm and (c) 3 µm.

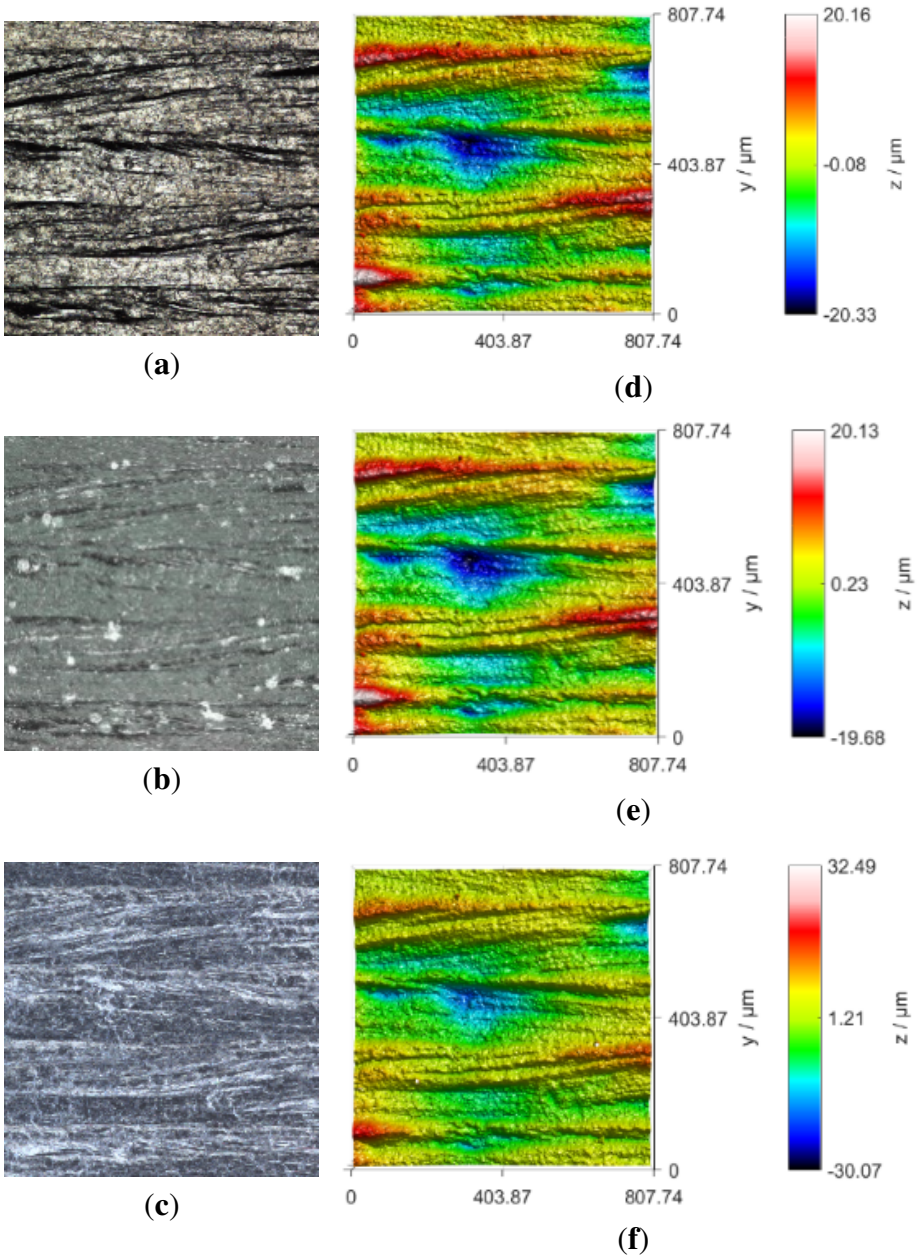

Fig. 3.8 EBPBF titanium alloy top surface measured using 20× magnification, lateral resolution at 2 µm, vertical resolution at 200 nm; focus stacked RGB images using (a) coaxial light, (b) polarised coaxial light and (c) ring light illumination. Corresponding height maps using (d) coaxial light, (e) polarised coaxial light and (f) ring light illumination.

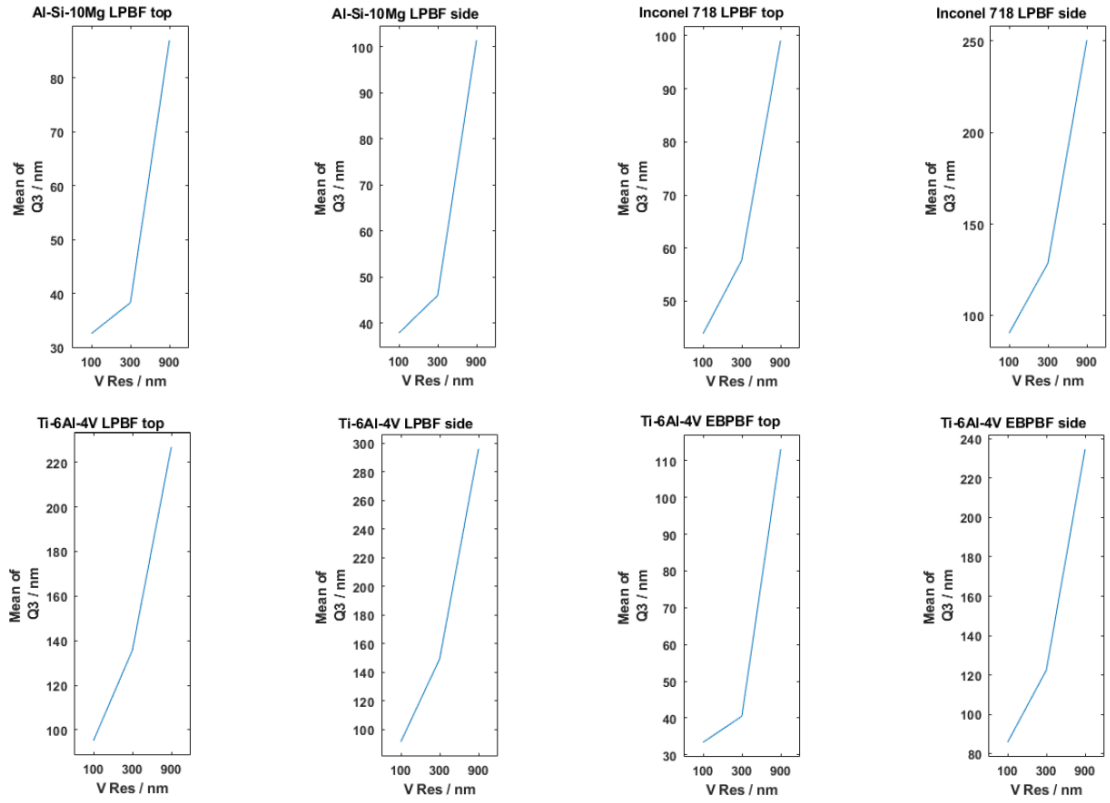

Fig. 3.9 Main effect plots for Q3 at 10× magnification.

Results for Q3

For the 10× magnification, R^2 was above 90% in all cases except for the Inconel 718 LPBF top (71.5%) and Ti-6Al-4V LPBF top (87.3%). For the 20× magnification, R^2 was above 90% in all cases except Inconel 718 LPBF top (76.3%). For the 50× magnification, R^2 was above 90% in all cases except Inconel 718 LPBF side (82.9%) and Ti-6Al-4V LPBF top (60.8%). In summary, a good fitting was obtained for the majority of cases, but not for all of them.

At 10× magnification (Figure 3.9), vertical resolution was the only significant factor ($p<0.05$). In all cases, Q3 increased with larger vertical resolution values (lower resolution).

At 20× (Figure 3.10), vertical resolution was still a significant factor (as for the 10× magnification) and Q3 still increased with lower vertical resolution values in all cases. However, lateral resolution was also found to be a significant factor, albeit Q3 varied much

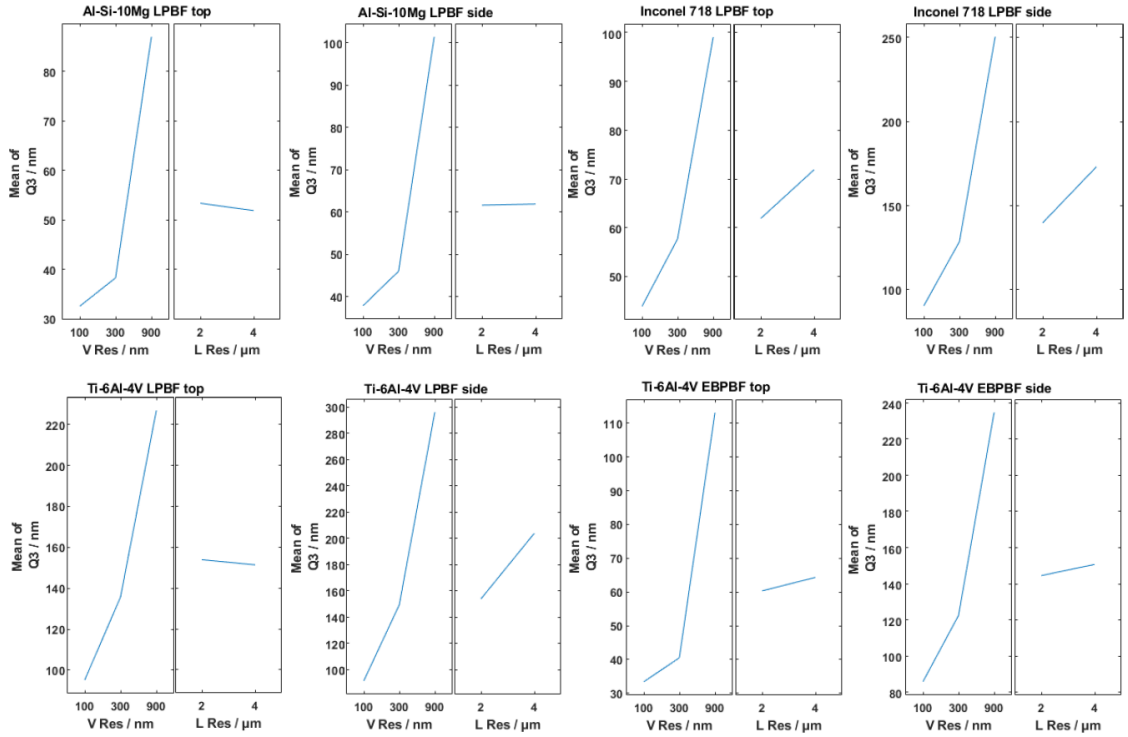

Fig. 3.10 Main effect plots for Q3 at 20× magnification.

less with lateral resolution and there was no consistent trend (in several cases it decreased, in a few cases oscillated, in a small number of cases increased).

At 50× magnification (Figure 3.11), vertical resolution was found as the only significant factor (as for the 10× magnification). Q3 increased at lower vertical resolution, in all cases.

For Q3, the full factorial models fitted well. The worse fitting performance was for Inconel 718 LPBF top, followed by Ti-6Al-4V LPBF top, and by Inconel 718 LPBF side. At all magnifications, vertical resolution was the most significant factor, and Q3 always increased at lower vertical resolution. Illumination type was never a significant factor. Lateral resolution was significant only at 20×, albeit with limited influence on Q3 when compared to vertical resolution.

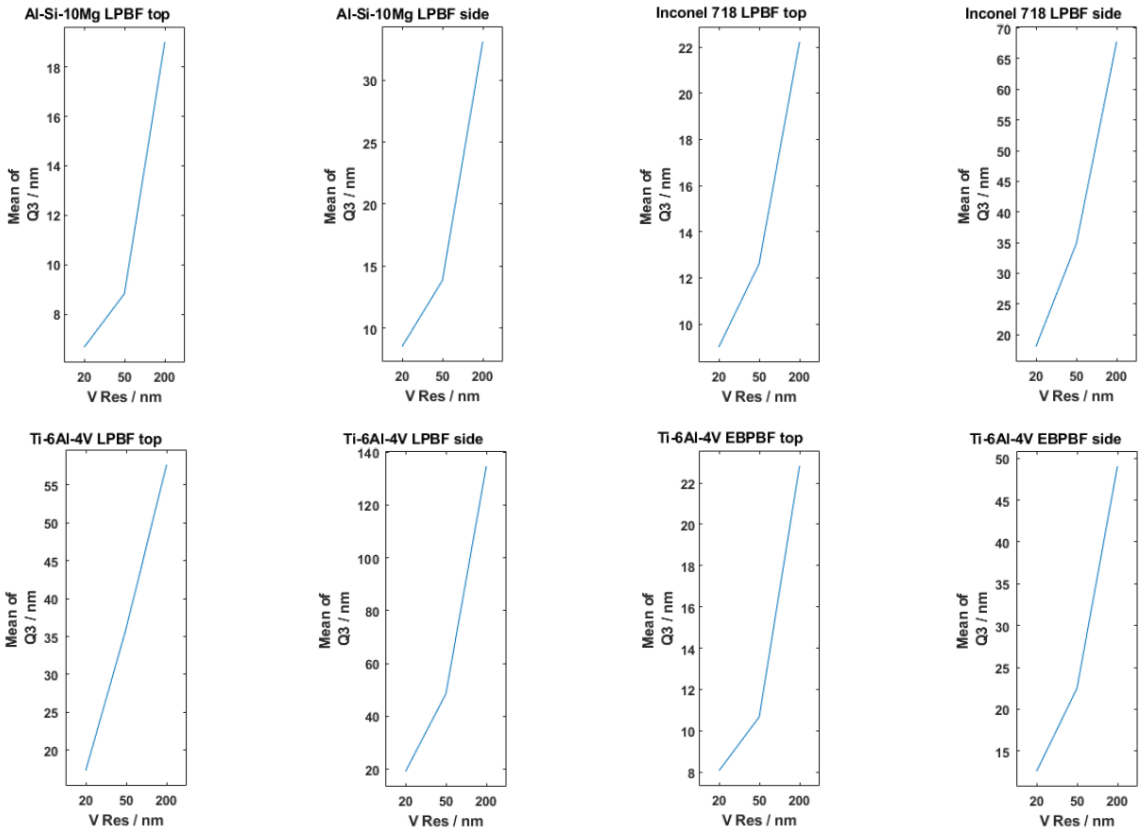

Fig. 3.11 Main effect plots for Q3 at 50× magnification.

Results for NMP

At 10× magnification, R^2 was above 80% only for Inconel 718 LPBF top, with the worst fitting for the Al-Si-10Mg LPBF side (73.1%). At 20× magnification, R^2 was above 80% only for Inconel 718 LPBF side (84.1%), with the worst fitting for Al-Si-10Mg LPBF top (55.6%). Similarly, at 50× magnification, R^2 was above 80% only for Ti-6Al-4V LPBF top (81.3%), Ti-6Al-4V LPBF side (90.6%) and Ti-6Al-4V EBPBF side (82.5%) with the worst fitting for Ti-6Al-4V EBPBF top (72.7%). In summary, the full factorial models for NMP were characterised by relatively good fitting.

At 10× magnification (Figure 3.12), illumination type and lateral resolution were found to be significant. For illumination type, except for Al-Si-10Mg which showed no consistent trend, for top surfaces, higher NMP were observed with coaxial and lower NMP with ring illumination, whilst the opposite was observed for side surfaces. Concerning lateral resolution, NMP always decreased, with lower lateral resolution.

At 20× magnification (Figure 3.13), lateral resolution was still significant (as at 10× magnification), with lower lateral resolution still leading to decreasing NMP. Illumination type was not found significant, but vertical resolution was, almost as important as lateral, with lower vertical resolutions also leading to a decrease of NMP.

At 50× magnification (Figure 3.14), the same situation was observed as at 20× magnification. Lateral resolution was found significant, and NMP decreased with lower lateral resolutions as previous. Vertical resolution was also found to be significant, and usually as the resolution became lower, NMP decreased, as with 20× magnification.

For NMP, lateral resolution was observed as a consistently relevant factor at all magnifications: reducing lateral resolution lead to decreasing NMP. Illumination type was only significant at 10×, but with inconsistent effects (i.e. varying with surface orientation and type of material). Vertical resolution was significant at 20× and 50× magnifications, with lower resolution leading to decrease in NMP as observed for lateral resolution.

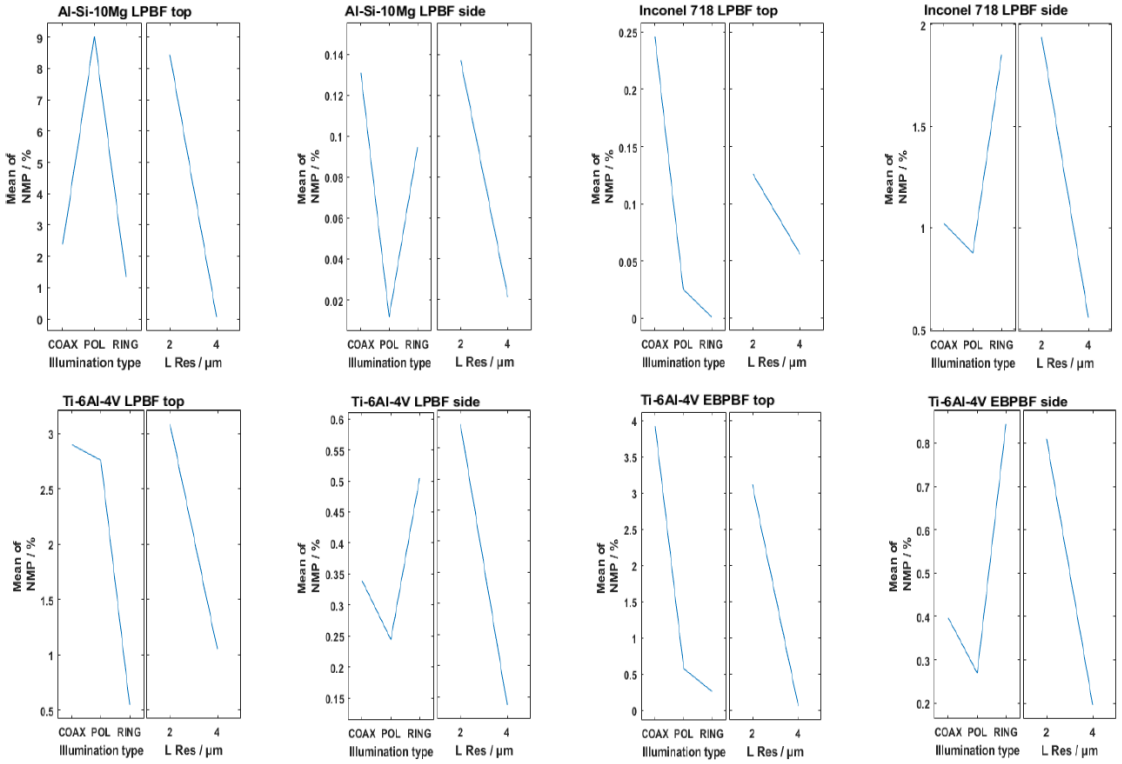

Fig. 3.12 Main effect plots for NMP at 10× magnification.

Results for surface texture parameters, *Sa*

At 10× magnification, R^2 was above 98% in all cases, with six out of eight models above 99%. At 20× magnification, R^2 was above 83% in all cases except for Al-Si-10Mg LPBF top (76.1% and for five cases R^2 was above 90%. At 50× magnification, R^2 was above 90% in all cases except for Al-Si-10Mg LPBF side (80.5%) and Ti-6Al-4V LPBF side (82.9%). In summary, the full factorial models for *Sa* were characterised by relatively good fitting.

At 10× magnification (Figure 3.15), lateral resolution was significant, with lower lateral resolution leading to a decrease of *Sa*, except for in two cases, where it led to a slight increase (although never more than 0.5 µm). Illumination type was the other significant factor, with *Sa* decreasing from coaxial to polarised to ring illumination, except for two cases. Variations of *Sa* obtained when changing settings within the limits of the DOE were confined within a micrometre in most cases.

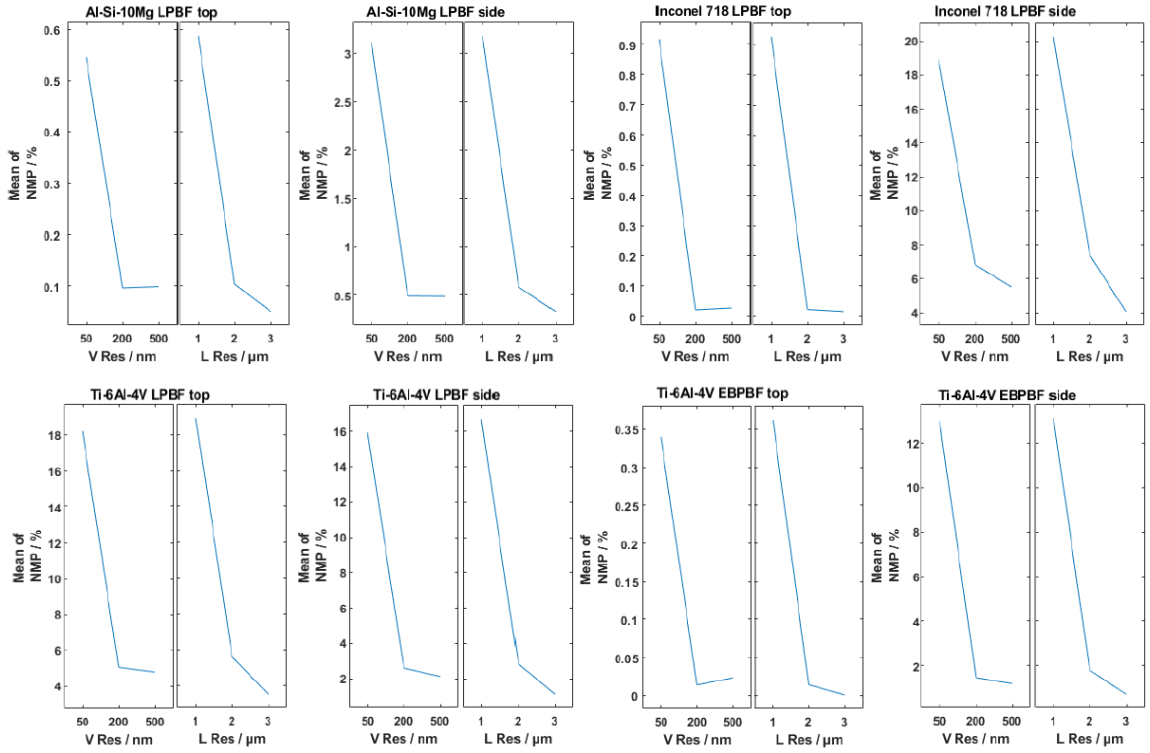

Fig. 3.13 Main effect plots for NMP at 20× magnification.

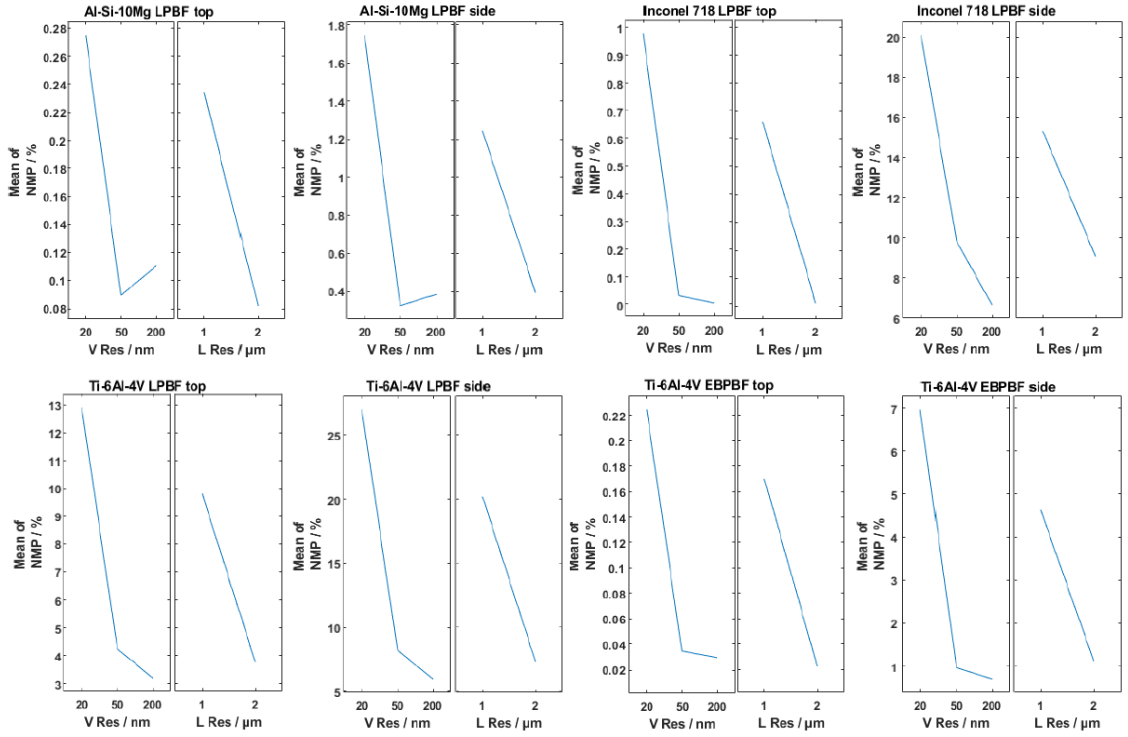

Fig. 3.14 Main effect plots for NMP at 50× magnification.

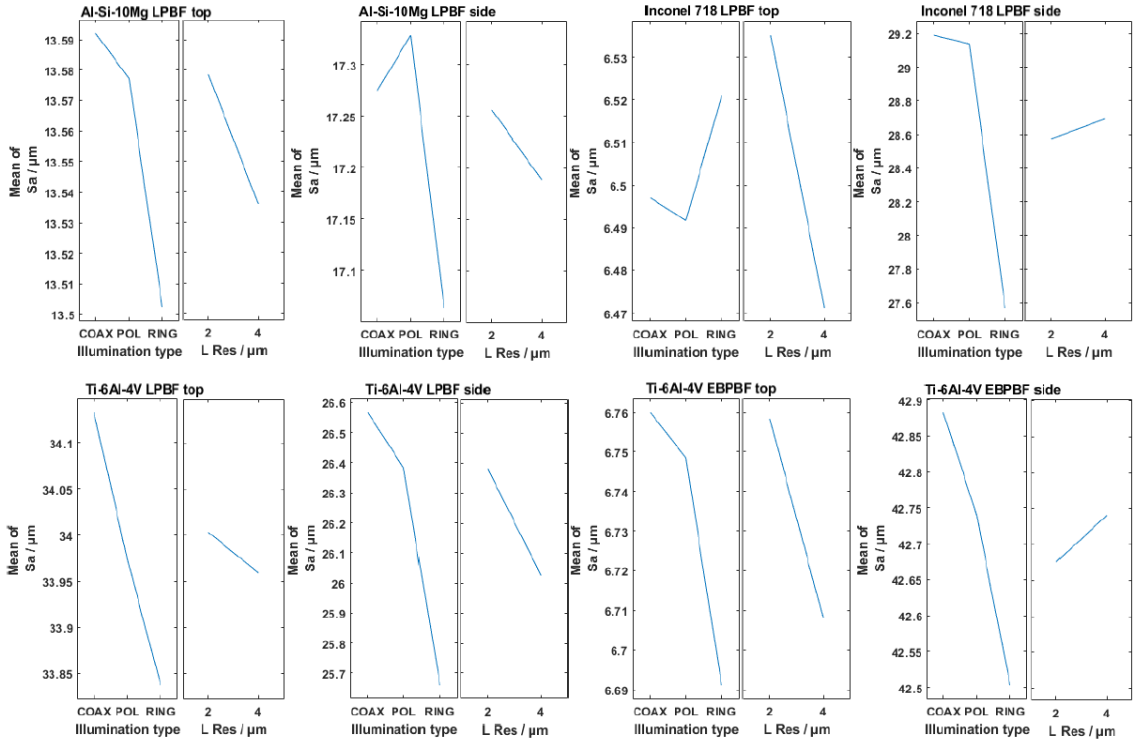

Fig. 3.15 Main effect plots for surface parameter, *Sa*, at 10× magnification.

At 20× magnification (Figure 3.16), only illumination type was significant. No clear trends were observed for illumination type, except that coaxial illumination would frequently lead to higher *Sa* values and ring light leading to lower *Sa*, in any case down to a fraction of a micrometre.

At 50× magnification (Figure 3.17), only illumination type was significant for all cases, as seen at 20× magnification. Inconsistent trends were observed with illumination type, with coaxial frequently leading to lower *Sa* values and ring light frequently leading to higher *Sa* values, nevertheless, in most cases the parameter still only varies within a micrometre of the average value for that surface.

For *Sa*, the quality of model fitting was acceptable/good in almost all cases. Lateral resolution and illumination type were found to be significant, albeit generally resulting in inconsistent trends. Lower lateral resolution often (but not always) led to slight decreases of *Sa*, whilst effects of illumination type were found dependent on the surface. For all cases,

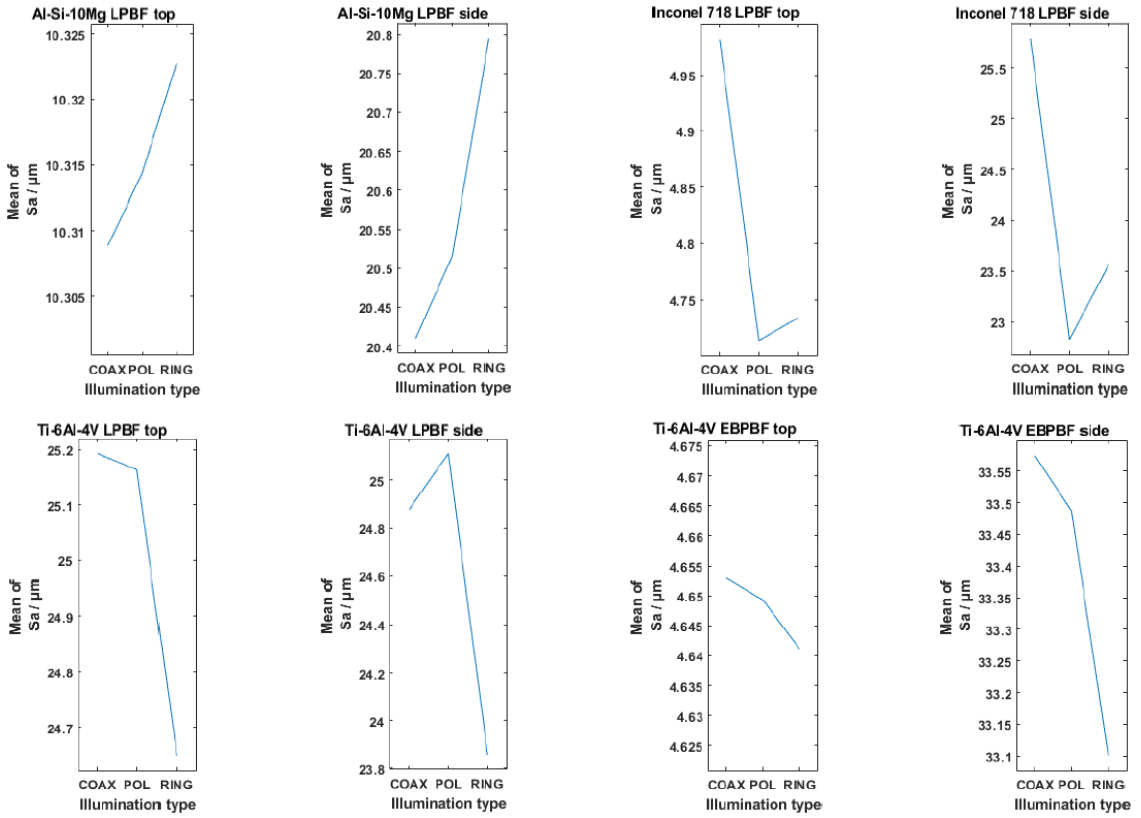

Fig. 3.16 Main effect plots for surface parameter, *Sa*, at 20× magnification.

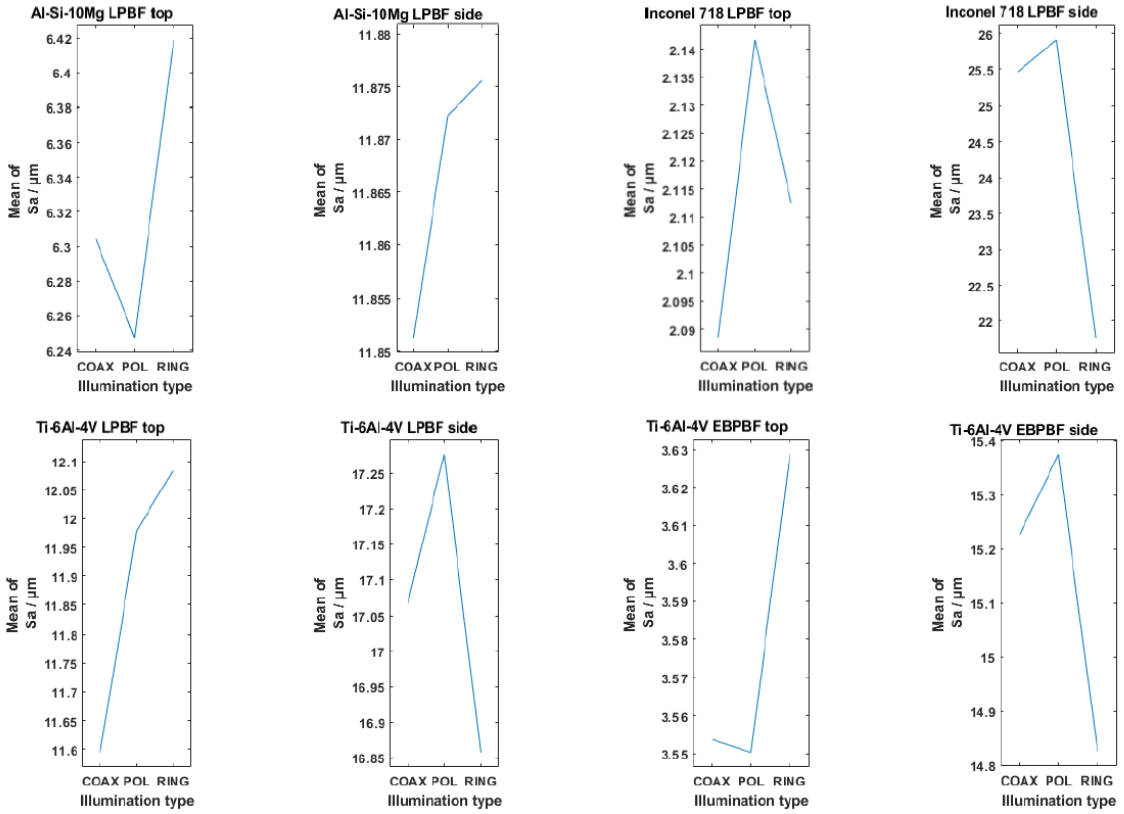

Fig. 3.17 Main effect plots for surface parameter, *Sa*, at 50× magnification.

both illumination type and lateral resolution induced variations of *Sa* that were found within a micrometre, usually one or two orders of magnitude smaller than the actual *Sa* values.

3.3.3 Summary of the results

Looking at the FV performance in computing texture parameters that summarise height properties, the FV measurement appears relatively stable with variations in the parameter value *Sa* for any surface and objective within 5% of the average value, often within a micrometre.

Concerning the actual quality of measured topography height values, measured by local repeatability error as computed by the instrument itself, then vertical resolution appears as the most significant factor. Finally, the number of non-measured points was found to associate most generally to the lateral resolution as a significant factor for all objectives, however the determination of non-measured points is not fully understood and may even be related to a thresholding operation applied to the distribution of the repeatability error (previous indicator), thus likely to be subjected to difficult to predict oscillations in correspondence of even the smaller changes (non-linear behaviour which is difficult to capture by linear regression modelling).

Regarding the measurement control parameters themselves, the following general trends can be extracted.

Vertical resolution: vertical resolution was always significant ($p < 0.05$) for Q3, with higher resolutions leading to lower Q3 values as shown in Figures 3.9, 3.10 and 3.12. Lower vertical resolutions consistently led to higher Q3 values, indicating on average a larger repeatability error. A possible interpretation of this is that if the instrument has fewer focal planes to consider, it may have fewer chances to find the maximum contrast point in the images available in the vertical stack and may need to rely more on interpolation. However, higher vertical resolutions also led to higher NMP at higher magnifications (at 20× and 50×),

as seen in Figures 3.13 and 3.14. Finally, from the ANOVA there was not enough evidence to confirm the influence of vertical resolution on *Sa*.

Lateral resolution: higher lateral resolutions generally led to higher NMP. This can be explained by assuming that lower lateral resolution imply the use of larger windows to compute contrast, and thus lower probability of contrast computation being inconclusive. There was not enough evidence from the ANOVA to confirm the influence of lateral resolution on Q3. Lower resolutions also usually led to smaller *Sa* values as it is considered that lower resolution act as a low-pass filter, i.e. introducing a smoothing effect in the reconstructed topography (as shown in Figure 3.7). In a few cases (some side surfaces at higher magnifications, as shown in Appendix A), the trend was inverted, presumably because of *Sa* being influenced by individual topography features (over the small measurement area) covering a higher percentage of the field of view.

Illumination type: the ANOVA was inconclusive regarding the effects of illumination type on Q3 and NMP, except at 10× magnification, where usually smoother surfaces (top surfaces) benefitted more from ring light illumination (lower NMP). The influence of illumination type on the *Sa* parameter was consistently observed. Usually, ring light illumination led to lower *Sa* at lower magnifications (10×, 20×), as shown in Figures 3.15 and 3.16. A not-so-consistent but inverted trend was observed at 50×, possibly because of individual features occupying a significant percentage of the field of view.

3.4 Discussion

3.4.1 General assumptions from the results

A natural question that arises after conducting an experimental study focused on a specific set of samples is can the results be generalised to different scenarios (different materials, manufacturing processes, surface geometries). Although this chapter only considered metal

additive surfaces, concentrating solely on PBF technologies, it is apparent that a wide array of surface topographies was still generated, because of the variability arising from the exploration of multiple combinations of manufacturing processes, materials and surface orientations. Within this chapter, surface topographies ranging from smooth to rough, from highly reflective to poorly reflective, from low to high aspect-ratio were covered. It is, therefore, reasonable to assume that surfaces originating from different manufacturing processes, but ultimately similar in terms of topographic complexity and possibly optical properties, may lead to similar behaviour with FV technology.

3.4.2 The meaning of measurement quality

In the majority of cases pertaining to the characterisation of surface topography in industrial scenarios, the role of surface measurement is to produce an assessment of "roughness" quantified in terms of texture parameters, such as the *Sa* parameter from the ISO 25178-2 standard, which was evaluated in this chapter. If the role of surface metrology is to compute texture parameters, then it was shown how results were relatively similar across different FV measurement set-ups (though the area size was below those recommended in the standard). This is mostly because of the averaging effects of texture parameters such as *Sa*, where local discrepancies between topographic reconstructions are easily absorbed in the computation of summary indicators that apply to the entire measured field [127]. However, when considering the accuracy of the actual individual, reconstructed topographic features, then more detailed investigations are needed. An indicator such as NMP (percentage of non-measured points), which was used in this chapter, only provides information about whether the instrument deemed the acquired raw information reliable enough to produce a point height estimate, which may not necessarily mean that the measurement is correct. Analogously, an indicator such as Q3 (upper quartile of repeatability error), which was also used in this chapter, only

indicates the instrument's own assessment of repeatability, which again does not consider the possibility of local bias, and thus lack of accuracy, in the measurement.

Previous work on the generation of statistical topography models from repeated measurements [48, 83] shows that more comprehensive assessment of measurement quality, intended as true metrological performance and thus useable to obtain an uncertainty estimate, may be possible as long as a more accurate measurement result (traceable) is available to act as reference. However, such comparison is at the moment missing for the experimental campaign carried out in this study, and the challenge of understanding how uncertainty should be computed and associated to surface topography characterisation is currently unsolved [128].

In summary, it is possible to say that values of parameters such as *Sa* are relatively consistent across measurement set-ups, but it is not possible to say whether the metrological quality of the reconstructed topographies (in particular in terms of accuracy) is better or worse in some set-ups versus others. This is because neither NMP nor Q3 are suitable indicators for accuracy, as comparison with a more accurate reference and appropriate, supporting statistical models is needed.

3.4.3 General advice on FV configuration for the measurement of metal AM surfaces

As the results have hopefully shown, there is no such thing as a 'metal additive surface'. When looking at PBF methods, if the material, orientation, or process (laser vs electron beam) is changed, different surfaces will be generated, each one with different topography and optical properties, thus presenting different challenges for FV measurement. However, a few general indications for the measurement control parameters: vertical resolution, lateral resolution, and illumination type can be provided for someone performing a measurement of a metal additive surface with a FV instrument.

Vertical resolution should be balanced to improve the repeatability error of the measurement whilst not leading to too many non-measured points. It was observed that whilst improved vertical resolutions lead to lower Q3 it also increased NMP. Top surfaces generally possess lower NMP from measurement, so it can be suggested that improved vertical resolutions may be used when measuring top surfaces. Side surfaces however typically result in higher NMPs, likely because of hard-to-measure features of the surface, such as particles. For side surfaces, the use of lower vertical resolutions may be suggested, as it would allow for a reduction in NMP. This would likely come at the cost of quality (Q3, repeatability error) and lower *Sa*,, so a trade-off may be sought, depending on application needs.

Lateral resolution should be chosen based on the smallest scale that is of interest to capture in the measurement. However, the user ought to use the lowest resolutions that can still capture the features of interest, as it was observed that lower lateral resolutions lead to lower NMP and, in case of lower magnifications, also lower *Sa*. As observed by visual inspection (Figure 3.7), lateral resolution influences the smallest scale of spatial frequencies that are captured on the surface, therefore it is important to ensure that this smoothing effect of worse resolution is kept to a minimum whilst insuring good coverage in the measurement of the surface.

Illumination type should be chosen based on the type of surface, material and orientation and the ability to adequately illuminate the surface without causing issues with contrast in the image (under- or over-exposure), which can be seen in Figure 3.8. Higher NMP were observed with coaxial and lower NMP with ring illumination for top surfaces, whilst the opposite was observed for side surfaces suggesting that coaxial light can capture aspects of the side surface better than ring light.

Ultimately, regardless of measurement setup, texture parameters such as *Sa* are not going to be affected that much by changing measurement process parameters. Observed variations for *Sa* were confined to 5% (typically within one micrometre range) of the average for that

measured. However, when considering the accuracy of the actual detail of the reconstruction of the measured topography as opposed to surface texture parameters, then the above findings should be considered with additional care.

3.5 Conclusions

From the work in this chapter, a concise list of guidelines and recommended optimum instrument settings can be listed as key findings. These findings are:

- AM surfaces vary significantly between surface orientation and material, therefore a procedure to determine suitable measurement parameters should be performed for each new test case.
- Correct objective magnification should be chosen based on the scale of interest required from the measurement, i.e. smaller features require higher magnification.
- Vertical resolution values should be minimised to improve the repeatability of the measurement, but not as much to cause large regions of non-measured points or excessive measurement time.
- Lateral resolution values should be chosen based on the smallest scale that is of interest to capture in the measurement - not too small as to increase the high frequency components on the surface and increase non-measured points or too high as to introduce an excessive smoothing effect on high frequency components on the surface that relate to features of interest.
- Any illumination choice should adequately illuminate the surface without causing issues with contrast in the image (under- or over-exposure)
- Illumination choice is dependent on the surface, material and orientation.

- Top surfaces benefit from ring light illumination which contributes to reduced non-measured points and repeatability error.
- Side surfaces benefit from coaxial illumination to reduce non-measured points, but at a cost of increasing repeatability error. Ring light illumination acts in the opposite way, increasing non-measured points but reducing repeatability error.

This chapter explored FV measurement of metal additive surfaces. The sensitivity of FV measurement to control parameters which are commonly set during the measurement, specifically magnification, vertical resolution, lateral resolution and illumination type, was studied as FV measurement was applied to surfaces of additive parts fabricated with aluminium alloy Al-Si-10Mg; nickel super alloy Inconel 718; and titanium alloy Ti-6Al-4V, produced by LPBF or EBPBF, and oriented horizontally or vertically with respect to the build direction.

The results indicate that there is a wide array of surface topographies and optical properties represented by metal additive surfaces. Despite the variability, some general conclusions can be drawn by building regression models on full factorial design of experiments. In particular, the computation of surface texture parameters such as *Sa* (ISO 25178-2 [57]) are mostly unaffected by the various set-ups explored. However, other indicators such as local repeatability error in height determination and the percentage of non-measured points are significantly affected by the control parameters, albeit the magnitude of such effects, and the generated trends, may vary with surface type. The contribution of this chapter is a method for sensitivity analysis based on regression modelling, useful for exploring the behaviour of any measurement instrument when applied to a wide range of measured surfaces. Finally, this chapter once more highlights the underlying, currently unsolved challenge of understanding how uncertainty should be computed and associated to surface topography data.

Although this chapter provides useful guidelines for AM users to improve the quality of their FV measurement results, a more thorough investigation is needed to understand specifically what topographic properties (local slope, aspect ratio, optical properties, etc.)

affect FV behaviour and performance and to what extent. This is likely to imply a more extensive experimentation based on artificial surfaces and systematic testing of combinations. Another challenge is to properly unravel the internal mechanism of the specific FV instrument which may prove hard because of understandable needs for IP protection, but is nevertheless necessary for a fuller understanding of how the measurement control parameters affect actual performance. Finally, a proper assessment of FV measurement performance should include a connection to a more accurate reference which allows the investigation of trueness and traceability.

Using the findings from this chapter will allow for a useful recommendations regarding measurement settings when using the FV instrument to capture metal AM surfaces.

Chapter 4

Comparison and validation of surface topography segmentation methods

The work in this chapter has been submitted to the journal, Surface Topography: Metrology and Properties [129] and has been presented at the euspen/ASPE special interest group conference in Nantes [130].

4.1 Introduction

Once the surface has been measured using optimised parameters, such as following guidelines as suggested in Chapter 3, with good coverage and reduced repeatability errors, then the surface can be characterised. Compared to the conventional parameter based characterisation pipeline, features-based characterisation can provide additional information on the surface topography as well as offer dimensional measurement of features on the surface, however, these approaches also need to be investigated to ensure optimised parameters are being used.

In a feature-based characterisation scenario involving metal PBF surfaces, where the target is the isolation and characterisation of spatter and particles on as-built surfaces, the choice of an appropriate segmentation method is paramount. As surface topography data is

commonly available as height maps, i.e. matrices of height values (scalars) distributed along the rows and columns of a regular grid [115], potentially applicable segmentation methods are commonly found in the domain of image processing (a height map is mathematically equivalent to a grayscale, digital image [115]). In this chapter, three methods of feature-based segmentation were investigated: morphological segmentation on edges [57, 63] and active contours [116], both derived from the domain of image processing and recently adapted to operate on topography data, and contour stability analysis [84, 122], an original method developed directly for areal topography data. Implementations of the three methods were applied to a selected set of surfaces belonging to the test case, and their performance was quantitatively compared.

4.2 Methodology

4.2.1 Sample surfaces

To perform the comparison, three PBF surfaces obtained at differing build orientations LPBF top (0°) surface, EBPBF angled (30°) surface and EBPBF side (90°) surface) were measured using FV microscopy [56, 44] optimised for measurement following the work in Chapter 3, and subjected to the segmentation approaches which were optimised to isolate particles and spatter on the surface. The three surfaces were chosen as representative of a large range of scenarios, with the LPBF top surface typically featuring the least number of features, the EBPBF side surface featuring the most, and the angled EBPBF surface featuring an intermediate number of spatter and particles. Example measured topographies from the three samples are shown in Figure 4.1.

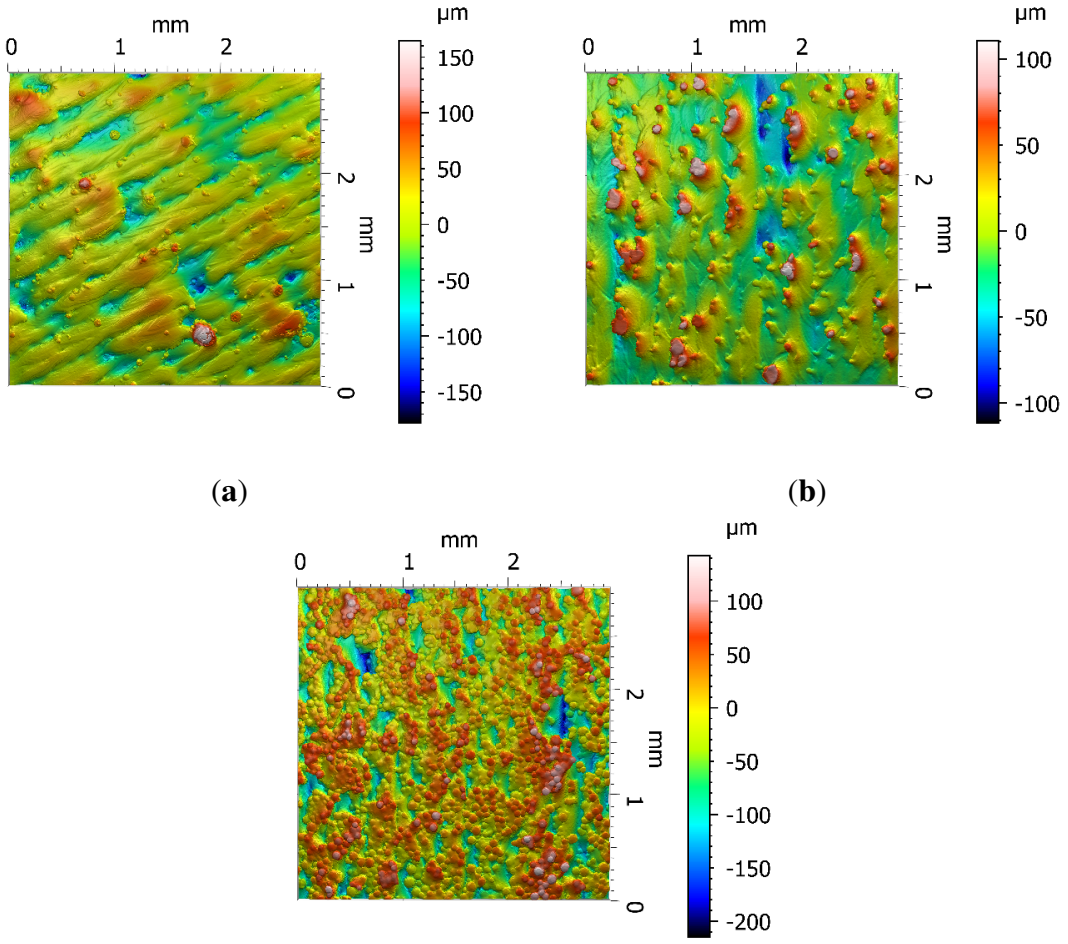

Fig. 4.1 Example surface topography height maps (a) LBPF top surface (b) EBPBF angled surface and (c) EBPBF side surface

4.2.2 Segmentation using contour stability analysis

Contour stability analysis was originally presented in reference [84], where it was applied to identify particles and spatter features on LPBF surfaces. Contour stability analysis is essentially an edge detection method that privileges sharp transitions, so it preferentially works for features delimited by steep "walls", which applies to most particles/spatter formations in the test case. In contour stability analysis, the measured topography is sectioned by a series of slicing planes at decreasing height starting from the top. Each slicing plane results in a series of cross-sectional contours. Each contour is tracked as its shape changes moving down through the sequence of slicing planes. Those contours that change minimally (i.e. within a small, predefined threshold), are defined as stable, and are representative of steep feature boundaries in the original, sectioned topography. In order to efficiently track multiple contours across many slicing planes, the method implements a spatial binning process for the contour maps and considers as stable those portions of contours that do not exit their original bins. Once the more stable contours are identified and cleaned via a sequence of morphological operations, those forming closed loops are extracted and used to isolate features [84]. In this chapter, contour stability analysis was implemented for particle and spatter detection with the following parameters.

- An S-filter of nesting index 8 μm and an L-filter of nesting index 250 μm were applied to remove noise and the underlying large-scale waviness which may confuse the contour stability analysis.
- Contour stability was run with the following settings: the threshold for maximum lateral movement of contour points across slicing planes was set to 2 μm over a vertical range of 5 μm (computed with a series of vertically stacked slicing planes set 0.25μm apart); to connect edges that are detected by the algorithm into closed regions that represent feature objects on the surface, morphological dilation and erosion over a three pixel structuring element was applied in the segmentation binary mask.

4.2.3 Morphological segmentation on edges

Morphological segmentation consists of partitioning the topography into hills or dales, as described in ISO 25178-2 [57] and elsewhere [60]. Hills are areas from which maximum uphill paths lead to one specific peak and dales are areas from which maximum downhill paths lead to one specific pit. As a rough surface will typically result in a multitude of hills or dales, methods have been defined to simplify the partitioning by aggregating individually less relevant (i.e. smaller) hills or dales to larger ones [60]. The most widespread aggregation methods are area pruning and Wolf (i.e. height) pruning [60], respectively based on merging hills/dales with smaller footprint areas, or smaller local height/depth, to larger ones. Morphological segmentation into hills/dales can be performed using a variant, specifically designed to detect edges [60, 118]. In this variant, an artificial topography is created, containing the absolute values of the local slope of the original topography. This topography is partitioned with dale-based segmentation [118, 131]. The method is colloquially referred to as morphological segmentation on edges [118] because local concentrations of large slopes (visible as dale crests in the absolute slope map) are typically representative of edges in the original topography. Morphological segmentation on edges was recently applied to the identification of spatter and un-melted particles in PBF surfaces [63], using the following steps.

a) An L-filter with nesting index 250 μm is applied to suppress large scale (waviness) components on the surface. As for contour stability analysis, this step is designed to remove topography components which may confuse the actual segmentation algorithm.

b) Sobel operators are applied to produce a gradient magnitude map of the surface (particles and spatter would possess high gradients around the edge of the feature).

c) The gradient magnitude map was taken as absolute value (that is, negative slopes are turned into positive, so that high-slope regions appear as crests surrounding low-sloped regions - dales in the gradient map). Finally, morphological segmentation into dales

was applied and pruning of these segmented regions was performed by thresholding the heights above three standard deviations of the mean height to isolate the top-most regions of the segmentation map, which are most likely to correspond to protruded formations such as spatter and particles.

In this chapter, morphological segmentation on edges was implemented for particle and spatter detection, following the method proposed in reference [63]. The following parameters were adopted.

a) An S-filter with nesting index at 8 μm and an L-filter with nesting index 250 μm were applied to extract the roughness surface.

b) Sobel operators were applied to produce the gradient magnitude map, later turned into absolute values.

c) Morphological segmentation into dales was applied. Threshold-based isolation of the top-most regions, with varying thresholds depending on the surface condition.

For the LPBF top surface, the threshold was applied at the value of the mean height, plus one times the standard deviation; for the EBPBF angled surface, the threshold was set at the mean height plus half standard deviation; and for the EBPBF side surface the threshold was set at the mean height. These values were chosen as optimised to isolate the top-most regions corresponding to the protruding formations.

4.2.4 Segmentation using active contours

Active contours is a method that, starting from an initial guess, iteratively refines the position of a closed contour that is meant to separate the region of interest from its surroundings [116, 119–121, 132]. Strictly speaking, active contours should be regarded as an edge refinement method, not an edge identification method, however, the method is always paired

to an initial contour rough-guessing method, so that the combination of both steps represent an actual edge identification. Starting from the initial guess, active contours makes use of mathematical models that mimic energy minimisation, to iteratively move the contour towards its most stable position (moving outwards or inwards, depending on the variant). The final stable position is assumed as the boundary of the feature being isolated. In this chapter, active contours was implemented for particle and spatter detection by subjecting the surface topography to a L-filter with nesting index 70 μm. The index was chosen based on the approximate size of individual particles, to remove larger topographical features. On the L-filtered surface, a thresholding operation was applied at 90% of the height range on the surface for the LPBF top surface and the EBPBF angled surface, and at 70% of the height range for the EBPBF side surface. The thresholding is designed to isolate the top-most regions of the filtered topography, which are most likely to correspond to protruded formations such as spatter and particles. On the resulting threshold map, topologically disconnected isles were isolated, then some filtered out based on size, horizontal aspect ratio and height (in the corresponding height map) when not consistent with typical spatter and particles of known geometric attributes. Boundaries extracted from the final isle map were individually used as initial contour rough guesses for running the active contours algorithm. Active contours was run using 100 iterations, and the geodesic 'edge' method [132] with negative contraction bias (leading to outwards growth of the contour). The output of each run was a segmentation mask that could be applied to the surface topography to isolate the spatter/particle features.

4.2.5 Comparison of segmentation methods

A performance comparison of the segmentation methods applied to the test cases was carried out by designing a series of quantitative performance indicators. The performance aspects targeted by the indicators were a) the feature identification capability, i.e. the capability

of producing segments containing the targeted features; and b) the accuracy in feature boundary identification, i.e. the capability of segmentation to place segment boundaries corresponding to actual feature boundaries. All the quantitative performance indicators assume the availability of a reference, ideal segmentation result, where each targeted feature is appropriately represented by a segment, and where the feature boundaries exactly correspond to the segment boundaries. The reference segmentation result can be compared with the result of each investigated method, to assess performance of the latter. However, due to lack of an optimal segmentation method whose performance is recognised as ideal for the selected test case, a segmentation result was hand-drawn for each test surface to act as a comparison reference. Clearly though, adopting a reference result created by a human operator is susceptible to bias and repeatability/reproducibility issues because of the presence of subjective assessment [62]. The performance indicators illustrated in the following assume that any segmentation result, whether generated by one of the compared methods or manually generated by the operator, is available in the form of a map of identifiers (IDs). A map of IDs is a grid of ID values, the same size as the original height map, so that each location (map point) in the height map is univocally associated to one and only one segment (the one represented by the ID value associated to that point). To maintain the useful parallel to digital images, map points will be referred to as "pixels" from now onwards. The following definitions for the quantitative performance indicators assume the pre-processing steps shown in see Figure 4.2.

For each subset of the height map containing an individual feature (Figure 4.2a), the corresponding reference, ideal segmentation result is assumed available (Figure 4.2b). Notice that in the ideal result, the feature has been identified (i.e. there is a segment covering the region occupied by the feature), and the feature boundary has been correctly localised (i.e. the segment boundaries do coincide with the actual feature boundaries). In Figure 4.2c, the result of a segmentation algorithm to be evaluated is shown. Clearly, whilst a segment has

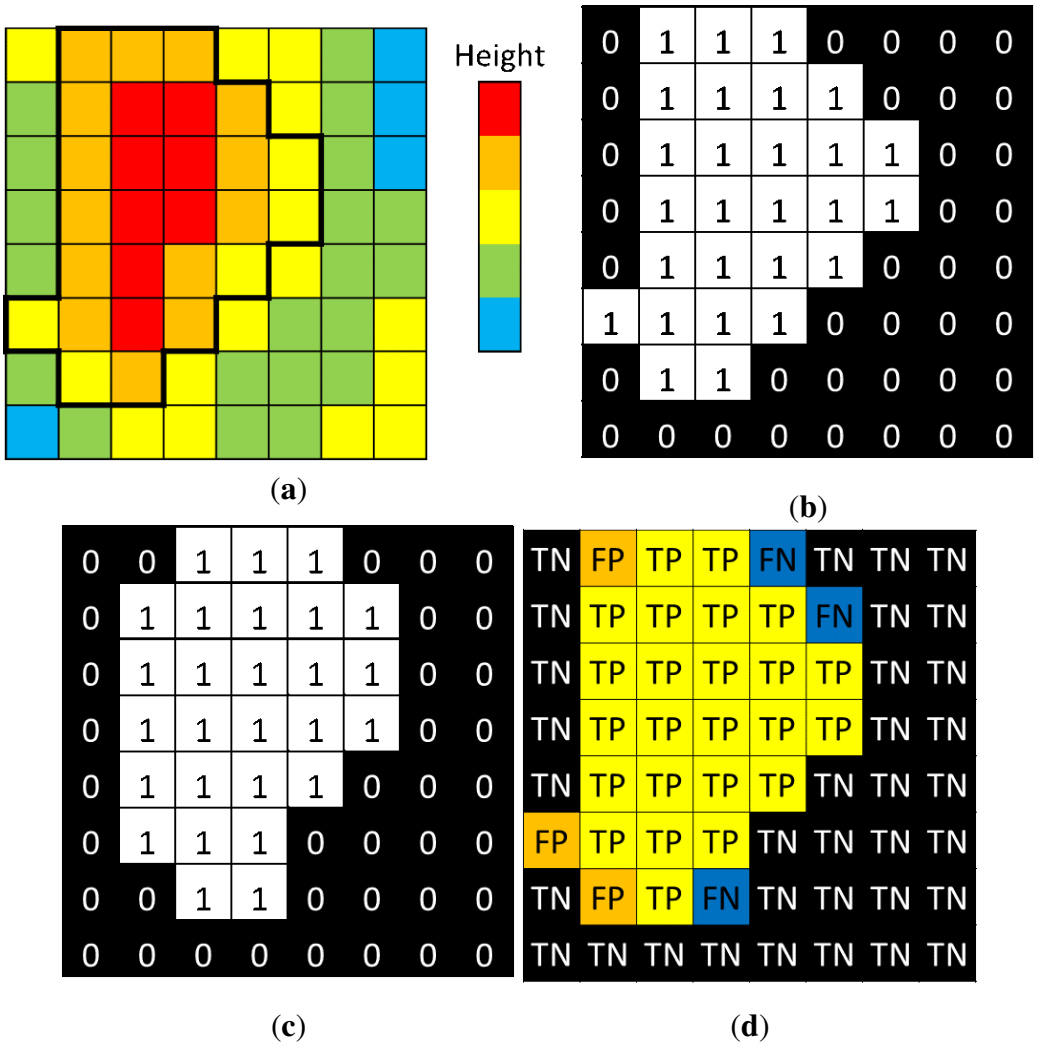

Fig. 4.2 Pre-processing for the quantitative performance indicators for individual feature assessment showing (a) portion of surface topography (height map) where a feature instance is visible, highlighted by the thick black contour (b) ideal segmentation result drawn by hand; (c) result of one of the segmentation algorithms; (d) classification of the individual cells from comparing the segmentation result with the reference, ideal one.

Class	Description	Short name (feature-centric)
TP (true positive)	1-valued segmentation pixel overlaid to a feature pixel in the height map	Feature pixel
FP (false positive)	1-valued segmentation pixel overlaid to a background pixel in the height map	Excess (feature) pixel
TN (true negative)	0-valued segmentation pixel overlaid to a background pixel	Background pixel
FN (false negative)	0-valued segmentation pixel overlaid to a feature pixel	Missing (feature) pixel

Table 4.1 Classification of pixels in the segmentation map depending on whether they correspond to features or background pixels.

been created approximately corresponding to the position of the actual feature (i.e. successful identification), the segment boundaries do not correspond exactly to the feature boundaries, leading to different statuses associated with the segment pixels, depending on where they fall with respect to the actual feature (Figure 4.2d). Such statuses can be derived from the results of a binary classifier and are summarised in Table 1.

The following performance indicators, originally devised for binary classifiers, can be adopted to describe the performance of segmentation with respect to an individual feature.

$$\begin{aligned}\text{Precision}\ (\text{positive predictive value} - \text{PPV}) &= \frac{TP}{TP+FP} \\ &= \frac{\text{no. feature pixels}}{\text{no. feature pixels} + \text{no. excess pixels}}\end{aligned} \tag{4.1}$$

High precision implies a low number of excess pixels, a 100% precision implies zero excess pixels.

$$\begin{aligned}\text{Recall}\ (\text{sensitivity, true positive rate} - \text{TPR}) &= \frac{TP}{TP+FN} \\ &= \frac{\text{no. feature pixels}}{\text{no. feature pixels} + \text{no. missing pixels}}\end{aligned} \tag{4.2}$$

High recall implies a low number of missing pixels, a 100% recall implies zero missing pixels.

$$\begin{aligned}\text{Specificity } (\text{selectivity, true negative rate} - \text{TNR}) &= \frac{TP}{TP+FP} \\ &= \frac{\text{no. background pixels}}{\text{no. background pixels } + \text{ no. excess pixels}}\end{aligned} \tag{4.3}$$

Similar to the concept of metrological precision, high specificity implies a low number of excess pixels (i.e. pixels wrongly recognised as belonging to the feature). However, different to precision, the viewpoint is the identification of the background.

The above indicators can be computed for each individual feature and its associated portion of the segmentation map. Once repeated for all the individual features presented on a test surfaces, they can be aggregated into performance statistics (e.g. mean and standard deviation of each indicator).The indicators provide information intuitively related to metrological accuracy in feature boundary identification. To quantify performance in feature identification, the number of features that have no corresponding pixels in the segmentation map (i.e. the number of totally ignored features) is counted and compared to the total number of features present in the analysed region (from the reference segmentation result). The following ratio is defined:

$$\text{Identification error ratio } = \frac{\text{no. ignored features}}{\text{no. total features}} \tag{4.4}$$

The identification performance is defined as the complement of the identification error ratio:

$$\begin{aligned}\text{Identification performance } &= \frac{\text{no. identified features}}{\text{no. total features}} \\ &= \frac{(\text{no. total features } - \text{ no. ignored features})}{\text{no. total features}}\end{aligned} \tag{4.5}$$

In addition, the indicators applied to individual features can be applied to all pixels within the image to offer a complementary assessment of the segmentations approaches with respect to the whole surface. This is done by comparing the binary maps. Alongside this, an indicator for the accuracy of the segmentation approach can be used to describe the performance with respect to the whole image:

$$\text{Accuracy} = \frac{TP+TN}{TP+FP+TN+FN} = \frac{\text{no. feature pixels } + \text{ no. background pixels}}{\text{no. total pixels}} \tag{4.6}$$

Accuracy provides an overall view of classification performance. However, the result is skewed by different number of feature and background pixels in the analysed region of the segmentation map. Therefore, the following balanced form can be adopted:

$$\begin{aligned}\text{Balanced accuracy} &= \frac{\frac{TP}{TP+FP} + \frac{TN}{TN+TP}}{2} = \frac{TPR+TNR}{2} \\ &= \text{arithmetic average of recall and specificity}\end{aligned} \tag{4.7}$$

4.3 Results

In Figures 4.3, 4.6 and 4.9, segmentation maps are shown from the different segmentation methods applied to the LPBF top surface. Pixels are coloured based on the comparison with the ideal reference classification results. Note that the coloured maps have been obtained by aggregating the comparison results obtained for each individual feature (particle or spatter). Missing (feature) pixels are shown in blue, thus particles/spatter features that are shown as entirely blue are ignored features that reduce the overall identification performance of the method. On the contrary, identified (or partially identified) features are marked with yellow pixels (feature pixels). For those, excess pixels (orange) and missing pixels (blue) provide

an indication of boundary detection performance. Figures 4.4, 4.7 and 4.10 show boxplots of all the performance metrics calculated on individual objects that are found on both the reference and the segmentation approach for each surface. Each object is considered as a whole regardless of how small the overlap of matching pixels might be; this is to determine how effective the segmentation is for specific features on the surface. Figures 4.5, 4.8 and 4.11 show the values of the performance parameters calculated over the whole surface as determined by the binary classification tests shown in Figures 3, 6 and 9. These results only give a general assessment of the segmentation and do not consider the effectiveness of boundary detection.

4.3.1 LPBF top surface

For the LPBF top surface (Figure 4.3), where there is an expected low number of features (particles and spatter) on the surface, the morphological segmentation on edges resulted in the lowest identification performance of 0.087 (about 9% identified features). Contour stability identified more features with an identification performance of 0.621. Active contours resulted in the highest identification performance with a score of 0.776.

Figure 4.4 shows specificity, precision and recall calculated on the matched features for the LPBF top surface. For morphological segmentation on edges, the boxplots were calculated for nine matched features. The boxplot for contour stability was calculated on sixty-four matching features and active contours was calculated on eighty matching features. Morphological segmentation on edges has the highest scores for precision and specificity, both with low dispersion. For precision, contour stability and active contours have higher dispersion whilst contour stability possesses a much higher median value very close to unity. Active contours has the highest scores and significantly low dispersion for recall, performing better than the others, suggesting that it is often the best approach to identify most of the

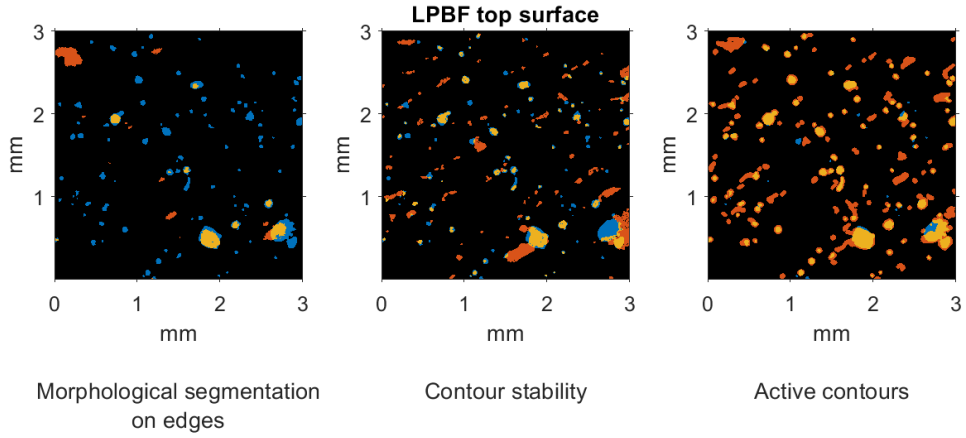

Fig. 4.3 Binary classification test results between the manual reference and the segmentation approach for LPBF top surface, in the figure, yellow represents matching pixels, orange represents excess pixels and blue denotes missing pixels.

spatter formations and particles present on the surface. All three approaches result in high scores and low dispersion for specificity, with all values greater than 0.99.

As shown in Figure 4.5 for the whole surface, morphological segmentation on edges possesses the lowest scores for balanced accuracy and recall. However, morphological segmentation on edges results in the highest values for precision and specificity. Contour stability appears to be not as precise as morphological segmentation on edges. Otherwise, the performance parameters for contour stability fall between the two other approaches with a comparably higher score for specificity. Active contours does result in a high score for recall, suggesting that it does identify a lot of the features as found in the reference, consistent with the highest score for accuracy. However, lower scores of precision and specificity suggest that active contours generally overestimate both the size and number of relevant features, a result that can be visualised in Figure 4.3.

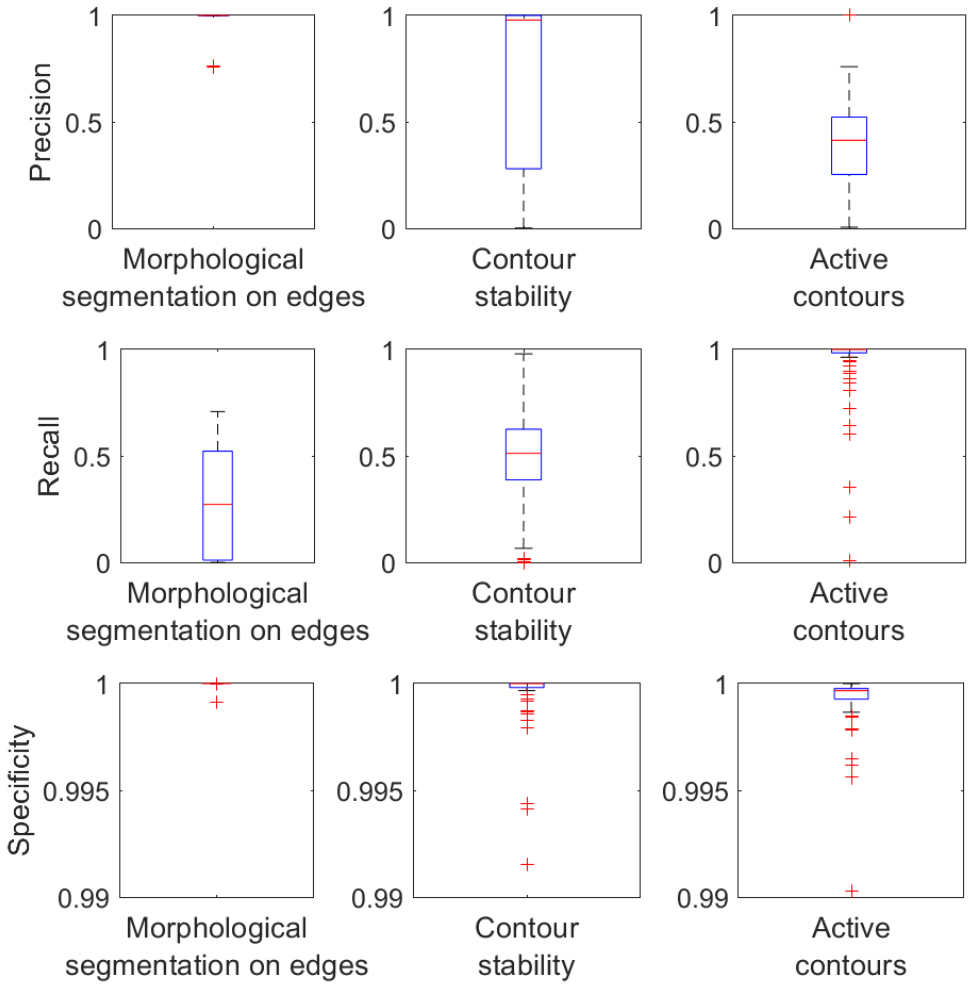

Fig. 4.4 Precision, recall and specificity for matched features on the LPBF top surface.

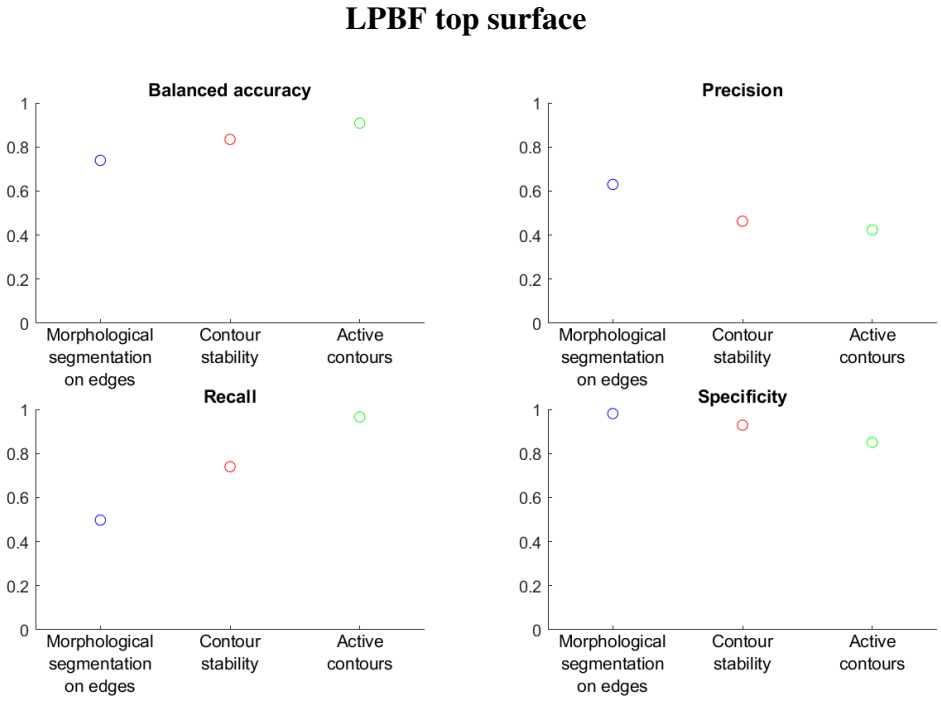

Fig. 4.5 Performance indicators calculated over the whole datasets for the LPBF top surface

4.3.2 EBPBF angled surface

The EBPBF angled surface (Figure 4.6), features an increased number of particles and spatter formations with respect to the LPBF top surface. Morphological segmentation on edges resulted in an identification performance of 0.574. Contour stability resulted in the lowest score for this surface, with an identification performance of 0.465. Active contours resulted in the highest identification performance, with a score of 0.929.

Figure 4.7 shows the boxplots for individual matching features between the reference and segmentation results for the EBPBF angled side surface. For morphological segmentation on edges, the boxplots were calculated for seventy-three matched features. The boxplots for contour stability were calculated on fifty-nine matching features, whilst for active contours they were calculated on 118 matching features. As shown in Figure 4.1 and Figure 4.6, there are some particles that appear adhered to layer edges and as groups of particle clusters. In Figure 4.7, a relatively high dispersion of the scores for all segmentation methods is observed

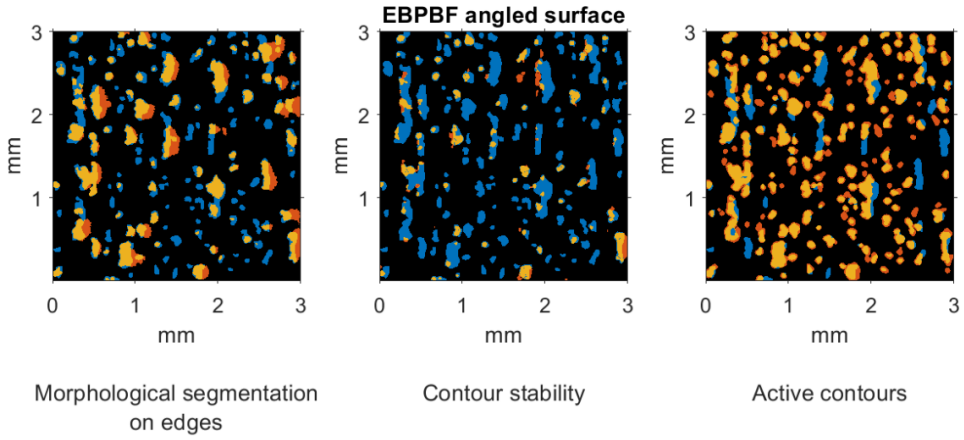

Fig. 4.6 Binary classification test results between the manual reference and the segmentation approach for EBPBF angled surface, in the figure, yellow represents matching pixels, orange represents excess pixels and blue denotes missing pixels.

when compared to the top surface, with exception of contour stability, likely due to the difficulty in defining contours on particle clusters that have low gradients. Morphological segmentation on edges results in high scores for precision and specificity but lower scores for recall. Contour stability possesses the highest scores and lowest dispersion for both precision and specificity. Active contours result in the highest score and lowest dispersion for recall, with the interquartile range (IQR) above 0.8, following a similar trend as previously observed for the LPBF surface (Figure 4.4).

For the performance indicators calculated over the whole image, morphological segmentation on edges, as shown in Figure 4.8, resulted in the highest value of balanced accuracy and very high values for precision and recall. Contour stability still has reasonably high values for precision and recall, but with a much lower specificity leading to a lower balanced accuracy. Active contours, whilst having a high recall and a good precision, has the lowest specificity suggesting that, whilst there was good agreement between the method and the reference, there was still some over-estimation of features.

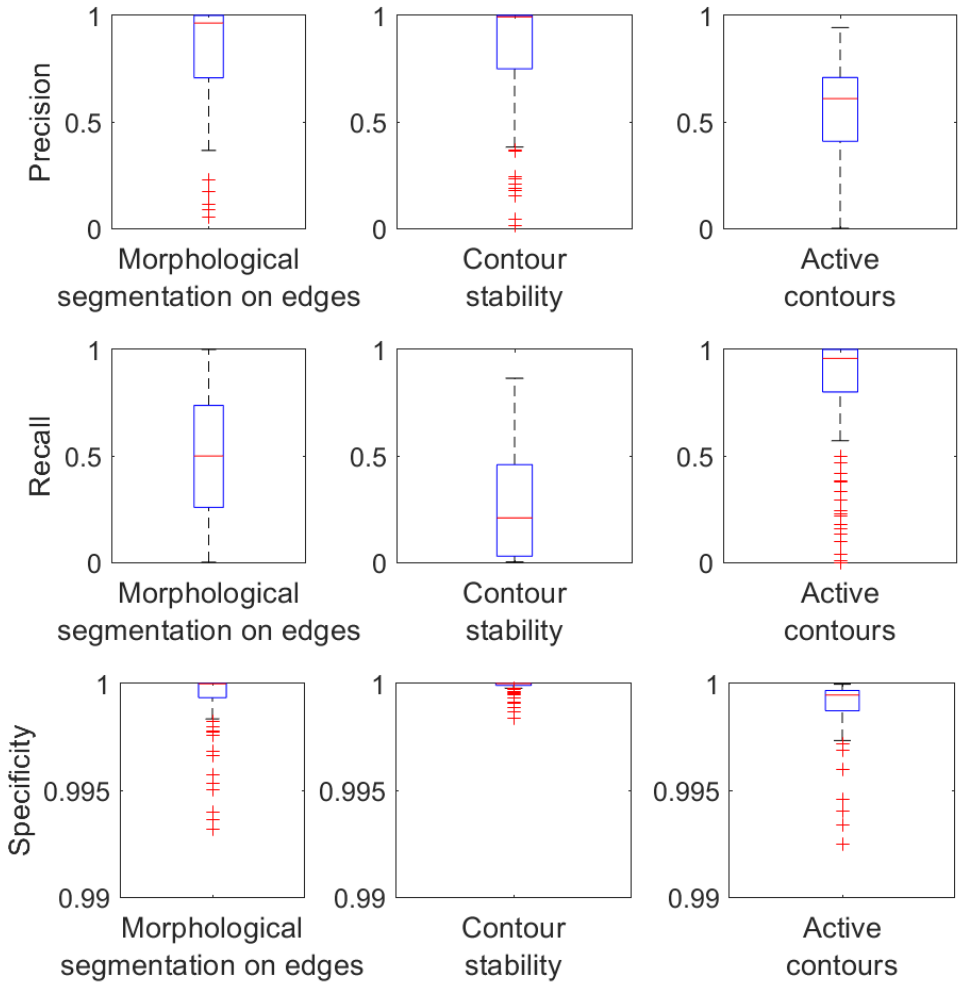

Fig. 4.7 Precision, recall and specificity for matched features on the EBPBF angled surface.

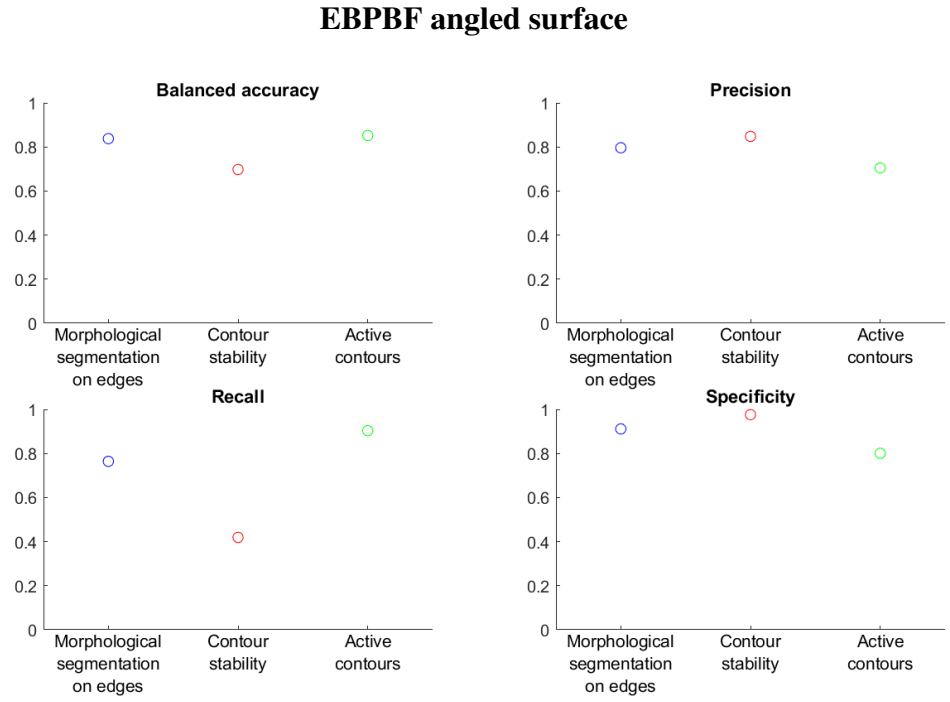

Fig. 4.8 Performance indicators calculated over the whole datasets for the EBPBF angled surface

4.3.3 EBPBF side surface

The EBPBF side surface (Figure 4.9), featured the highest number of spatter formations and particles, with an increased occurrence of particle clusters. Morphological segmentation on edges resulted in the lowest identification performance with a value of 0.313. Contour stability identified more features with an identification performance of 0.417. Active contours resulted in the highest identification performance with a score of 0.600.

The boxplots for the individual matching features for the EBPBF side surface are shown in Figure 4.10. Due to the further increase in the number of features and increased presence of agglomerations, there appears to be an even greater dispersion for most of the performance metrics across the segmentation approaches. For morphological segmentation on edges, the boxplots were calculated for 36 matched features. The boxplots for contour stability were calculated on 48 matching features, whilst those for active contours were calculated on 69 matching features.

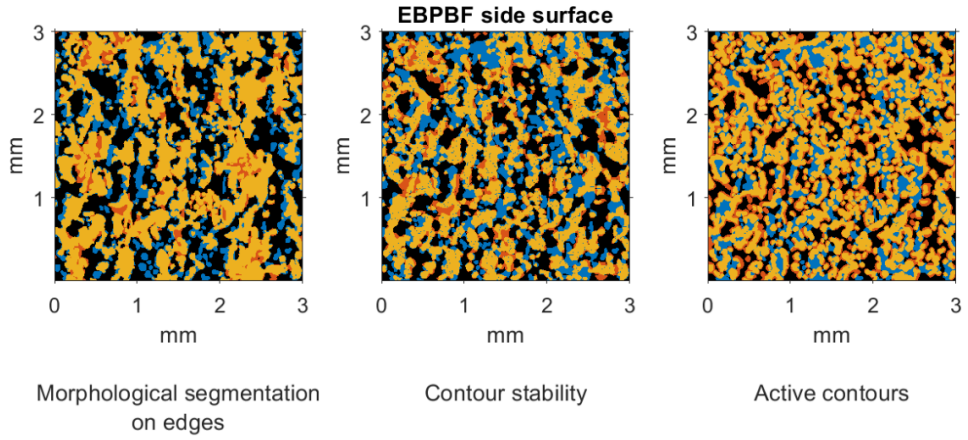

Fig. 4.9 Binary classification test results between the manual reference and the segmentation approach for EBPBF side surface, in the figure, yellow represents matching pixels, orange represents excess pixels and blue denotes missing pixels.

In Figure 4.10, morphological segmentation on edges results in the highest values and lowest dispersion for precision and specificity, with both contour stability and active contours possessing higher dispersion and lower median scores. For recall, there is a very large dispersion for active contours, however, the median is significantly lower when compared to contour stability. Whilst contour stability has the highest score for recall, it also has high dispersion. In addition, contour stability possesses the largest IQR for specificity – which is also greater than the greatest result found across all the surfaces considered.

The performance indicators calculated over the whole image can be seen in Figure 4.11. Morphological segmentation on edges appears to have performed the best for the EPBPF side surface, with the highest value of balanced accuracy and very high values for precision and recall. Contour stability still has reasonably high values for precision and recall, but with a much lower specificity leading to a lower balanced accuracy (not shown). Active contours, whilst having a high recall and a good precision, has the lowest specificity suggesting overestimation of feature size.

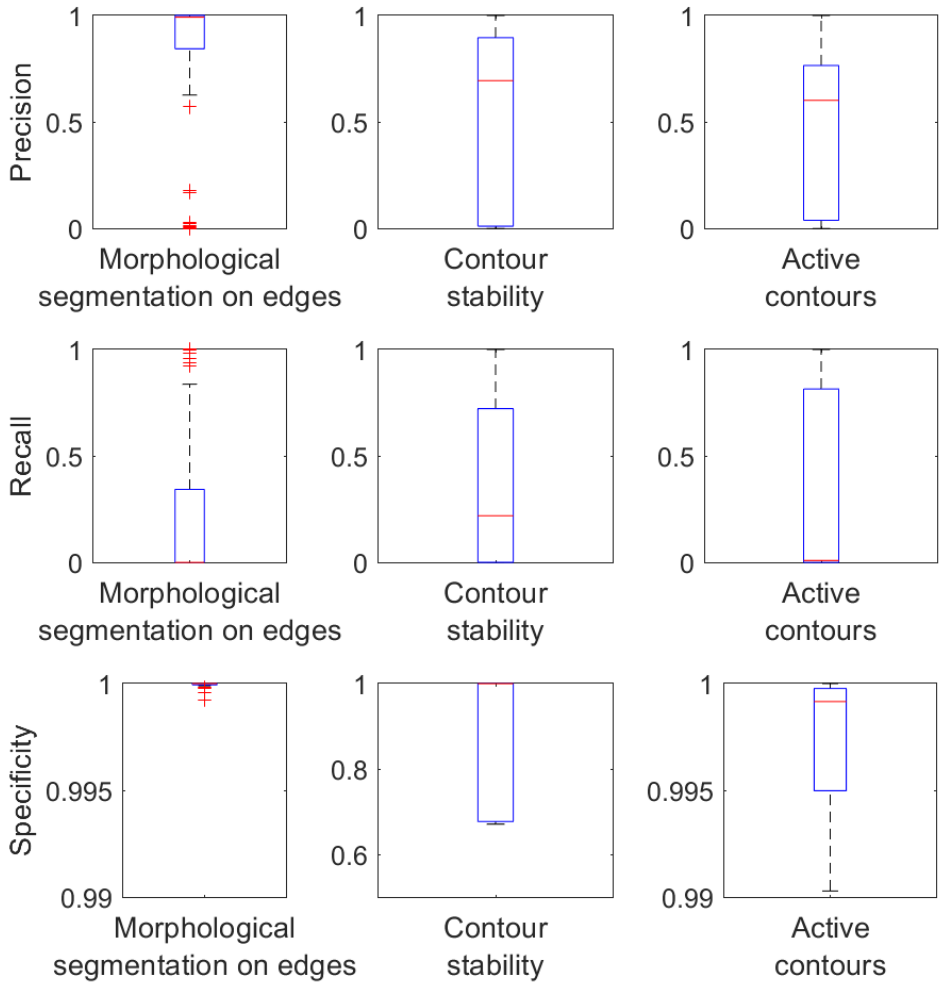

Fig. 4.10 Precision, recall and specificity for matched features on the EBPBF side surface.

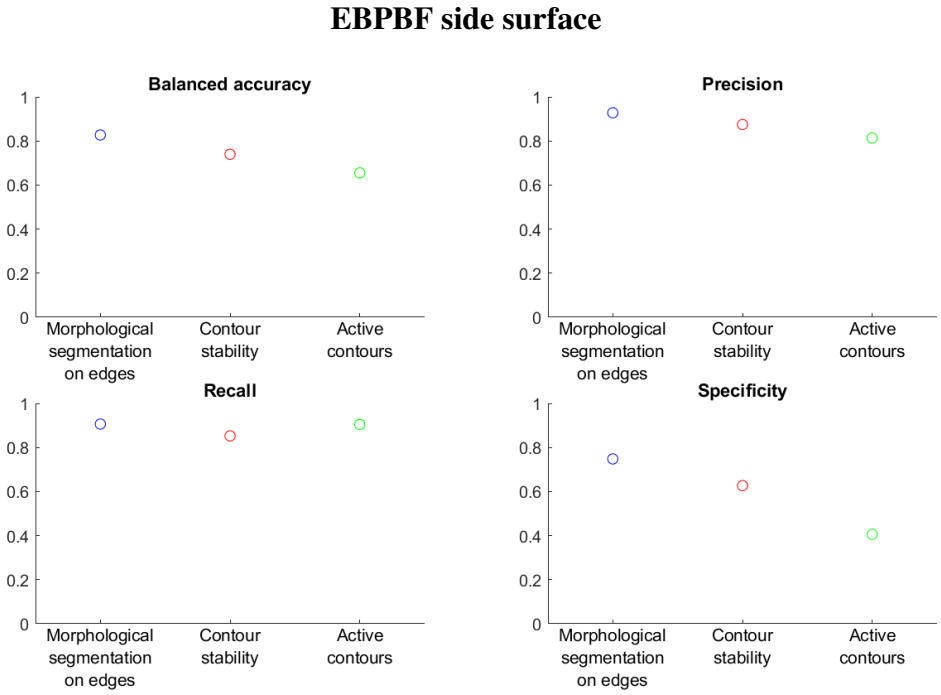

Fig. 4.11 Performance indicators calculated over the whole datasets for the EBPBF side surface

4.3.4 Summary of the comparison results

For identification performance, active contours scored the highest across all surface cases with morphological segmentation on edges resulting in the lowest scores for the LPBF top surface and the EBPBF side surface. Contour stability performed reasonably for all surface cases. It appears that the EBPBF angled surface was the easiest surface to segment, as reflected by the highest scores for each approach. On the contrary, the lowest score for identification performance was observed for morphological segmentation on edges on the LPBF top surface. The results for the individual matched objects (particles, spatter and particle cluster formations) show a trend for higher dispersion for the scores (lower agreement) with increasing complexity (from LPBF top surfaces to EBPBF side surfaces) which suggests that, as the individual features on the surface get more complex, all segmentation approaches find it more difficult to identify features that agree with the reference segmentation. Consistently, morphological segmentation on edges reported high scores and a lower dispersion

for precison and recall, whilst active contours generally had the higher scores for recall. Contour stability generally performed better than active contours for precision and specificity, and showed scores for recall improving with increasing complexity of the surface. When comparing the result for the whole surface, the increasing complexity and number of features is reflected in the balanced accuracy, with the lowest values found on the EBPBF side surface and the highest scores found on the LPBF top surface. The lowest values for precision were found on the LPBF top surface where all methods were unable to identify many of the spatter and particle features. In general, there is a trade-off between recall and specificity across all three methods. Active contours is generally a good approach, with low precision and specificity but high recall. On the contrary, morphological segmentation on edges, whilst leading to lower recall, possesses higher scores for precision and specificity. Essentially, active contours will find all objects found in the reference, but at the cost of oversizing feature boundaries. Morphological segmentation on edges may struggle to identify all objects in the reference but will more closely track the edges of the object boundaries. Contour stability falls between the other two methods in terms of performance, but is particularly weak when confronted with agglomerated particles, resulting in lower scores for recall on surfaces where these types of features are present.

4.4 Discussion

4.4.1 Limits of the segmentation validation method

A reference segmentation result is necessary to compute the performance indicators that have been proposed in this chapter. However, in the absence of an ideal segmentation method to use as a reference, the use of a manually obtained segmentation result has been suggested. Clearly, the reliance on a result obtained by a human operator is prone to be affected by subjective bias, and such bias is not only operator-dependent, but may also be

application dependent, as operators may find different challenges when processing different types of surfaces. Visual understanding of reconstructed, digital topographies is affected by many confounding factors, including the influence of measurement error, and - for complex topographic objects - lack of definition of what an actual feature may look like, or even worse, how exactly a feature boundary may be identified. In addition, performance degrades with increased feature count, as the operator is more likely to cause errors when large numbers of features must be manually assessed. These issues should be considered when assessing the reliability and reproducibility of the results presented by this chapter. Regardless, the goal of this research is to highlight the need for a quantitative evaluation of segmentation performance, and several relevant, quantitative indicators has been provided.

4.4.2 Additional computational costs of segmentation

The segmentation methods illustrated in this chapter have been compared solely in terms of their performance on a specific test case. It is important to point out the fact that such performance is normally not obtained out-of-the-box, and each segmentation method requires a long tuning process, in order to perform optimally on each class of surfaces and target features. When choosing a segmentation method, the number and complexity of actions and decisions involved in tuning the method for the test case should be considered as well. For example, morphological segmentation on edges run with default parameters will always result in over-segmentation, even if the original topography is only moderately complex [62]. Subsequent post-processing to reduce the number of segments is typically required which, however, requires the careful tuning of several parameters (as described in Section 2.3). Contour stability also requires careful tuning of several parameters. In addition, contour stability was designed to preferentially address steep edges, and performs relatively weakly when encountering locally smooth gradients, such as those observed with agglomerated particles in the test case (see Section 3.2). Active contours is possibly the approach requiring

the most involving set-up, in particular because of the need to perform a rough-guess of the initial contours, which requires a whole new topography pre-processing step. Ultimately, thus, the choice of a segmentation method may also be dictated by complexity of its set-up and fine-tuning, which in turn may be affected by application-dependent circumstances. Other challenges have been found to be consistently shared across applications. For example, for all the test cases and all the methods investigated, filtering was required to remove larger-scale topographic formations which can confuse the segmentation process. Though this aspect has not been covered in detail in this chapter, the identification of optimal filtering parameters is often challenging and still subject to trial and error. Initial set-up is important for any segmentation approach and it is important that the user is experienced with both surface characterisation and the processes that produce the surface in order to meaningfully determine the features being assessed.

4.4.3 Measurement uncertainty for feature-based characterisation

Measurement uncertainty for feature-based segmentation and characterisation should be provided, just as measurement uncertainty for areal topography datasets has been previously investigated [48, 128, 133]. Estimation of uncertainty in feature-based characterisation is an important challenge to the adoption of these methods, requiring understanding of the influence factors associated with the topography data from the measurement as well as how this error may propagate through the various stages of the segmentation and characterisation.

4.5 Conclusions

- LPBF top surface was found to be hardest to segment - with morphological segmentation on edges unable to identify most of the particles as determined by the reference.
- EBPBF side surface was found to be the easiest surface to segment for all approaches.

- There is a trade-off between recall and specificity for all segmentation methods.
- Active contours results in low precision, but high recall - it will find more features but over-estimate their boundaries.
- Morphological segmentation on edges results in high precision, but low recall - it can better define the contours of features compared to the reference, but often does not identify features.
- Contour stability falls between the two other methods proposed, but is weaker when dealing with agglomerated features where contours that may resolve separate particles are not as clearly defined.
- The methodology proposed can allow for a comprehensive assessment of segmentation performance, that could allow for optimisation.
- In future, use of virtual reference with pre-defined features would allow for assessment independent of bias: operator or application dependent.

Feature based characterisation is a way to assess surface topography that is complementary to texture parameters, and in some cases may provide richer information content, as features can be defined that more closely match the subject of interest in any specific surface investigation scenario. Segmentation, the act of partitioning a surface topography into regions (segments) plays a fundamental role in feature-identification. In particular, the accuracy of a segmentation method at identifying region boundaries directly influences the accuracy in the assessment of a feature geometrical properties. This chapter presents a method to compare segmentation results and quantitatively assess their performance under different viewpoints related to both the capability of identifying features, and the capability to accurately delimit feature boundaries. The method is based on computing a series of quantitative performance indicators and requires a reference (ideal segmentation result) on which to compare. In the

absence of an ideally performing, algorithmic segmentation method acting as a reference, the ideal result is currently produced manually by an expert operator. Manual generation may create issues of reproducibility, especially on complex surfaces with many features. However, if multiple segmentation methods are compared with each other using the same reference result, the method can provide a comparative, comprehensive assessment of segmentation performance. Future work would see the methodology proposed used to compare segmentation methodologies and settings in order to optimise the segmentation methods for specific features, such as particles and particle clusters, as well as further developing segmentation approaches to target different features present on the additive manufactured surface. Other future work would see the methodology applied to a virtual surface, to provide defined features that can be assessed independent of various bias: operator dependent and application dependent.

Chapter 5

Characterisation of surface topography for EBPBF surfaces produced at different build orientations

The work in this chapter has been presented to the Surface Topography: Metrology and Properties conference in Lyon [134].

5.1 Introduction

Once optimised parameters can be identified for feature based characterisation, such as using methods from Chapter 4, these approaches can be used to meaningfully and accurately identify and segment topographic features on a surface. In this chapter, surface orientation is identified as a variable that influences surface topography: both the parameter values and features found present on the surface.

The study of how surface topography in additively manufactured parts is affected by build orientation is important for understanding the behaviour of additive manufacturing processes. For metal powder bed fusion (PBF), whilst top surfaces contain topographic formations that

are the result of the scanning strategy adopted for the build, side surfaces differ greatly with respect to the build angle and result from a series of combined effects, such as the staircase effect, the bonding between layers, and the interaction of the part with the surrounding powder bed [1, 84, 135]. Process-induced topographic formations can significantly influence the choices for surface post processing.

Most of the research investigating surface texture of metal AM parts has focused on laser powder bed fusion (LPBF). Whilst electron beam powder bed fusion (EBPBF) is similar, as it is also a powder bed fusion process, it features some rather significant differences in the surfaces it produces [9]. Test parts (artefacts) are commonly adopted to investigate surface topography, with many of them designed to possess many surfaces at differing orientations with respect to the build [6].

For assessing the topography of AM surfaces, most researchers have used ISO 4287 profile parameters [52], the most commonly used parameter being *Ra*, the arithmetic mean deviation of the assessed profile [80, 103, 136, 137]. Areal parameters – defined within ISO 25178-2 [57]– have been used less often. The most commonly adopted areal parameters have been , *Sa*, the arithmetic mean height of the scale-limited surface (the areal equivalent to *Ra*) and *Sq*, the root mean square height of the scale limited surface [82, 89–91].

In recent work on metal AM surfaces, ways to describe the complex topography via approaches alternative to texture parameters have been investigated, based on the characterisation of topographic formations that populate the typical metal additive surface (weld tracks, spatter formations, particles) [84, 117, 63, 122]. These alternative approaches have been collectively referred to as feature-based characterisation [62].

Surface texture parameters offer quantitative assessments of surfaces which can allow for comparison. Many parameters describe the distribution of heights from a mean plane, with others describing other properties (such as those of the material ratio curve), but in general all parameters capture properties that pertain to the entire region that has been measured which

are only indirectly linked to properties of topographic features of relevance that populate the surface. On the contrary, feature-based approaches allow for the segmentation of selected localised topographic formations on which individual geometric dimensional properties can evaluated. These properties can be evaluated as individual measurements or further aggregated to offer an enhanced assessment of groups of features.

In this work, a hybrid approach is proposed where EBPBF surfaces, acquired by means of areal topography measurement, are decomposed and analysed using feature-based characterisation techniques. Particles and spatter are separated from the surface and characterised in terms of their properties, whilst the remaining topography, deprived of particles, is described in terms of ISO 25178-2 areal field texture parameters. The decomposition approach is particularly relevant as a means to describe how the topography of EBPBF surfaces varies as a function of build angle: particles (individual or in clusters) and spatter formations (on top surfaces) are typically present in varying amounts at different tilts; as they are protruded, particles and spatter can influence significantly the computation of any areal field texture parameter, thus rendering the characterisation of the substrate surface often impossible. Because particles and spatter are typically welded to the substrate, even their mechanical removal does not produce a reliable surface for the computation of texture parameters because of the modification they leave behind in the regions where they were attached, thus a solution for masking particles and spatter out from the topography is preferable. In addition, being able to separate particles and spatter from their surroundings allows also for the selective computation of their geometrical and positional properties. Therefore, for any surface, separation of particles and spatter from the substrate enables the computation of particle number, size, spatial distribution, tendency to form aggregates, etc, which in turn leads to the possibility of describing surfaces as a function of build orientation in a more informative and comprehensive way.

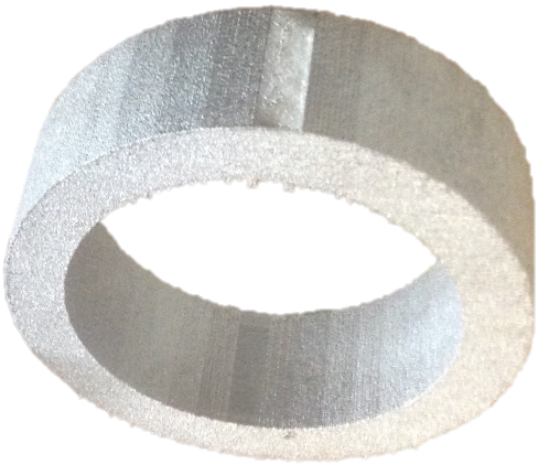

Fig. 5.1 'Bracelet' test part

5.2 Methodology

5.2.1 Measurement test part

A 'Bracelet' test part made of Ti6Al4V (125 × 125 × 25) mm was manufactured using EBPBF with an Arcam A2XX. The part has an outer side surface made of 36 planar facets with local orientations varying in 10° increments (0°, 10°, 20°, etc.). Before measurement, all the support structures were removed, and all the surfaces were cleaned using compressed air. Any further post-processing would have increased the risk of removing meaningful, process-related features from the surfaces.

5.2.2 Measurement strategy

Measurement was performed using the Alicona G5 focus variation (FV) microscope instrument [44]. Focus variation has been demonstrated to be a suitable technology for the measurement of metal AM surfaces and has been optimised using the work found in Chapter 3.1. The following settings for the FV instrument were adopted: 20× objective lens (NA 0.4, field of view (0.81 × 0.81) mm); lateral resolution: 3.51 μm; vertical resolution: 12 nm; ring

light illumination; measured area (3 × 3) mm, stitched. Magnification and the extent of the measured areas were chosen to capture a sufficiently representative portion of the surfaces, suitable for the identification of a large number of particles and spatter formations, and for the characterisation of the underlying substrate via texture parameters.

5.2.3 Feature-based segmentation

The measured surfaces were first levelled by subtraction of the least-squares mean plane. Particles and spatter formations were then identified by application of a segmentation method (i.e. spatial partitioning of the measured field) based on active contours, an edge detection method originally developed for image processing [116, 119]. Details on the implementation of the method to make it suitable to operate on surface topography can be found in Chapter 4. In brief, an initial guess on the position of the features and their boundaries must be made (i.e. an initial contour estimate) from which the active contour method proceeds by iterative refinement, until a final contour, accurately delimiting each feature of interest, is obtained [116, 119–121, 132].

In this chapter, active contours have been implemented for particle and spatter detection as follows. In order to create the initial mask for the active contour procedure, the surface topography was subject to filtering operations (an S-filter with nesting index of 5 µm and an L-filter with nesting index of 70 µm). This index was chosen through experimentation to accentuate particles on the surface (diameters typically between 45 µm to 100 µm [11]), to remove a significant part of any larger topographical features. On the L-filtered surface, a height thresholding operation was applied, meant to isolate the topmost regions of the filtered topography, most likely belonging to protruded formations such as spatter and particles. Thresholding was performed using different threshold values depending on surface orientation (see Table 5.1). On the resultant binary mask (=1 for regions above the threshold), topologically disconnected isles were isolated, then some were filtered out based

Table 5.1 Optimised threshold values adopted for height thresholding depending on surface orientation.

Surface orientation (°)	**Threshold (%)**	**Rationale**
0	0.975	2·std. dev. above mean height
10	0.975	
20	0.975	
30	0.823	Smr^1 on material ratio curve
40	0.748	
50	0.765	
60	0.718	0.75·std. dev. above mean height
70	0.720	
80	0.719	
90	0.722	
100	0.646	0.5·std. dev. above mean height
110	0.645	
120	0.645	
130	0.647	
140	0.646	
150	0.647	
160	0.645	
170	0.645	
180	0.645	

on size, aspect-ratio and height (in the corresponding height map) not consistent with known geometric attributes of typical spatter formations and particles.

Boundaries extracted from the final isle map were individually used as initial contour guesses for running the active contour algorithm. The active contour runs over 100 iterations, using the geodesic active contours 'edge' method [120] and has a negative contraction bias (leading to growth). The output was a final segmentation mask that can be applied to the surface topography to remove spatter/particle features.

5.2.4 Feature-based characterisation of surface texture

The segmentation masks were firstly used to determine the percentage particle coverage, which is simply the area of surface covered by spatter and particles as a percentage of the measured area.

Then, the masks were used to remove spatter and particles from the original height map datasets, so that the underlying surface could be characterised by using conventional texture parameters. Removal consisted in "voiding" the regions previously occupied by particles/spatter (i.e. flagging such regions as "non-measured"), so that they would not be included in the computation of texture parameters.

Finally, by using the segmentation masks and the height information of the initial levelled topography, the following properties of the features identified on the surface could be computed: feature count, feature height and feature area.

The feature count is determined by the number of individual unconnected components found in the segmentation mask.

The height is algorithmically determined by subtracting the mean height value around a region of maximum height, from the mean height value of an extended region around the outer edge of the feature.

The feature area is calculated by multiplying the number of pixels within the feature boundary by the pixel sizing.

All assessments were performed on repeat measurements, so that boxplots could be generated to assess quantitative differences of results obtained for different surface orientations.

5.2.5 Parameter-based characterisation of surface texture

Texture parameters were computed both on the original surface topographies (i.e. as measured) and on those resulting from removal of spatter and particle features as described in the previous section. In both cases, computations were performed using MountainsMap by Digi-

talSurf [126]. For computing texture parameters, the following operations were performed on the topography datasets: levelling by least-squares mean plane subtraction; S-filter of nesting index 0.008 mm; and L-filter of nesting index 0.25 mm. From the resultant SL surface, the following ISO 25178-2 areal texture parameters were calculated: *Sa* – arithmetic mean height of scale-limited surface, *Sq* – root mean square height of the scale-limited surface, *Ssk* – skewness of the scale-limited surface, *Sku* – kurtosis of the scale-limited surface and *Sz* – maximum height of the scale limited surface. All the computations were performed on repeat measurements, so that boxplots could be generated to assess quantitative differences of results obtained for different surface orientations.

5.3 Results

5.3.1 Visualisation of the surface

As highlighted from the example surfaces shown in Figure 5.2, as the surface orientation changes, so does the complexity of the surface. Generally, as the surface orientation increases, the number of particles increases as well as the range of heights on the surface. The 0° orientation surface (Figure 5.2a) mostly consist of weld tracks with very little presence of particles or spatter. For the 30° orientation surface (Figure 5.2b), which would be orientated upwards in the build, some staircasing effects are visible, in addition to spatter formations and particles present individually and in agglomerated form. For angles greater than 90°, such as those in Figure 5.2c and Figure 5.2d, the topographies appear dominated by particles. However, there is a difference between the 90° orientation surface and downwards oriented (150° orientation) surface, with the former made of smaller individually represented particles and the downwards surface featuring large agglomerations of many particles. This finding is consistent with a known phenomenon of powder bed fusion, where in downwards facing layers, because of the energy applied on the layers above, surfaces are formed which are

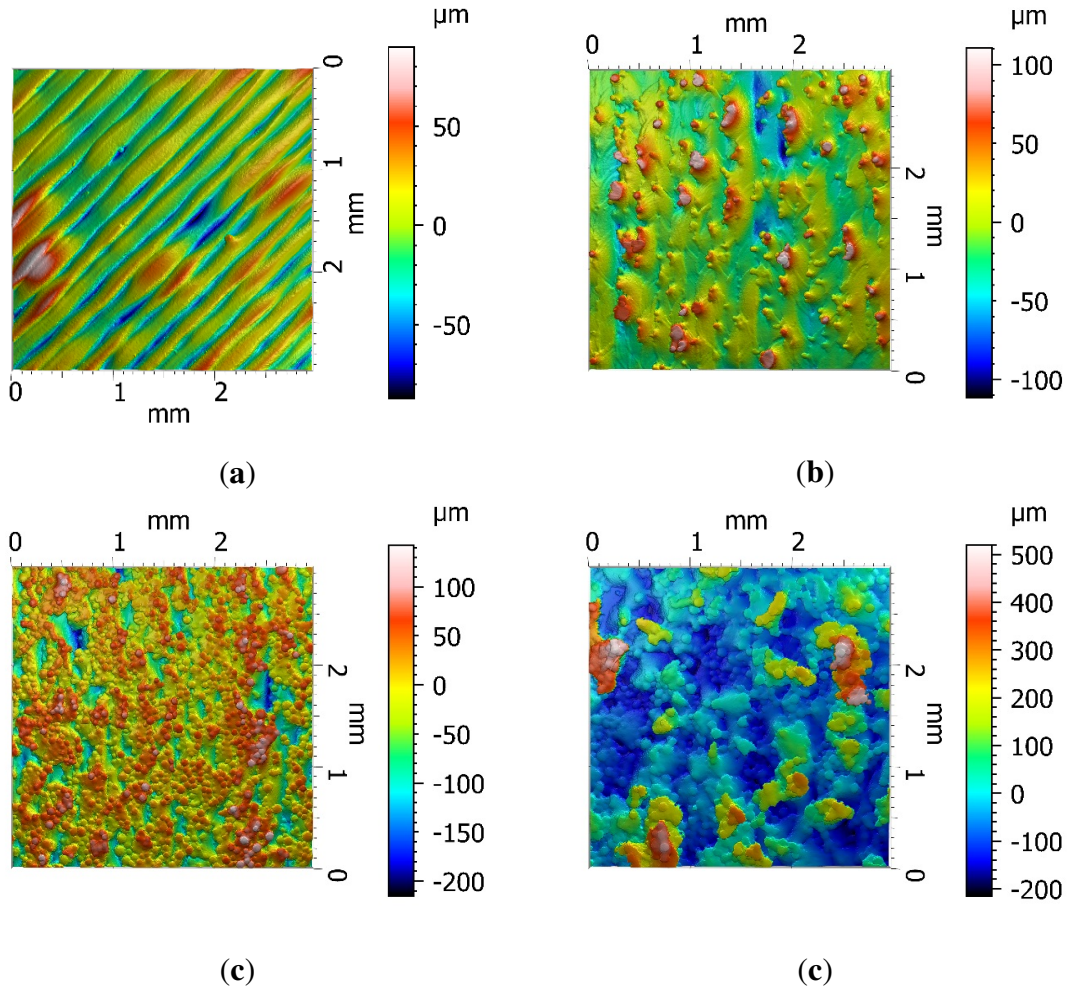

Fig. 5.2 Example levelled surface topography height maps for varying surface orientations: (a) 0° (b) 30°, (c) 90°, and (d) 150°.

dominated by inter-layer bonding with the surrounding powder bed. On the contrary, vertical surfaces are mostly subjected to partial melting and sintering of powder particles adjacent to the part.

5.3.2 Feature-based characterisation

Active contours approach

Active contours is applied to the same surface shown in Figure 5.3a (the same 30° orientation surface previously shown in Figure 5.2b). In Figure 5.3b, the surface has been filtered to

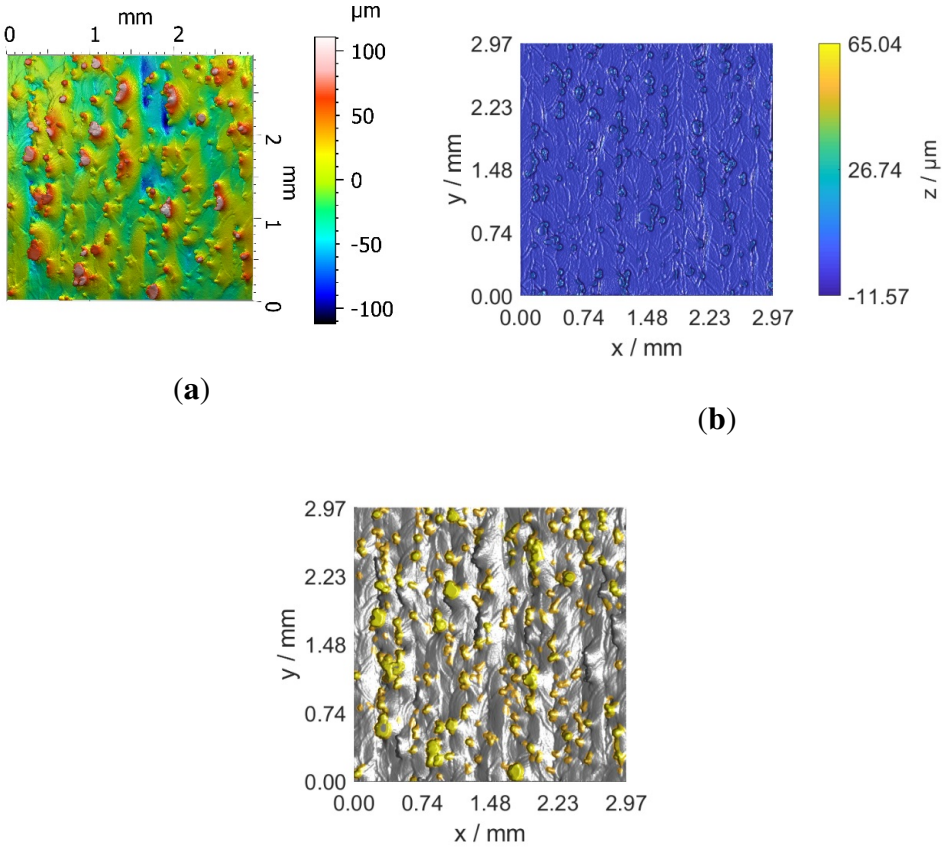

Fig. 5.3 Example application of the active contours method to surface built with 30° orientation; (a) initial surface topography, (b) filtered surface, and (c) results from active contours overlaid on the initial surface topography.

extenuate and pronounce the particles on the surface, as explained in Section 5.2.3 for the creation of the mask needed as the starting point of the active contours algorithm. The results of segmentation are shown in Figure 5.3c.

The application of active contours to all the example datasets shown in Figure 5.3 , results in the segmentations shown in Figure 5.4. For the 0° orientation surface only a small spatter particle is identified. For the rest of the surfaces, there are different types of objects as visually identified in Figure 5.3. For the 30° orientation surface (Figure 5.4b) there are particles identified alongside the edges of the weld tracks and some spatter/particles, with a small number of visible particles not identified as objects. The number of objects is higher in

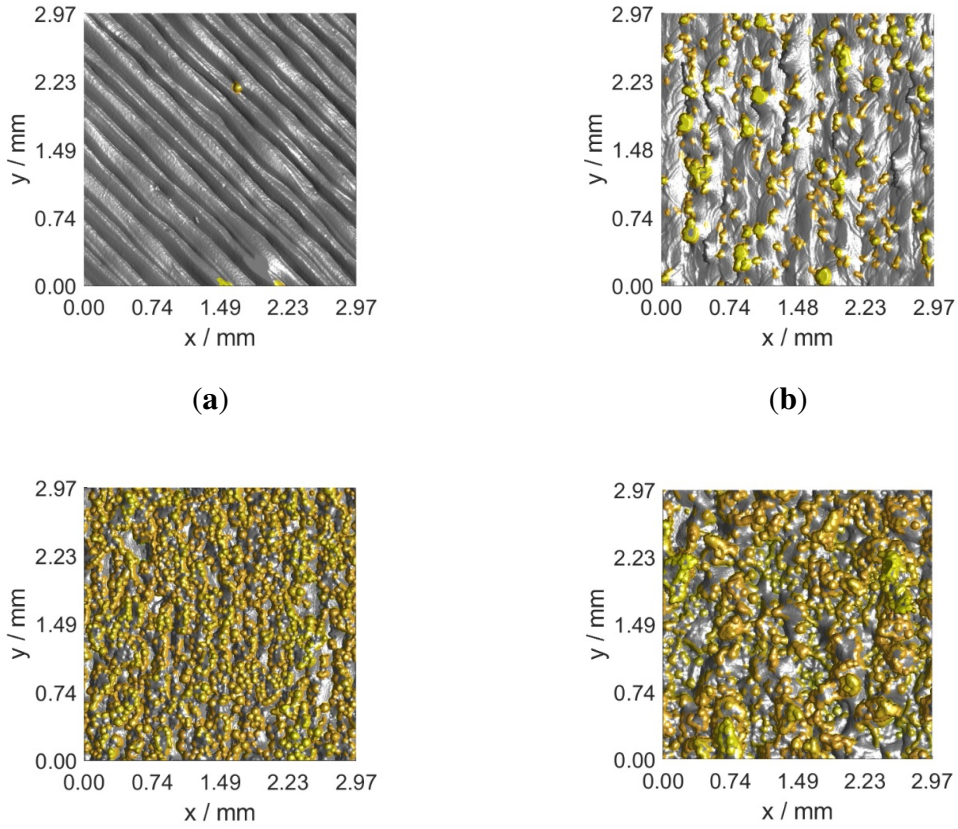

Fig. 5.4 Example segmentation results achieved by the active contours method for surfaces built with (a) 0° orientation, (b) 30° orientation, (c) 90° orientation, and (d) 120° orientation. Yellow highlights a region of an identified particle, whilst the grey represents the rest of the surface.

Figure 5.4c and Figure 5.4d, with the 90° orientation surface possessing a higher number of smaller objects and the 120° orientation surface containing a decrease in number but an increase in size.

Characterisation of feature attributes

The values of the selected feature attributes (as defined in Section 5.2.4) can be visualised using boxplots, as a function of surface orientation. Figure 5.5 shows the number of identified features (feature count). The general trend for feature count is that there is an increasing

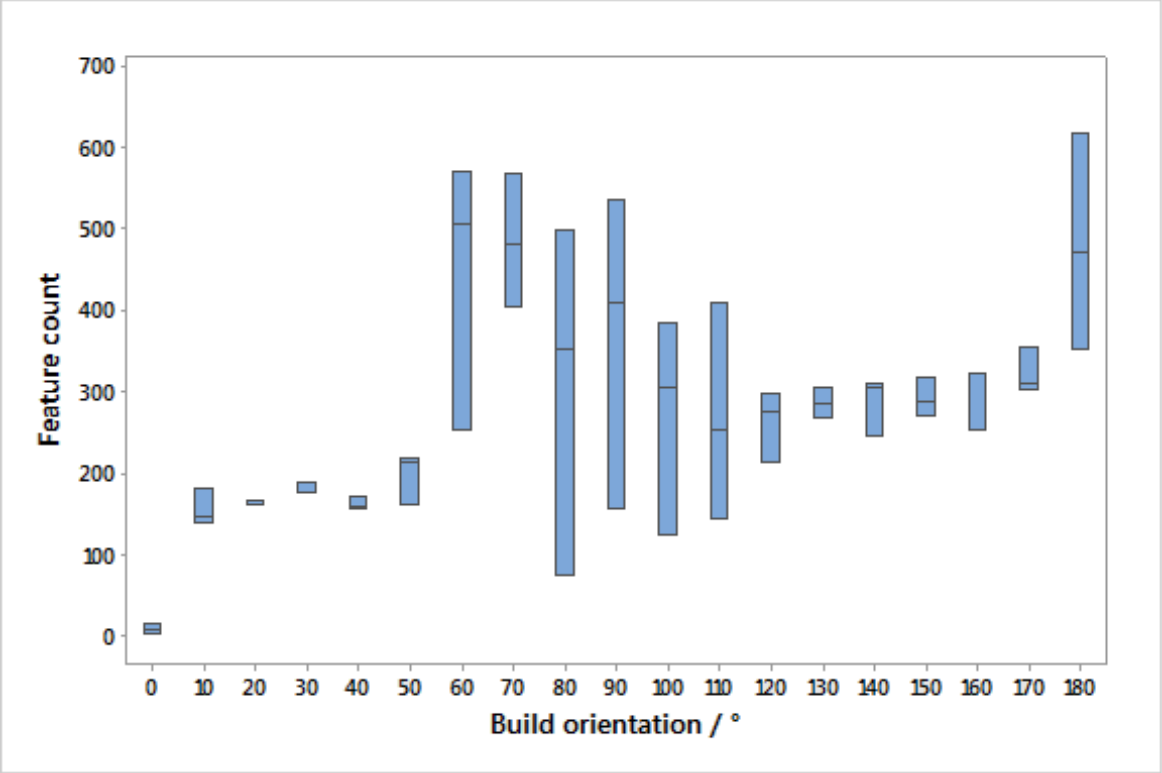

Fig. 5.5 Boxplots of feature count with respect to surface orientation

number of features with increasing build angle; a trend which can also be visualised for the example segmentations results shown in Figure 5.4. Between the 60° to 110° orientation surfaces there is an increase in the dispersion of the results; this may be attributed to the increased difficulty encountered by the segmentation approach in defining the feature boundaries. In fact, at these orientations, there is an increasing number of particles/spatter formations located in clusters or close to the edges of the build layer (producing a visible staircase effect). The proximity of neighbouring particles/spatter formations influences the result of the active contours edge refinement leading to this larger variation, suggesting that the segmentation could be optimised.

The behaviour of the feature height attribute (defined in Section 5.2.4), is illustrated in Figure 5.6. The trend of the attribute value indicates increasing feature height for smaller orientation angle up until to 50°, after which the value decreases and reaches a plateau for

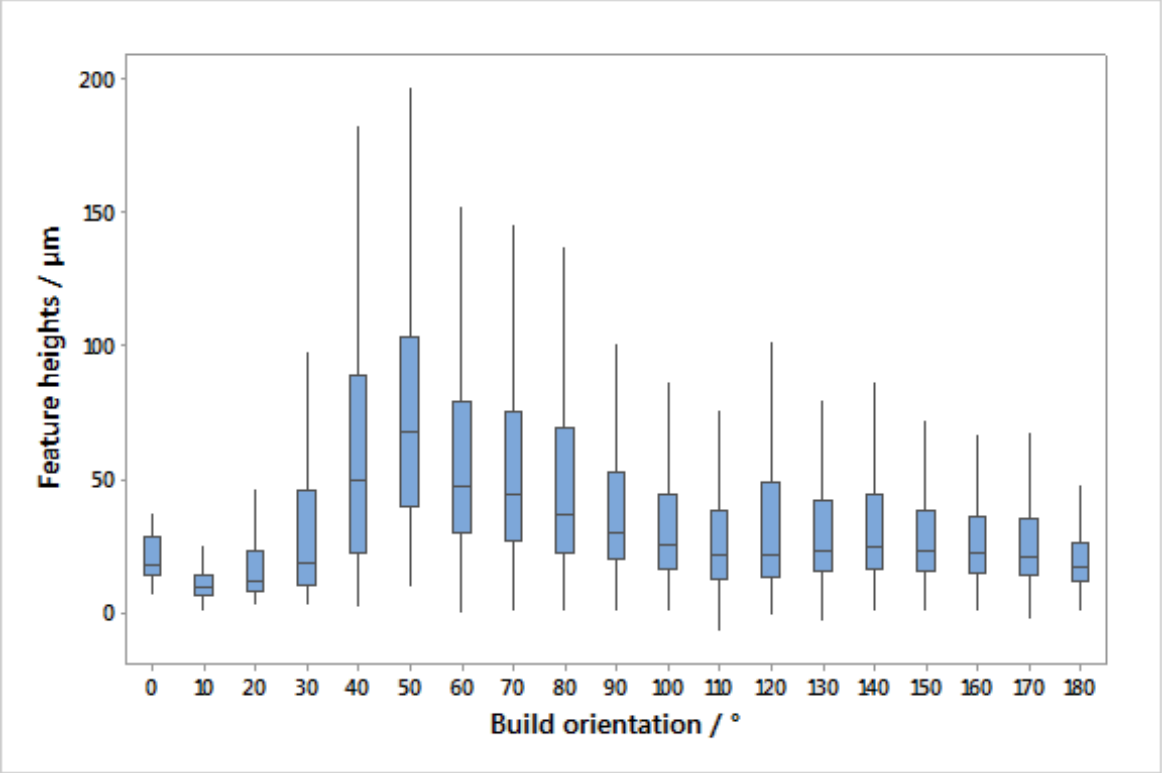

Fig. 5.6 Boxplots of feature height with respect to surface orientation

orientation angles greater than 100°. An explanation for the initial increase of feature height could be the staircase effect confusing the segmentation algorithm: the border of each layer creates a protruded ridge, very well visible on the tilted surface and of height comparable or superior to that of particles and spatter. The segmentation method is therefore tricked into falsely identifying the ridges as if they were large agglomerates of particles thus leading to biased estimations of feature attributes, including feature height. For orientation angles greater than 100°, the surfaces are downward facing within the build chamber, meaning that there is greater occurrence of excess energy penetrating the powder bed leading to sintering and welding of excess powder. As seen in Figure 5.4d, and reflected in the choice of threshold in Table 5.1, the particles/ spatter formations on these surfaces are found at much lower heights, away from the bulk surface, when compared to upwards-facing surfaces (0° to 80° orientation angles).

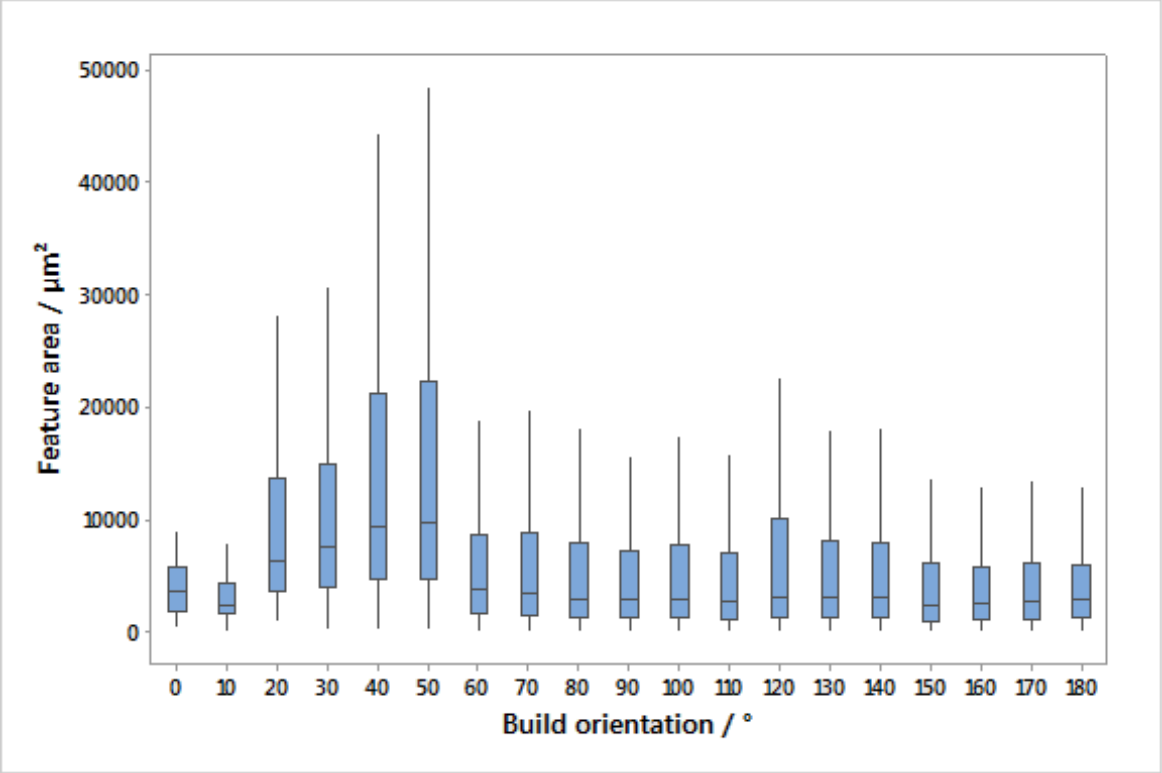

Fig. 5.7 Boxplots of feature area with respect to surface orientation

Feature area, defined in Section 5.2.4 as the area of a topologically isolated feature, is plotted against build orientation in Figure 5.7. Generally, feature areas appear to be somewhat consistent in value across orientations, with some for surfaces between 20° to 50° orientation. The increase takes place at roughly the same orientations where an increase of feature height is observed, which could be interpreted again as an effect of the segmentation algorithm mistakenly identifying staircase ridges as large agglomerates of particles.

Figure 5.8a shows the 30° orientation surface after regions containing the identified particles/spatter formations have been voided to facilitate the computation of texture parameters on the substrate. From this point onwards, this type of surfaces will be referred to as feature-deprived surface, in reference to the fact that the features targeted by the procedure (particles and spatter) have been removed. The total area occupied by the voided regions can be used as a measure of the percentage particle coverage, as the total area occupied by the

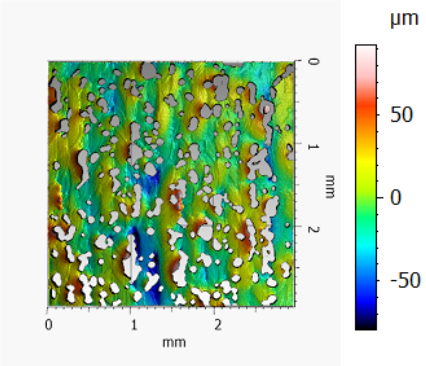

(**a**)

Parameter	Original	Feature deprived	Unit
% particle coverage	0	27.1	%
Sa	8.0	4.3	µm
Sq	12.8	6.5	µm
Ssk	1.09	-0.21	
Sku	8.74	11.4	
Sz	166.0	116.1	µm

(**b**)

Fig. 5.8 Example of characterisation applied to surface built with 30° orientation showing (a) surface topography height map with particles removed, and (b)texture parameter values as computed on the original and feature-deprived surface.

particle and spatter features expressed as a percentage of the measured area, as reported in Figure 5b.

When the feature-deprived surface shown in Figure 5.8a is compared to the original topography still containing all the features (Figure 5.2c), a reduction of height range can be observed, corresponding to the removal of spatter/particles, which are typically protruded on the surface. Such reduction of heights is appreciable by looking at the variations of the texture parameter values, as reported in Figure 5.8b.

Figure 5.9 shows boxplots of the percentage or surface area covered by particles (% particle coverage) with respect to the surface orientation of that surface, computed from three surface regions. For the 0° orientation surface there is almost no coverage, whilst the covered area as a percentage slowly increases steadily up to the 80° orientation surface where it appears to reach a plateau at a coverage between 50 % to 60 %. This trend can be visibly identified on the topographies, as in Figure 5.4, and can also be determined by considering the increasing number of features with respect to surface orientation even though they generally possess a similar distribution of values for feature area, shown in Figure 5.7.

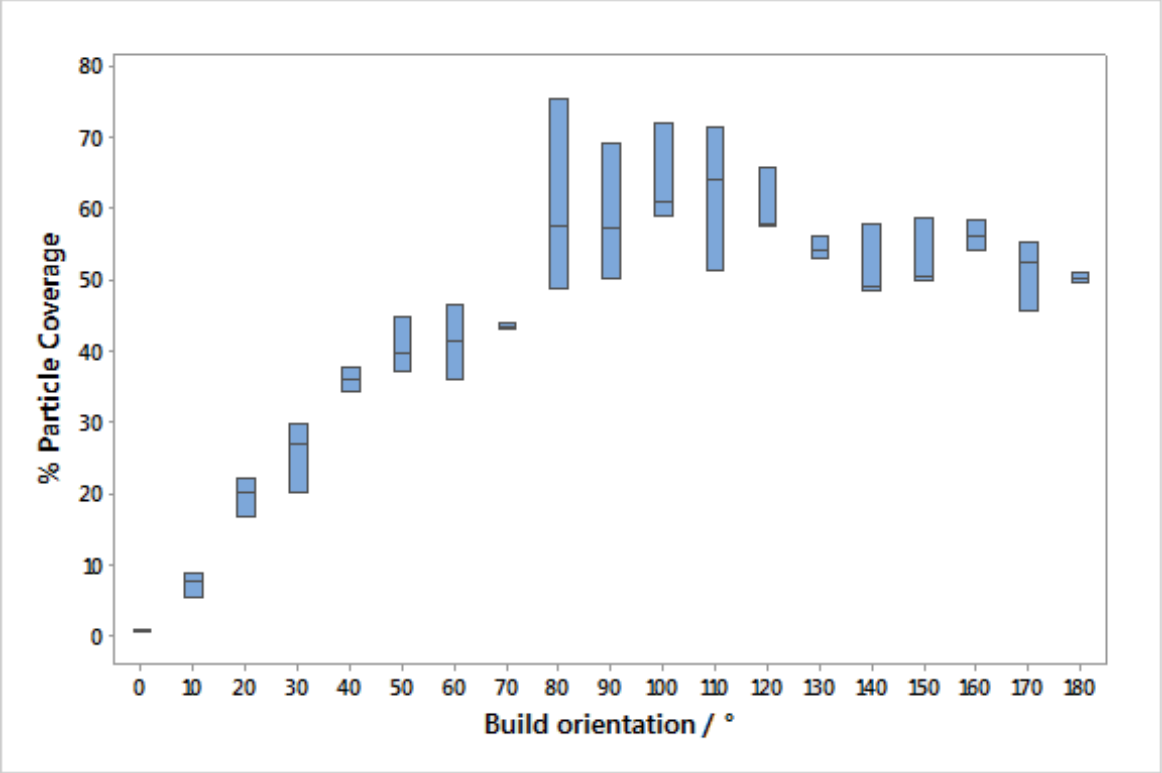

Fig. 5.9 Boxplots of percentage particle coverage with respect to surface orientation

Characterisation of the particle-deprived surface with texture parameters

For the graphs comparing the particle deprived surface to the non-deprived surface, the feature-deprived surface determined by the active contours approach is referred to as surface 'F', whilst the original surface, and thus is conventionally assessed, is referred to as the 'O' surface. Figure 5.8 shows an example surface that has been characterised after particles/spatter has been removed.

Figures 5.10 and 5.11 show the variation of the areal surface texture parameters for *Sa* and *Sq*, respectively. These parameters are some of the more commonly used parameters to assess the surface texture and are both parameters that investigate an average distance from the mean plane. Both trends for the *Sa* and *Sq* show a sinusoidal pattern with respect to surface orientation, with the parameter value generally increasing up to the 70° orientation, decreasing to the 110° orientation, increasing again until the 150° orientation then decreasing

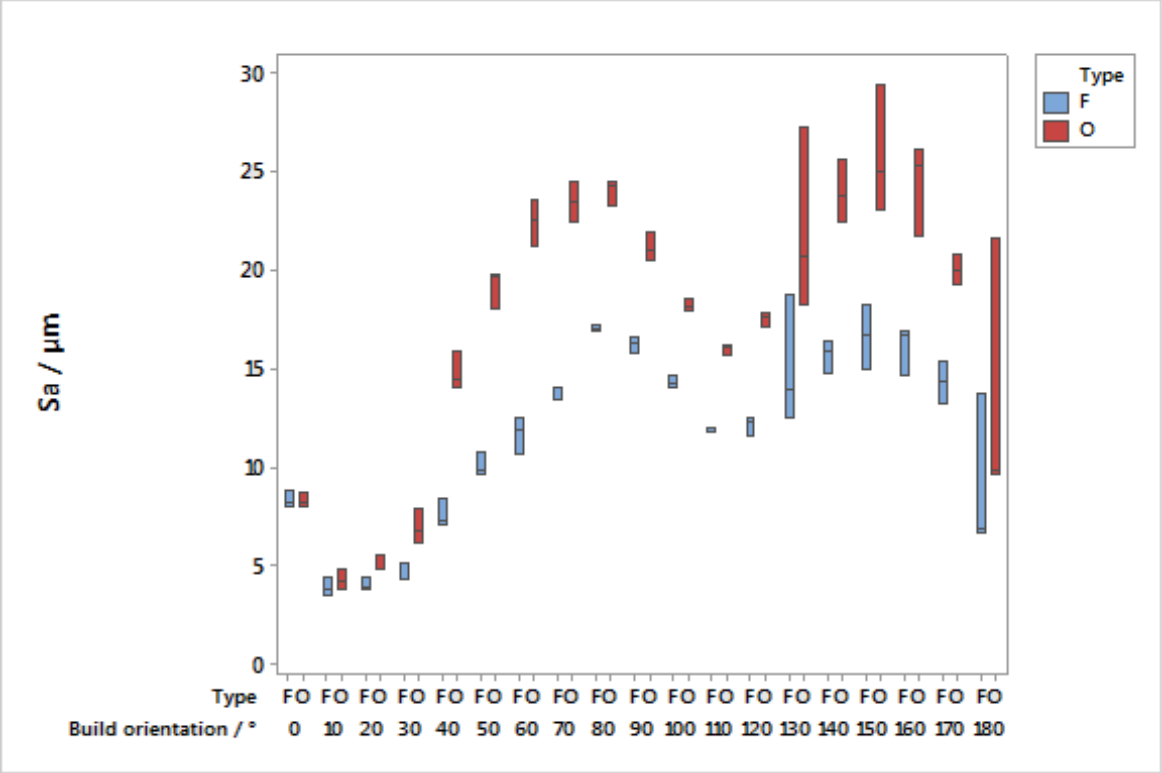

Fig. 5.10 Boxplots of surface parameter, *Sa*, for feature-deprived surface and original surface with respect to build orientation

for both types of surface. Between the feature-deprived ('F') and original ('O') surfaces, there is a general shift of decreased values - suggesting the particles/spatter contributes to these values. There is generally a more significant reduction of parameter values as a result of removing the features after the 50° orientation surface.

For *Sz*, the boxplots with respect to surface orientation can be shown in Figure 5.13. For the parameter, *Sz*, there appears to a general increase in value with increasing build orientation angle. Although not always significant, there is often a reduction of value for *Sz* as a result of removing the particle/spatter features, with a more significant reduction after the 90° orientation surface. As this is an extreme parameter, surface 'F' may be affected by segmentation error and how well the boundaries are defined, with some leftover spikes or walls due to inaccurate particle boundary identification, however, the influence and value of extreme pits may also influence this value. For downward facing surfaces of

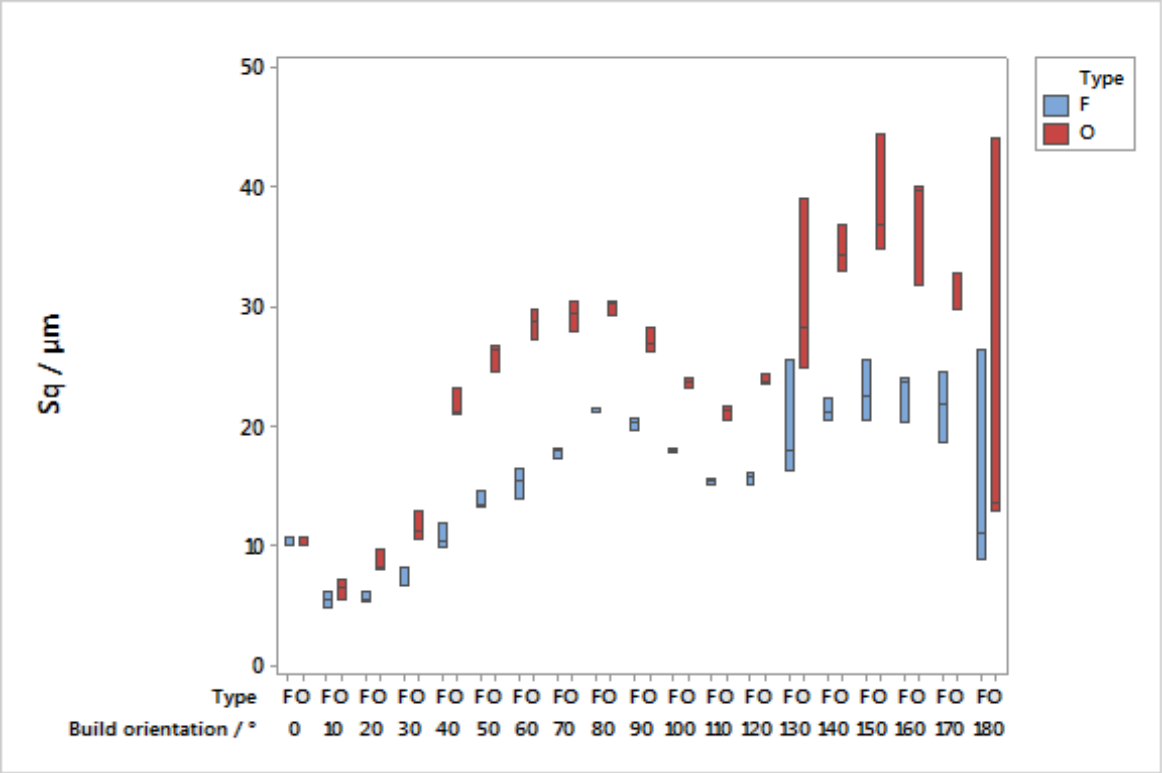

Fig. 5.11 Boxplots of surface parameter, *Sq*, for feature-deprived surface and original surface with respect to build orientation

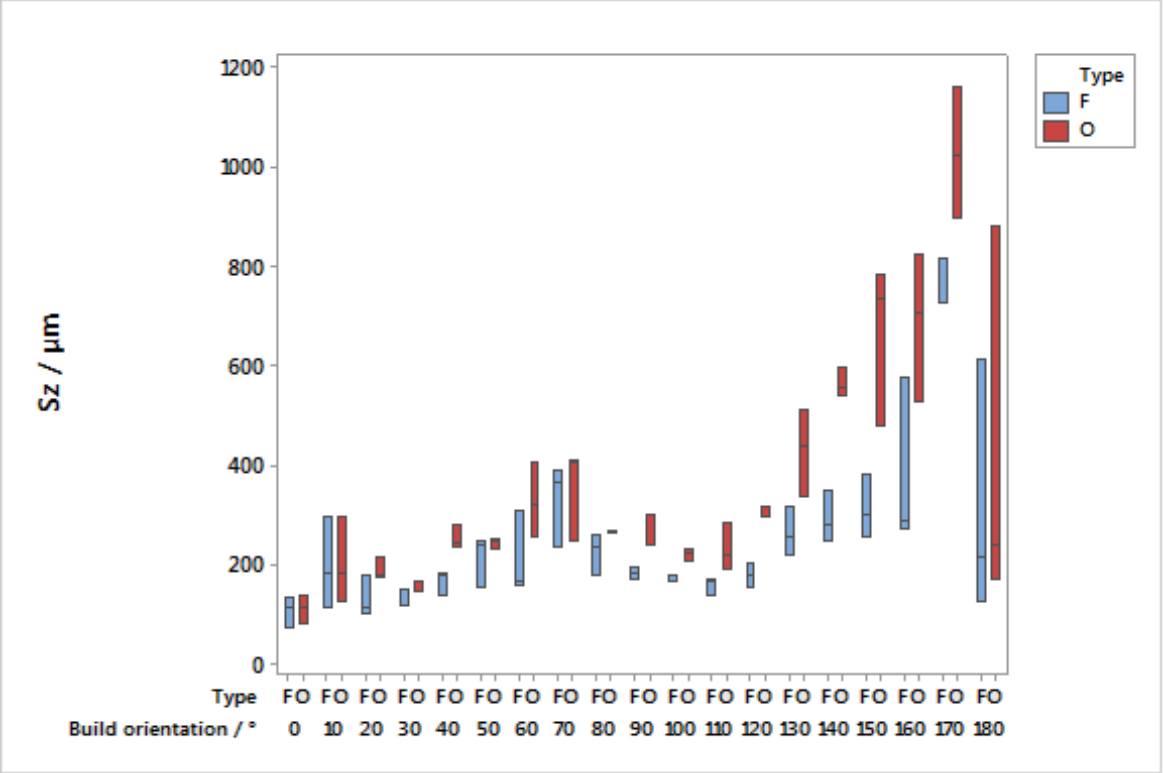

Fig. 5.12 Boxplots of surface parameter, *Sz*, for feature-deprived surface and original surface with respect to build orientation

the original surface (surface 'O'), when melting any build layer above a previous layer, the thermal energy can penetrate further down through the part which increases the probability of sintering particles from the powder bed to the outer surface, contributing to a larger spread of data.

Figure 5.13 and Figure 5.14 show the areal surface parameters for skewness and kurtosis respectively. These parameters characterise the probability distribution of the height values of the topography. Skewness is a measure of symmetry around the mean line, the skewness parameter, *Ssk*, possesses a value of zero for a normal distribution, has negative values when the bulk of the material is above the mean line and positive values when the surface is below the mean line. In Figure 5.13, there is a trend for decreasing values of *Ssk* from 20° to 100° orientation with a small increase in value as the orientation increases after 110° orientation. When comparing the trends between surface 'F' and 'O', removing the spatter/particles shifts

the parameter, *Ssk*, towards lower, and eventually negative, values; which is to be expected because positive height content (particles) are removed from the probability distribution.

Kurtosis is a measure of flatness (or peakedness) of the distribution. *Sku* is a positive value parameter, with values of 3 representing a normal distribution, values higher than this represent a spikier probability distribution and is indicative of a generally flatter surface with spikes, whilst a value lower than 3 represents a flatter distribution and is indicative of a bumpier, but smoother surface. For Figure 5.14, the values of *Sku* is greater than 3 for all surfaces, suggesting that the surfaces are relatively flat with some spikes. For the conventionally assessed surface (surface 'O') between 10° and 170° orientation, the trend is a parabolic centred around 90° orientation with increased values at 10° and 170° orientation. For surface 'F', the particle removed surface has the opposite trend with decreased values at 10° and 170° orientation and the highest values of *Sku* generally around the 90° orientation – the values. The higher values of *Sku* for surface 'F' could be due to the leftover spikes or walls due to inaccurate particle boundary identification.

5.4 Discussion

Feature-based characterisation approaches overcome some limitations of conventional parameters on the assessment of surface topography, by offering assessment of individual topographic formations that can be visualised on the surface as opposed to broad statistical assessments of the height distribution. Feature-based approaches are an information-rich method to describe topography [138], meaning that they can consider the test case and prior knowledge of the process to isolate meaningful components of the surface and better describe the link between surface topography and the parameters of the manufacturing process. With these approaches, the surfaces can be assessed to determine the intensity of finishing required by investigating the proportion of features present that have to be removed, as well as characterise the underlying surface independent of those features. By removing the particles/spatter

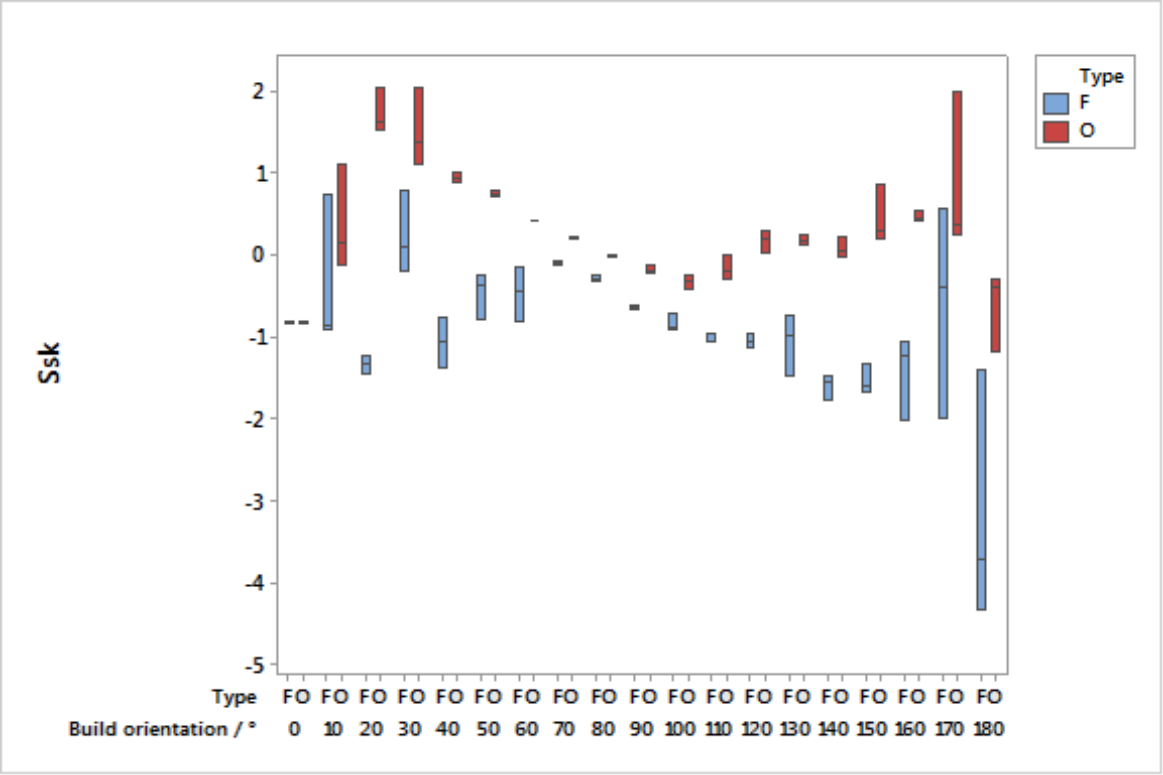

Fig. 5.13 Boxplots of surface parameter, *Ssk*, for feature-deprived surface and original surface with respect to build orientation

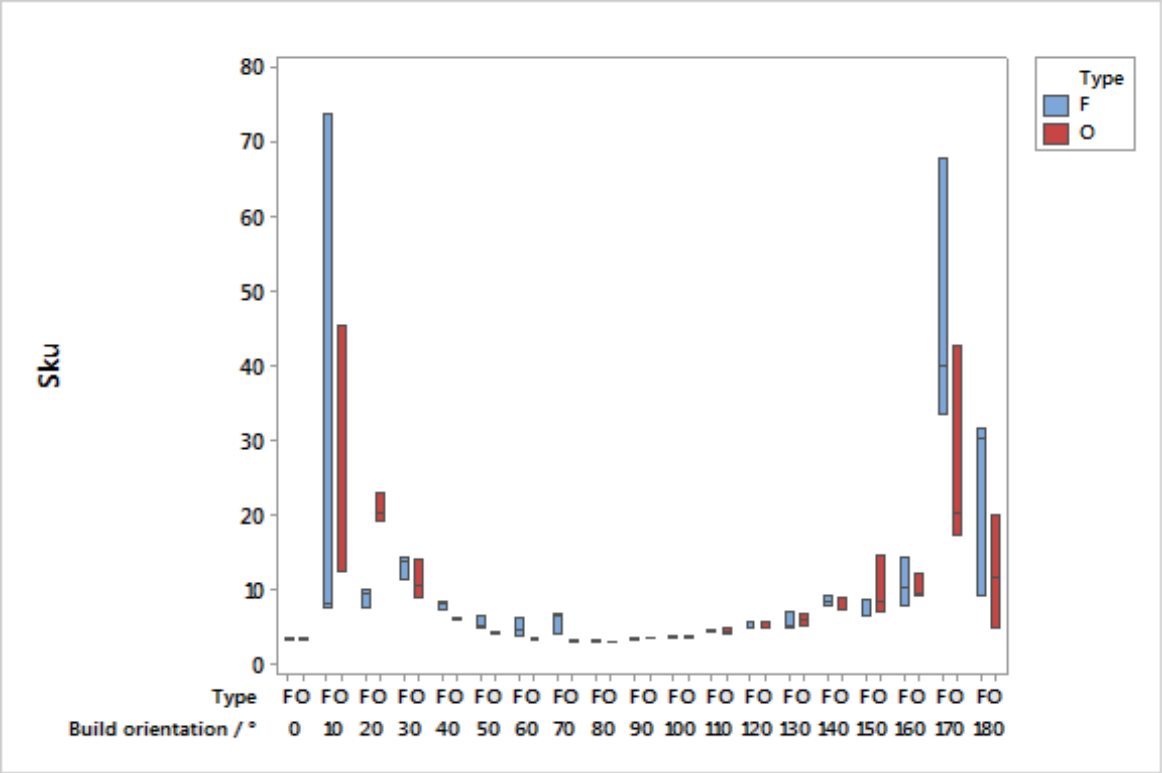

Fig. 5.14 Boxplots of surface parameter, *Sku*, for feature-deprived surface and original surface with respect to build orientation

and observing the changes in the values of surface parameters, the weighting of these features on the surface parameters can be understood.

The complications and limitations with feature-based approaches are on how to present the resultant information. The results of the feature-based characterisation depend on how the features and dimensional attributes are defined. Operators must always make considerations on how they define a feature within the topography, ensuring that the segmentation approach meaningfully determines the boundaries of these features. The dimensional assessment of percentage coverage and other attributes of the features also require definition, to ensure that meaningful parameters can be extracted and compared. One consideration when considering any results for a particle removed surface is that with larger percentages of removed particles (such as those at higher orientations) the surface has less data-points from which to calculate a parameter, which can contribute to an increase in error.

5.5 Conclusion

- Active contours segmentation enables the extraction and characterisation of signature features of the EBPBF process.
- As the surface orientation with respect to build increases, so does the complexity of the surface.
- Generally, the number of particle-like features appears to increase with build orientation.
- When removing features from the topography, there is generally a significant reduction in the *Sa* and *Sq* parameters.

- Future work would compare the feature-deprived results to surfaces subject to particle-removing finishing operations to verify the characterisation results of the underlying surface.

Active contours segmentation enables the extraction and characterisation of signature features of the EBPBF process. With this, a better understanding of the link between the surface topography and parameters of the manufacturing process can be obtained in comparison to conventional surface texture characterisation. Feature-based characterisation using active contours has been applied to surfaces with varying surface orientations, showing a trend for increasing proportion of particles/spatter with increasing surface orientations. Future work would see this approach applied to finished AM components to assess whether surface texture parameters for the underlying surface can be accurately determined and characterised. In addition, the segmentation methods could be used to target other signature features of the PBF.

Chapter 6

Monitoring the evolution of surface topography

The work in this chapter has been presented at the euspen conference in Venice [122].

6.1 Introduction

Finishing operations are applied for a variety of reasons to additively manufactured (AM) components, such as for the removal of supports, part accuracy improvements and other surface texture improvements [1]. Operations, such as shot peening [26], grinding [29] and laser polishing [114], are often applied to improve the surface quality of AM parts. It is known that finishing operations applied to a surface leave a characteristic "fingerprint" related to the operation itself. Examples are shot craters (as a result of shot peen size and shape), the uncovering of sub-surface features and creation of tool marks (as a result of the grinding process removing the upper surface, until the bulk material is reached), the appearance of weld tracks and re-melt features (as a result of the re-melt laser strategy) [114].

Commonly, areal surface texture parameters, such as those given in ISO 25178-2 [57, 40] are used to describe a change in surface topography as a reduction or increase in nominal

value. However, texture parameters only quantify an overall change of textural properties, and are often not suitable to capture the changes that individual surface topography formations (surface features) undergo during the modification process. In the literature on finishing operations applied to AM surfaces, qualitative assessments of changes pertaining to surface features are often performed through visual observation of, for example, images taken via optical or scanning electron microscopy. However, rigorous, quantitative techniques to perform such assessment from measured data, other than computing texture parameters, are currently lacking. Topography measuring instruments are now capable of acquiring areal topography information to a high level of detail [40], so that geometrical and dimensional information pertaining to individual topography features can now, at least in theory, be processed.

In this work, the possibility to apply feature-based characterisation to the investigation of topography modifications occurring as a consequence of finishing operations in AM processes is investigated through the development of an original approach. The approach consists of the following steps:

- A sample specimen is designed, featuring one or multiple custom surface features designed to survive the finishing process with minimal modifications. These features are designed to act as relocation landmarks.
- The sample is manufactured, measured as-is, subjected to the finishing operation, and then re-measured.
- The landmark features are used to relocate the two measured datasets with respect to each other.
- Feature-based characterisation is used to identify and isolate the topographic formations of interest, and track their evolution through the modification process.

The approach is illustrated as it is applied to investigate the topography evolution of samples fabricated via electron beam powder bed fusion (EBPBF), and subjected to a variety of finishing processes, including shot peening, grinding and laser polishing.

6.2 Methodology

6.2.1 Samples

A titanium alloy (Ti6Al4V) block was fabricated by EBPBF using the Arcam A2XX. The block dimensions are (35 × 25 × 75) mm built at 0° orientation.

6.2.2 Relocation landmarks

Through practical investigation, micro milling can be applied to the AM surface with limited effects on the local topography. (1 × 0.5) mm rectangles with rounded corners were milled to a depth of 300 µm over the additive surface to act as fiducial markers. The bottom surface of these features is used for vertical alignment and applied in an L shape to give three areas to level from. The layout of the relocation landmarks and the principle for preserving them are shown in Figure 6.1.

6.2.3 Measurement strategy

Measurement is performed using the Alicona G5 focus variation (FV) microscope instrument [44], which has been optimised using the work found in Chapter 3.1. The following settings for the FV instrument are adopted: 20× objective lens (NA 0.4, field of view (0.81 × 0.81) mm); lateral resolution: 3.51 µm; vertical resolution: 12 nm; ring light illumination; measured area (5 × 5) mm, stitched.

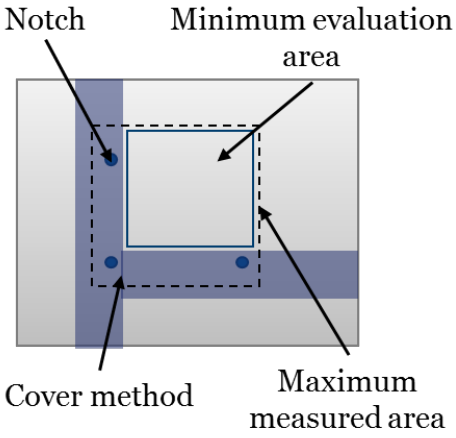

Fig. 6.1 Layout of relocation landmarks showing measured area and covered regions

Table 6.1 Finishing operations and key parameter values

Finishing operation	Key parameters and values
Shot peening	ASH110 cast steel shot approx. 280 μm Ø, Almen intensity 0.2 mm to 0.25 mm A, 200% coverage, 0° impact angle
Grinding	P80 grit flap wheel, 100 mm/s spindle speed, 0° attack angle, 12 N contact force, 3 passes
Laser polishing	500 W 1090 nm laser, 350 μm spot size, 225 W laser power, 30 μm hatch, 500 mm/s scan speed, 0° angle from nominal, argon shielding

6.2.4 Finishing operations

Finishing is then applied to the surface using the following techniques and parameters which were deemed optimal from previous evaluation, shown in table 6.1. The affected area is to be suitably contained as to not interfere and damage the fiducial markers.

6.2.5 Re-measurement and registration of topographies

Re-measurement is performed using identical measurement settings, with the fiducial markers used to identify the approximate region for re-measurement.

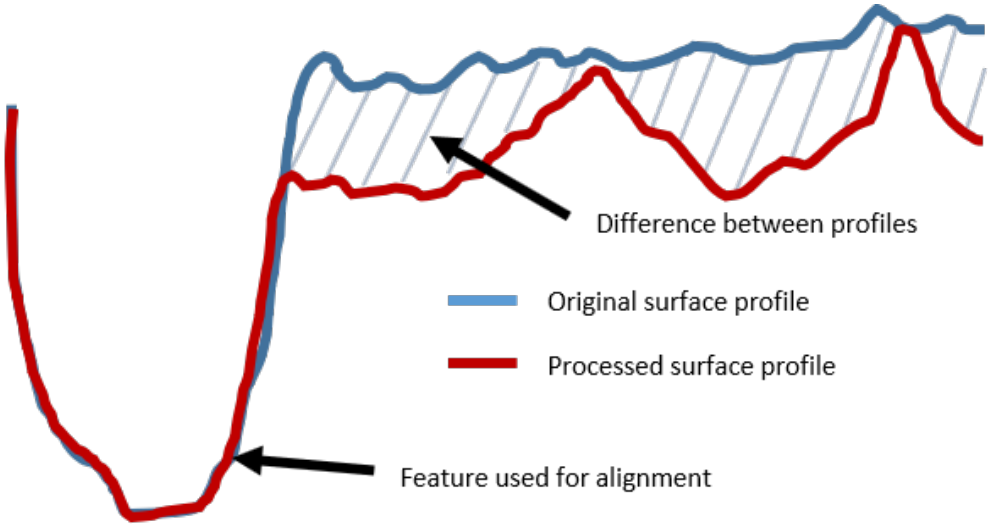

Fig. 6.2 Principle for the alignment of two topographies using a measured reference geometry

Alignment is performed following the methodology found in [48] and [83]. The notches on both surfaces were used as reference geometry to align the pre- and post-finished surfaces using the unaffected regions to provide alignment in x,y and z (see Figure 6.2). These notch pairs (between the pre- and post-condition) are used to offer coarse alignment of the two surfaces, which is then followed by iterative closest point alignment. This procedure determines the transform required to align the initial topography (used as a fixed reference) and the processed surface with six degrees of freedom (which includes a z alignment). The transformation value is used on the post-finished surface and a raster scanning procedure is applied to output an aligned topography in the same coordinate system as the fixed reference surface. With these aligned topographies, the same (3×3) mm area is extracted from both topographies over the area that is affected by the finishing process.

6.2.6 Surface texture characterisation

Conventional analysis is performed on an extracted region of the as-built surface and finished surface. Using MountainsMap by DigitalSurf [126], an F-operator is applied by levelling the least-squares mean plane, followed by an applied S-filter at nesting index of 5 µm and an

L-filter at nesting index of 0.8 mm. Areal surface texture parameters *Sa*, *Sq*, *Ssk*, *Sku* and *Sz* were used to quantify the surface texture [9]. These parameters were compared both before and after finishing. The material ratio curve is also plotted for the heights on the levelled surfaces (pre- and post-finishing) on the levelled surface.

6.2.7 Feature-based evaluation of surface topography

After alignment, an active contours approach (as found in Chapters 4 and 5) is applied to the surface topographic data of the side surfaces to identify and isolate particle/spatter features on the AM as-built surface. Feature attributes, such as feature height were computed on the as-built surface. For the post-finishing surface, the segmentation map of the as-built (pre-finished) surface is overlaid and feature properties were computed to compare the influence of the finishing operation on these features.

Segmentation is performed using active contours, similarly applied in Chapters 4 and 5. In order to create the initial mask for the active contour procedure, the surface topography was subject to an S-filter with nesting index of 5 μm and an L-filter with nesting index of 70 μm. This index was chosen through experimentation to accentuate particles on the surface (diameters typically between 45 μm to 100 μm [11]), to remove a significant part of any larger topographical features. On the SL surface, a height thresholding operation was applied at the *Smr*1 (corresponding to the lowest height boundary of the surface peak region), meant to isolate the topmost regions of the filtered topography, most likely belonging to protruded formations, such as spatter and particles. Using the threshold mask as the initial guess, active contours was run using 100 iterations, and the geodesic 'edge' method [132] with negative contraction bias (leading to outwards growth of the contour) - see Section 4.2.4.

The segmentation mask for the pre-finished surface is applied to both the pre- and post-finished surfaces in order to evaluate properties of features as they evolve as a result of the finishing operation. Using the segmentation masks and the height information of the initial

levelled topography, the feature height, absolute height of the top of the feature and absolute height of the bottom of the feature are computed. The feature height is algorithmically determined using a material ratio curve applied to only the heights of the individual feature. From this material ratio curve, the fitted maximum height value (the absolute feature height at the top) is subtracted from the fitted minimum height value (the absolute feature height at the bottom) resulting in the feature height.

6.3 Results

6.3.1 Surface texture characterisation

0° orientation surface - linishing

Figure 6.3a and 6.3b shows the aligned topographies of the pre- and post-linished region with the same coordinate system. What can be seen is that there is a large change between the two topographies and a noticeable drop in height as a result of the linishing tool removing the upper layer, and this affect is noticable in Figure 6.3c and 6.3d, the material ratio curves. There is a valley region on the surface that appears to have 'survived' the machining process in the initial topography, however, this is not as visible in the filtered surfaces (Figures 6.3e and 6.3f). The as-built surface topography is characterised by the presence of weld tracks which become clearer when filtered, whilst the linished surface is characterised by the presence of machining marks.

Between the parameters, there is a change in *Ssk* and *Sku*, which is visible in the material ratio curves, but almost no change in the parameters *Sa* and *Sq*. The *Sz* parameter shows a lower value for the linished surface, however, this result has been skewed by the presence of the large and deep machining defect.

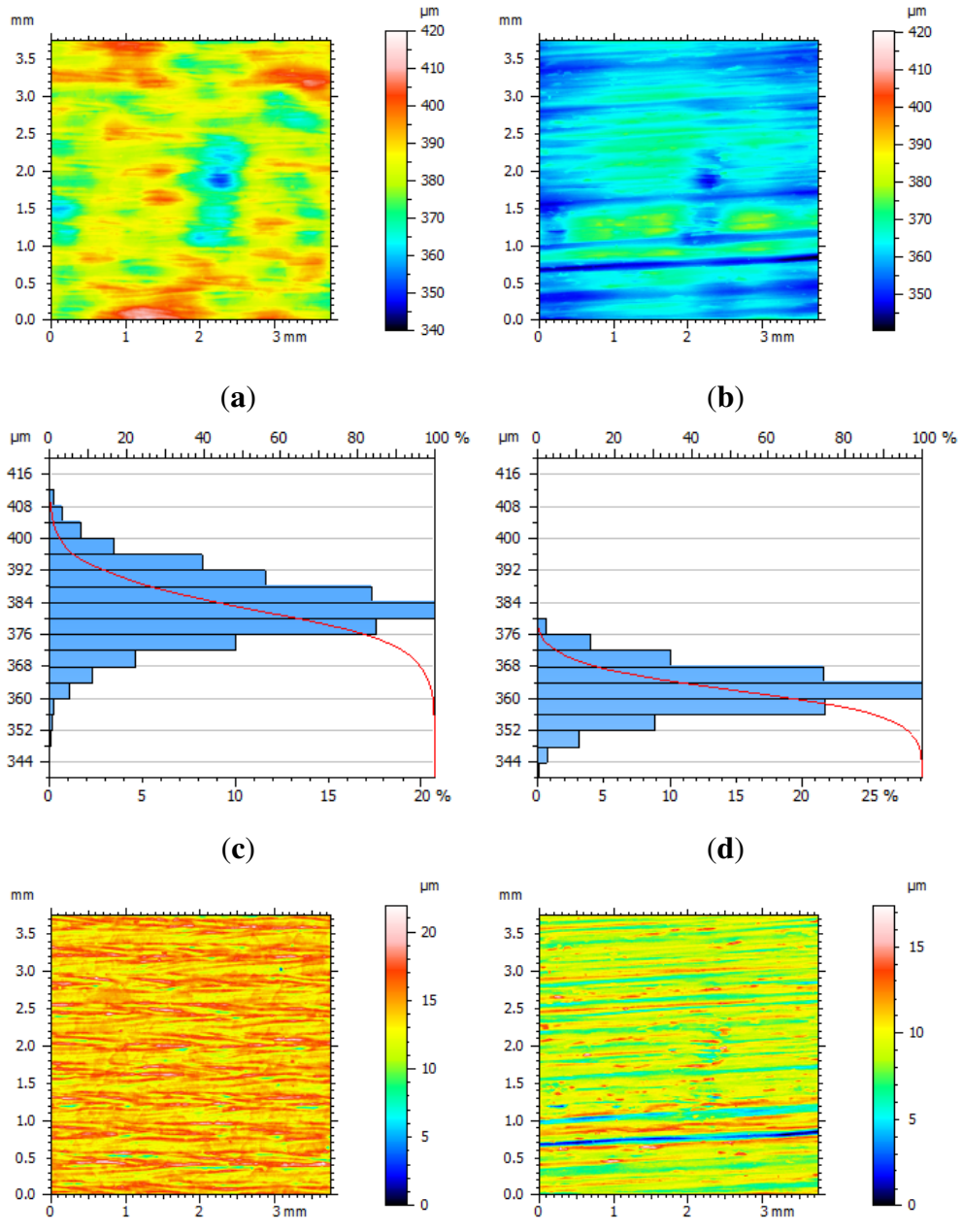

(g)

Parameter	Value	Unit
Sa	1.3	µm
Sq	1.7	µm
Ssk	-0.01	
Sku	3.57	
Sz	21.9	µm

(h)

Parameter	Value	Unit
Sa	1.3	µm
Sq	1.8	µm
Ssk	-0.396	
Sku	4.72	
Sz	17.4	µm

Fig. 6.3 Surface characterisation of 0° surface subjected to linishing, showing: the surface topography height maps of the (a) measured pre- surface and (b) measured post- surface; the material ratio curves of (c) measured pre- surface and (d) measured post- surface; the surface topography height maps of the (e) filtered pre- surface and (f) filtered post- surface; and the characterisation results of the (g) filtered pre- surface and (h) filtered post- surface.

0° orientation surface - laser polishing

Between the pre- and post-laser polished surfaces (Figures 6.4a and 6.4b respectively), there is a large change as a result of the finishing process, with the post-laser polished surface possessing no weld tracks from the as-built scanning strategy. It is also clear that there has been some material build-up as a result of the laser polishing; there also appears to be a component of waviness similar between the topographies. The material ratio curves for the levelled measured surfaces (Figure 6.4c and Figure 6.4d) represent this build-up of material for the laser-polished surface, however, they do somewhat fall within the same absolute heights between processes, suggesting the surface is generally 'evolved' by the process and is not just simply removed (as compared to linishing). The characteristic toolmarks of the as-built surface (more clearly shown in Figure 6.4e) and the laser polished surface (shown in Figure 6.4f) are similar in that they are weld tracks, however, the size and scale is clearly different as a result of the difference between the beam settings between the AM system and the post-processing system. Figures 6.4g and 6.4h show a significant reduction in values for surface parameters *Sa* and *Sq* between the pre- and post-laser polished surface, the difference between the *Ssk* and *Sku* is also visible in the material ratio curves. The maximum height parameter, *Sz*, does appear to increase after laser polishing, however, this does appear to be a result of a small defect valley produced which can skew the value of the parameter.

0° orientation surface - shot peening

Shot peening applied to the 0° orientation surface (shown in Figure 6.5b) appears to preserve the underlying waviness components whilst reforming the weld tracks seen in the pre-shot peened surface (Figure 6.5a). Figures 6.5c and 6.5d show the material ratio curves for the pre- and post-shot peened surfaces respectively that does not appear to have a large change in the overall distribution of heights, apart from a very small reduction in values at the upper heights of the surface - a result of the shot peening stamping the upper heights of the surface.

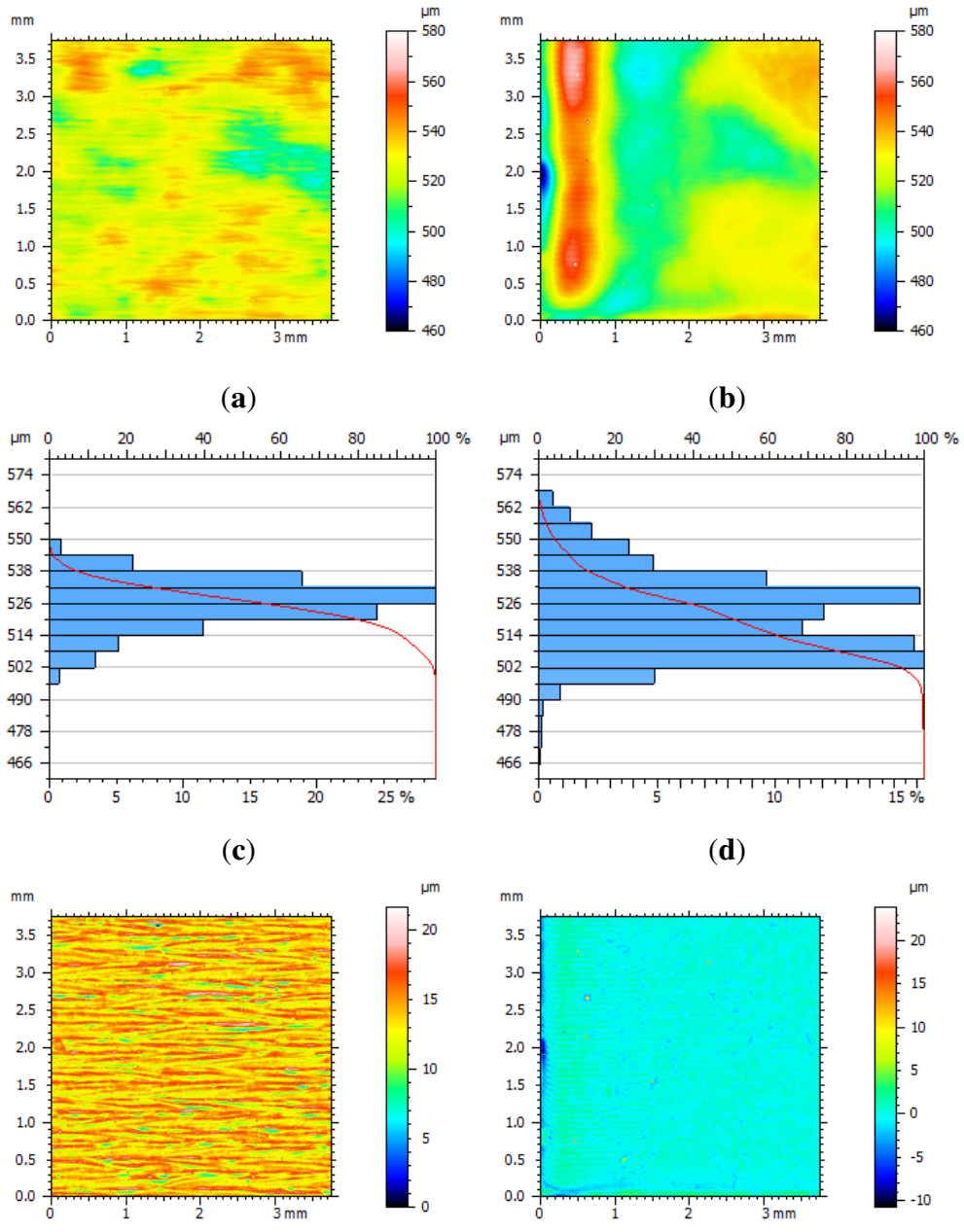

Parameter	Value	Unit
Sa	1.4	µm
Sq	1.9	µm
Ssk	-0.197	
Sku	3.67	
Sz	21.6	µm

(g)

Parameter	Value	Unit
Sa	0.5	µm
Sq	0.8	µm
Ssk	1.57	
Sku	60.5	
Sz	34.7	µm

(h)

Fig. 6.4 Surface characterisation of 0° surface subjected to laser polishing, showing: the surface topography height maps of the (a) measured pre- surface and (b) measured post-surface; the material ratio curves of (c) measured pre- surface and (d) measured post- surface; the surface topography height maps of the (e) filtered pre- surface and (f) filtered post-surface; and the characterisation results of the (g) filtered pre- surface and (h) filtered post-surface.

Between the filtered surfaces, the shot-peened surface (Figure 6.5f) shows crater-like features as a result of the impact of the metal shot, and when compared to the pre-shot peened surface (Figure 6.5), there appears to be remnants of the weld tracks. For the parameters results tables (Figures 6.5g and 6.5h) there isn't much change between these surfaces apart from the *Ssk*, which is reflected in the change of the upper heights in Figure 6.5d.

90° orientation surface - linishing

The 90° orientation (side) surfaces are dominated by particles/spatter (see Figure 6.6a). When subjected to an automated linishing process (Figure 6.6b) there are some flattened regions that correspond to the locations of some particle/spatter regions that sit higher on the surface; it appears the machining settings were not optimised for this surface test case as many lower regions on the surface still possess the same surface as the as-built condition. The effect of the linishing operation in removing material at the top of the surface is visible when comparing the material ratio curves (Figures 6.6c and 6.6d) with a large shift of heights downwards where the material is removed by the linishing process. For the filtered surfaces, there are similar features of particles and spatter in both the pre-linished surface (Figure 6.6e) and the post-linished surface (Figure 6.6f) as the finishing process has not effectively removed all of these features. In Figure 6.6, there are visible plateau regions with machining toolmarks as seen in the initial topography, reducing the range of heights in the finished surface. As the finishing process was not optimal, there is only a small reduction in the areal height parameters, *Sa*, *Sq* and *Sz* as expected with a process that removes the upper heights of the surface seen between Figures 6.6g and 6.6h. For the areal surface texture parameters, *Ssk* and *Sku*, there is not enough change in the overall distrubtion of heights (visualised in the material ratio curves) to lead to large changes in these parameters between surface condition.

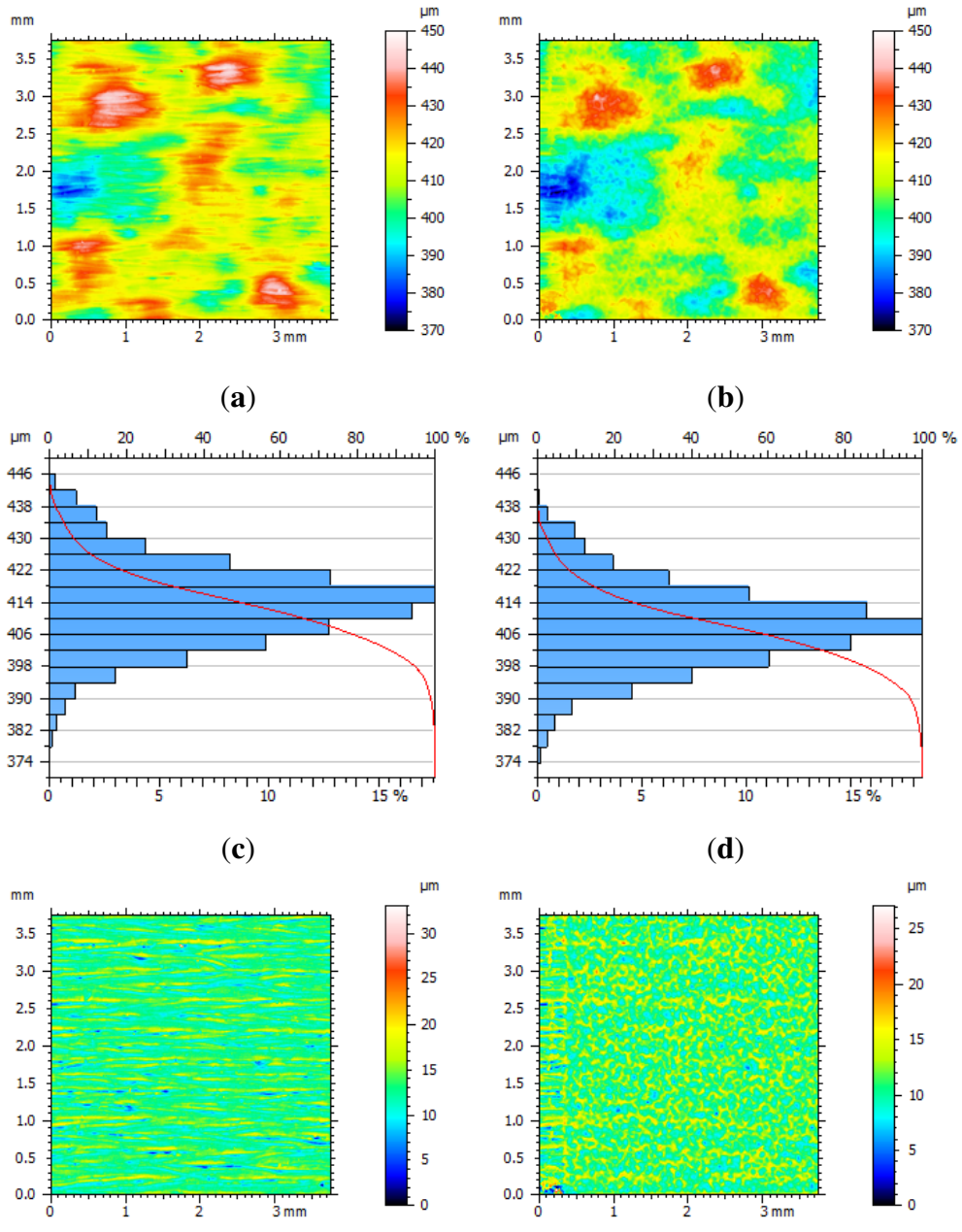

(**a**) (**b**)

(**c**) (**d**)

(**e**) (**f**)

Parameter	Value	Unit
Sa	1.4	µm
Sq	1.9	µm
Ssk	-0.12	
Sku	4.24	
Sz	33.0	µm

(**g**)

Parameter	Value	Unit
Sa	1.4	µm
Sq	1.8	µm
Ssk	0.184	
Sku	3.98	
Sz	27.1	µm

(**h**)

Fig. 6.5 Surface characterisation of 0° surface subjected to shot peening, showing: the surface topography height maps of the (a) measured pre- surface and (b) measured post- surface; the material ratio curves of (c) measured pre- surface and (d) measured post- surface; the surface topography height maps of the (e) filtered pre- surface and (f) filtered post- surface; and the characterisation results of the (g) filtered pre- surface and (h) filtered post- surface.

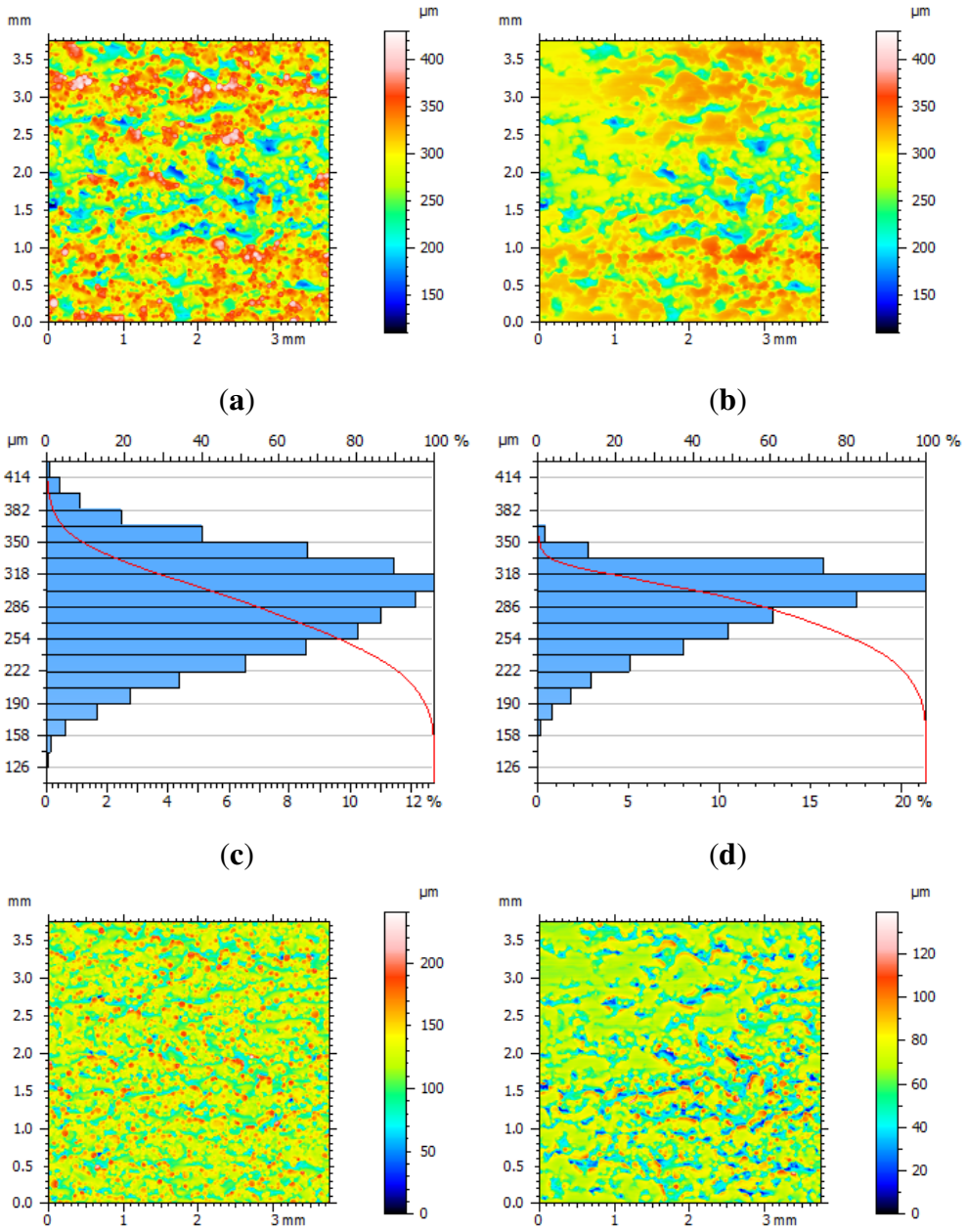

Parameter	Value	Unit
Sa	19.8	µm
Sq	25.0	µm
Ssk	-0.06	
Sku	3.03	
Sz	240	µm

(g)

Parameter	Value	Unit
Sa	12.4	µm
Sq	16.1	µm
Ssk	-0.482	
Sku	3.40	
Sz	139	µm

(h)

Fig. 6.6 Surface characterisation of 90° surface subjected to linishing, showing: the surface topography height maps of the (a) measured pre- surface and (b) measured post- surface; the material ratio curves of (c) measured pre- surface and (d) measured post- surface; the surface topography height maps of the (e) filtered pre- surface and (f) filtered post- surface; and the characterisation results of the (g) filtered pre- surface and (h) filtered post- surface.

90° orientation surface - laser polishing

The levelled measured topography of the pre- and post-laser polished 90° orientation surfaces are shown in Figures 6.7a and 6.7b respectively. The pre-laser polished surface is typical of an as-built side surfaces (as in Figure 6.6a) and dominated by particles/spatter, whilst the laser-polished surface shows a significant change in the topographic formations on the surface; instead dominated by laser remelting weld tracks. There is preservation of the underlying waviness of the surface, with both the pre- and post-laser polished surface showing a similar region of lower heights in the centre of the height map. There is a significant change in the distribution of heights as result of the laser polishing (comparing Figure 6.7c and 6.7d), with the post-laser polished material ratio curve having a smaller distribution and a lower mean value than the pre-laser polished material ratio curve; this significant change in topography is also shown in the filtered surface topography height maps. Figure 6.7e shows particle/spatter features with a large range of height, compared to Figure 6.7f, which is completely devoid of particle/spatter and is replaced with only the resultant surface of the scanning strategy. For the areal surface texture parameters (Figure 6.7g and 6.7h), there is a significant reduction in the values for Sa, Sq and Sz as a result of the laser-polishing; remelting characteristically causes the particle/spatter material to flow.

90° orientation surface - shot peening

The effect of shot peening on the 90° orientation surface can be visualised by comparing Figure 6.8a (pre-shot peened) to Figure 6.8b (post-shot peened). As a result of the shot peening process, there is a reduction of the top heights of the surface with preservation of the overall waviness and regions of the bottom surface; due to the difficulty of shot peening in penetrating recesses, which is dependent on the size of the shot. The material ratio curves (Figures 6.8c and 6.8d) also show a reduction of heights at the upper regions of the surface, with a more significant shift than found for the 0° orientation surface finished using shot

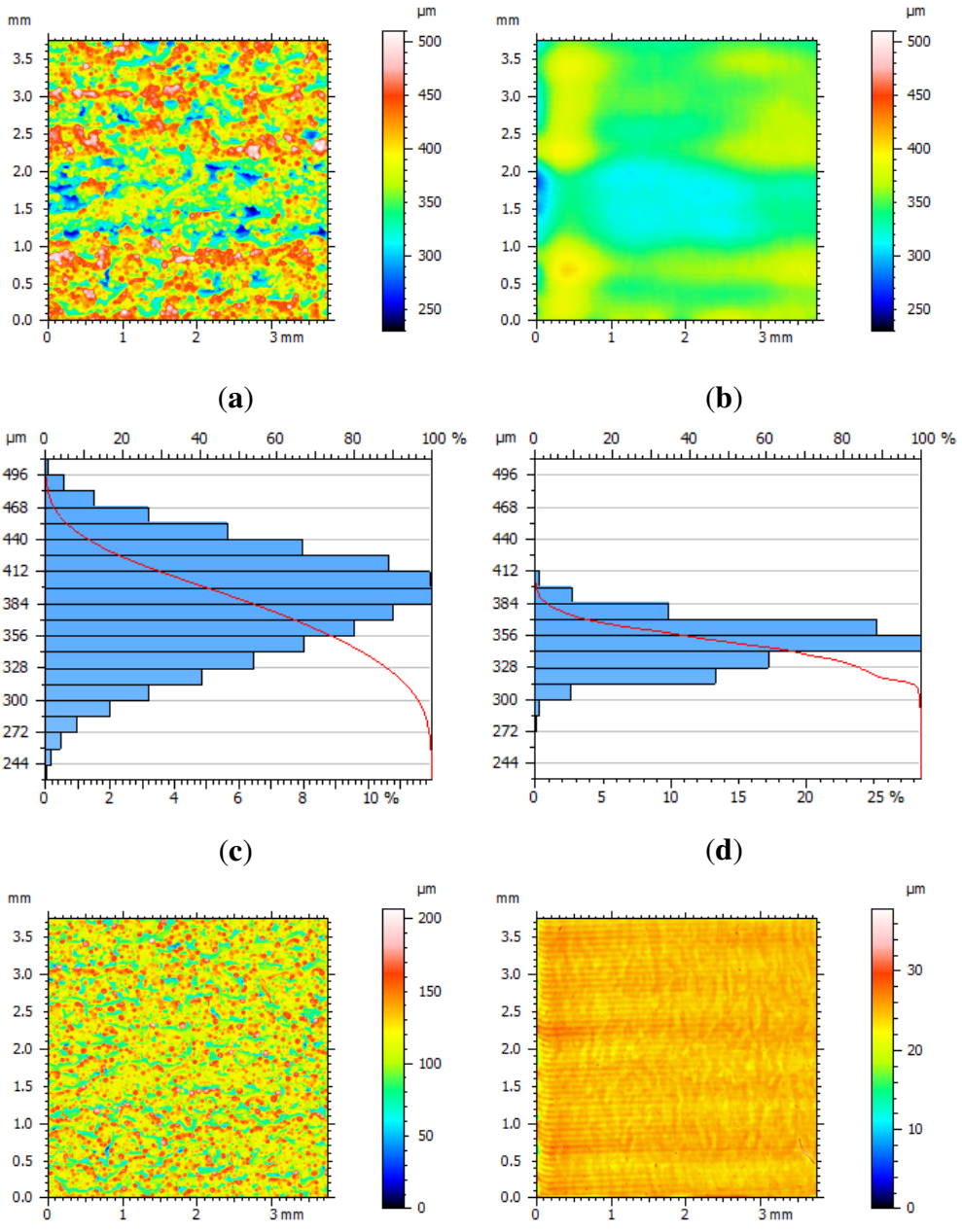

(**a**) (**b**)

(**c**) (**d**)

(**e**) (**f**)

Parameter	Value	Unit
Sa	19.0	µm
Sq	23.8	µm
Ssk	-0.171	
Sku	2.94	
Sz	206	µm

(**g**)

Parameter	Value	Unit
Sa	0.7	µm
Sq	1.0	µm
Ssk	-2.5	
Sku	35.7	
Sz	37.8	µm

(**h**)

Fig. 6.7 Surface characterisation of 90° surface subjected to laser polishing, showing: the surface topography height maps of the (a) measured pre- surface and (b) measured post- surface; the material ratio curves of (c) measured pre- surface and (d) measured post- surface; the surface topography height maps of the (e) filtered pre- surface and (f) filtered post- surface; and the characterisation results of the (g) filtered pre- surface and (h) filtered post- surface.

peening (Figure 6.5). Between the filtered pre-shot peened surface (Figure 6.8e) and the post-shot peened surface (Figure 6.8f), there is reduction of the total height range, as well as a change from particle/spatter to crater-like pits distributed randomly across the surface. For the surface texture parameters (Figure 6.8g and 6.8h), there is a reduction in *Sa*, *Sq* and *Sz* as a result of the shot peening process; this is a more significant reduction when compare to the effect of shot peening on the 0° orientation surface, seen in Figure 6.5.

6.3.2 Feature-based characterisation of side surfaces

90° orientation surface - linishing

Due to the presence of particle/spatter features on the side surface, these surfaces were subject to an active contours segmentation approach as described in Section 6.2.7. Figure 6.9a shows a segmentation mask, the result of the feature-based segmentation approach, applied to the pre-linished surface. The result of this segmentation is a good determination of the majority of particle/spatter features on the as-built surface and a surface dominated by these features. Figure 6.9b shows the same segmentation mask applied to the post-linished surface, which highlights the inability of the linishing process to remove many of these particles/spatter; likely a result of sub-optimal processing parameters or poor work-holding. In general, the affected regions within Figure 6.9b, correspond to the boundaries of the particle/spatter clusters with a flatter topography were the material has been removed. Figure 6.10 shows the results of the feature-based characterisation of the height of these segmented features for the surface in both conditions (pre and post). From Figure 6.10a, there is a reduction in the values for feature heights between pre- and post-linishing, in addition to a reduced dispersion. When comparing the absolute height of the bottom of the features (Figure 6.10c), these boxplots possess similar dispersion and values; a result of a preservation of the bottom of these features as well as suggesting good alignment. When comparing the similarity of the absolute bottom height values to the reduction between the absolute top height values

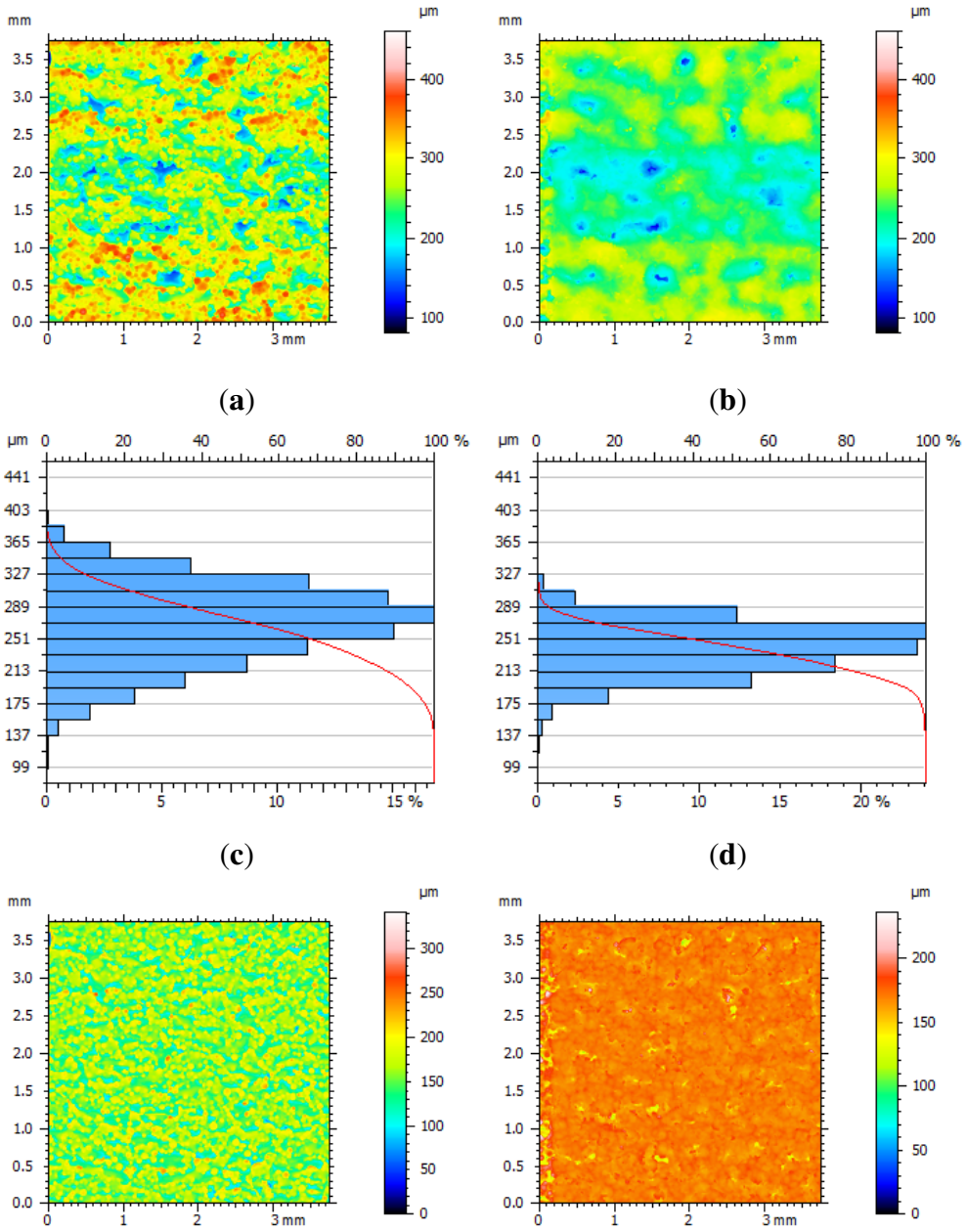

Parameter	Value	Unit
Sa	19.1	µm
Sq	24.1	µm
Ssk	-0.154	
Sku	3.22	
Sz	342	µm

(g)

Parameter	Value	Unit
Sa	4.2	µm
Sq	6.8	µm
Ssk	-1.78	
Sku	33.1	
Sz	236	µm

(h)

Fig. 6.8 Surface characterisation of 90° surface subjected to shot peening, showing: the surface topography height maps of the (a) measured pre- surface and (b) measured post- surface; the material ratio curves of (c) measured pre- surface and (d) measured post- surface; the surface topography height maps of the (e) filtered pre- surface and (f) filtered post- surface; and the characterisation results of the (g) filtered pre- surface and (h) filtered post- surface.

of features in Figure 6.10b, the change in feature height shown in Figure 6.10a is clearly a result of this reduction; the linishing process does reduce feature height by removing the material at the top of these features.

90° orientation surface - laser polishing

The segmentation mask within Figure 6.11a shows a good segmentation of features; with the majority of particles/spatter identified. When this mask is applied to Figure 6.11b, it is apparent that none of these features are able to survive the laser polishing process. When the feature-based characterisation is applied to both surfaces, there is a significant reduction in the values and dispersion of feature height as a result of laser-polishing, with the median height value reducing from approximately 40 μm to 5 μm. However, this reduction of feature height is not only the result of the significant reduction in the values for the absolute top height of the features (Figure 6.11b), but also a small reduction in the absolute bottom height of the features between pre- and post-laser polishing (as shown in Figure 6.11c). Assuming good alignment, this small reduction of value and dispersion for the absolute bottom height suggests that laser-polishing completely re-melts and re-forms the surface allowing material to flow into, fill and settle at a lower height than the as-built surface.

90° orientation surface - shot peening

The segmentation approach applied to the pre-shot peened surface shows good segmentation of features (Figure 6.13a), with many particles/spatter features identified. In Figure 6.13b, there is a resultant random surface with limited correspondence between particles/spatter and the crater-like pits produced through shot peening; suggesting this approach is sufficient at removing the particles/spatter features but leaving few clear corresponding features. At the leftmost edge of the post-shot peened surface measured region (Figure 6.13b), there is an unaffected region (likely a result of covering), where there is a match between features

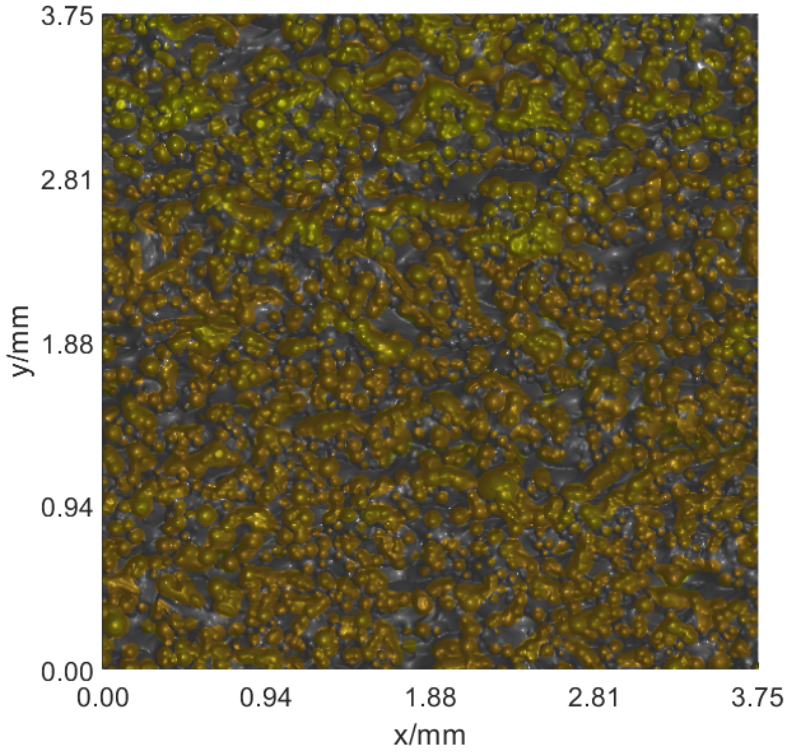

(**a**)

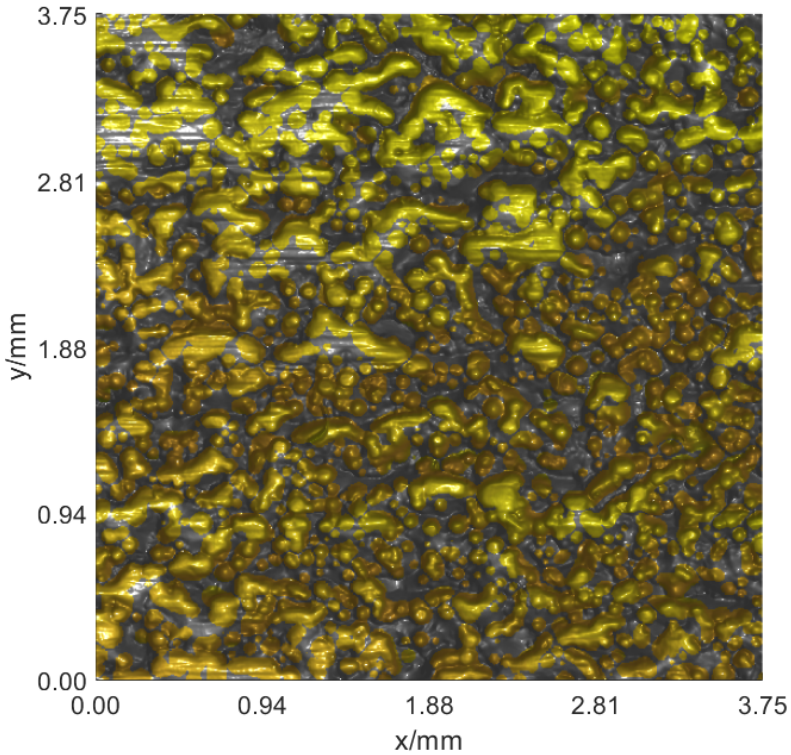

(**b**)

Fig. 6.9 Segmentation mask for as-built surface applied to (a) pre- and (b) post-linished 90° orientated surface. Where yellow denotes pixels within identified feature boundaries and grey denotes background pixels. An artificial reflection is added to enhance visualisation (may produce white regions).

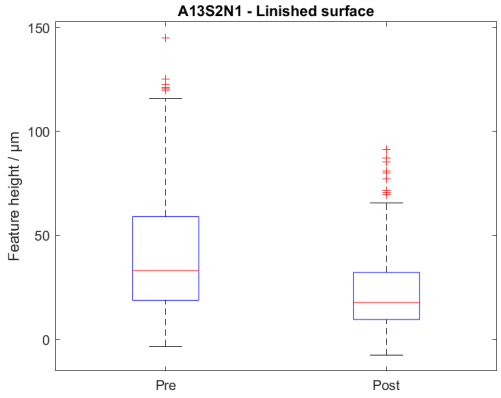

(**a**)

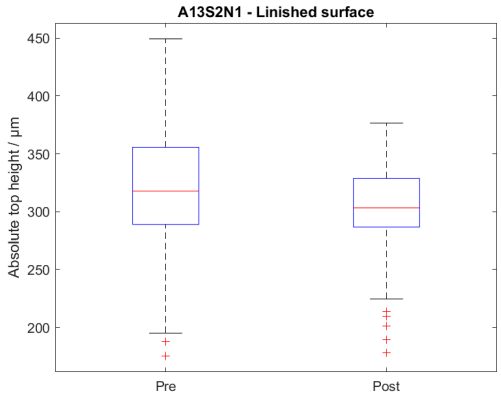

(**b**)

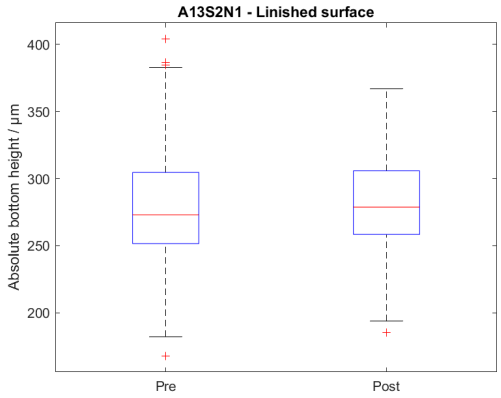

(**c**)

Fig. 6.10 Feature attributes for pre- and post-linished side surface showing (a) feature height, (b) absolute top height of feature and (c) absolute bottom height of a feature

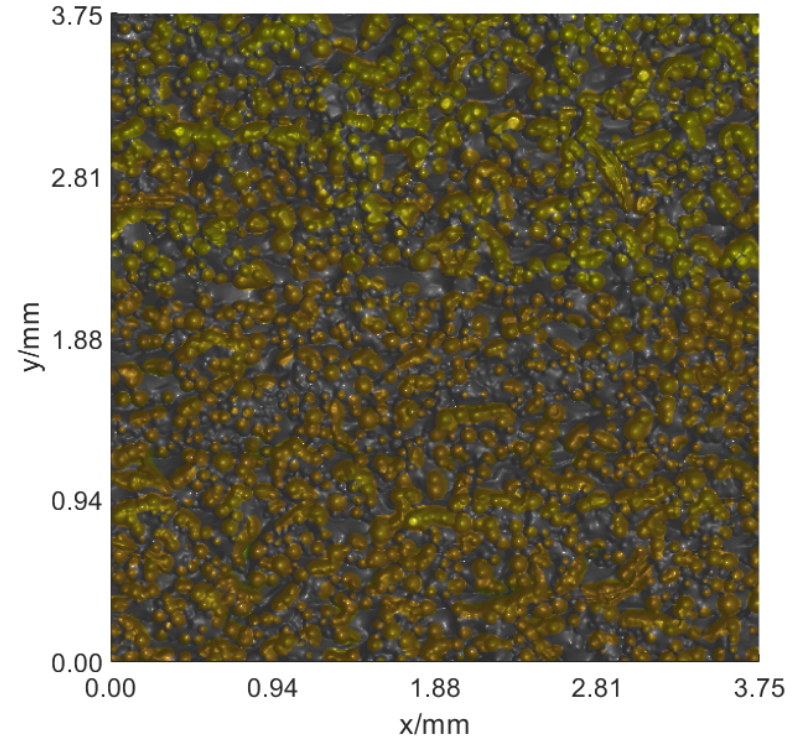

(**a**)

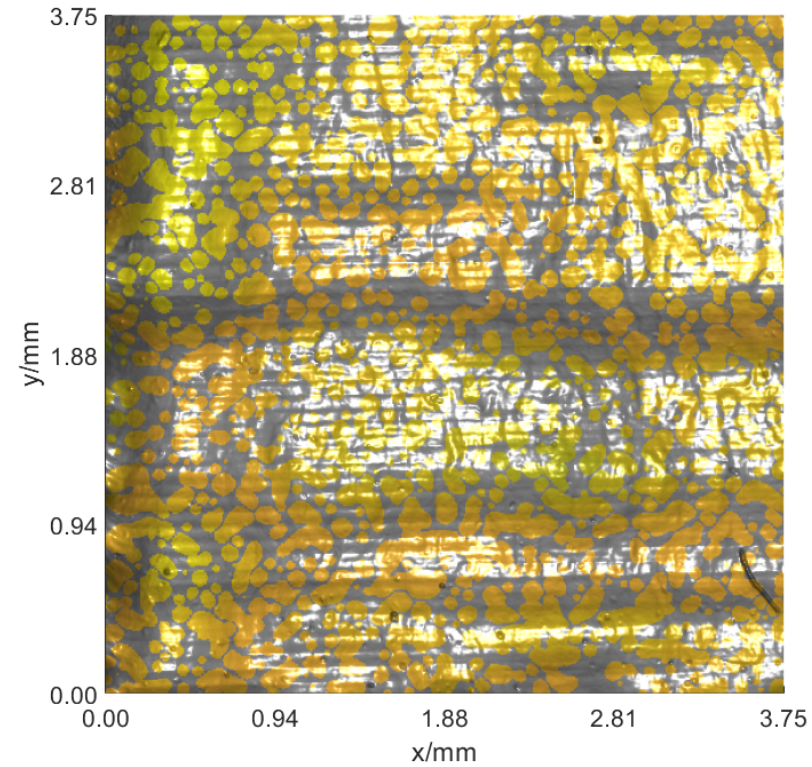

(**b**)

Fig. 6.11 Segmentation mask for as-built surface applied to (a) pre- and (b) post-laser polished 90° orientated surface. Where yellow denotes pixels within identified feature boundaries and grey denotes background pixels. An artificial reflection is added to enhance visualisation (may produce white regions).

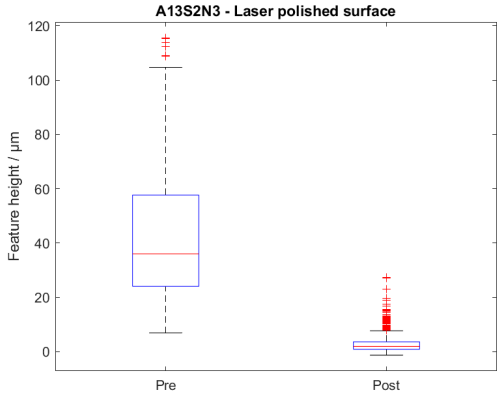

(**a**)

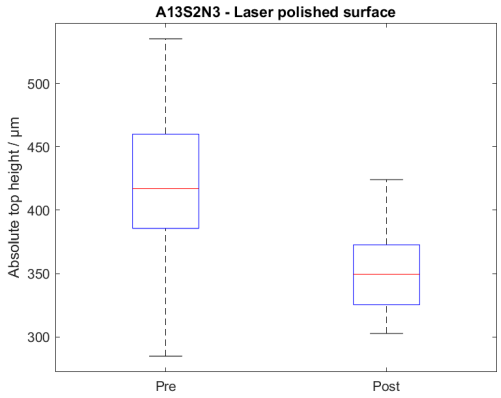

(**b**)

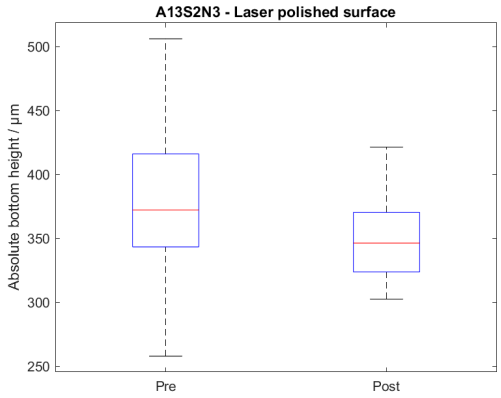

(**c**)

Fig. 6.12 Feature attributes for pre- and post-laser polished side surface showing (a) feature height, (b) absolute top height of feature and (c) absolute bottom height of a feature

and particles/spatter for the pre- and post-shot peening condition. There is overlap of the dispersions between the absolute bottom height of the features (Figure 6.14c) for the pre- and post-shot peened surfaces and assuming good alignment, the small reduction in absolute bottom height values are due to the impact of the metal shot compressing the material. There is a more significant shift in the absolute top heights of features, shown in Figure 6.14b, which can explain the large shift in feature height values calculated from these values (Figure 6.14a); this reduction of feature height is not as effective for shot peening as for laser polishing.

6.4 Discussion

Traditionally, an operator might only be able to approximate a material removal rate, and would only see change in topography using surface texture parameters. Through the use of an unaffected relocation landmark, registration and alignment in six degrees of freedom can be used to see changes in the distribution of heights and the material ratio in absolute terms; so that material removal or evolution can be seen in terms of an absolute shift in heights on the surface.

Accurate registration is required for a meaningful analysis of the correspondence between a surface before and after a finishing operations causes an alteration to the surface topography as well as for further characterisation of areal surface texture parameters or the dimensional properties of surface features. With perfect alignment, only the influence of the finishing operation on the surface topography and any uncertainty within the measurement of the topography should explain differences between the surfaces in a pre- and post-condition. Residual displacement errors should aim to be smaller than the pixel distance, but there is still some benefit to a coarse alignment to locate surfaces within the same global coordinate system in terms of understanding how the material ratio and distribution of heights as a result

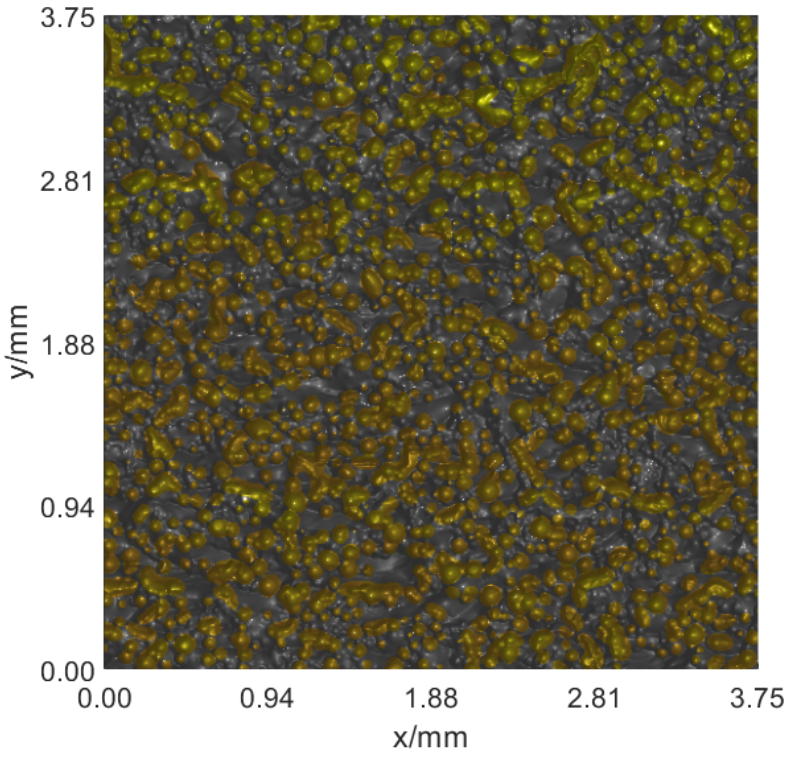

(**a**)

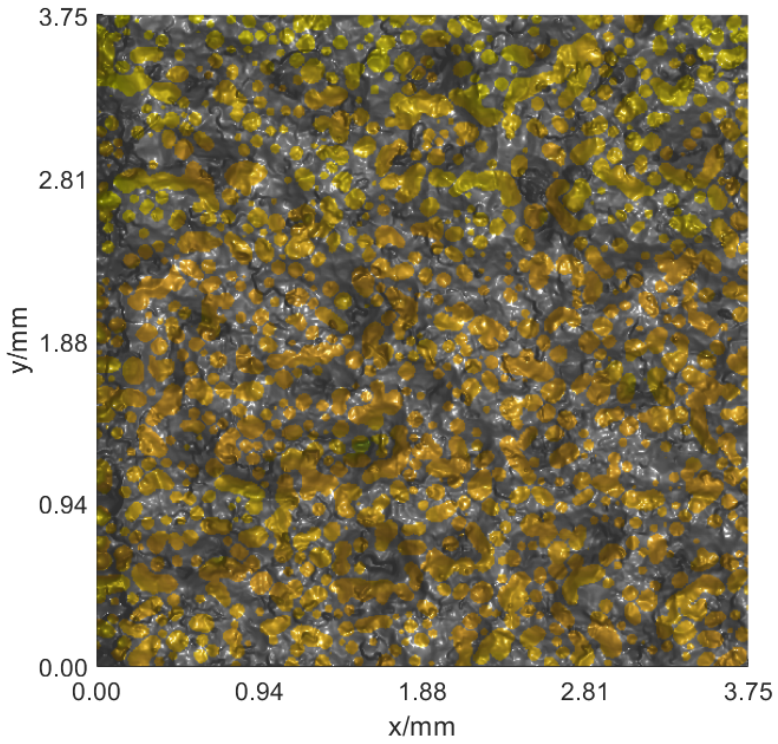

(**b**)

Fig. 6.13 Segmentation mask for as-built surface applied to (a) pre- and (b) post-shot peened 90° orientated surface. Where yellow denotes pixels within identified feature boundaries and grey denotes background pixels. An artificial reflection is added to enhance visualisation (may produce white regions).

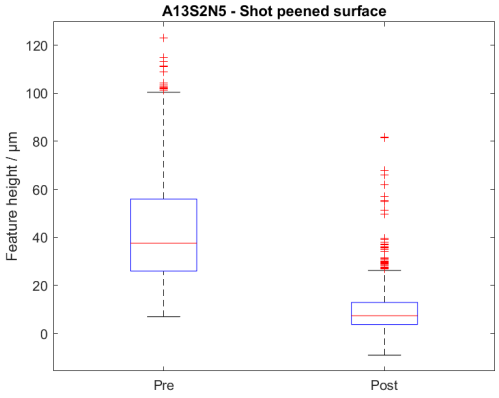

(a)

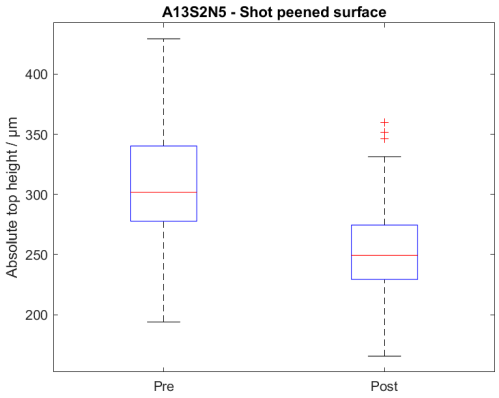

(b)

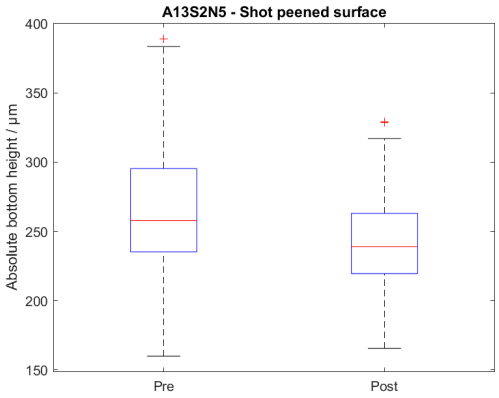

(c)

Fig. 6.14 Feature attributes for pre- and post-shot peened side surface showing (a) feature height, (b) absolute top height of feature and (c) absolute bottom height of a feature

of finishing parameters change absolutely. However, the determination of the validity and efficacy of a registration result is still required.

Within this study, only single measurements were assessed for each test case and whilst this might be acceptable to suggest benefits of the proposed methodology, repeats and the assessment of measurement uncertainty should be considered in future; especially in terms of the additional processing steps applied in this approach. Knowledge of uncertainty with respect to registration and relocation is fundamental for the later assessment of uncertainty of topographic comparison and the traceability chain of the whole analysis approach. These issues should be considered when comparing the effect of a finishing operation on an AM surface, however, the goal of this research is to offer a methodology that can take advantage of knowledge about the finishing process, fiducial markers in the form of relocation landmarks and the three-dimensional nature of areal surface topography to better understand the evolution of a surface.

6.5 Conclusion

- An original method using fiducial markers and registration algorithms can be used to align topographic information in the same coordinate system for comparable characterisation is presented - opposed to using parameter-based assessments on measurement data not necessarily on the exact same region of the surface.
- Change in surface texture can not always be observed through looking at parameters, however, shifts in the material ratio curve are visible between finishing condition for all surfaces.
- Each finishing operation leaves characteristic marks on the surface:

  - Linishing appears to reduce surface heights by material removal of the upper surface, leaving plateau regions as it removes the tops of particle structure - not-affecting lower height regions on the surface.
  - Laser polishing results in a surface completely devoid of features of the original AM surface - leaving only characteristic marks of the laser process.
  - Shot peening leaves craters as a result of the process, but is sometimes unable to access and alter bottom regions of smaller valley features.
  - Both laser polishing and shot peening processes do not appear to affect low spatial frequency components of the surface.

- By overlaying the feature-based segmentation from the pre-condition surface over the
- Changes in characterised feature height between pre-condition segmentation result applied over pre- and post-finished surfaces can visibly be explained by the application of the respective process.
- Validation of this approach in terms of accuracy and uncertainty is required for future adoption.

An original method has been presented for the investigation of evolving topographies as a consequence of finishing operations. Conventionally, changes of surface topography as a result of are characterised using parameter-based assessments not necessarily on the exact same region of the surface, from which numerical differences between parameters can be compared. In contrast, the method presented is based on combining topography registration based on fiducials, with feature-based characterisation for the identification of relevant topography formations, in order to track how they change as a consequence of the finishing operation in terms of absolute changes in heights on the surface. Overall, different finishing operations can be understood to have different effects depending on the initial

topography as well as in terms of how they either remove material (such as with linishing) or re-form the surface to produce a finished surface.

Further work will apply this methodology to other finishing operations, AM processes and surface orientations to offer further understanding of the evolution of the features on the AM surface. Other work would be an investigation into methods to validate the registration of topographies and the determination of measurement uncertainty for assessments made on registered topographies.

Chapter 7

Conclusions

7.1 Thesis summary

The aim of the Thesis was to develop methods for measuring and characterising the surface topography of as-built and post-processed additive manufactured (AM) parts.

The objectives of the Thesis were to determine the optimum instrument settings and good practice for the measurement of surface topography of additive surfaces using focus variation (FV) - addressed in Chapter 3, develop methodologies to identify and describe/ define features on the powder bed fusion (PBF) surface, such as investigating variation of features with respect to build orientation - addressed in Chapter 4 and Chapter 5 and to develop methodologies that can quantitatively monitor the evolution of surface topography before and after post processing - addressed in Chapter 6.

The work in this Thesis focused mostly on the use of FV and the measurements of metal PBF - more specifically electron beam powder bed fusion (EBPBF) - in various surface conditions; built at differing orientations and subjected to various finishing operations. From the assessment of the literature in Chapter 2, there is a clear need for good practice in terms of the measurement instrument settings as well as for the characterisation approaches being applied to metal PBF surfaces in both pre- and post-processing conditions. By first evaluating

the optimum settings for measurement for PBF surfaces, good practice can be determined and applied to capture more accurate measurements. Secondly, with more accurate measurement data, novel characterisation approaches (such as feature-based characterisation) can then be applied to better understand the AM process in terms of the features present on the surface and how they relate to the build process. Finally, for PBF surfaces that are subject to finishing operations, there is need for greater understanding of the influence of these operations have on the features of the surface, as well as whether they can be applied adaptively to achieve a similar final surface.

Chapter 3 showed that PBF surfaces vary with different materials and processes, resulting in differing surface topographies, however, general trends can be drawn by building regression models on full factorial design of experiments. From the assessment of metrics, such as non-measured points, the upper quartile of repeatability error and the surface texture parameter, *Sa*, assessed over the measured topography against measurement settings, the influence of changing these parameters can be determined. The contribution of this work is a methodology that uses a sensitivity analysis applied to the regression model to plot trends in order to contribute to the understanding of the influence of the measurement setting for specific surface test cases. With the general trends from this analysis, good practice can be defined for FV microscopy.

Feature-based characterisation offers a richer information content than conventional surface texture parameters as features can be defined more closely to match aspects of the topography, but accurate segmentation is fundamental. Prior to the application of novel feature-based approaches on AM surfaces, which is the second objective, there is a need to ensure that the result of a segmentation result is valid and accurate in determining the boundary of a feature. The contribution of Chapter 4 is a methodology that can quantitatively assess the performance of a segmentation approach given a reference result to compare against. As there are a variety of segmentation methods in the literature, binary classification

testing offers a way to make use of segmentation masks (binary masks denoting only the pixels within a feature) and produce metrics that can be used to characterise a result against a reference, allowing for comparison between segmentation approaches. With the ability to measure the validity and efficacy of a segmentation approach with respect to a desired result, these algorithms can be optimised to specific surfaces.

From the results of the comparison and validation methodology in Chapter 4, the active contours approach has been shown as a suitable method to segment the AM surface and is applied in Chapter 5 to meet the second objective by investigating the particles/spatter features on the AM surface. The contribution of Chapter 5 is a case study showing the application of a feature-based approach (active contours) to a variety of surfaces built at differing orientations. The active contours approach offers an additional assessment of the changing surface topography with respect to build orientation in the form of proportional assessments of particles/spatter on the surface, characterisation of the underlying surface deprived of features and the characterisation of feature attributes. When applied to the surfaces built at varying orientation, there is an increasing proportion of particle/spatter as the surface angle increases towards surfaces that face into the powder bed. Along with any assessment made on the underlying surface, this trend of increasing particles/spatter can be useful to adaptively inform the intensity of the finishing operation that can to be applied to these types of surface to meet functional or tolerance requirements.

Chapter 6 meets the third objective which is to develop methodologies to compare surfaces, before and after post processing. Using fiducial markers and areal topography measurement, an accurate registration and alignment of topographies both pre- and post-finishing can be achieved in six degrees of freedom. With alignment in the same global coordinate system, differences between topographies can be compared in absolute terms. As different finishing operations can have a different material removal or altering mechanism, there are different effects on the topography making their choice important when trying to

achieve a desired surface texture and/or functionality. The contribution of this chapter is a novel approach for the comparison of topographies through registration using preserved fiducial markers. This registration allows for the monitoring of the evolution of a topography in terms of a global coordinate system, in addition to the application of the feature-based characterisation methods used in Chapter 5 to assess the dimensional changes of feature properties from the initial topography as a result of a finishing operation.

7.2 Contributions to the field

The main contributions are summarised concisely by Chapter, they consist of the key findings and important observations of the work within the Thesis. From the literature review in Chapter 2, the key findings and observations in relation to the aims and objectives of the Thesis were:

- PBF is commonly used to produce metal AM parts, producing unique measurement challenges to surface texture measurement instruments - EBPBF requires further study.
- Surfaces produced by PBF are rough and contain a large range of components over a large scale of spatial wavelengths - from small ripples to particles/spatter to weld tracks.
- FV appears as a suitable measurement technique to overcome many of the measurement challenges presented by PBF, but requires optimisation of its measurement parameters.
- Parameters are mostly used to characterise the surface, which is most often to relate to either the build process parameters or to assess effectiveness of finishing operations.
- Feature-based characterisation can offer an alternative to parameters, by characterising dimensional properties of defined and segmented surface features. But there are no methods for comparison or validation of these approaches.

- Feature-based characterisation and various segmentation approaches are already being applied to PBF surfaces to isolate particles on the surface, however, active contours segmentation is not currently used for AM test cases.

- Finishing operations are required for most PBF surfaces produced, which are assessed using parameter-based characterisation typically measured before or after over representative regions of the surface - it is uncommon for feature-based characterisation to be applied.

For Chapter 3, which dealt with FV measurement of metal PBF surfaces, the following guidelines for the optimisation of measurement were:

- AM surfaces vary significantly between surface orientation and material, therefore a procedure to determine suitable measurement parameters should be performed for each new test case.

- Correct objective magnification should be chosen based on the scale of interest required from the measurement, i.e. smaller features require higher magnification.

- Vertical resolution values should be minimised to improve the repeatability of the measurement, but not as much to cause large regions of non-measured points or excessive measurement time.

- Lateral resolution values should be chosen based on the smallest scale that is of interest to capture in the measurement - not too small as to increase the high frequency components on the surface and increase non-measured points or too high as to introduce an excessive smoothing effect on high frequency components on the surface that relate to features of interest.

- Any illumination choice should adequately illuminate the surface without causing issues with contrast in the image (under- or over-exposure)

- Illumination choice is dependent on the surface, material and orientation.
  - Top surfaces benefit from ring light illumination which contributes to reduced non-measured points and repeatability error.
  - Side surfaces benefit from coaxial illumination to reduce non-measured points, but at a cost of increasing repeatability error. Ring light illumination acts in the opposite way, increasing non-measured points but reducing repeatability error.

Chapter 4 presented a method to quantitatively assess the performance of a segmentation approach given a reference result, from this chapter the key findings were:

- LPBF top surface was found to be hardest to segment - with morphological segmentation on edges unable to identify most of the particles as determined by the reference.
- EBPBF side surface was found to be the easiest surface to segment for all approaches.
- There is a trade-off between recall and specificity for all segmentation methods.
- Active contours results in low precision, but high recall - it will find more features but over-estimate their boundaries.
- Morphological segmentation on edges results in high precision, but low recall - it can better define the contours of features compared to the reference, but often does not identify features.
- Contour stability falls between the two other methods proposed, but is weaker when dealing with agglomerated features where contours that may resolve separate particles are not as clearly defined.
- The methodology proposed can allow for a comprehensive assessment of segmentation performance, that could allow for optimisation.

- In future, use of virtual reference with pre-defined features would allow for assessment independent of bias: operator or application dependent.

Chapter 5 contributed a case study investigating the particles/spatter features on the AM surface using active contours feature-based characterisation on surfaces built at different orientations. The findings of this chapter were:

- Active contours segmentation enables the extraction and characterisation of signature features of the EBPBF process.
- As the surface orientation with respect to build increases, so does the complexity of the surface.
- Generally, the number of particle-like features appears to increase with build orientation.
- When removing features from the topography, there is generally a significant reduction in the *Sa* and *Sq* parameters.
- Future work would compare the feature-deprived results to surfaces subject to particle-removing finishing operations to verify the characterisation results of the underlying surface.

Chapter 6 contributes a method to compare surfaces before and after finishing in the same location and same global coordinate system using fiducials and registration in 6 degrees of freedom. The following key findings and important observations from this chapter were:

- An original method using fiducial markers and registration algorithms can be used to align topographic information in the same coordinate system for comparable characterisation is presented - opposed to using parameter-based assessments on measurement data not necessarily on the exact same region of the surface.

- Change in surface texture can not always be observed through looking at parameters, however, shifts in the material ratio curve are visible between finishing condition for all surfaces.
- Each finishing operation leaves characteristic marks on the surface:
  - Linishing appears to reduce surface heights by material removal of the upper surface, leaving plateau regions as it removes the tops of particle structure - not-affecting lower height regions on the surface.
  - Laser polishing results in a surface completely devoid of features of the original AM surface - leaving only characteristic marks of the laser process.
  - Shot peening leaves craters as a result of the process, but is sometimes unable to access and alter bottom regions of smaller valley features.
  - Both laser polishing and shot peening processes do not appear to affect low spatial frequency components of the surface.
- By overlaying the feature-based segmentation from the pre-condition surface over the
- Changes in characterised feature height between pre-condition segmentation result applied over pre- and post-finished surfaces can visibly be explained by the application of the respective process.
- Validation of this approach in terms of accuracy and uncertainty is required for future adoption.

7.3 Areas for future work

There are many areas of future work that can be carried out in order to further the aims and objectives in developing methods for the measurement and characterisation of surface

topography of additively manufactured parts both before and after finishing. From the state of the art in Chapter 2, the general theme of future work for surface texture metrology for AM is good practice, for both measurement and characterisation approaches.

Regarding the focus variation measurement of metal PBF surfaces in Chapter 3, the future work required is a more thorough investigation into the relationship between the topographic properties of features on the AM surface and the behaviour of the FV instrument, which might also investigate measurement noise. This investigation would need to make use of extensive experimentation using purposely fabricated surface features and a systematic testing of combinations of measurement settings. In addition to this, any future work assessing the FV instrument should make use of an accurate reference in order to ascertain traceability of the measurements. The methodology of this chapter using regression modelling on full factorial design of experiments can also be applied to other measurement systems in order to determine general trends that can contribute to optimisation and good practice. Additional work could apply aspects of the methodology proposed in this Chapter to determine FV instrument measurement uncertainty, which could be further applied to more measurement instrument technologies.

For Chapter 4, where a methodology to allow for the comparison and validation of a segmentation result is presented, future work could include the use of a virtual computer-generated topography in order to assess and optimise the parameters of the various segmentation approaches. With the creation of a surface with known feature number, location and sizing, the virtual surface can be used to produce an ideal reference from which to compare and validate against. In addition, the methodology can be applied to validate and compare segmentation approaches that are used to isolate other types of features on the AM surface. Other work could be to use mathematically defined surfaces, which can be used as reference surfaces, to ascertain measurement uncertainty for feature-based segmentation and characterisation.

For Chapter 5, future work could be to apply the methodology for evaluating the surface topography to more measurements from surfaces built at differing build orientations with the goal of building predictive models for these surfaces including particle coverage that can be used to optimise part designs prior to build to reduce finishing requirements or to use predictions to assist automated systems that can adaptively finish surfaces to requirement. In addition, other work could involve comparing the results of the underlying surface texture devoid of particles to a surface that has had components removed via finishing in order to validate the approach, whilst other work could investigate other features of the AM surface to determine how they vary with build orientation.

The methodology in Chapter 6 can be expanded to other finishing operations and different initial surfaces, including taking progressive measurements between multiple processing steps, to determine optimum methods and combinations required to achieve desired surface texture. A similar methodology can also be applied to fatigue testing samples in order to assess the evolution of surface topography as a result of finishing operations in terms of absolute heights, as well as offer an explanation for fatigue failure in terms of changing features on the surface (i.e. pits). Most importantly, a method to verify and validate the alignment and registration procedure is required alongside an investigation into the measurement uncertainty for this approach.

Across all of the work in the Thesis, along with good practice, there is an essential need for the determination of measurement uncertainty for areal surface topography data in order to validate these approaches and their accuracy in a traceable way.

References

[1] Gibson I, Rosen D and Stucker B 2014 Design for additive manufacturing *Additive Manufacturing Technologies: 3D Printing, Rapid Prototyping, and Direct Digital Manufacturing* (New York: Springer New York) chap Chapter 17, pp 399–343 2nd ed

[2] ISO 17296-2 2016 Additive manufacturing — General principles Part 2 : Overview of process categories and feedstock

[3] Frazier W E 2014 Metal additive manufacturing: A review *Journal of Materials Engineering and Performance* **23** 1917–1928

[4] Ding D, Pan Z, Cuiuri D and Li H 2015 Wire-feed additive manufacturing of metal components: technologies, developments and future interests *International Journal of Advanced Manufacturing Technology* **81** 465–481

[5] Friel R J and Harris R A 2013 Ultrasonic additive manufacturing A hybrid production process for novel functional products *Procedia CIRP* **6** 35–40

[6] Townsend A, Senin N, Blunt L, Leach R and Taylor J 2016 Surface texture metrology for metal additive manufacturing: a review *Precision Engineering* **46** 34–47

[7] Leach R K, Bourell D, Carmignato S, Donmez A, Senin N and Dewulf W 2019 Geometrical metrology for metal additive manufacturing *CIRP Annals* **[In press]**

[8] Körner C, Bauereiß A and Attar E 2013 Fundamental consolidation mechanisms during selective beam melting of powders *Modelling and simulation in materials science and engineering* **21** 085011

[9] Körner C 2016 Additive manufacturing of metallic components by selective electron beam melting — a review *International Materials Reviews* **61** 361–377

[10] Liu B, Wildman R, Tuck C, Ashcroft I and Hague R 2011 Investigation the Effect of Particle Size Distribution on Processing Parameters Optimisation in Selective Laser Melting Process *22nd Annual International Solid Freeform Fabrication Symposium - An Additive Manufacturing Conference, SFF 2011* 227–238

[11] Vock S, Klöden B, Kirchner A, Weißgärber T and Kieback B 2019 Powders for powder bed fusion: a review *Progress in Additive Manufacturing* **0** 0

[12] Khairallah S A, Anderson A T, Rubenchik A M and King W E 2017 Laser powder-bed fusion additive manufacturing: Physics of complex melt flow and formation mechanisms of pores, spatter, and denudation zones *Additive Manufacturing Handbook: Product Development for the Defense Industry* **108** 613–628

[13] Leach R K 2011 *Optical Measurement of Surface Topography* (Berlin, Heidelberg: Springer Berlin Heidelberg)

[14] Shamsaei N, Yadollahi A, Bian L and Thompson S M 2015 An overview of Direct Laser Deposition for additive manufacturing; Part II: Mechanical behavior, process parameter optimization and control *Additive Manufacturing* **8** 12–35

[15] Kruth J P, Mercelis P, Van Vaerenbergh J, Froyen L and Rombouts M 2005 Binding mechanisms in selective laser sintering and selective laser melting *Rapid Prototyping Journal* **11** 26–36

[16] Calignano F, Manfredi D, Ambrosio E P, Iuliano L and Fino P 2013 Influence of process parameters on surface roughness of aluminum parts produced by DMLS *International Journal of Advanced Manufacturing Technology* **67** 2743–2751

[17] Wauthle R, Vrancken B, Beynaerts B, Jorissen K, Schrooten J, Kruth J P and Van Humbeeck J 2015 Effects of build orientation and heat treatment on the microstructure and mechanical properties of selective laser melted Ti6Al4V lattice structures *Additive Manufacturing* **5** 77–84

[18] Zakaria K, Ismail Z, Redzuan N and Dalgarno K W 2015 Effect of Wire EDM Cutting Parameters for Evaluating of Additive Manufacturing Hybrid Metal Material *Procedia Manufacturing* **2** 532–537

[19] Verhaagen B, Zanderink T and Fernandez Rivas D 2016 Ultrasonic cleaning of 3D printed objects and Cleaning Challenge Devices *Applied Acoustics* **103** 172–181

[20] Tan K L and Yeo S H 2017 Surface modification of additive manufactured components by ultrasonic cavitation abrasive finishing *Wear* **378-379** 90–95

[21] de Formanoir C, Michotte S, Rigo O, Germain L and Godet S 2016 Electron beam melted Ti-6Al-4V: Microstructure, texture and mechanical behavior of the as-built and heat-treated material *Materials Science and Engineering A* **652** 105–119

[22] Brandão A D, Gumpinger J, Gschweitl M, Seyfert C, Hofbauer P and Ghidini T 2017 Fatigue Properties of Additively Manufactured AlSi10Mg-Surface Treatment Effect *Procedia Structural Integrity* **7** 58–66

[23] Benardos P G and Vosniakos G C 2003 Predicting surface roughness in machining: A review *International Journal of Machine Tools and Manufacture* **43** 833–844

[24] Thomas T R 2013 Roughness and function *Surface Topography: Metrology and Properties* **2** 014001

[25] Bagehorn S, Wehr J and Maier H J 2017 Application of mechanical surface finishing processes for roughness reduction and fatigue improvement of additively manufactured Ti-6Al-4V parts *International Journal of Fatigue* **102** 135–142

[26] AlMangour B and Yang J M 2016 Improving the surface quality and mechanical properties by shot-peening of 17-4 stainless steel fabricated by additive manufacturing *Materials and Design* **110** 914–924

[27] Iquebal A S, Amri S E, Shrestha S, Wang Z, Manogharan G P and Bukkapatnam S 2017 Longitudinal milling and fine abrasive finishing operations to improve surface integrity of metal AM components *Procedia Manufacturing* **10** 990–996

[28] Atzeni E, Barletta M, Calignano F, Iuliano L, Rubino G and Tagliaferri V 2016 Abrasive Fluidized Bed (AFB) finishing of AlSi10Mg substrates manufactured by Direct Metal Laser Sintering (DMLS) *Additive Manufacturing* **10** 15–23

[29] Beaucamp A, Namba Y and Charlton P 2015 Process mechanism in shape adaptive grinding (SAG) *CIRP Annals - Manufacturing Technology* **64** 305–308

[30] Yasa E, Kruth J P and Deckers J 2011 Manufacturing by combining Selective Laser Melting and Selective Laser Erosion/laser re-melting *CIRP Annals - Manufacturing Technology* **60** 263–266

[31] Mohammad A, Mohammed M K and Alahmari A M 2016 Effect of laser ablation parameters on surface improvement of electron beam melted parts *International Journal of Advanced Manufacturing Technology* **87** 1033–1044

[32] Longhitano G A, Larosa M A, Munhoz A L J, Zavaglia C A d C and Ierardi M C F 2015 Surface finishes for Ti-6Al-4V alloy produced by direct metal laser sintering *Materials Research* **18** 838–842

[33] Lyczkowska E, Szymczyk P, Dybała B and Chlebus E 2014 Chemical polishing of scaffolds made of Ti-6Al-7Nb alloy by additive manufacturing *Archives of Civil and Mechanical Engineering* **14** 586–594

[34] Salmi M, Huuki J and Ituarte I F 2017 The ultrasonic burnishing of cobalt-chrome and stainless steel surface made by additive manufacturing *Progress in Additive Manufacturing* **2** 31–41

[35] Kumbhar N N and Mulay A V 2018 Post Processing Methods used to Improve Surface Finish of Products which are Manufactured by Additive Manufacturing Technologies: A Review *Journal of The Institution of Engineers (India): Series C* **99** 481–487

[36] BIPM 2012 *International vocabulary of metrology – Basic and general concepts and associated terms (VIM)* 3rd ed (Paris, France: Bureau International des Poids et Mesures))

[37] BIPM 2008 *Evaluation of measurement data — Guide to the expression of uncertainty in measurement* (Paris, France: Bureau International des Poids et Mesures)

[38] Bell S 2001 *Good Practice Guide No. 11 - Introductory Guide to Uncertainty of Measurement* 2 (Crown Publishing)

[39] Ferrucci M, Leach R K and Haitjema H 2018 Dimensional metrology *Basics of precision engineering* ed Leach R K S S T (Boca Raton, London, New York: CRC Press) chap 5, pp 151–204

[40] Leach R K 2013 Characterisation of areal surface texture *Characterisation of Areal Surface Texture* ed Leach R K (Springer Berlin Heidelberg)

[41] Thompson A 2018 *Surface texture measurement of metal additively manufactured parts by X-ray computed tomography* Ph.D. thesis University of Nottingham

[42] ISO 25178-601 2010 Geometrical product specifications (GPS) — Surface texture : Areal Part 601 : Nominal characteristics of contact (stylus) instruments

[43] ISO 25178-604 2013 Geometrical product specifications (GPS) — Surface texture : Areal Part 604 : Nominal characteristics of non-contact (coherence scanning interferometry) instruments

[44] ISO 25178-606 2015 Geometrical product specification (GPS): Surface texture: Areal, Part 606: Nominal characteristics of non-contact (focus variation) instruments

[45] ISO 25178-607 2019 Geometrical product specifications (GPS) — Surface texture: Areal — Part 607: Nominal characteristics of non-contact (confocal microscopy) instruments

[46] Townsend A, Pagani L, Scott P and Blunt L 2017 Areal surface texture data extraction from X-ray computed tomography reconstructions of metal additively manufactured parts *Precision Engineering* **48** 254–264

[47] Thompson A, Senin N, Maskery I, Körner L, Lawes S and Leach R K 2018 Internal surface measurement of metal powder bed fusion parts *Additive Manufacturing* **20** 126–133

[48] Thompson A, Senin N, Giusca C and Leach R K 2017 Topography of selectively laser melted surfaces: A comparison of different measurement methods *CIRP Annals* **66** 543–546

[49] Pagani L, Qi Q, Jiang X and Scott P J 2017 Towards a new definition of areal surface texture parameters on freeform surface *Measurement* **109** 281–291

[50] Pagani L, Zanini F, Carmignato S, Jiang X and Scott P J 2018 Generalization of profile texture parameters for additively manufactured surfaces *Journal of Physics: Conference Series* **1065** 212019

[51] Leach R K 2014 *Fundemental principals of nanometrology* (Oxford, UK: Elsevier)

[52] ISO 4287 2005 Geometrical product specification (GPS) - Surface texture: Profile method - Terms, definitions and surface texture parameters

[53] ISO 4288 1998 Geometrical Product Specifications (GPS)- Surface texture: Profile method- Rules and procedures for the assessment of surface texture

[54] Whitehouse D J 2010 *Handbook of surface and nanometrology* (Boca Raton, USA: CRC Press)

[55] Nikolaev N, Petzing J and Coupland J 2016 Focus variation microscope: linear theory and surface tilt sensitivity *Applied Optics* **55** 3555

[56] Helmli F 2013 Focus variations instruments *Optical measurement of surface topography* ed Leach R K (Springer Berlin Heidelberg) chap 7, pp 131–166

[57] ISO 25178-2 2012 Geometrical product specifications (GPS) - Surface texture: Areal - Part 2: Terms, definitions and surface texture parameters

[58] Leach R K 2014 *Good Practice Guide No. 37 - Introductory Guide to Uncertainty of Measurement* 2 (Crown Publishing)

[59] Blateyron F 2013 The Areal Field Parameters *Characterisation of Areal Surface Texture* ed Leach R K (Berlin, Heidelberg: Springer Berlin Heidelberg) pp 15–43

[60] Scott P J 2004 Pattern analysis and metrology: the extraction of stable features from observable measurements *Proceedings of the Royal Society of London. Series A: Mathematical, Physical and Engineering Sciences* **460** 2845–2864

[61] Wolf G W 1991 A FORTRAN subroutine for cartographic generalization *Computers and Geosciences* **17** 1359–1381

[62] Senin N, Moretti M and Blunt L A 2013 Identification of individual features in areal surface topography data by means of template matching and the ring projection transform *Surface Topography: Metrology and Properties* **2** 014007

[63] Lou S, Jiang X, Sun W, Zeng W, Pagani L and Scott P 2019 Characterisation methods for powder bed fusion processed surface topography *Precision Engineering* **57** 1–15

[64] Rowe W B 2014 Mechanics of Abrasion *Principles of Modern Grinding Technology* ed Rowe W B (Oxford, UK: Elsevier) chap 17, pp 341–363 2nd ed

[65] Bagherifard S, Beretta N, Monti S, Riccio M, Bandini M and Guagliano M 2018 On the fatigue strength enhancement of additive manufactured AlSi10Mg parts by mechanical and thermal post-processing *Materials and Design* **145** 28–41

[66] Evans C J, Paul E, Dornfield D, Lucca D A, Byrne G, Tricard M, Klocke F, Dambon O and Mullany B A 2003 Material removal mechanisms in lapping and polishing *CIRP Annals - Manufacturing Technology* **52** 611–633

[67] Yamazaki T 2016 Development of A Hybrid Multi-tasking Machine Tool: Integration of Additive Manufacturing Technology with CNC Machining *Procedia CIRP* **42** 81–86

[68] Bordin A, Sartori S, Bruschi S and Ghiotti A 2017 Experimental investigation on the feasibility of dry and cryogenic machining as sustainable strategies when turning Ti6Al4V produced by Additive Manufacturing *Journal of Cleaner Production* **142** 4142–4151

[69] Oyelola O, Crawforth P, M'Saoubi R and Clare A T 2016 Machining of Additively Manufactured Parts: Implications for Surface Integrity *Procedia CIRP* **45** 119–122

[70] Polishetty A, Shunmugavel M, Goldberg M, Littlefair G and Singh R K 2017 Cutting Force and Surface Finish Analysis of Machining Additive Manufactured Titanium Alloy Ti-6Al-4V *Procedia Manufacturing* **7** 284–289

[71] Bruschi S, Bertolini R and Ghiotti A 2017 Coupling machining and heat treatment to enhance the wear behaviour of an Additive Manufactured Ti6Al4V titanium alloy *Tribology International* **116** 58–68

[72] Kumar S S and Hiremath S S 2016 A Review on Abrasive Flow Machining (AFM) *Procedia Technology* **25** 1297–1304

[73] Beaucamp A T, Namba Y, Charlton P, Jain S and Graziano A A 2015 Finishing of additively manufactured titanium alloy by shape adaptive grinding (SAG) *Surface Topography: Metrology and Properties* **3** 024001

[74] Maamoun A, Elbestawi M and Veldhuis S 2018 Influence of Shot Peening on AlSi10Mg Parts Fabricated by Additive Manufacturing *Journal of Manufacturing and Materials Processing* **2** 40

[75] Temmler A, Willenborg E and Wissenbach K 2011 Design surfaces by laser remelting *Physics Procedia* **12** 419–430

[76] Richter B, Blanke N, Werner C, Vollertsen F and Pfefferkorn F E 2019 Effect of Initial Surface Features on Laser Polishing of Co-Cr-Mo Alloy Made by Powder-Bed Fusion *Jom* **71** 912–919

[77] Rosa B, Mognol P and Hascoët J y 2015 Laser polishing of additive laser manufacturing surfaces *Journal of Laser Applications* **27** S29102

[78] Alfieri V, Argenio P, Caiazzo F and Sergi V 2017 Reduction of surface roughness by means of laser processing over additive manufacturing metal parts *Materials* **10** 30

[79] Vaithilingam J, Goodridge R D, Hague R J, Christie S D and Edmondson S 2016 The effect of laser remelting on the surface chemistry of Ti6al4V components fabricated by selective laser melting *Journal of Materials Processing Technology* **232** 1–8

[80] Boschetto A, Bottini L and Veniali F 2017 Roughness modeling of AlSi10Mg parts fabricated by selective laser melting *Journal of Materials Processing Technology* **241** 154–163

[81] Guo C, Ge W and Lin F 2015 Effects of scanning parameters on material deposition during Electron Beam Selective Melting of Ti-6Al-4V powder *Journal of Materials Processing Technology* **217** 148–157

[82] Fox J C, Moylan S P and Lane B M 2016 Effect of Process Parameters on the Surface Roughness of Overhanging Structures in Laser Powder Bed Fusion Additive Manufacturing *Procedia CIRP* **45** 131–134

[83] Senin N, Thompson A and Leach R K 2017 Characterisation of the topography of metal additive surface features with different measurement technologies *Measurement Science and Technology* **28** 095003

[84] Senin N, Thompson A and Leach R K 2018 Feature-based characterisation of signature topography in laser powder bed fusion of metals *Measurement Science and Technology* **29** 045009

[85] de Groot P 2017 The Meaning and Measure of Vertical Resolution in Optical Surface Topography Measurement *Applied Sciences* **7** 54

[86] Gomez C, Su R, Thompson A, DiSciacca J, Lawes S and Leach R K 2017 Optimization of surface measurement for metal additive manufacturing using coherence scanning interferometry *Optical Engineering* **56** 111714

[87] Southon N, Stavroulakis P, Goodridge R and Leach R K 2018 In-process measurement and monitoring of a polymer laser sintering powder bed with fringe projection *Materials and Design* **157** 227–234

[88] Zhang B, Ziegert J, Farahi F and Davies A 2016 In situ surface topography of laser powder bed fusion using fringe projection *Additive Manufacturing* **12** 100–107

[89] Triantaphyllou A, Giusca C L, Macaulay G D, Roerig F, Hoebel M, Leach R K, Tomita B and Milne K A 2015 Surface texture measurement for additive manufacturing *Surface Topography: Metrology and Properties* **3** 024002

[90] Grimm T, Wiora G and Witt G 2015 Characterization of typical surface effects in additive manufacturing with confocal microscopy *Surface Topography: Metrology and Properties* **3** 014001

[91] Sidambe A T 2017 Three dimensional surface topography characterization of the electron beam melted Ti6Al4V *Metal Powder Report* **72** 200–205

[92] Cabanettes F, Joubert A, Chardon G, Dumas V, Rech J, Grosjean C and Dimkovski Z 2018 Topography of as built surfaces generated in metal additive manufacturing: A multi scale analysis from form to roughness *Precision Engineering* **52** 249–265

[93] Townsend A, Racasan R and Blunt L 2018 Surface-specific additive manufacturing test artefacts *Surface Topography: Metrology and Properties* **6** 024007

[94] Gora W S, Tian Y, Cabo A P, Ardron M, Maier R R, Prangnell P, Weston N J and Hand D P 2016 Enhancing Surface Finish of Additively Manufactured Titanium and Cobalt Chrome Elements Using Laser Based Finishing *Physics Procedia* **83** 258–263

[95] Sun Y Y, Gulizia S, Oh C H, Fraser D, Leary M, Yang Y F and Qian M 2016 The Influence of As-Built Surface Conditions on Mechanical Properties of Ti-6Al-4V Additively Manufactured by Selective Electron Beam Melting *JOM* **68** 791–798

[96] Rosa B, Mognol P and Hascoët J y 2015 Laser polishing of additive laser manufacturing surfaces *Journal of Laser Applications* **27** S29102

[97] Demir A G and Previtali B 2017 Additive manufacturing of cardiovascular CoCr stents by selective laser melting *Materials & Design* **119** 338–350

[98] Leach R K and Haitjema H 2010 Bandwidth characteristics and comparisons of surface texture measuring instruments *Measurement Science and Technology* **21** 32001–9

[99] Todhunter L D, Leach R K, Lawes S D A and Blateyron F 2017 Industrial survey of ISO surface texture parameters *CIRP Journal of Manufacturing Science and Technology* **19** 84–92

[100] Safdar A, He H Z, Wei L Y, Snis A and Chavez De Paz L E 2012 Effect of process parameters settings and thickness on surface roughness of EBM produced Ti-6Al-4V *Rapid Prototyping Journal* **18** 401–408

[101] Yakout M, Cadamuro A, Elbestawi M A and Veldhuis S C 2017 The selection of process parameters in additive manufacturing for aerospace alloys *International Journal of Advanced Manufacturing Technology* **92** 2081–2098

[102] Koutiri I, Pessard E, Peyre P, Amlou O and De Terris T 2018 Influence of SLM process parameters on the surface finish, porosity rate and fatigue behavior of as-built Inconel 625 parts **255** 536–546

[103] Strano G, Hao L, Everson R M and Evans K E 2013 Surface roughness analysis, modelling and prediction in selective laser melting *Journal of Materials Processing Technology* **213** 589–597

[104] Weißmann V, Drescher P, Bader R, Seitz H, Hansmann H and Laufer N 2017 Comparison of Single Ti6Al4V Struts Made Using Selective Laser Melting and Electron Beam Melting Subject to Part Orientation *Metals* **7** 91

[105] Staub A, Spierings A B and Wegener K 2018 Selective Laser Melting at High Laser Intensity: Overhang Surface Characterization and Optimization *DDMC 2018: Fraunhofer Direct Digital Manufacturing Conference. Proceedings* 296–301

[106] Campbell R I, Martorelli M and Lee H S 2002 Surface roughness visualisation for rapid prototyping models *CAD Computer Aided Design* **34** 717–725

[107] Ahn D, Kim H and Lee S 2009 Surface roughness prediction using measured data and interpolation in layered manufacturing *Journal of Materials Processing Technology* **209** 664–671

[108] Barari A, Kishawy H A, Kaji F and Elbestawi M A 2017 On the surface quality of additive manufactured parts *International Journal of Advanced Manufacturing Technology* **89** 1969–1974

[109] Bacchewar P B, Singhal S K and Pandey P M 2007 Statistical modelling and optimization of surface roughness in the selective laser sintering process *Proceedings of the Institution of Mechanical Engineers, Part B: Journal of Engineering Manufacture* **221** 35–52

[110] Alrbaey K, Wimpenny D, Tosi R, Manning W and Moroz A 2014 On optimization of surface roughness of selective laser melted stainless steel parts: A statistical study *Journal of Materials Engineering and Performance* **23** 2139–2148

[111] Ghany K A and Moustafa S F 2006 Comparison between the products of four RPM systems for metals *Rapid Prototyping Journal* **12** 86–94

[112] Lamikiz A, Sánchez J A, López de Lacalle L N and Arana J L 2007 Laser polishing of parts built up by selective laser sintering *International Journal of Machine Tools and Manufacture* **47** 2040–2050

[113] Löber L, Flache C, Petters R, Kühn U and Eckert J 2013 Comparison of different post processing technologies for SLM generated 316l steel parts *Rapid Prototyping Journal* **19** 173–179

[114] Ma C P, Guan Y C and Zhou W 2017 Laser polishing of additive manufactured Ti alloys *Optics and Lasers in Engineering* **93** 171–177

[115] Senin N and Blunt L 2013 Characterisation of individual areal features *Characterisation of Areal Surface Texture* ed Leach R K (Berlin, Heidelberg) chap 8, pp 179–216

[116] MacAulay G D, Senin N, Giusca C L, Leach R K and Ivanov A 2015 Review of feature boundary identification techniques for the characterization of tessellated surfaces *Surface Topography: Metrology and Properties* **3** 013002

[117] Krishna A V, Flys O, Reddy V V, Leicht A, Hammar L and Rosen B g 2018 Potential approach towards effective topography characterization of 316L stainless steel components produced by selective laser melting process *Proc. 18th Int. euspen Conf., Venice, Italy, Jun*

[118] Senin N, Blunt L A, Leach R K and Pini S 2013 Morphologic segmentation algorithms for extracting individual surface features from areal surface topography maps *Surface Topography: Metrology and Properties* **1** 015005

[119] Zhu H 2012 *Measurement and characterisation of micro/nano scale structured surfaces* Ph.D. thesis University of Huddersfield

[120] Vicent C, Ron K and Guillermo S 1997 Geodesic Active Contours *International Journal of Computer Vision* **22** 61–79

[121] Gonzales R C and Woods R E 2018 *Digital Image Processing, 4th edition* 4th ed (New York, NY: Pearson)

[122] Newton L, Senin N, Smith B and Leach R 2018 Feature-based characterisation of evolving surface topographies in finishing operations for additive manufacturing *Proc. 18th Int. euspen Conf., Venice, Italy, Jun*

[123] Newton L, Senin N, Gomez C, Danzl R, Helmli F, Blunt L and Leach R K 2019 Areal topography measurement of metal additive surfaces using focus variation microscopy *Additive Manufacturing* **25** 365–389

[124] Danzl R, Helmli F and Scherer S 2011 Focus variation - A robust technology for high resolution optical 3D surface metrology *Strojniski Vestnik/Journal of Mechanical Engineering* **57** 245–256

[125] Hiersemenzel F, Claverley J D, Petzing J N, Leach R K and Helmli F S 2013 Areal surface topography measurement of high aspect ratio features using the focus variation technique *Harmnst 2013* 2–3

[126] Digital Surf 2018 Mountains® surface imaging & metrology software

[127] Leach R K 2013 *Characterisation of Areal Surface Texture* (Berlin, Heidelberg: Springer Berlin Heidelberg)

[128] Haitjema H 2015 Uncertainty in measurement of surface topography *Surface Topography: Metrology and Properties* **3** 035004

[129] Newton L, Senin N, Smith B, Chatzivagiannis E and Leach R K 2019 Comparison and validation of surface topography segmentation methods for feature-based characterisation of metal powder bed fusion surfaces *Surface Topography: Metrology and Properties* **[Submitted]**

[130] Newton L, Senin N, Smith B, Chatzivagiannis E and Leach R K 2019 Comparison and validation of surface topography segmentation methods for feature-based characterisation of metal powder bed fusion surfaces *ASPE/euspen Special Interest Group Meeting: Advancing Precision in Additive Manufacturing, Nantes, France, September*

[131] Blunt L and Xiao S 2011 The use of surface segmentation methods to characterise laser zone surface structure on hard disc drives *Wear* **271** 604–609

[132] Whitaker R T 1998 A Level-Set Approach to 3D Reconstruction from Range Data *International Journal of Computer Vision* **29** 203–231

[133] MacAulay G D and Giusca C L 2016 Assessment of uncertainty in structured surfaces using metrological characteristics *CIRP Annals - Manufacturing Technology* **65** 533–536

[134] Newton L, Senin N, Smith B, Chatzivagiannis E and Leach R K 2019 Feature-based characterisation of ti6al4v electron beam powder bed fusion surfaces fabricated at different orientations *Proc. 22nd Met. Props, Lyon, France, Jul.*

[135] Jamshidinia M and Kovacevic R 2015 The influence of heat accumulation on the surface roughness in powder-bed additive manufacturing *Surface Topography: Metrology and Properties* **3** 014003

[136] Chen Z, Wu X, Tomus D and Davies C H 2018 Surface roughness of Selective Laser Melted Ti-6Al-4V alloy components *Additive Manufacturing* **21** 91–103

[137] Mumtaz K and Hopkinson N 2009 Top surface and side roughness of Inconel 625 parts processed using selective laser melting *Rapid Prototyping Journal* **15** 96–103

[138] Senin N and Leach R K 2018 Information-rich surface metrology *Procedia CIRP* **75** 19–26

Appendix A

Design of experiment results for optimisation of focus variation

A.1 Coefficient of determination (R^2) results for each ANOVA model

The coefficient of determination (R^2) results for each general linear model analysed through ANOVA are shown in the Figures below. These are a measure of the goodness of fit of the the regression line between the predicted values as determined by the general linear model and the observed responses for each surface test case (e.g. Al-Si-10Mg LPBF Top) and each respective metric (e.g. Q3 / nm). Theoretically, if the model could explain 100% of the variance, the predicted values would always equal the observed values and all data points would fall on the fitted regression line. In total for each objective magnification there were 24 general linear models created from the full factorial design of experiments highlighted in Section 3.2.3.

10× magnification			
Surface	R^2 **values**		
	Q3 / nm	**NMP / %**	**Sa / µm**
Al-Si-10Mg LPBF Top	0.989	0.971	0.993
Al-Si-10Mg LPBF Side	0.990	0.731	0.995
Inconel 718 LPBF Top	0.715	0.987	0.981
Inconel 718 LPBF Side	0.997	0.867	0.992
Ti-6Al-4V LPBF Top	0.873	0.899	0.986
Ti-6Al-4V LPBF Side	0.993	0.840	0.997
Ti-6Al-4V EBPBF Top	0.985	0.931	0.980
Ti-6Al-4V EBPBF Side	0.996	0.806	0.997

Table A.1 Coefficient of determination (R^2) results for the 10× objective ANOVA models

20× magnification			
Surface	R^2 **values**		
	Q3 / nm	**NMP / %**	**Sa / µm**
Al-Si-10Mg LPBF Top	0.979	0.556	0.761
Al-Si-10Mg LPBF Side	0.978	0.663	0.827
Inconel 718 LPBF Top	0.763	0.649	0.999
Inconel 718 LPBF Side	0.969	0.841	0.948
Ti-6Al-4V LPBF Top	0.943	0.776	0.865
Ti-6Al-4V LPBF Side	0.941	0.761	0.924
Ti-6Al-4V EBPBF Top	0.939	0.574	0.978
Ti-6Al-4V EBPBF Side	0.911	0.758	0.925

Table A.2 Coefficient of determination (R^2) results for the 20× objective ANOVA models

50× magnification			
Surface	R^2 **values**		
	Q3 / nm	**NMP / %**	**Sa / µm**
Al-Si-10Mg LPBF Top	0.989	0.768	0.967
Al-Si-10Mg LPBF Side	0.975	0.750	0.805
Inconel 718 LPBF Top	0.920	0.775	0.988
Inconel 718 LPBF Side	0.829	0.787	0.979
Ti-6Al-4V LPBF Top	0.608	0.813	0.966
Ti-6Al-4V LPBF Side	0.998	0.906	0.829
Ti-6Al-4V EBPBF Top	0.989	0.727	0.994
Ti-6Al-4V EBPBF Side	0.984	0.825	0.977

Table A.3 Coefficient of determination (R^2) results for the 50× objective ANOVA models

A.2 Main effects plots for each ANOVA model

From the ANOVA analysis, the main effects plots are created to show the differences between level mean of the response for each factor level. A difference indicates there is a main effect but not any interaction. For all following figures in this section of the appendix, the vertical scale is the same for all graphs grouped by surface type.

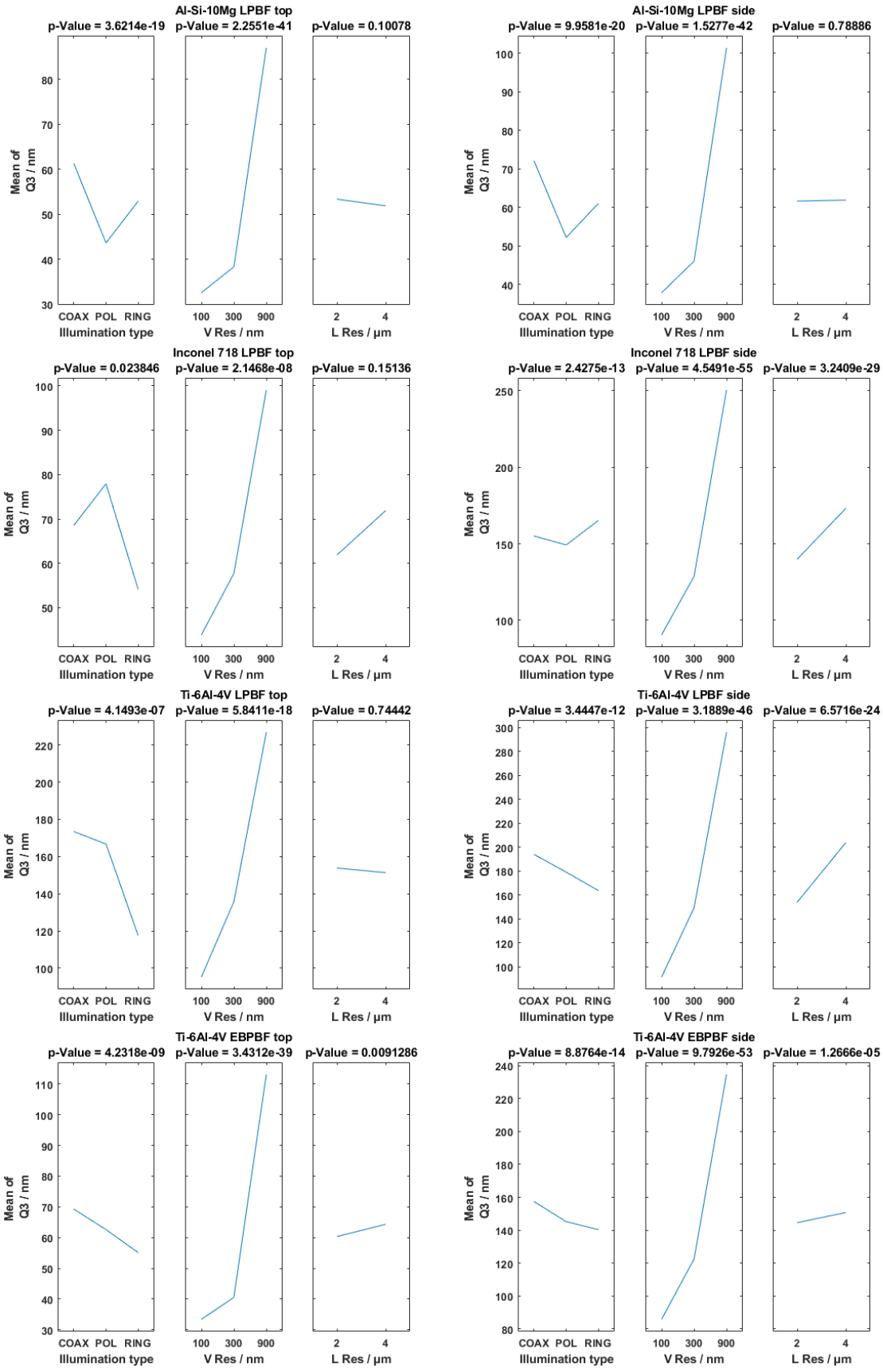

Fig. A.1 Main effects plots for Q3 for the 10× magnification

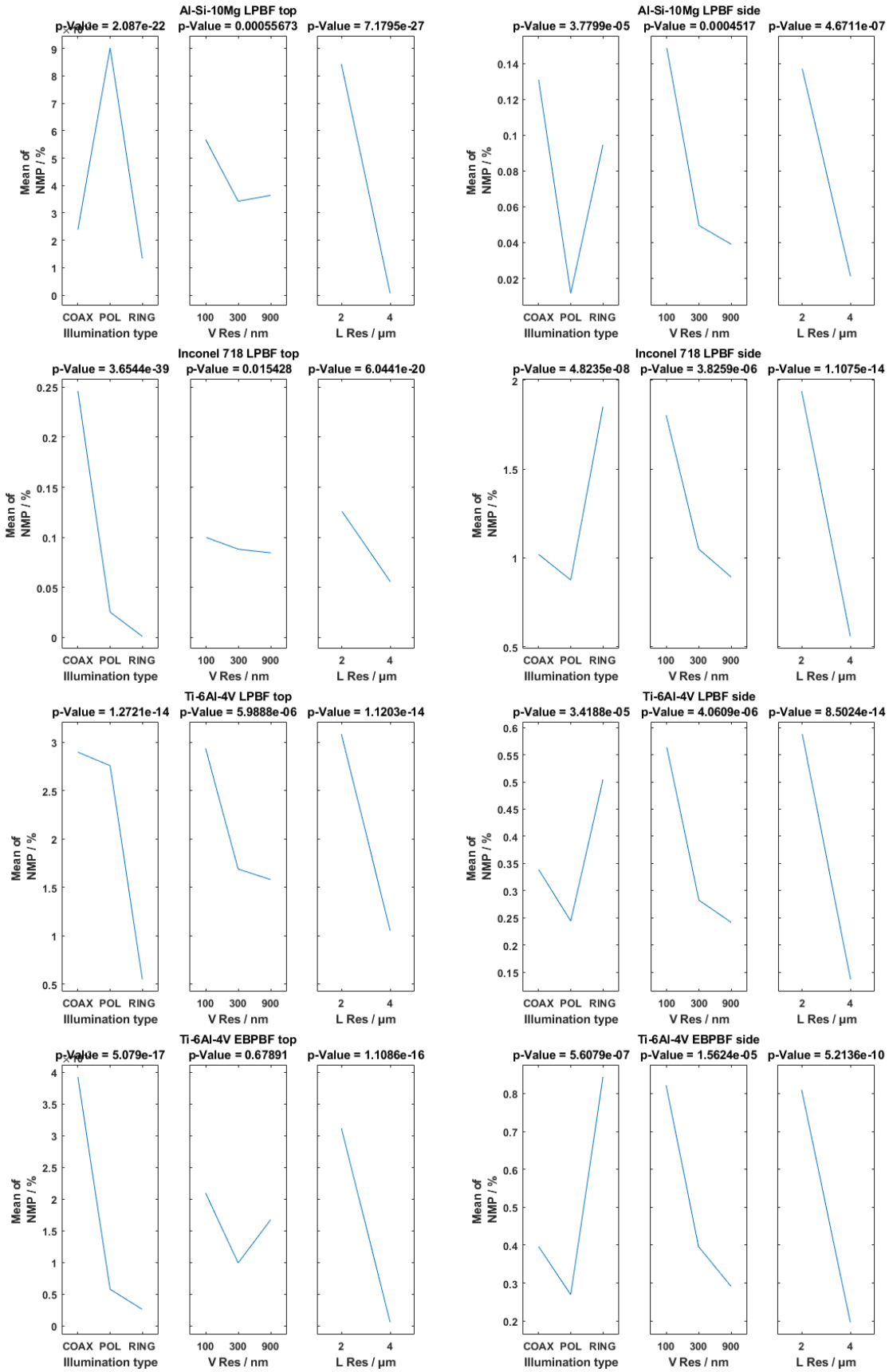

Fig. A.2 Main effects plots for NMP for the 10× magnification

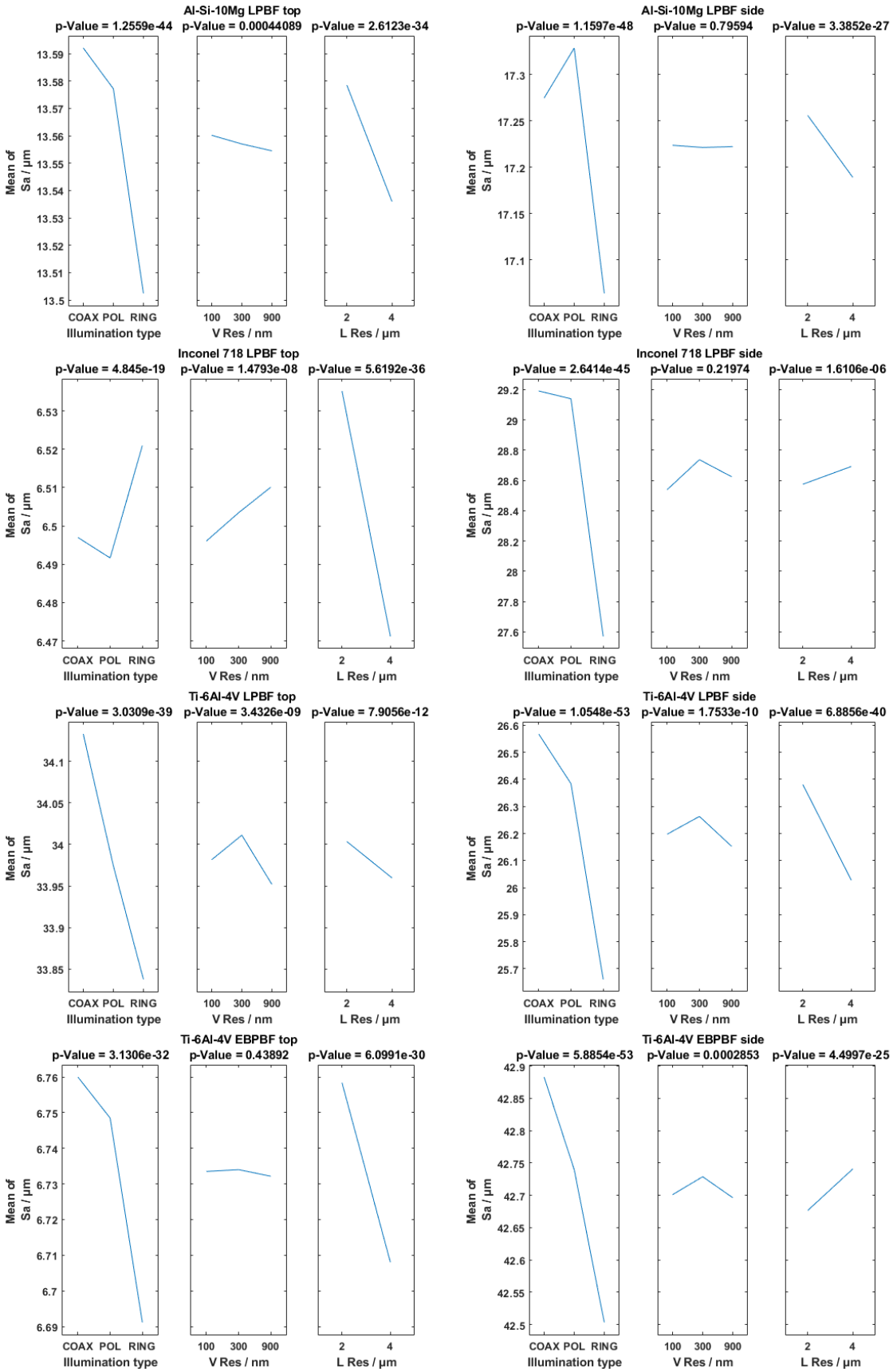

Fig. A.3 Main effects plots for *Sa* for the 10× magnification

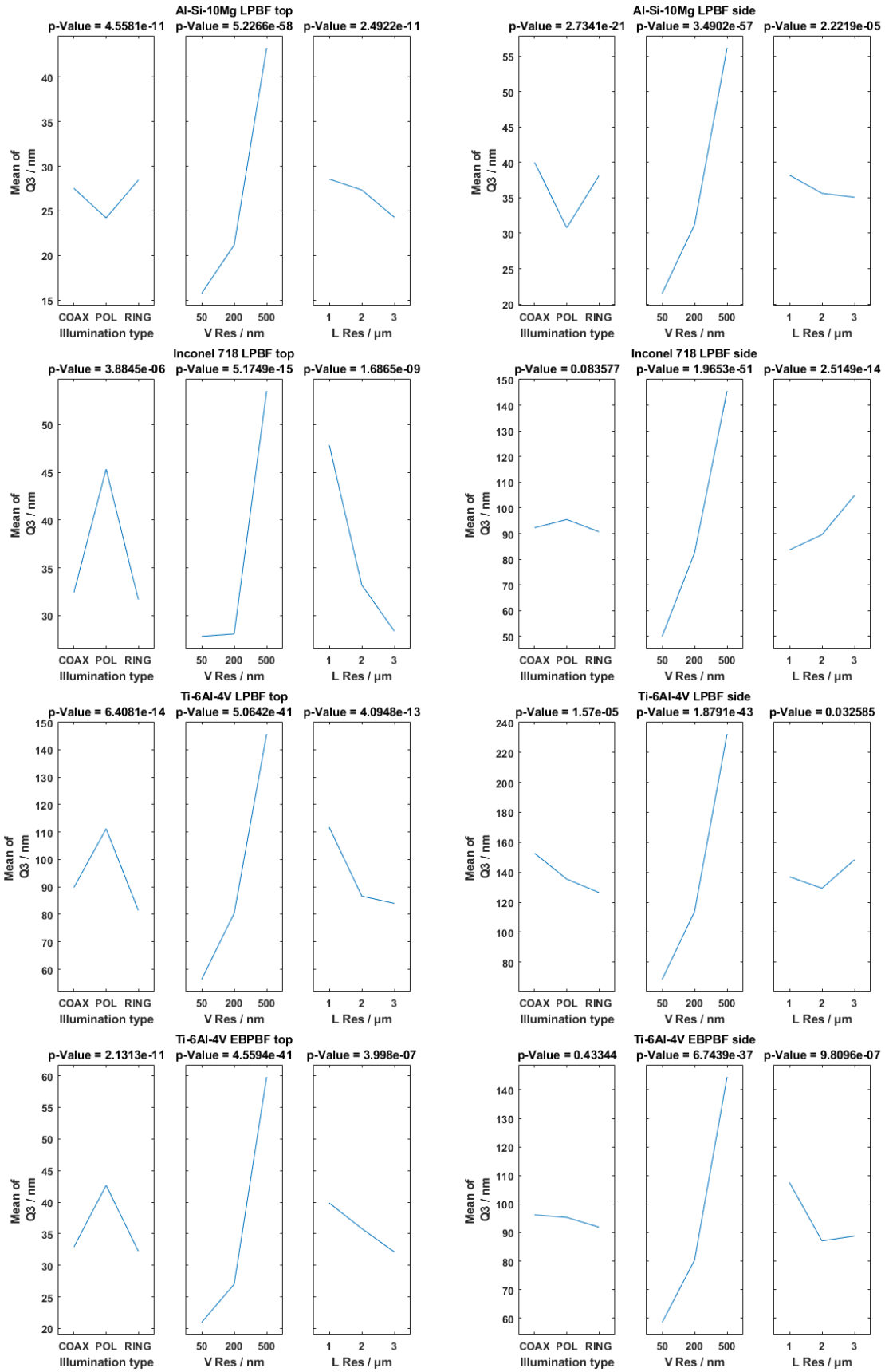

Fig. A.4 Main effects plots for Q3 for the 20× magnification

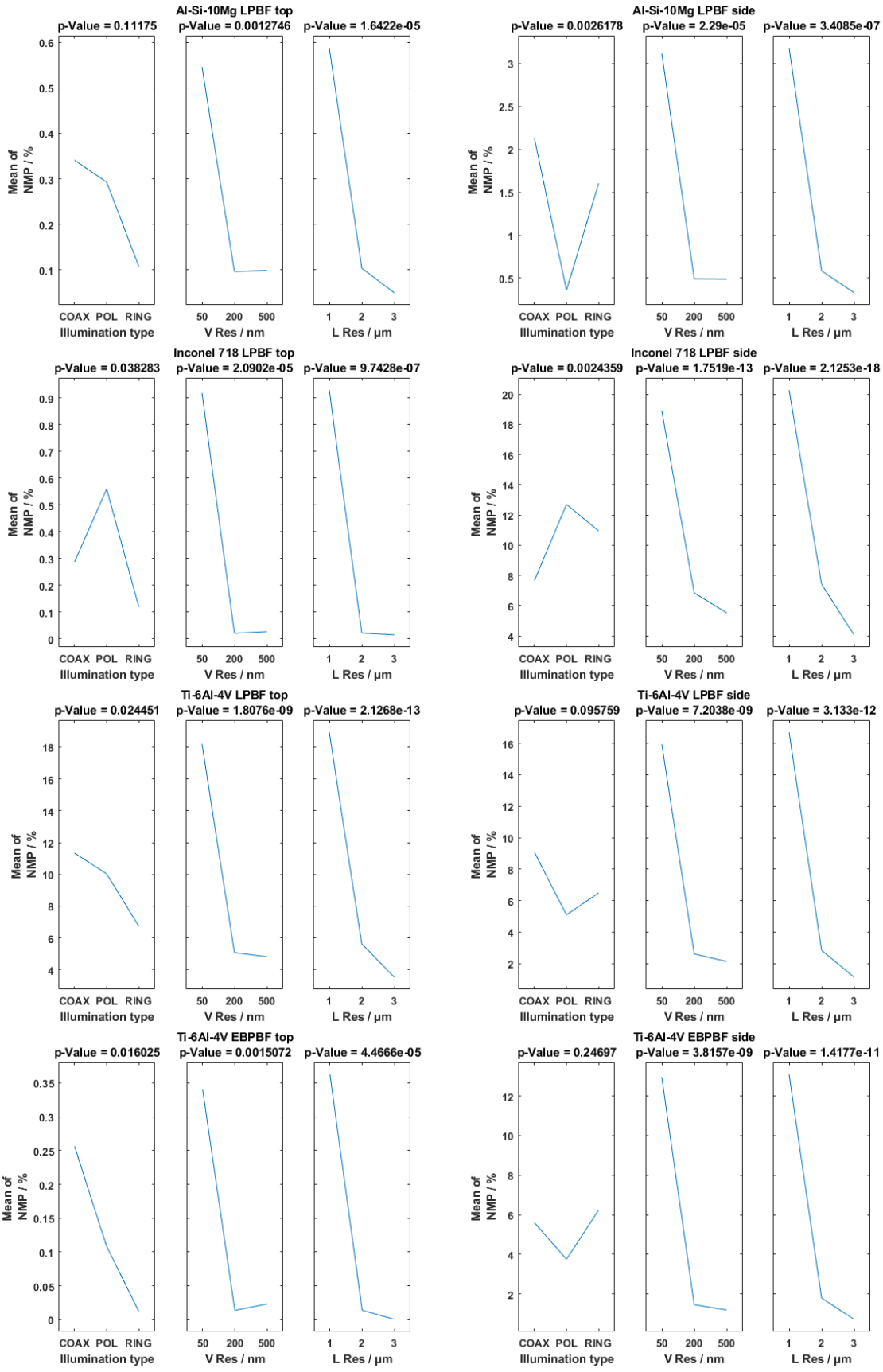

Fig. A.5 Main effects plots for NMP for the 20× magnification

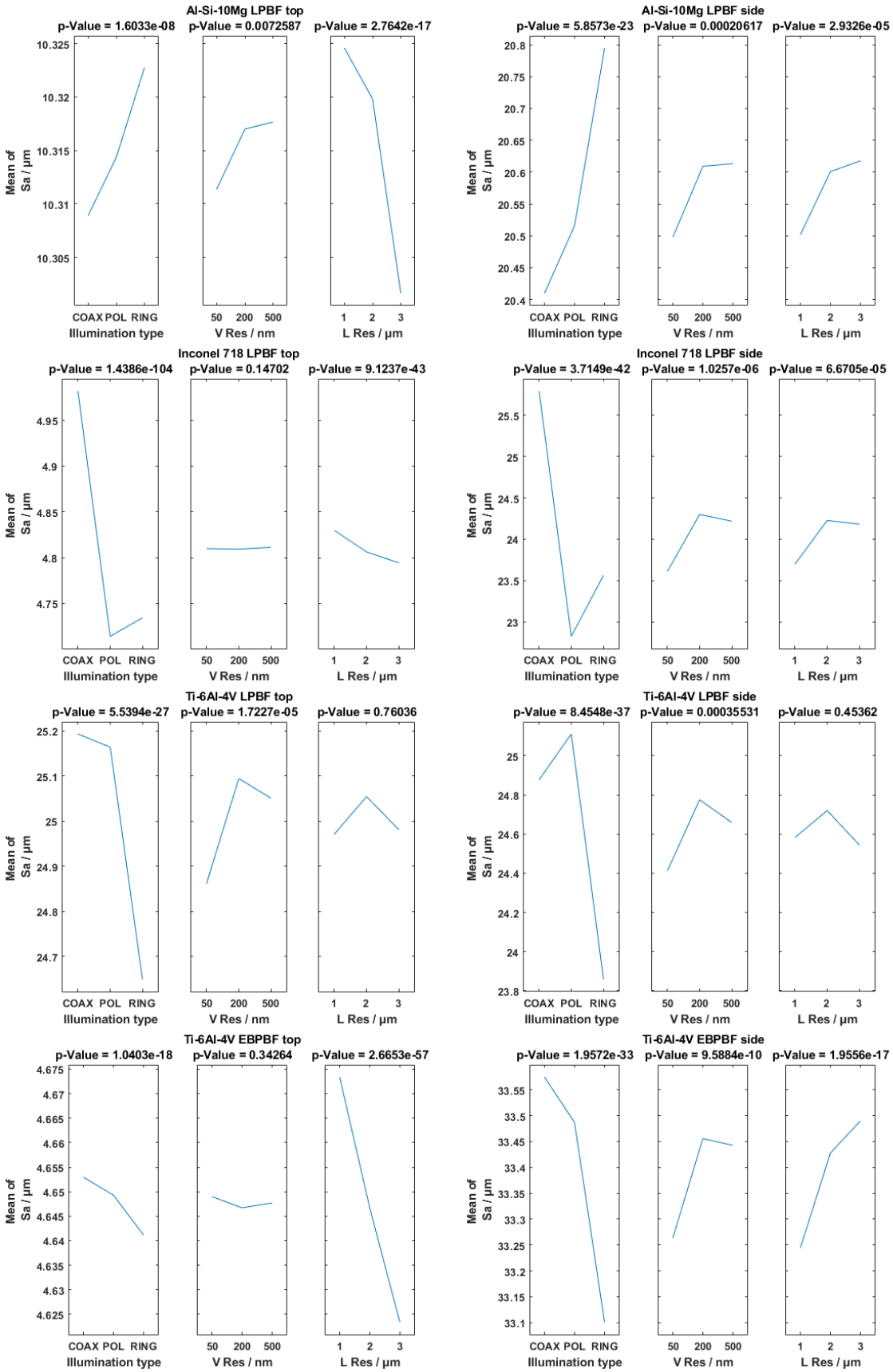

Fig. A.6 Main effects plots for *Sa* for the 20× magnification

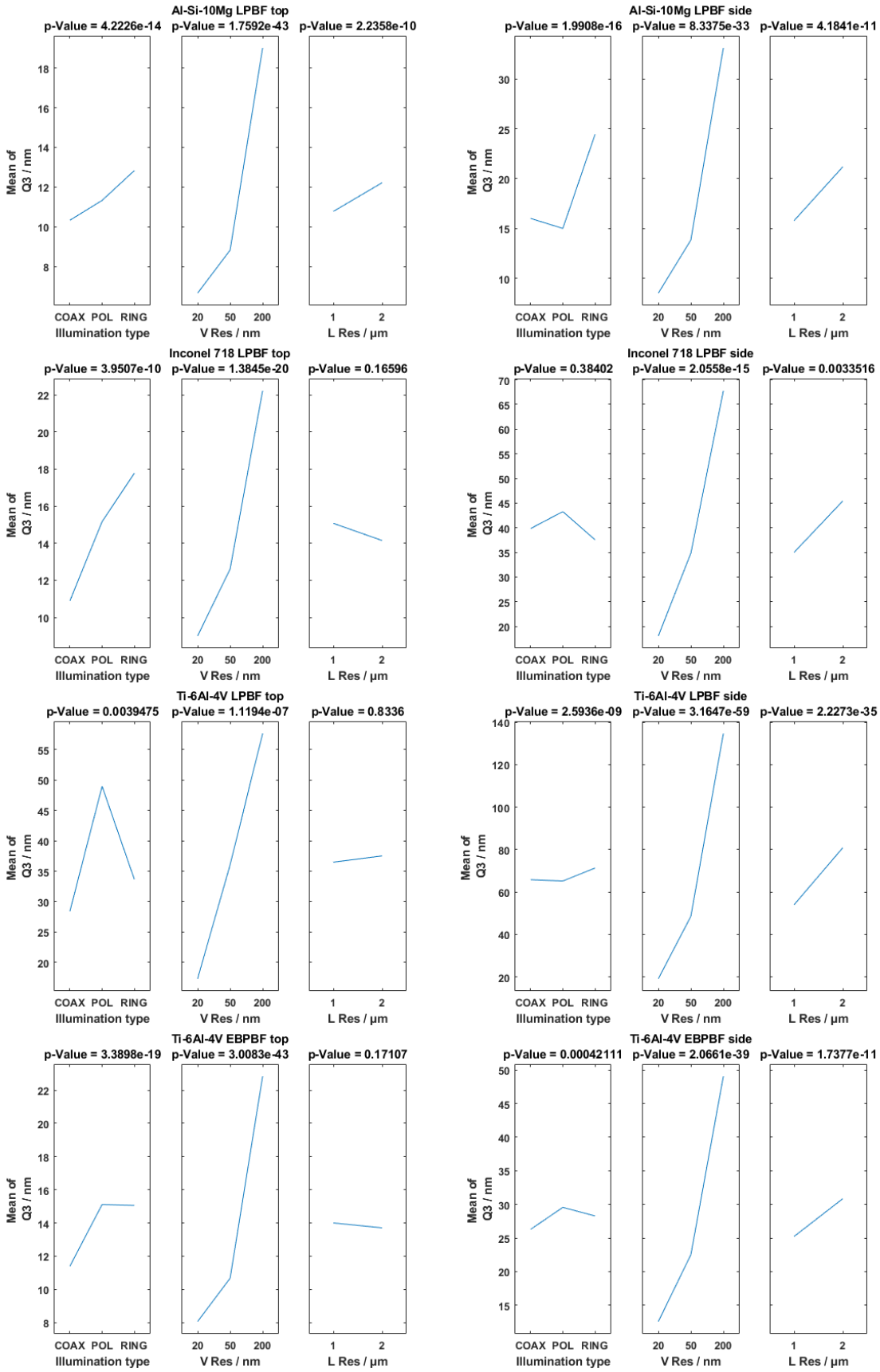

Fig. A.7 Main effects plots for Q3 for the 50× magnification

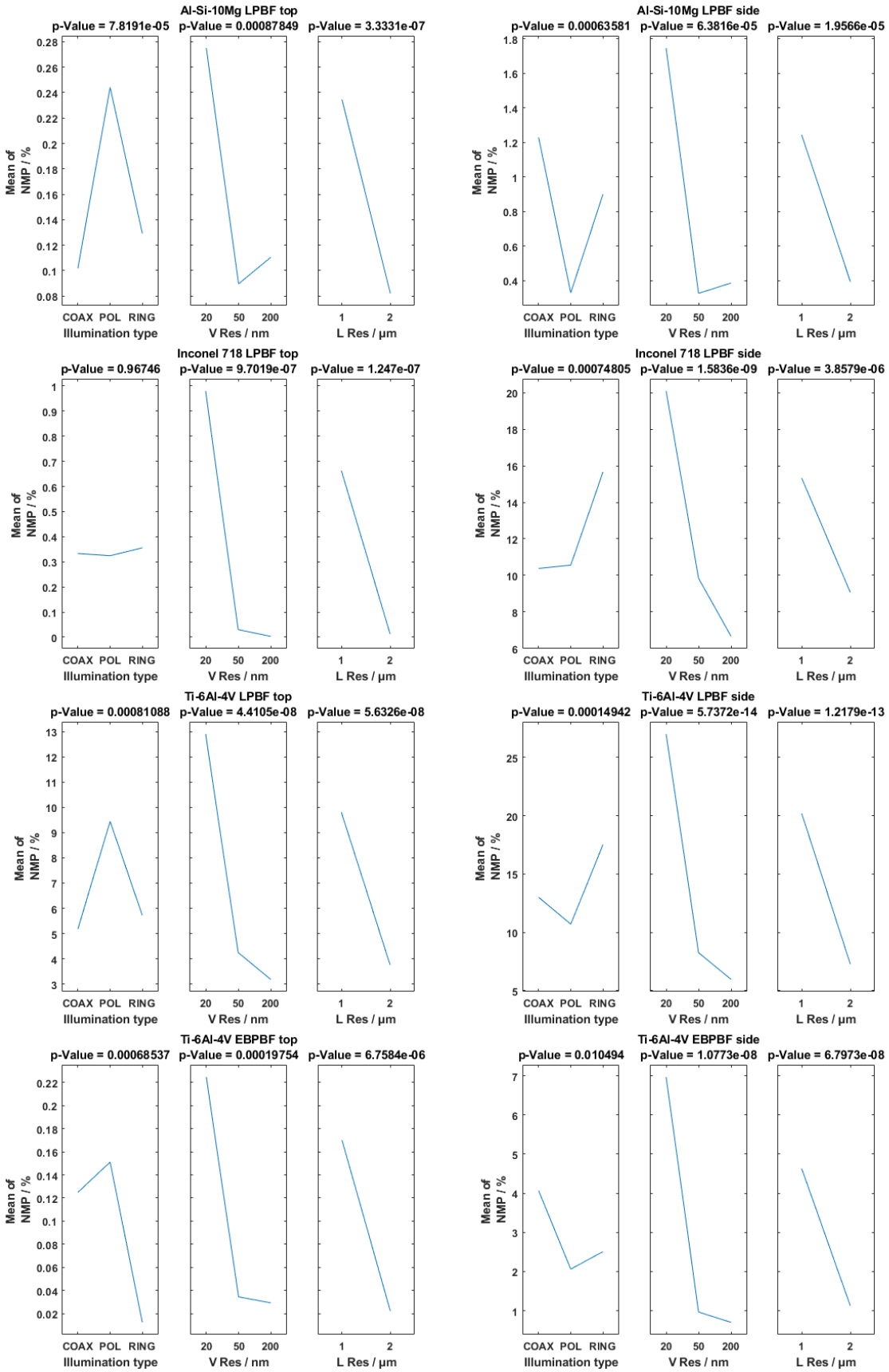

Fig. A.8 Main effects plots for NMP for the 50× magnification

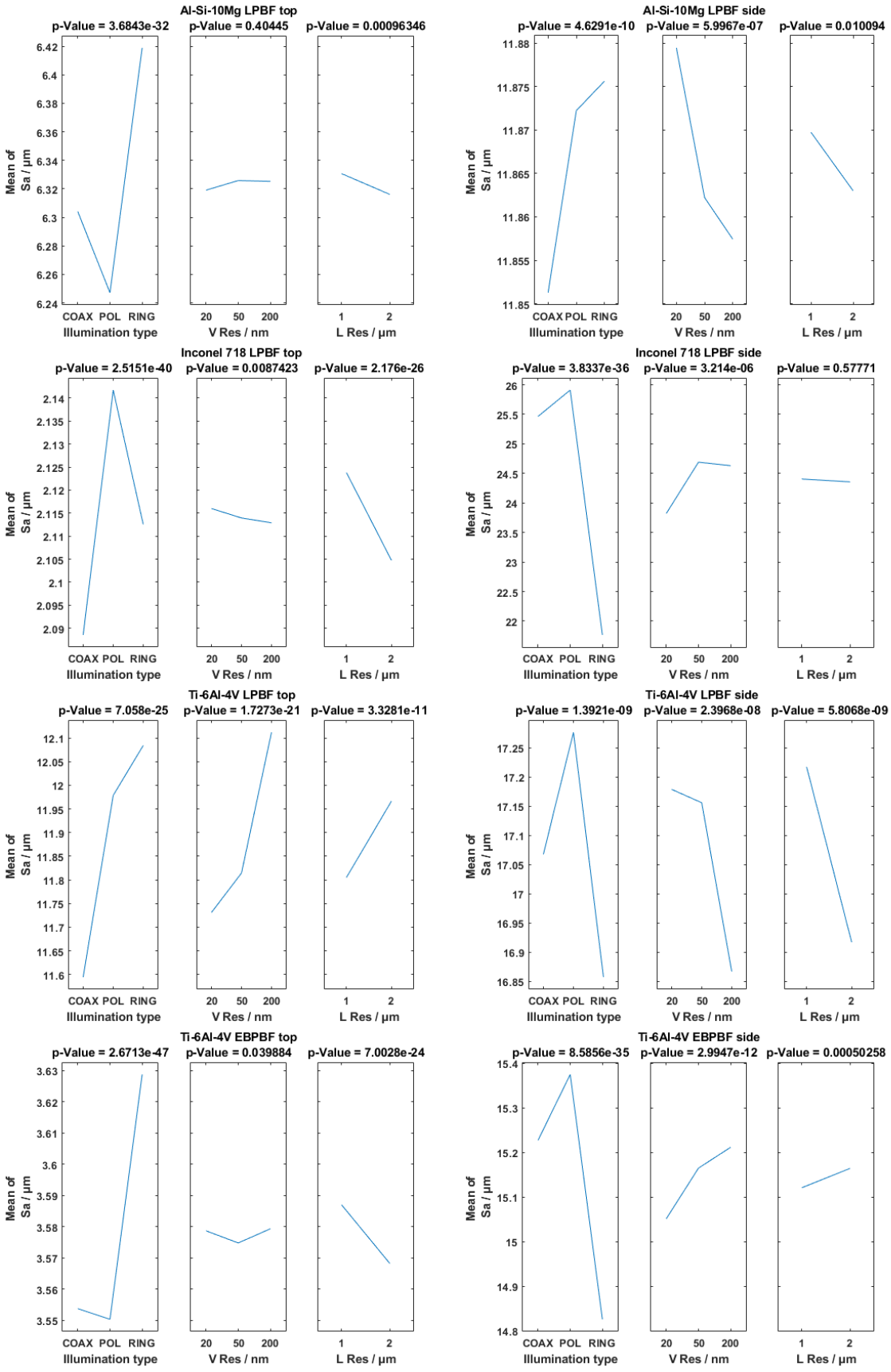

Fig. A.9 Main effects plots for *Sa* for the 50× magnification